

**TECHNO-ECONOMIC STUDY FOR SUGARCANE BAGASSE TO
LIQUID BIOFUELS IN SOUTH AFRICA:
A COMPARISON BETWEEN BIOLOGICAL AND
THERMOCHEMICAL PROCESS ROUTES**

by

Nadia H Leibbrandt

Dissertation presented for the Degree

of

**DOCTOR OF PHILOSOPHY
(Chemical Engineering)**

in the Department of Process Engineering
at the University of Stellenbosch

March 2010

Promoter/s

Professor JH Knoetze

Professor JF Görgens

STELLENBOSCH

DECLARATION

I, the undersigned, hereby declare that the work contained in this dissertation/assignment/thesis is my own original work and that I have not previously in its entirety or in part submitted it at any university for a degree.

A handwritten signature in black ink, appearing to read 'M. M. M. M.', written diagonally across the page.

Signature

1 March 2010

Date

ACKNOWLEDGEMENTS

I would like to thank the following people for the roles each of them have played in my work and my life in the last four years:

Professor Hansie Knoetze for his invaluable support, wisdom and guidance throughout the last four years and over the last eleven years of my study career.

Professor Johann Görgens for his motivation and guidance and for introducing me to the fascinating world of biofuels.

Colleagues and friends at the Process Engineering Department of Stellenbosch University, with special thanks to Dr Cara Schwarz, Dr Lafras Moolman and Dr Marion Carrier, for encouragement and support at times when it was much needed.

Dr Mark Laser and Professor Lee Lynd at Dartmouth College, NH, USA, for hosting me at their department and providing me with a platform on which the process modelling was based. My sincere gratitude also goes to Dr John Hannon, for his friendly hospitality during my stay.

Dr Carlos Martín, for providing additional information on fermentation with their adapted yeast.

TSB Sugar for their financial support, without which this project could not have been initiated, and to Nico Stolz, for his unfailing support and involvement in this project. It has been a pleasure experience working with an industry partner that is always available and enthusiastic.

The Centre for Renewable and Sustainable Energy Studies, for providing invaluable financial support.

To my mom and dad, Tertius, Tina, Cliff and Ross, I am blessed to have such a supportive family who have always believed in me and I love you all for that.

Finally, to my husband, Grant, who keeps expanding my horizons and who is always there to provide love, support, and if all else fails, a glass of diluted ethanol!

ABSTRACT

A techno-economic feasibility study was performed to compare biological and thermochemical process routes for production of liquid biofuels from sugarcane bagasse in South Africa using process modelling. Processing of sugarcane bagasse for the production of *bioethanol*, *pyrolysis oil* or *Fischer-Tropsch liquid fuels* were identified as relevant for this case study. For each main process route, various modes or configurations were evaluated, and in total eleven process scenarios were modelled, for which fourteen economic models were developed to include different scales of biomass input.

Although detailed process modelling of various biofuels processes has been performed for other (mainly first world) countries, comparative studies have been very limited and mainly focused on mature technology. This is the first techno-economic case study performed for South Africa to compare these process routes using data for sugarcane bagasse. The technical and economic performance of each process route was investigated using the following approach:

- Obtain **reliable data** sets from literature for processing of **sugarcane bagasse** via biological pretreatment, hydrolysis and fermentation, fast and vacuum pyrolysis, and equilibrium gasification to be sufficient for process modelling.
- Develop **process models** for eleven process scenarios to compare their energy efficiencies and product yields. In order to reflect currently available technology, conservative assumptions were made where necessary and the measured data collected from literature was used. The modelling was performed to reflect energy-self-sufficient processes by using the thermal energy available as a source of heat and electricity for the process.
- Develop **economic models** using cost data available in literature and price data and economic parameters applicable to South Africa.

- **Compare** the three process routes using technical and economic results obtained from the process and economic models and identify the most promising scenarios.

For *bioethanol* production, experimental data was collected for three pretreatment methods, namely steam explosion, dilute acid and liquid hot water pretreatment performed at pretreatment solids concentrations of 50wt%, 10wt% and 5wt%, respectively. This was followed by enzymatic hydrolysis and separate co-fermentation. *Pyrolysis* data for production of bio-oil via fast and vacuum pyrolysis was also collected. For *gasification*, data was generated via equilibrium modelling based on literature that validated the method against experimental data for sugarcane bagasse gasification. The equilibrium model was used to determine optimum gasification conditions for either gasification efficiency or syngas composition, using sugarcane bagasse, fast pyrolysis slurry or vacuum pyrolysis slurry as feedstock. These results were integrated with a downstream process model for *Fischer-Tropsch synthesis* to evaluate the effect of upstream optimisation on the process energy efficiency and economics, and the inclusion of a shift reactor was also evaluated. The effect of process heat integration and boilers with steam turbine cycles to produce process heat and electricity, and possibly electricity by-product, was included for each process.

This analysis assumed that certain process units could be successfully scaled to commercial scales at the same yields and efficiencies determined by experimental and equilibrium modelling data. The most important process units that need to be proven on an industrial scale are pretreatment, hydrolysis and fermentation for bioethanol production, the fast pyrolysis and vacuum pyrolysis reactors, and the operation of a two-stage gasifier with nickel catalyst at near equilibrium conditions. All of these process units have already been proven on a bench scale with sugarcane bagasse as feedstock.

The *economic models* were based on a critical evaluation of equipment cost data available in literature, and a conservative approach was taken to reflect 1st plant technology. Data for the cost and availability of raw materials was obtained from the

local industry and all price data and economic parameters (debt ratio, interest and tax rates) were applicable to the current situation in South Africa. A sensitivity analysis was performed to investigate the effects of likely market fluctuations on the process economics.

A summary of the technical and economic performances of the most promising scenarios is shown in the table below. The **bioethanol** process models showed that the liquid hot water and dilute acid pretreatment scenarios are not energy self-sufficient and require additional fossil energy input to supply process energy needs. This is attributed to the excessive process steam requirements for pretreatment and conditioning due to the low pretreatment solid concentrations of 5wt% and 10wt%, respectively.

The critical solids concentration during dilute acid pretreatment for an energy self-sufficient process was found to be 35%, although this was a theoretical scenario and the data needs to be verified experimentally. At a pretreatment level of 50% solids, steam explosion achieved the highest process thermal energy efficiency for bioethanol of 55.8%, and a liquid fuel energy efficiency of 40.9%.

Both **pyrolysis** processes are energy self-sufficient, although some of the char produced by fast pyrolysis is used to supplement the higher process energy demand of fast compared to vacuum pyrolysis. The thermal process energy efficiencies of both pyrolysis processes are roughly 70% for the production of crude bio-oil that can be sold as a residual fuel oil. However, the liquid fuel energy efficiency of fast pyrolysis is 66.5%, compared to 57.5% for vacuum pyrolysis, since fast pyrolysis produces more bio-oil and less char than vacuum pyrolysis.

ENERGY EFFICIENCIES and ECONOMIC RESULTS for SELECTED SCENARIOS Economic
results are given for 600MW bagasse input scenarios.

Process route	Bioethanol	Pyrolysis	Pyrolysis	Fischer-Tropsch	Fischer-Tropsch	Fischer-Tropsch
Scenario description	Steam explosion	Fast	Vacuum	Equilibrium gasifier 1	Equilibrium gasifier 1 with shift reactor	Equilibrium gasifier 2
Energy efficiencies						
Liquid fuel	40.9%	66.5%	57.5%	52.9%	49.4%	41.7%
Liquid fuel+thermal energy	55.8%	69.7%	70.0%	64.7%	54.0%	38.3%
Liquid fuel + electricity and/or char	41.9%	69.7%	69.0%	50.9%	49.0%	41.5%
Economic results						
Total project investment cost [US\$ million]	\$432.90	\$141.68	\$124.14	\$705.04	\$794.48	\$719.62
Liquid fuel production costs [\$US/GJ HHV]	\$23.0	\$6.95	\$8.16	\$21.6	\$28.4	\$29.7

The process energy efficiencies (LHV basis) are defined as follows: 1) Liquid fuel= (energy in liquid fuel)/ (energy in feed-energy in electricity - energy in char) (all in thermal units).
2) Liquid fuel + thermal energy= (thermal energy in liquid fuel + thermal energy in intermediate lignin, char or gas)/energy in feed (all in thermal units).
3) Liquid fuel + electricity and/or char= (energy in liquid fuel + electric energy + energy in char)/energy in feed (energy units).

Taking kinetic and practical considerations into account, two sets of operating conditions were determined for two **equilibrium gasifier** modes. Equilibrium Gasifier 1 was aimed at maximising the gasification efficiency, while the hydrogen/carbon monoxide syngas ratio was set to 2 for Equilibrium Gasifier 2 in order to maximise downstream Fischer-Tropsch liquid yields according to the stoichiometry of the synthesis reaction. The resulting operating conditions for Equilibrium Gasifier 1 were 1100K, an equivalence ratio of 0.25 and a steam to biomass ratio of 0.75 for atmospheric gasification of bagasse at 5% moisture, resulting in a gasification efficiency of 75%. In order to obtain a syngas ratio of 2, the steam to biomass ratio had to be raised to 2.25, reducing the

gasification efficiency to 60%. The equilibrium model data was verified by comparing it to experimental data measured in a two-stage gasifier.

Results obtained from the **Fischer-Tropsch** process models showed that Fischer-Tropsch liquid yields will increase from 40% (conversion of feed energy to Fischer-Tropsch liquids) to 45%, when Equilibrium Gasifier mode 2 is used instead of Equilibrium Gasifier 1. The addition of a shift reactor led to the same increase in liquid yields. However, the best thermal process and liquid fuel energy efficiencies of 64.7% and 52.9%, respectively, were obtained by using Equilibrium Gasifier 1, without inclusion of a shift reactor, since the total process energy consumption was lower and more electricity is produced as by-product. The process energy efficiencies were comparable with data in literature for similar process configurations. The liquid yields obtained from pyrolysis slurry gasification were found to be 4-10% lower compared to the scenarios for bagasse.

Considering current technology for the production of transport grade liquid fuels, it was found that Fischer-Tropsch processing achieves higher liquid fuel energy efficiencies than bioethanol production because all the biomass including lignin is utilised during thermochemical processing. However, improvements in pretreatment and fermentability will increase the end product energy efficiency of bioethanol processes to similar levels than those reported for advanced gasification systems. Pyrolysis is a very efficient process for the production of crude bio-oil and char, although upgrading does not currently offer significant energy benefits compared to other transport fuel process routes.

The **economic analysis** showed that, at liquid fuel production costs of \$US 23.0/GJ for bioethanol and \$US 21.6/GJ for Fischer-Tropsch liquids, these liquid biofuels can be produced at comparable costs. Bioethanol can compete with the petroleum industry at a crude oil price of \$US 81.0/barrel, while the breakeven oil price for Fischer-Tropsch liquids is \$US 77.3/barrel. However, due to the significantly higher capital investment required for a Fischer-Tropsch facility, bioethanol processing achieved the highest rate

of return (IRR) and return on investment (ROI) of 14.4% and 8.2%, respectively, for production of transport fuels. These returns are not sufficient to justify investment and based on the current market situation the South African government will have to provide subsidy schemes if these technologies are to be commercialised. However, likely changes in product prices that are expected to occur in the next few years will lead to drastic changes in this analysis. On the other hand, the economics of pyrolysis is very attractive from an investment point of view. Vacuum pyrolysis produces crude bio-oil at \$8.16/GJ and an internal rate of return of 40.5% (ROI of 37.6%); while the production costs of fast pyrolysis crude bio-oil is \$6.95/GJ at an internal rate of return of 34.2% (ROI of 29.4%). In all cases, scale played an important role and other than pyrolysis, the small 145MW scale scenarios were not economical. Production of Fischer-Tropsch liquids from gasification of pyrolysis slurry was also found to be uneconomical for sugarcane bagasse in this case study.

The sensitivity analysis showed that the most important factors affecting the economics are the assumed cost for bagasse, the selling price of fuel products and especially the price of electricity, which is expected to rise significantly in the next three years. If the South African government is to grant the price increase requested by Eskom, the national electricity distributor, the production costs for Fischer-Tropsch liquids and bioethanol could fall to \$7.7/GJ and \$10.6/GJ, at an internal rate of return of 21 and 29%, respectively.

The work presented in this study has made a valuable contribution to provide a base set of process and economic models applicable to South Africa that can be further developed and updated as these technologies advance. Also, the study offers a direct comparison between second generation biological and thermochemical process routes for liquid biofuels production based on a consistent framework. In addition, it has provided investors and decision makers with a consistent framework to compare these technologies and clarify the opportunities that each can offer in the unique South African context.

TABLE OF CONTENTS

DECLARATION	II
ACKNOWLEDGEMENTS	III
ABSTRACT	I
TABLE OF CONTENTS	VII
LIST OF FIGURES	XI
LIST OF TABLES	XIV
1. INTRODUCTION	1
1.1 PROJECT MOTIVATION AND OUTLINE OF THESIS	3
REFERENCES	7
2. LITERATURE BACKGROUND	9
2.1 BIOLOGICAL PROCESSING	9
2.1.1 Biomass Preparation and Pretreatment	10
2.1.2 Hydrolysis and Fermentation	12
2.2 THERMOCHEMICAL PROCESSING	14
2.2.1 Pyrolysis	14
2.2.2 Gasification for Fischer-Tropsch Synthesis	16
2.3 PROCESS MODELLING	19
REFERENCES	25
3. MODELLING OF BIOLOGICAL FERMENTATION AND PYROLYSIS PROCESSES	29
SUMMARY	29
3.1 INTRODUCTION	30
3.2 METHODOLOGY	32
3.2.1 Biological Processing Process Model	32
3.2.2 Pyrolysis Process Model	41

3.3 RESULTS AND DISCUSSION	45
3.3.1 Bioethanol Process Energy Requirements	45
3.3.2 Pyrolysis Process Energy Requirements	48
3.3.3 Process energy efficiencies	49
3.4 CONCLUSIONS	55
REFERENCES	57
4. MODELLING OF GASIFICATION AND DOWNSTREAM FISCHER-TROPSCH PROCESSING	59
SUMMARY	59
4.1 INTRODUCTION	61
4.2 METHODOLOGY	65
4.2.1 Gasification Section Equilibrium Modelling	65
4.2.2 Fischer-Tropsch Synthesis Process Modelling	67
4.3 RESULTS AND DISCUSSION	75
4.3.1 Gasification Section Equilibrium Modelling	75
4.3.2 Fischer-Tropsch Process Modelling	84
4.6 CONCLUSIONS	90
4.6.1 Gasification Equilibrium Modelling	90
4.6.2 Fischer-Tropsch Process Modelling	91
REFERENCES	93
5. BIOLOGICAL AND THERMOCHEMICAL PROCESS ROUTES: COMPARISON OF TECHNICAL PERFORMANCE	95
SUMMARY	95
5.1 INTRODUCTION	96
5.2 COMPARISON OF RESULTS	97
5.2.1 Comparison of process modelling results from this study for all process routes	97
5.2.2 Comparison of process modelling results for transport fuels production from this study with literature data	100
5.3 CONCLUSIONS	104
REFERENCES	105
6. ECONOMIC MODELLING FOR BIOETHANOL, PYROLYSIS AND FISCHER-TROPSCH PROCESS ROUTES	107
SUMMARY	107
6.1 INTRODUCTION	108
6.2 METHODOLOGY	110
6.2.1 Feedstock Availability and Delivery Costs	113

6.2.2 Process Equipment and Operating Costs	116
6.3 ECONOMIC MODELLING RESULTS AND ANALYSIS	118
6.3.1 Capital Investment	118
6.3.3 Fuel Production Costs	122
6.3.4 Investment Analyses and Sensitivity	125
6.4 CONCLUSIONS	132
REFERENCES	134
7. CONCLUSIONS	136
7.1 TECHNICAL PERFORMANCE of BIOETHANOL, PYROLYSIS and GASIFICATION FOLLOWED BY FISCHER-TROPSCH PROCESSING	136
7.1.1 Energy consumption and conversion of feed energy to liquid products	136
7.1.2 Process and liquid fuel energy efficiencies	141
7.2 PRODUCTION COSTS AND ECONOMIC PERFORMANCE of BIOETHANOL, PYROLYSIS and GASIFICATION FOLLOWED BY FISCHER-TROPSCH SYNTHESIS	142
7.3 CONTRIBUTIONS	145
8. RECOMMENDATIONS FOR FUTURE WORK	148
8.1 BIOETHANOL PROCESSES FOR SUGARCANE BAGASSE	148
8.2 PYROLYSIS PROCESSES FOR SUGARCANE BAGASSE	149
8.3 GASIFICATION AND FISCHER-TROPSCH PROCESSES FOR SUGARCANE BAGASSE	151
REFERENCES	153
APPENDIX A1 REACTION DATA FOR BIOETHANOL MODELS	154
APPENDIX A2 REACTION DATA FOR PYROLYSIS MODELS	156
APPENDIX A3 ASPENPLUS® RESULTS FOR BIOETHANOL PROCESS MODELS	158
APPENDIX A4 ASPENPLUS® RESULTS FOR PYROLYSIS PROCESS MODELS	166
APPENDIX A5 HEAT INTEGRATION CALCULATIONS FOR BIOETHANOL, PYROLYSIS AND FISCHER-TROPSCH PROCESS MODELS	170

APPENDIX A6 PROCESS FLOW DIAGRAMS FOR BIOETHANOL AND PYROLYSIS PROCESS MODELS	171
APPENDIX B1 ADDITIONAL DATA FOR EQUILIBRIUM MODELLING OF BAGASSE AND SLURRY GASIFICATION	207
B1.1 Calculation of heat of formation for bagasse and bagasse-derived feedstocks	208
APPENDIX B2 STATISTICAL DATA FOR EQUILIBRIUM GASIFIER MODELLING	214
B-2.1 PARETO CHARTS FOR STANDARDIZED FOR SYNGAS RATIO	214
B-2.2 PARETO CHARTS FOR STANDARDIZED FOR SYNGAS COMPOSITION	215
B-2.3 PARETO CHARTS FOR STANDARDIZED FOR GASIFICATION SYSTEM EFFICIENCY	217
B-2.4 PARETO CHART FOR STANDARDIZED FOR GASIFIER DUTY	218
APPENDIX B3 DETERMINATION OF GASIFIER OPERATING CONDITIONS USING EQUILIBRIUM MODELLING	219
B3.1 H ₂ /CO molar ratio	221
B3.2 Sum of H ₂ and CO molar fractions	221
B3.3 System efficiency	223
B3.4 Combined variable	223
APPENDIX B4 ASPENPLUS® RESULTS FOR FISCHER-TROPSCH PROCESS MODELS	226
APPENDIX B5 PROCESS FLOW DIAGRAMS FOR FISCHER-TROPSCH PROCESS MODELS	232
APPENDIX C1 GENERAL INPUT DATA FOR ECONOMIC MODELS	239
APPENDIX C2 PROCESS EQUIPMENT COST DATA	242
APPENDIX C3 ECONOMIC RESULTS SUMMARY	249

LIST OF FIGURES

Figure 1.1 Mind map for outline of thesis and work flow	5
Figure 2.1 Simplified process steps required for bioethanol production without inclusion of heat integration (McMillan, 1997).	10
Figure 2.2 Main processing units for Fischer Tropsch fuel production from biomass	18
Figure 3.1 Schematic of process flow for bioethanol production.	33
Figure 3.2 Schematic of ethanol recovery process flow in bioethanol process.	38
Figure 3.3 Process flow diagram for pyrolysis process. The dashed lines are only applicable to fast pyrolysis.	42
Figure 3.4(a) Comparison of process steam requirements for bioethanol process: a) Different pretreatment methods for bagasse investigated in this study. b) Dilute acid pretreatment of various feedstocks at different solid levels obtained from this and other studies.	Error! Bookmark not defined.
Figure 3.5 Distribution of total process input energy consumed in the process and captured in oil, char and electricity products for pyrolysis processes.	49
Figure 3.6 Distribution of total process feed energy captured in process steam, electricity and ethanol for bioethanol processes.	50
Figure 3.7 Process energy efficiencies and liquid fuel efficiencies for bioethanol and pyrolysis processes.	51
Figure 3.8 Liquid fuel energy efficiencies at different levels of heat integration for bioethanol using steam explosion and fast pyrolysis processes.	53
Figure 4.1 Representation of different biomass feedstocks on a ternary C-H-O diagram (redrawn from Ptasiński et al, 2007).	62
Figure 4.2 Simplified process flow diagram of Fischer-Tropsch downstream processing.	68
Figure 4.3 Comparison of equilibrium modelling results from this study with prediction modelling and experimental data for bagasse gasification (1 bar, 11% moisture, equivalence ratio=0.18, steam biomass ratio=1.9).	76
Figure 4.4 Effect of temperature on equilibrium gas compositions for bagasse gasification. (1 bar, 5% moisture, equivalence ratio=0.25, steam biomass ratio=0.5).	77
Figure 4.5 Effect of equivalence ratio on equilibrium gas composition for bagasse gasification (1100K, 1 bar, 5% moisture, steam biomass ratio=0.5)	78
Figure 4.6 Effect of pressure on equilibrium gas composition for bagasse gasification (1100K, 5% moisture, equivalence ratio=0.25, steam biomass ratio=0.5).	80
Figure 4.7 Effect of steam biomass ratio on dry equilibrium gas composition for bagasse (1100K, 1bar, 5% moisture, equivalence ratio=0.25).	80
Figure 4.8 Combined effects of steam biomass ratio (wt/wt) and bagasse moisture content (wt%) on predicted (a) equilibrium gas H ₂ /CO ratio (R ² =0.98) and (b) gasification efficiency (R ² =0.99). Temperature=1100K, pressure=1bar, equivalence ratio=0.25.	81
Figure 4.9 Combined effects of steam biomass ratio (wt/wt) and equivalence ratio predicted gasifier duty (R ² =0.88). Temperature=1100K, pressure=1bar, moisture=5%. Positive values indicate a net heat input to the gasifier.	82
Figure 4.10 Combined effects of steam biomass ratio (wt/wt) and fast pyrolysis slurry moisture content (wt%) on predicted gasification efficiency (R ² =0.98).	83

Figure 4.11 Total energy consumption of Fischer-Tropsch processes for different feedstocks and gasifier configurations.	87
Figure 4.12 Process energy efficiencies for Fischer-Tropsch processing scenarios for different feedstocks.	88
Figure 5.1 Typical ranges of end product process energy efficiencies for bioethanol and Fischer-Tropsch processes calculated from process models in literature and this study. The integrated biorefinery includes both bioethanol and Fischer-Tropsch facilities that operate at efficiencies of 50% and 30%, respectively (based on mature technology).	100
Figure 6.1 Map of sugar mills in northern region of South Africa (Garmap Pty Ltd.).	115
Figure 6.2 Effect of feedstock delivery distance on energy costs and feedstock prices of bagasse and pyrolysis slurry.	115
Figure 6.3 Breakdown of capital investment costs for bioethanol scenarios (\$US ₂₀₀₉).	119
Figure 6.4 Breakdown of capital investments for pyrolysis processes (\$US ₂₀₀₉).	120
Figure 6.5 Breakdown of capital investments for Fischer-Tropsch scenarios (\$US ₂₀₀₉).	121
Figure 6.6 Production costs and breakeven oil prices for liquid biofuels from sugarcane bagasse (\$US ₂₀₀₉).	123
Figure 6.7 World crude oil price statistics for the past 12 years (Energy Information Administration, 2009).	124
Figure 6.8 Comparison of liquid fuel production costs as a function of end-product process energy efficiencies from this study and literature data.	125
Figure 6.9 Sensitivity of liquid fuel production costs to total capital investment (% variation from base case), on-site price of feedstock (bagasse and trash) and selling prices of by-products (% variation from base case).	127
Figure 6.10 Effect of electricity price on the return on investment for a 600MW BIG/GCC cogeneration plant. Cost data was obtained from Jin et al, 006.	129
Figure 6.11 Internal rate of return results for best performing process scenarios for production of bioethanol, crude bio-oil and Fischer-Tropsch fuels.	130
Figure 6.12 Sensitivity of internal rate of return for conversion of bagasse to bioethanol with steam explosion, fast pyrolysis oil and Fischer-Tropsch liquids using G1 gasifier mode.	131
Figure 7.1 Sensitivity of internal rate of return for conversion of bagasse to bioethanol with steam explosion, fast pyrolysis oil and Fischer-Tropsch liquids using G1 gasifier mode.	145
Figure B-2.1 Pareto chart of standardised effects on H ₂ /CO ratio of equilibrium gas for bagasse gasification. ANOVA R ² =0.98.	214
Figure B-2.2 Pareto chart of standardised effects on H ₂ /CO ratio of equilibrium gas for fast pyrolysis slurry gasification. ANOVA R ² =0.96.	214
Figure B-2.3 Pareto chart of standardised effects on H ₂ /CO ratio of equilibrium gas for vacuum pyrolysis slurry gasification. ANOVA R ² =0.97.	215
Figure B-2.4 Pareto chart of standardised effects on sum of H ₂ +CO of equilibrium gas for bagasse gasification. ANOVA R ² =0.96.	215
Figure B-2.5 Pareto chart of standardised effects on sum of H ₂ +CO of equilibrium gas for fast pyrolysis slurry gasification. ANOVA R ² =0.97.	216
Figure B-2.6 Pareto chart of standardised effects on sum of H ₂ +CO of equilibrium gas for vacuum pyrolysis slurry gasification. ANOVA R ² =0.97.	216

Figure B-2.7 Pareto chart of standardised effects on system efficiency for bagasse gasification. ANOVA $R^2=0.99$.	217
Figure B-2.8 Pareto chart of standardised effects on system efficiency for fast pyrolysis slurry gasification. ANOVA $R^2=0.98$.	217
Figure B-2.9 Pareto chart of standardised effects on system efficiency for vacuum pyrolysis slurry gasification. ANOVA $R^2=0.98$.	218
Figure B-2.10 Pareto chart of standardised effects on gasifier duty bagasse gasification. ANOVA $R^2=0.88$.	218

LIST OF TABLES

Table 3.1 Process design specifications for bioethanol production using different pretreatment methods	35
Table 3.2 Additional fossil input energy required for bioethanol process using different pretreatment methods.	46
Table 3.3 Process energy requirements for pyrolysis processes as a percentage of total energy input (HHV)	48
Table 4.1 Rectisol unit design parameters	70
Table 4.2 Fischer-Tropsch synthesis reactor fractional conversions	71
Table 4.3 Operating conditions for equilibrium gasification of bagasse-derived feedstocks at 1100K, 1 bar and an equivalence ratio of 0.25.	84
Table 4.4 Input parameters and gas compositions for equilibrium gasifiers used in Fischer-Tropsch process modelling.	85
Table 5.1 Comparison of energy efficiencies for bioethanol, pyrolysis and Fischer-Tropsch processing of sugarcane bagasse.	98
Table 6.1 Cost data for feedstocks, products and utilities (USD ₂₀₀₉)	111
Table 6.2 Operating costs for bioethanol scenarios	116
Table 7.1 Technical and economic performance of the most important process route scenarios for bioethanol, pyrolysis and Fischer-Tropsch processing.	138
Table A1.1 Composition and heating value of sugarcane bagasse supplied by local producer.	154
Table A1.2 Chemical formulas and property data sources for biomass components used in AspenPlus® process models.	154
Table A1.3 Stoichiometric pretreatment reactions and fractional conversion data used for bioethanol process models.	155
Table A1.4 Stoichiometric reactions and conversion data assumed for saccharification and fermentation reactors and conversion data used for bioethanol models.	155
Table A2.1 Fast Pyrolysis reactor calculated product yields	156
Table A2.2 Vacuum Pyrolysis reactor calculated product yields	157
Table A3.1 Summary of unit design assumptions and performance results for bioethanol process models.	159
Table A3.1 (continued) Detailed unit design assumptions and performance results for bioethanol process models.	160
Table A3.1 (continued) Detailed unit design assumptions and performance results for bioethanol process models.	161
Table A3.1 (continued) Detailed unit design assumptions and performance results for bioethanol process models.	162
Table A3.2 Breakdown of process energy demands determined for process models for bioethanol scenarios.	164
Table A3.3 Summary of energy balance obtained from process models for bioethanol scenarios.	165
Table A4.1 Detailed unit design assumptions and performance results for pyrolysis process models.	167
Table A4.1 (continued) Detailed unit design assumptions and performance results for pyrolysis process models.	168

Table A4.2 Summary of energy balance obtained from process models for pyrolysis scenarios.	169
Table A5.1 Calculation of the effect of heat integration on the liquid fuel energy efficiencies of bioethanol production using steam explosion, fast pyrolysis and bagasse gasification using EG1 followed by Fischer-Tropsch synthesis.	170
Table B1.1 Operating conditions for central composite design for gasification runs of each feedstock.	207
Table B1.2 Feedstock compositions, lower heating values and heats of formation used in equilibrium modelling.	209
Table B1.3 Output file from CEA program for equilibrium modelling of bagasse gasification: central composite design run 1	210
Table B3.1 ANOVA R ² values for STATISTICA model	220
Table B3.2 Fitted parameters from desirability profiling for H ₂ /CO molar ratio	222
Table B3.3 Fitted parameters from desirability profiling for the Sum of H ₂ and CO molar fractions	222
Table B3.4 Fitted parameters from desirability profiling for system efficiency	225
Table B3.5 Fitted parameters from desirability profiling for H ₂ /CO ratio, Sum of H ₂ and CO and system efficiency	225
Table B3.6 Model predictions for adjusted conditions for all feedstocks according to practical considerations	225
Table B4.1 Detailed unit design assumptions and performance results for Fischer-Tropsch process models.	227
Table B4.1 (continued) Detailed unit design assumptions and performance results for Fischer-Tropsch process models.	228
Table B4.2 Breakdown of process energy requirements for Fischer-Tropsch processes	231
Table C1.1 General specifications used for economic models in AspenIcarus [®]	239
Table C1.2 Main Investment Analysis parameters for economic models	240
Table C1.3 Basis for bagasse availability and delivery cost calculations.	241
Table C.2.3 Process equipment specifications and equipment model library cost data for pyrolysis processes	246
Table C2.4 Equipment mapping specifications and quoted cost data for Fischer-Tropsch scenarios	247
Table C2.5 Equipment model library cost data for Fischer-Tropsch scenarios	248
Table C3.1 Summary of economic results for selected scenarios of bioethanol, pyrolysis and Fischer-Tropsch process routes.	249
Table C3.2 Breakdown of total capital investment for bioethanol process scenarios	250
Table C3.3 Breakdown of total capital investment for pyrolysis process scenarios	250
Table C3.4 Breakdown of total capital investment for Fischer-Tropsch process scenarios	251
Table C3.5 Summary of economic indicators for bioethanol steam explosion scenarios	252
Table C3.6 Summary of economic indicators for vacuum pyrolysis scenarios.	253
Table C3.7 Summary of economic indicators for fast pyrolysis scenarios	254
Table C3.8 Summary of economic indicators for Fischer-Tropsch (EG1) bagasse scenarios	255
Table C3.9 Summary of economic indicators for Fischer-Tropsch (EG1) with shift and (EG2) bagasse scenarios	256

1. INTRODUCTION

The ever-increasing global energy demand and inevitable depletion of fossil fuel resources has led to increasing interest in renewable energy in recent years. Moreover, the environmental effects of global warming are undeniable and the production and use of fossil derived transport fuels has contributed 15% of the total man-made CO₂ since preindustrial times (Fuglestvedt et al, 2008). This has led to an initiative from over 160 countries who first signed the Kyoto protocol in Japan in 1997, committing themselves to actively combat greenhouse gas emissions by signing mandatory targets, of which South Africa is a voluntary signatory. Therefore, the White Paper on Renewable Energy 2003 is committed to deliver a 10 000 GWh renewable energy contribution to the current energy infrastructure by 2013. Based on this, the South African Biofuels draft strategy is aiming for a 4.5% market penetration of biofuels into the existing fuel market, which will be equal to 75% of the renewable energy target (Department of Minerals and Energy, 2006).

In view of this, the biorefinery concept has become a major consideration. Biomass is the most abundant renewable carbon-based fuel on earth, and the use of low cost lignocellulosic biomass to produce liquid fuels, valuable chemicals and to generate power, presents many potential economic, social and environmental benefits. In a South African context, food security is naturally a concern, since the use of primary agricultural feedstocks in Brazil and the United States for bioethanol production has often received criticism due to the negative impact on food supply (Grunwald, 2008). However, the South African government has established that one third of the currently unutilised high potential land in South Africa is sufficient to supply enough biomass from dedicated and energy crops, with an insignificant effect on food prices. In turn, the development of such an industry will create jobs and reduce unemployment by 1.3%, while achieving South Africa's clean energy targets (Department of Minerals and Energy, 2006).

A key issue is to obtain a low-cost, readily available feedstock. Agricultural residues contain between 55 and 75% total carbohydrate, (McMillan, 1997) offering a feedstock with a high fuel producing potential. South Africa has well developed agricultural industries and the maize and sugar industry are the largest producers of residues. The sugar industry has been exploring possible processing options to add value to sugarcane bagasse. Bagasse is the fibrous residue produced after sugar is extracted from the cane, and has a higher heating value of 19.25 MJ/kg (Mbohwa and Fukuda, 2003). As a feedstock, it bears no cost for growing, harvesting or preliminary physical processing, making it ideal for a biorefinery. For each kilogram of sugar, 1.25 kg bagasse is formed (Botha and Von Blottnitz, 2006). The South African sugar industry currently produces about 8 million tonnes of bagasse per year (www.data.un.org). Normally, most of the bagasse is burned in inefficient boilers to supply the energy needs of the mill. However, recent improvements in boiler technology has led to a significant amount of surplus bagasse becoming available, and approximately 50% of the bagasse is sufficient to supply the energy needs for sugar mills using modern boilers and cogeneration systems (Botha and Von Blottnitz, 2006). As a result, many sugar mills have replaced their conventional low-pressure boilers and back-pressure turbines with more efficient high temperature and pressure boilers coupled with condensing/extraction steam turbines (CEST) (Mbohwa and Fukuda, 2003).

The surplus bagasse is then available to produce by-products, which could include electricity, biofuels, or industrial chemicals. Finding the most economical combination of products would require careful consideration of several factors, such as technological advances, market-related issues, infrastructure, social policies and government strategies. Probably the most important advantage that a biorefinery would offer the sugar industry is the degree of flexibility with respect to product range from utilisation of the same primary feedstock for multiple products, providing a buffer during market fluctuations that often affect this industry.

Since the South African government has earmarked biofuels as the major contributor to its 2013 renewable energy target, the production of liquid biofuels is being incentivised

by offering biofuels producers a fuel levy exemption that is currently charged on conventional transport fuels. There are various processing options available for the production of liquid biofuels from lignocellulosic materials, including biological and thermochemical routes. Currently, the preferred biological processing route for lignocellulose is enzymatic hydrolysis followed by fermentation, either by separate or simultaneous hydrolysis and fermentation. For thermochemical process routes, pyrolysis and gasification with downstream Fischer-Tropsch synthesis are being developed. The question is which process route will lead to the maximum energy efficiency and profitability, based on the technology that is currently available.

1.1 PROJECT MOTIVATION AND OUTLINE OF THESIS

A detailed techno-economic study for cellulosic biofuels in South Africa has never been done, especially for comparison of biological and thermochemical processing based on near-term available technologies. This study aims to compare the technologies of the different process routes, which can be applied to any location, but then continues to compare the economic feasibility of each process route, which is specifically applicable to South African market conditions and investment parameters. Although it is necessary to consider future development possibilities, the best or preferred technology to be pursued will ultimately depend on factors that are specific to the socio-political, technological and resource challenges of this country. In addition, the question of whether the current state of the art biofuel technologies can compete with the conventional petroleum-based fuel industry needs to be addressed.

The main purpose of this study as outlined in Figure 1.1 was therefore to

- develop **process models** in AspenPlus® for the biological and thermochemical process routes currently available to produce liquid biofuels from sugarcane bagasse for either the transport or industrial fuel market, **using data either measured or modelled for bagasse** and including heat integration, based on

- currently available technology** and designs for energy self-sufficient processes. The selected processes include
- Transport quality *bioethanol* production via biological fermentation coupled with utilisation of the solid residues for cogeneration. The three pretreatment methods considered were dilute acid pretreatment, steam explosion and liquid hot water pretreatment, and the **minimum required solid concentration** during dilute acid pretreatment for a self-sustainable process is determined (**Chapter 3**).
 - *Pyrolysis* to produce crude bio-oil suitable for an industrial fuel and char as a by-product. The two pyrolysis modes considered were fast and vacuum pyrolysis (**Chapter 3**).
 - Equilibrium modelling to *optimise gasification* of sugarcane bagasse, as well as pyrolysis slurries, followed by *Fischer-Tropsch synthesis*. Several process configurations were evaluated including different gasification optimisation approaches and inclusion of a shift reactor, and equilibrium modelling optimisation results were validated using experimental results for bagasse (**Chapter 4**).
- *Comparison of the technical performance* of the three processing routes based on the process modelling results (**Chapter 5**). **Biological and thermochemical process routes** were **compared** on an equivalent basis for processing of sugarcane bagasse to produce liquid biofuels. In addition, the results were compared with literature to assess the possible scope for improvements in technical performance.
- Develop **economic models** for the most promising process scenarios for bioethanol production, pyrolysis and Fischer-Tropsch synthesis and compare the production costs and investment opportunities (**Chapter 6**). The economic models developed in AspenIcarus[®] were specifically relevant to the **South African sugar industry**.

- Recommend the best current technologies based on an internal rate of return above 12% and a return on investment of at least 30%, which is considered to be the minimum for investment in new technologies, and suggest future work needed for commercialisation.

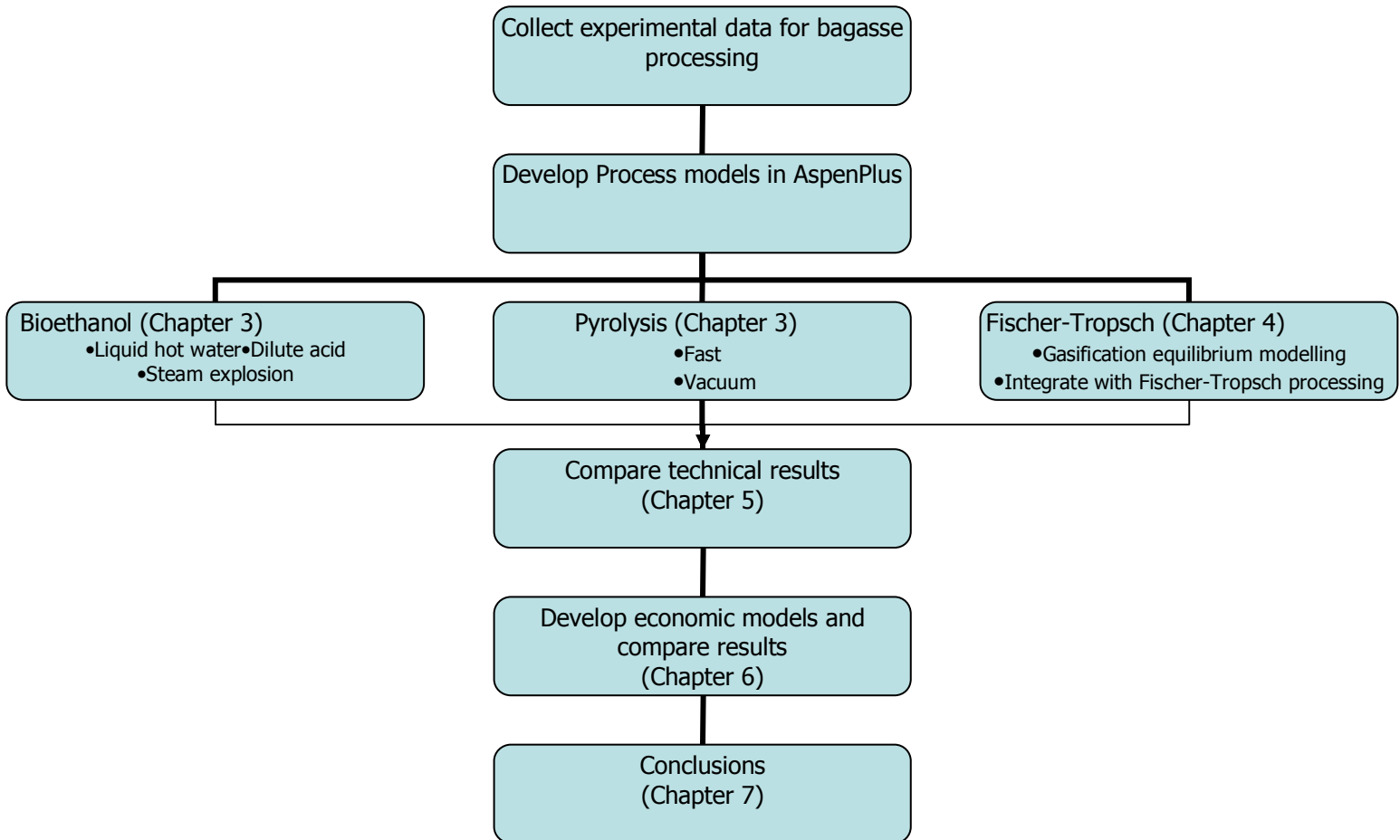


Figure 1.1 Outline of thesis and work flow

At this stage, it is important to note that the relevant minimum scales of the three process routes studied here are not necessarily similar. While there would be sufficient feedstock available at a typical South African sugar mill to feed a small bioethanol or pyrolysis facility, a Fischer-Tropsch process would only be economic at much larger scales and would require a consortium of sugar mills to co-feed to a central facility. More than likely, this would also not be mills from the same sugar company, and may therefore be considered as a more advanced scenario. Furthermore, both bioethanol

production and pyrolysis are process routes that have been considered for bagasse in the past in other countries (Alonso et al, 2006, Rocha et al, 2002, Kadar et al, 2004, Gnansounou et al, 2005). For the sugar industry, these two routes therefore pose less risk in terms of novelty, as well as required capital investment, since Fischer-Tropsch plants are known to require significantly higher capital investments (Wright and Brown, 2007). Therefore, in view of the difference in the level of application of these process routes, bioethanol and pyrolysis is discussed in Chapter 3, while the more advanced, larger scale option for Fischer-Tropsch synthesis is discussed in Chapter 4.

REFERENCES

Botha, T. and H. v. Blottnitz (2006). "A comparison of the environmental benefits of bagasse-derived electricity and fuel ethanol on a life-cycle basis." *Energy Policy* 34: 2654–2661.

Department of Minerals and Energy (2006). "Draft Biofuels Industrial Strategy of the Republic of South Africa." Official report.

Fuglestvedt, J., T. Berntsen, G. Myhre, K. Rypdal and R. B. Skeie (2008). "Climate forcing from the transport sectors." *Proceedings of the National Academy of Sciences of the United States of America* 105(2): 454-458.

Grunwald, M. (2008). The clean energy scam. *Time magazine*, 28 March.

Mbohwa, C. and S. Fukuda (2003). "Electricity from bagasse in Zimbabwe." *Biomass and Bioenergy* 25: 197-207.

McMillan, J. D. (1997). "Bioethanol production: status and prospects." *Renewable Energy* 10(213): 295-302.

www.data.un.org. 20 October 2009.

2. LITERATURE BACKGROUND

The literature available in the field of biofuels in general is vast and many reviews have been published to describe the different process options. The aim of this chapter is to provide the reader with a brief overview of the most important theory and state of the art technology, and reference is made to other, more detailed reviews applicable to each process route where necessary.

2.1 BIOLOGICAL PROCESSING

Bioethanol is the main biofuel product currently being considered for biological processing of lignocellulose. Although biobutanol is a superior fuel, since it has a higher energy density that is close to that of gasoline, lower volatility and better blending potential with gasoline (Ramey, 2007), certain technical difficulties are still being addressed to make it economically feasible. Anhydrous (99.5%) bioethanol can be used as a replacement transport fuel or an additive and oxygen enhancer for petrol. Bioethanol is produced via biological fermentation of the fermentable sugars obtained from carbohydrates, i.e. monosaccharides that can be utilised by ethanogenic micro organisms to produce ethanol.

Bagasse is a lignocellulosic material and the polysaccharides have to be hydrolysed to form monosaccharides before bioconversion can take place. Lignocellulose is made up of three main components, namely cellulose, hemicellulose and lignin, with a small amount of ash. Sugarcane bagasse typically contains approximately 40% cellulose, 22% hemicellulose, 25% lignin, 3-4% ash and the balance consists of extractives and uronic acids. (Kadam, 2002). The key challenge associated with lignocellulosic bioconversion is overcoming its recalcitrant nature. Cellulose is insoluble in water and forms the skeletal structure of the biomass, while hemicellulose, which is soluble in dilute alkali, is bonded to the cellulose fibers to strengthen the plant. Lignin is a mononuclear aromatic polymer that is often also bound to cellulose fibers, forming a so-called lignocellulosic complex. Together, these form a crystalline structure, preventing hydrolytic agents from accessing the cellulose and making the material resistant to microbial conversion (Mosier et al,

2005). Therefore, prior to fermentation, pretreatment is required to render the biomass accessible for hydrolysis via enzymatic or acid attack. Figure 1.1 gives a general overview of bioethanol production via lignocellulose fermentation.

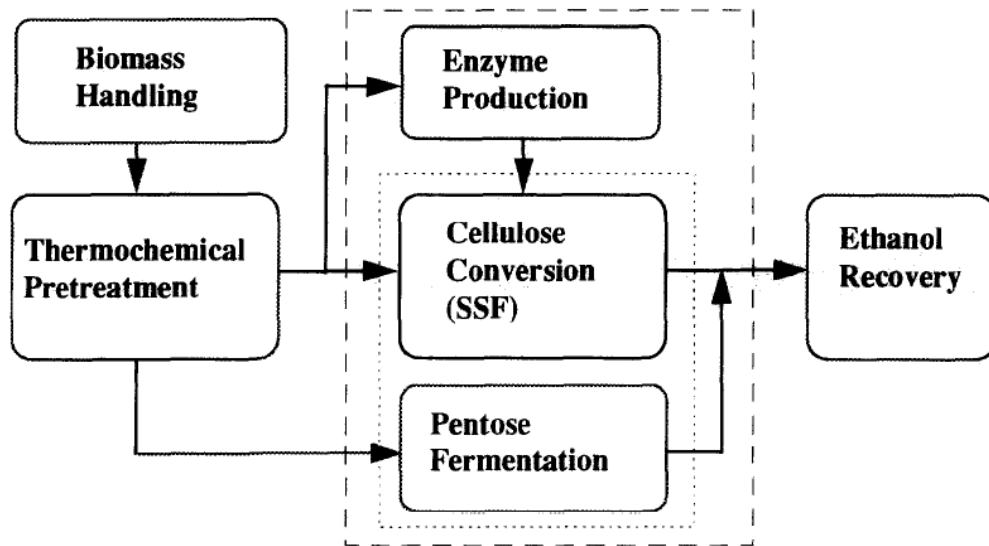


Figure 2.1 Simplified process steps required for bioethanol production without inclusion of heat integration (McMillan, 1997).

2.1.1 Biomass Preparation and Pretreatment

Biomass handling may include harvesting, transport and size reduction. The purpose of pretreatment is to increase the porosity and digestibility of the cellulose fibers and preserve any pentose released from hemicellulose solubilisation while limiting inhibitors, as well as energy requirements and cost. (Mosier et al, 2005). The formation of inhibitors such as acetic acid, furfural and phenolics often requires detoxification after pretreatment, which increases costs. Several methods, such as overliming, enzymatic detoxification and the use of activated carbon or ion exchange resins has also been discussed previously (Chandel et al, 2006).

Pre-treatment is currently a major cost factor for bioethanol production (Mosier et al, 2005). Milling is a form of physical pre-treatment that is often required to reduce the particle size for downstream processing. Wet, dry, vibratory ball or compression milling may be used, depending on the biomass. A wide variety of chemical pre-treatment methods have been explored and a detailed review can be found in Mosier et al, 2005. Based on the extent of previous research on bagasse, available data and economic considerations, three pretreatment technologies have been considered in this study. Two of these are hydrothermal, i.e. steam explosion with sulphuric acid catalyst and liquid hot water pretreatment, and one chemical, i.e. dilute acid pretreatment with sulphuric acid.

Hydrothermal methods have the benefit of not requiring chemicals or expensive disposal costs (Martín et al, 2005). Also, costs of neutralisation and conditioning after pre-treatment are eliminated since no acid is used, and the need for size reduction is greatly reduced or even eliminated as the particles break when cooked in water. This makes hydrothermal pretreatment attractive from an economical and environmental point of view. Laser et al, 2005 compared the results of steam- and liquid hot water pre-treatment on sugarcane bagasse and found that the results were highly affected by the different solids content of the two processes. After pre-treatment, simultaneous saccharification and fermentation was performed using *Trichoderma reesei* cellulase in combination with β -glucosidase and *Saccharomyces cerevisiae* as the fermenting organism. Liquid hot water pretreatment achieved a higher SSF conversion compared to steam explosion, the maximum being over 90% based on theoretical ethanol yield at 220°C for 2 minutes and solid concentrations below 5%, although above 5%, the yields dropped dramatically. Significant inhibition of the fermentation rate was observed and complications with pentosan preservation suggested that autohydrolysis was the cause. Autohydrolysis is the process by which acetic acid and other organic acids are released from hemicellulose, leading to decreased pentosan recoveries. This effect was more pronounced at high solids concentrations, and is also known to be dependent on reactor configuration (Mosier et al, 2005). With further improvements in reactor design, the potential for high yields of liquid hot water pre-treatment may therefore be realised.

Despite the lower xylan conversion of steam explosion, it has a major advantage in that high solid concentrations can be achieved, leading to lower energy requirements for downstream processing. Martin et al, 2002 achieved a xylan conversion of 71% using sulphuric acid-catalysed steam explosion of sugarcane bagasse, although fermentability was limited by a significant amount of inhibitors in the hydrolysate. However, in 2006, the same group succeeded in developing a genetically-engineered strain of xylose-utilising *Saccharomyces cerevisiae* through adaptation by cultivating it in a medium with high concentrations of inhibitors. This adapted strain was able to convert more than twice the amount of xylose to ethanol compared to the parent strain, resulting in an increase in total ethanol yield from 0.18 g/g to 0.38 g/g total sugars (Martin et al, 2006).

The most widely used dilute acid pre-treatments are based on sulphuric acid, although equipment corrosion increases capital costs and neutralisation is required prior to fermentation. Pre-grinding of the feedstock is necessary to reduce the size to 1 mm, which can account for up to 33% of process power requirements (Mosier et al, 2005). Nevertheless, dilute acid pretreatment currently achieves the highest conversions and the technology is well developed (Hamelinck et al, 2005). Aquilar et al, 2002 succeeded in hydrolysing 90% of the hemicellulose in sugarcane bagasse by treating it in 2% sulphuric acid at 122°C for 24 minutes.

2.1.2 Hydrolysis and Fermentation

After pretreatment, the cellulose is hydrolyzed, followed by biological fermentation of the pentose and hexose sugars. Although acid hydrolysis has been studied for many years and is well understood, enzymatic hydrolysis is now widely accepted as the most promising option to achieve high sugar yields with low environmental impacts (Gnansounou et al, 2005, Knauf and Moniruzzaman, 2004).

One of the most significant breakthroughs in bioethanol production from lignocellulose has been the development of simultaneous saccharification and fermentation (SSF) technology. During SSF, enzymatic cellulose hydrolysis is combined with hexose

fermentation in one vessel, thereby reducing the end-product inhibition effect of glucose on the cellulase enzyme and increasing ethanol yields, as well as decreasing capital investment costs (Lynd et al, 1999).

In its native form, *Saccharomyces cerevisiae* is only capable of fermenting hexose sugars (glucose, galactose, and mannose). On the other hand, pentoses (xylose and arabinose), can only be fermented by a few native strains and usually at low yields (McMillan et al, 1997). Further advances in microbiology have however led to novel micro-organisms that can ferment both sugars in the same tank at high yields (Martín et al, 2002). This process is called simultaneous saccharification with co-fermentation (*SSCF*), thereby reducing the capital investment costs even further. The production of lignocellulosic enzymes is also a subject receiving attention, as it plays a major role in the process economics. Currently, scientists are working on the next breakthrough to engineer an organism that can effectively ferment both hexose and pentose sugars whilst also producing cellulase enzymes, thus enabling the entire process of hydrolysis and fermentation to take place in one tank (Lynd et al, 1999). This is called Consolidated Bioprocessing (CBP). After fermentation, the ethanol product is recovered and purified, while the solid lignin residue is used to fuel a cogeneration plant to produce steam and electricity (McMillan et al, 1997).

Several lignocellulosic biorefineries are being developed. The SEKAB pilot facility in Sweden is primarily based on cellulose from softwood and produces 400-500 l ethanol from 2 tons of dry saw dust (www.biomatnet.org). Iogen also owns a demonstration plant capable of producing 1 million gallons bioethanol per year in Canada. In 2008, Abengoa Bioenergy started commissioning the world's first commercial biomass ethanol plant in Spain. The plant produces over 5 million litres of fuel grade ethanol per year from agricultural residues such as wheat straw (www.abengoabioenergy.es).

2.2 THERMOCHEMICAL PROCESSING

Liquid fuels can be produced from biomass via two thermal processing routes, namely pyrolysis or gasification. Pyrolysis produces a bio-oil product that can be upgraded to transport fuel quality or sold as a lower grade fuel oil. Gasification produces a gas that is rich in hydrogen and carbon monoxide and can be used to synthesise various fuels. For this study, Fischer-Tropsch synthesis was considered, since it is already being produced in South Africa from natural gas and coal and currently supplies 35% of the local fuel market (Department of Minerals and Energy, 2006).

2.2.1 Pyrolysis

Pyrolysis is a thermochemical process that occurs in an inert atmosphere, producing a mixture of condensable and non-condensable gases and a solid product called char. There are different modes of pyrolysis, including fast and vacuum pyrolysis. The keys to maximising the liquid yield are high heating rates, a moderate reaction temperature of around 500°C, short vapour residence times (less than 2 s) and rapid cooling of the vapours to prevent secondary cracking, which is undesirable as it reduces yield and alters the properties of the oil. Liquid yields of up to 80% (wet basis) can be achieved with fast pyrolysis. For detailed overviews of pyrolysis processes, the reader is referred to Bridgwater et al, 1999 and Hendriks and Zeeman, 2009.

Fast pyrolysis is designed to maximise the liquid product yield and is normally operated at around 500°C. After pyrolysis, the vapours are subjected to rapid quenching and the bio-oil fraction is recovered. Fluidised beds are normally used, where a carrier gas acts as a heat source for the biomass particles. High quantities of carrier gas are needed to ensure that all the particles are fluidised, although the gas is usually recycled. Piskorz et al, 1998, obtained liquid yields of 60% on an energy basis from fast pyrolysis of sugarcane bagasse.

With vacuum pyrolysis, slow heating rates are applied at around 300°C under vacuum. The solid residence times are higher, although the rapid and continuous removal of the vapours essentially simulates a fast pyrolysis process. Higher char product yields compared to fast pyrolysis are obtained at the cost of lower liquid yields, resulting in energy yields of 40% and 28% in bio-oil and char for bagasse, respectively, based on results from Stellenbosch University. Although there is no need for a carrier gas, the vacuum equipment is costly.

The bio-oil product is a brown liquid that generally has a heating value half that of conventional fuel oil (Bridgwater et al, 1999). At present, one of the main obstacles for the commercial acceptability of bio-oils is the physico-chemical instability of the oil and consequently poor storage capabilities (Pindoria et al, 1999, Das et al, 2004). Ash components in the char fines are carried over with the vapour product and act as a vapour cracking catalyst, which leads to polymerization and increases the viscosity of the oil product. De-ashing by pretreatment in water or mild acid prior to pyrolysis has proved effective in alleviating this (Das et al, 2004).

Another factor complicating the sale of bio-oil is the current lack of a reliable framework for rating the quality of the oil, as bio-oil has no universally accepted standard. Currently, further processing routes for bio-oil include combustion applications in turbines, engines or boilers or extraction of high-value chemicals. Although the technology for bio-oil upgrading to high-quality transport fuel products is feasible, further developments are needed for the process to be economical (Bridgwater, 2003, Huber et al, 2006, Zhang et al, 2007). One of the most attractive aspects of pyrolysis is the ability to store high-energy fuels in liquid or solid form to be transported and sold. One company that has been a leader in the development of fast pyrolysis technology is Dynamotive Energy Systems Corporation, who currently produces bio-oil and biochar at a 200 ton per day fast pyrolysis plant in Guelph, Ontario (www.dynamotive.com).

2.2.2 Gasification for Fischer-Tropsch Synthesis

Gasification is a high temperature process that occurs above 800°C. The mechanism involves three stages, the first being sequential drying of the biomass to release moisture, followed by pyrolysis to produce gas, oil and char, and finally partial oxidation (gasification) of the pyrolysis products to produce gases such as CO₂, CO, H₂ and other hydrocarbon gases. The last step is rate controlling, and some of the aerosols polymerise to form tar, which is known to cause deposition and corrosion in process equipment (Bridgwater, 2003).

Tar formation is one of the main challenges still faced in gasification technology and as such has become a widely researched subject. Tar formation can be minimised by operating closer to equilibrium conditions by increasing the temperature, equivalence ratio (ratio of amount of oxygen fed to the gasifier to amount of oxygen required for full combustion) or residence time. Gasifier modifications, such as two-stage gasification and secondary air injection, have also been shown to reduce tar formation (Devi et al, 2003). For example, De Filippis et al, 2004, succeeded in producing a tar free gas by two-stage gasification of sugarcane bagasse in the presence of a nickel catalyst. Hot gas cleaning of the producer gas for tar removal include catalytic cracking using dolomite or nickel, thermal cracking by partial oxidation or direct contact and mechanical removal with the use of cyclones, filters or scrubbers (Bridgwater, 2003, Devi et al, 2003). However, hot gas cleaning has not been commercialised yet and wet gas cleaning is currently used (Tijmensen et al, 2002).

Slagging is another phenomenon that occurs when gasification temperatures are higher than the ash melting temperature, and this can be problematic for materials with high ash contents of above 5%, especially if the ash is high in alkali oxides and salts, which lower the ash melting temperature (McKendry, 2002). Slagging entrained flow gasifiers may be used to handle slagging mixtures that are gasified at high temperatures (generally above 1200°C) (Boerrigter and Rauch, 2006). Additives may also be used to

raise ash fusion temperatures and avoid operational problems associated with slagging (Larson et al, 2006).

Apart from tar formation, gasification technology is relatively advanced and high hot gas efficiencies of 95-97% can be obtained (Bridgwater, 2003). Several commercial biomass gasification systems have been successfully demonstrated at large-scale and pilot operations and experience has shown that circulating fluidised bed gasifiers perform best in large-scale applications, while down-draft gasifiers are preferred for small-scale purposes. For downstream Fischer-Tropsch synthesis, high hydrogen yields are required, necessitating the use of steam as a co-gasifying agent, which reduces the overall efficiency to 70-80%. Either air or pure oxygen may be used for gasification; however, for downstream synthesis pure oxygen is preferred since air gasification leads to high amounts of inert nitrogen being present in the downstream process, which increases the size and cost of equipment. The main processing steps for Fischer-Tropsch synthesis are shown in Figure 2. 2.

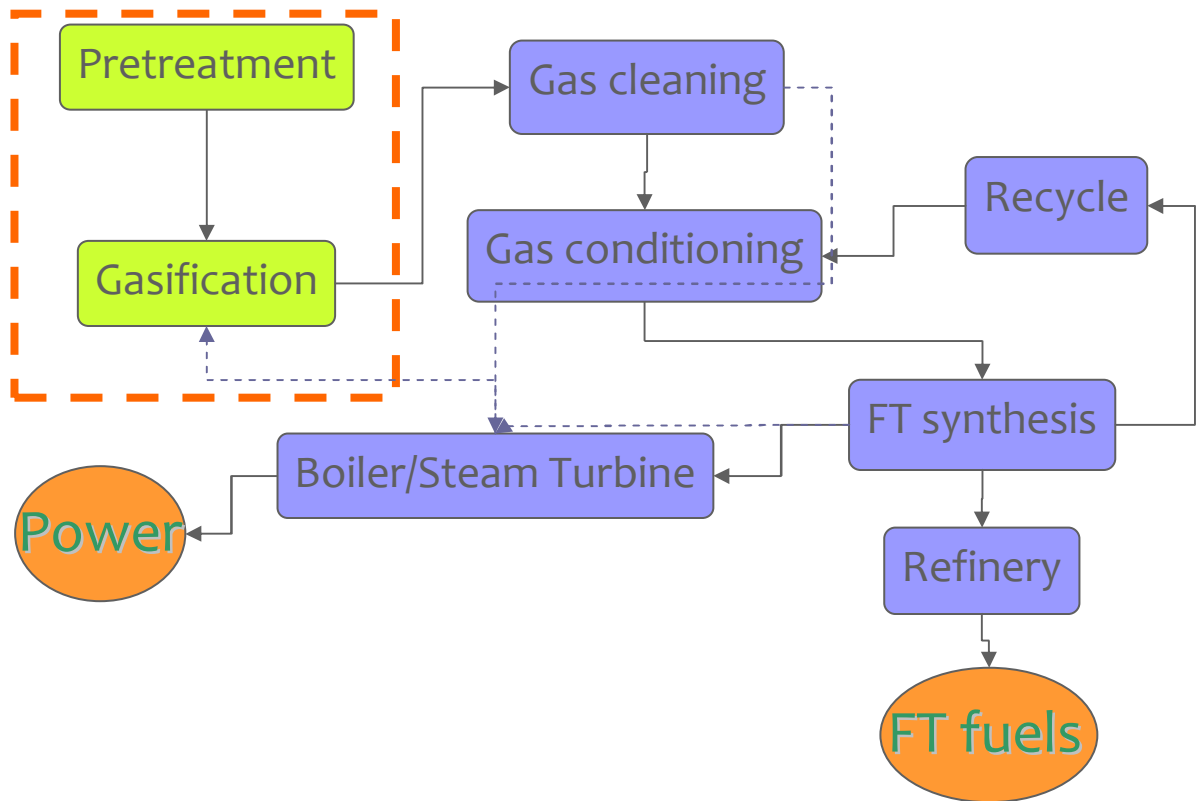


Figure 2.2 Main processing units for Fischer Tropsch fuel production from biomass

Pretreatment entails size reduction and drying, usually below 10% moisture. After gasification, the gas is cleaned to remove any tar and impurities. Conditioning is an optional step to adjust the gas mixture composition in order to maximise Fischer-Tropsch liquid recovery. Depending on the concentration of methane in the syngas, steam reforming may be employed. CO₂ removal is usually required if the off-gas from the synthesis reactor is recycled; however, for small scale applications, this is not economical (Hamelinck et al, 2003). CO₂ removal is normally performed in a Rectisol unit. If CO₂ removal is omitted, the synthesis reactor is run in a 'once-through' mode to prevent CO₂ build-up. This leads to lower FT liquid yields, but produces more electricity that can be exported as a by-product (Tijmensen et al, 2002). For more detailed reviews on gasification and Fischer-Tropsch technology, the reader may refer to Van Der Drift, 2002 and Boerrigter et al, 2002.

Depending on the gasifier and catalyst used, it may be necessary to adjust the H₂/CO ratio for maximum product recovery using the water-gas-shift reactor. The optimum H₂/CO ratio for Fischer-Tropsch synthesis is around 2.1:1 (Tijmensen et al, 2002). Normally, the use of an iron-based catalyst precludes the need for a water-gas shift, as this reaction occurs automatically in the presence of iron catalysts. Cobalt-based catalysts do not have this feature and the gas mixtures formed normally require adjustment, although these catalysts exhibit higher activities and are generally more selective.

During synthesis, hydrogen and carbon monoxide are reacted to form a mixture of hydrocarbon products. The product distribution is governed by polymerisation reaction kinetics, and is often expressed in terms of the chain growth factor, α . Depending on α , a mixture of lighter hydrocarbons ($< C_5$), gasoline components (C_5 - C_{10}), diesel (C_{10} - C_{20}) and wax ($>C_{20}$) is produced. According to Perry and Green, 1997, the maximum theoretical product concentrations for gasoline and diesel are 50 and 25%, respectively.

After synthesis, the liquid product is refined to transport diesel and petrol and the off-gas is used to fire a gas turbine, steam turbine or boiler for electricity and heat production, that is used to supply the energy needs of the plant, thereby increasing the overall process energy efficiency. Developments in thermochemical gasification for Fischer-Tropsch processing of the syngas are currently close to commercialisation. Choren has successfully demonstrated wood gasification to produce Fischer-Tropsch diesel at a 45MW input facility, and the full-scale commercial plant is set to start operation in 2012 (Van der Drift, 2002). FZK has is also developing a process for the gasification of fast pyrolysis slurry that will be obtained from 100MW pyrolysis plants fed with straw and wood waste to produce Fischer-Tropsch fuels (Van der Drift, 2002).

2.3 PROCESS MODELLING

Although experimental data for processing of sugarcane bagasse via biological or thermochemical means is available in literature, process modelling of biofuels production

from lignocellulose has mostly focused on other feedstocks such as corn stover, switchgrass and soft woods including poplar, willow and aspen (Aden et al, 2002, Hamelinck et al, 2003, Hamelinck et al, 2005, Ringer et al, 2006, Tijmensen et al, 2002), and optimisation of the gasification sections coupled with downstream processing integration has not been studied in the past. Cardona and Sánchez, 2007 developed AspenPlus® process models for ethanol production from sugarcane bagasse, but used data for wood chips. Also, the model did not include boiler and steam turbine sections, which limits the potential for heat integration.

Botha and Von Blottnitz, 2005 performed some groundwork on the environmental impacts of bioethanol from sugarcane bagasse in the South African context but did not consider the economics, and more importantly, their work did not include detailed process and economic modelling. In addition, they only considered biological processing and did not perform comparisons with alternative process routes. Gnansounou et al, 2005 compared the economics of four different processing options for a sweet sorghum factory in China. Sweet sorghum is similar to sugarcane, although the apparent purity is much inferior to that of sugarcane, and therefore the production of white sugar from sorghum is less economically favourable than sugar juice or molasses. In general, it was concluded that ethanol production is favourable above an ethanol price of \$0.46/ℓ.

Aden et al, 2002 developed detailed process and economic models for bioethanol from corn stover. They worked closely with engineering firms to review the process design and provide quoted costs for key equipment, and also obtained likely delivered enzyme costs from Genencor International and Novozyme Biotech. The specific capital investment for a 440MW plant converting 48.7% of the feedstock energy to ethanol and 4.5% to electricity was estimated to be \$1700/kW ethanol, resulting in a minimum ethanol selling price of \$282/m³ ethanol. Hamelinck et al, 2005, reported an ethanol efficiency of 35% and a capital investment of \$2100/kW ethanol for a 400MW plant. Taking electricity production into account, they calculated a total process efficiency of 38%.

The energy efficiency of a process can be expressed in many different forms. The most widely used definition for the total process efficiency is the sum of the thermal energy in liquid and solid fuel products and the electric energy in saleable electricity, which is generally referred to as the overall process energy efficiency. However, many would argue that, because the quality of energy contained in electricity and fuels are different, they cannot be compared directly. To address these differences, three definitions of energy efficiency are reported in this study by considering 1) only the liquid fuel as a product, 2) the liquid fuel plus all the thermal energy in by-products or intermediate products and 3) the liquid fuel and all the final products in the form of electricity and/or char.

The definition for the energy efficiency based on the **liquid fuel product only** was taken from Hamelinck et al, 2005, and effectively adjusts the basis feed energy by subtracting the portion of the feed energy that reports to by-products (in thermal units), as shown in Equation 1.1. The electric energy is converted to thermal energy by assuming that the electricity product could be directly produced from biomass at an electric conversion efficiency (η_{elec}) of 45%, based on a BIG/CC system (Hamelinck et al, 2005). The result therefore reflects the efficiency of the particular process to produce liquid fuels from the portion of the feed energy that is converted to liquid fuel energy, ignoring the contribution of by-products to the overall process energy efficiency.

The second energy efficiency is based on the energy converted to **liquid fuels plus thermal energy in intermediate or by-products**, as defined in Equation 1.2. This efficiency therefore enables all the different processes to be compared on a thermal energy basis before electricity generation, by adding the thermal energy in the liquid fuel product to the thermal energy in the lignin residue, gas or char.

Finally, the overall process energy efficiency is calculated by adding the energy in the **liquid fuel plus all final by-products**, including the thermal energy in the liquid fuel and char, and the electric energy in the electricity by-product (see Equation 1.3).

Liquid fuel energy efficiency:

$$\eta_{liquid\ fuel} = \frac{E_{th}fuel}{E_{th}biomass - E_{th}byproduct - \left(\frac{E_{elec}power}{\eta_{elec}} \right)} \quad [\text{Eq. 1.1}]$$

Liquid fuel plus thermal energy (intermediate and/or by-products) energy efficiency:

$$\eta_{thermal} = \frac{E_{th}fuel + E_{thermal}byproducts\ or\ intermediate\ products}{E_{th}biomass + E_{th}fossil} \quad [\text{Eq. 1.2}]$$

Liquid fuel plus final by-products energy efficiency:

$$\eta_{end\ product} = \frac{E_{th}fuel + E_{th}byproduct + E_{elec}power}{E_{th}biomass + E_{th}fossil} \quad [\text{Eq. 1.3}]$$

where E_{th} = thermal energy [MW] in liquid fuel, biomass, by-product (in this case char) or fossil fuel supplement (if required), E_{elec} =electric energy [MW_{elec}] in generated export power.

Bagasse is not the only agricultural residue available to the sugar industry. Alonso et al, 2006, investigated the production of bio-oil from cane trash, also called SCAR (sugarcane agricultural residue), during the off-season. Cane trash consists of the sugarcane leaf and cane tops and has an energy value and harvesting yield similar to that of bagasse. The minimum selling price for the bio-oil was estimated at \$100/ton

(\$6.67/GJ), while Ringer et al, 2007 estimated a minimum bio-oil selling price of \$7.62/GJ.

For Fischer-Tropsch fuels, a number of process models have been developed. Kreutz et al, 2008 compared Fischer-Tropsch synthesis from coal, biomass (switchgrass or mixed prairie grass) or various combinations of the two. For coal, an entrained flow integral quench gasifier was used, while a pressurized oxygen-fired bubbling fluidised bed gasifier was used for biomass using data from Gas Technology Institute's pilot plant. The efficiency for Fischer Tropsch liquids from biomass was around 45%, translating into a 50% (HHV) end-product process efficiency taking electricity into account. This group extended their work to evaluate future scenarios for the production of Fischer-Tropsch fuels, dimethyl ether or hydrogen from switchgrass (Larson et al, 2009). Different configurations were studied, and it was found that Fischer-Tropsch fuels and dimethyl ether can be produced at similar process energy efficiencies and production costs, while hydrogen could be more energy efficient and cheaper to produce, although this is not taking the cost and logistics of fuel distribution into account. A project funded by the Energy Centre of the Netherlands and Copernicus Institute at Utrecht University has also produced Fischer Tropsch models for willow wood (Hamelinck et al, 2003, Tjmensen et al, 2002). Here, data from various gasifiers were used, and different oxidative media and pressures were investigated. The best performing systems resulted in an end-product process energy efficiency of 40 to 45% (HHV).

Various studies have compared different process routes for biofuels from lignocellulose, although most have either been reviews and not dedicated process modelling applicable to a specific feedstock, or based on mature technology, and all have been applicable to either the United States or Europe. Wright and Brown, 2007 reviewed a selection of biological and thermochemical routes to compare the economics of cellulosic ethanol to thermochemical production of methanol, hydrogen or Fischer-Tropsch fuels. No clear cost differences between these technologies were observed, although hydrogen production via gasification achieved the highest fuel energy efficiency of 50%. Pyrolysis was however not considered, but more importantly, the data was obtained from

different sources, that used different assumptions of cost data, conversion efficiencies applicable to different feedstocks, biomass prices and availability, product selling prices, technology maturation etc.

Laser et al, 2009(a) developed process models to compare current state of the art dilute acid pretreatment of corn stover to produce bioethanol with mature technologies utilising ammonia fibre explosion and reported on the effect that future developments would have on production costs and energy efficiencies. Laser et al, 2009(b) compared fourteen scenarios for biological and thermochemical processing of lignocellulose, based on mature technology. They found that integrating biological and thermochemical processing would result in the highest overall efficiencies and economics in the long term. Bioethanol production followed by thermochemical conversion of the solid residue to Fischer-Tropsch liquids resulted in the highest efficiency of 80% and an internal rate of return of 40% at the current crude oil price of \$70/barrel. The main technological advances that would have to be achieved to reach this state of mature technology included effective pretreatment methods and commercial development of consolidated bioprocessing for bioethanol production, and large-scale feeding systems of low density feedstocks to pressurised gasifiers, complete tar cracking and tight heat integration.

Therefore, although several process modelling studies have been performed, modelling of second generation processes for the production of liquid fuels from sugarcane bagasse has been very limited to biological processes and also incomplete. In addition, detailed economic models of second generation biofuels processes have not been developed for South Africa, although the context would be very different compared to first world countries. A review of the literature therefore highlighted the need for an in-depth comparative study dedicated to the South African economic context and based on current technology, to include both biological and thermochemical process routes. This is an important and much needed knowledge base that needs to be developed if the government's goal of integrating the existing fuel market with 4.5% second generation biofuels by 2013 is to be realised.

REFERENCES

- Aden, A., M. Ruth, K. Ibsen, J. Jechura, K. Neeves, J. Sheehan and B. Wallace (2002). Lignocellulosic Biomass to Ethanol Process Design and Economics Utilizing Co-Current Dilute Acid Prehydrolysis and Enzymatic Hydrolysis for Corn Stover. Golden, Colorado, US, National Renewable Energy Laboratory.
- Aguilar, R., J. A. Ramírez, G. Garrote and M. Vazquez (2002). "Kinetic study of the acid hydrolysis of sugar cane bagasse." *Journal of Food Engineering* 55: 309-318.
- Alonso, P. W., P. Garzone and G. Cornaccia. (2006). "Agro-industry sugarcane residues disposal: The trends of their conversion into energy carriers in Cuba." *Waste Management*, doi:10.1016/j.wasman.2006.05.001.
- Boerrigter, H. and R. Rauch (2006). Syngas production and utilisation. The Netherlands, Biomass Technology Group (BTG).
- Boerrigter, H., H. d. Uil and H.-P. Calis (2002). "Green diesel from biomass via Fischer-Tropsch synthesis: New insights in gas cleaning and process design."
- Botha, T. and H. v. Blottnitz (2006). "A comparison of the environmental benefits of bagasse-derived electricity and fuel ethanol on a life-cycle basis." *Energy Policy* 34: 2654–2661.
- Bridgwater, A. V. (2003). "Renewable fuels and chemicals by thermal processing of biomass." *Chemical Engineering Journal* 91: 87–102.
- Bridgwater, A. V., D. Meier and D. Radlein (1999). "An overview of fast pyrolysis of biomass." *Organic Geochemistry* 30: 1479-1493.
- Cardona, C. A. and O. s. J. Sánchez (2006). "Energy consumption analysis of integrated flowsheets for production of fuel ethanol from lignocellulosic biomass." *Energy* 31: 2447-2459.
- Chandel, A. K., R. K. Kapoor, A. Singh and R. C. Kuhad (2006). "Detoxification of sugarcane bagasse hydrolysate improves ethanol production by *Candida shehatae* NCIM 3501." *Bioresource Technology*, doi:10.1016/j.biortech.2006.07.047.
- Das, P., A. Ganesh and P. Wangikar (2004). "Influence of pretreatment for deashing of sugarcane bagasse on pyrolysis products." *Biomass and Bioenergy* 27: 445-457.

De Filippis, P., C. Borgianni, M. Paolucci and F. Pochetti (2004). "Gasification process of Cuban bagasse in a two-stage reactor." *Biomass and Bioenergy* 27: 247-252.

Department of Minerals and Energy (2006). "Draft Biofuels Industrial Strategy of the Republic of South Africa."

Devi, L., K. J. Ptasinski and F. J. J. G. Janssen (2003). "A review of the primary measures for tar elimination in biomass gasification processes." *Biomass and Bioenergy* 24: 125 – 140.

Gnansounou, E., A. Dauriat and C. E. Wyman (2005). "Refining sweet sorghum to ethanol and sugar: economic trade-offs in the context of North China." *Bioresource Technology* 96: 985–1002.

Hamelinck, C. N., A. P. C. Faaij, H. Den Uil and H. Boerrigter (2003). "Production of FT transportation fuels from biomass; technical options, process analysis and optimisation, and development potential." NWS-E-2003-08.

Hamelinck, C. N., G. v. Hooijdonk and A. P. Faaij (2005). "Ethanol from lignocellulosic biomass: techno-economic performance in short-, middle- and long-term." *Biomass and Bioenergy* 28: 384-410.

Hendriks, A. and G. Zeeman (2009). "Pretreatments to enhance the digestibility of lignocellulosic biomass." *Bioresource Technology* 100: 10-18.

Huber, G. W., S. Iborra and A. Corma (2006). "Synthesis of Transportation Fuels from Biomass: Chemistry, Catalysts, and Engineering." *Chemical reviews* 106: 4044-4098.

Kadam, K. L., E. C. Rydholm and J. D. McMillan (2004). "Development and Validation of a Kinetic Model for Enzymatic Saccharification of Lignocellulosic Biomass." *Biotechnology Progress* 20(3): 698-705.

Knauf, B. M. and M. Moniruzzaman (2004). "Lignocellulosic biomass processing: A perspective." *International sugar journal* 106(1263): 147-150.

Kreutz, T. G., E. D. Larson, G. Liu and R. H. Williams (2008). "Fischer-Tropsch Fuels from Coal and Biomass." 25th Annual International Pittsburgh Coal Conference.

Larson, E. D., H. Jin and F. E. Celik (2009). "Large-Scale Gasification-Based Co-Production of Fuels and Electricity from Switchgrass." *Biofuels, Bioproducts and Biorefining* 3: 174-194.

Laser, M., D. Schulman, S. G. Allen, J. Lichwa, M. J. A. Jr. and L. Lynd (2002). "A comparison of liquid hot water and steam pretreatments of sugarcane bagasse for bioconversion to ethanol." *Bioresource Technology* 81: 33-44.

Laser, M., H. Jin, K. Jayawardhana and L. R. Lynd (2009)(a). "Coproduct of ethanol and power from switchgrass." *Biofuels, Bioproducts and Biorefining* 3: 195-218.

Laser, M., E. D. Larson, B. E. Dale, M. Wang, N. Greene and L. R. Lynd (2009)(b). "Comparative analysis of efficiency, environmental impact, and process economics for mature biomass refining scenarios." *Biofuels, Bioproducts and Biorefining* 3: 247-270.

Lynd, L. R., C. E. Wyman and T. U. Gerngross (1999). "Biocommodity Engineering." *Biotechnol. Prog* 15: 777-793.

Martín, C., M. Galbe, C. F. Wahlbom, B. Hahn-Hagerdal and L. J. Jonsson (2002). "Ethanol production from enzymatic hydrolysates of sugarcane bagasse using recombinant xylose-utilising *Saccharomyces cerevisiae*." *Enzyme and Microbial Technology* 31: 274-282.

Martín, C., M. Marcet, O. Almazan and L. J. Jönsson (2006). "Adaptation of a recombinant xylose-utilizing *Saccharomyces cerevisiae* strain to a sugarcane bagasse hydrolysate with high content of fermentation inhibitors." *Bioresource Technology* 98: 1767-1773.

Mbohwa, C. and S. Fukuda (2003). "Electricity from bagasse in Zimbabwe." *Biomass and Bioenergy* 25: 197-207.

McKendry, P. (2002). "Energy production from biomass (part 3): gasification technologies." *Bioresource Technology* 83: 55-63.

McMillan, J. D. (1997). "Bioethanol production: status and prospects." *Renewable Energy* 10(213): 295-302.

Mosier, N., C. Wyman, B. Dale, R. Elander, Y. Y. Lee, M. Holtzapple and M. Ladisch (2005). "Features of promising technologies for pretreatment of lignocellulosic biomass." *Bioresource Technology* 96: 673–686.

Pindoria, R. V., I. N. Chatzakis, J.-Y. Lim, A. A. Herod, D. R. Dugwell and R. Kandiyoti (1999). "Hydropyrolysis of sugar cane bagasse: effect of sample configuration on bio-oil yields and structures from two bench-scale reactors." *Fuel* 78(1): 55-63.

Piskorz, J. and M. P (1998). "Fast pyrolysis of sweet sorghum and sweet sorghum bagasse." *Journal of Analytical and Applied Pyrolysis* 46: 15-29.

Ramey, D. E. (2007). *Butanol: The alternative fuel*. NABC 19: Agricultural Biofuels: Technology, Sustainability and Profitability, South Dakota State University, College of Agriculture and Biological Sciences.

Ringer, M., V. Putsche and J. Scahill (2006). *Large-Scale Pyrolysis Oil Production: A Technology November 2006 Assessment and Economic Analysis*. Golden, Colorado, US, National Renewable energy Laboratory. NREL/TP-510-37779.

Tijmensen, M. J. A., A. P. C. Faaij, C. N. Hamelinck and M. R. M. v. Hardeveld (2002). "Exploration of the possibilities for production of Fischer-Tropsch liquids and power via biomass gasification." *Biomass and Bioenergy* 23: 129-152.

Van Der Drift, A. (2002). "An overview of innovative biomass gasification concepts." *Proceedings of the 12th European Conference and Technology Exhibition on Biomass for Energy, Industry and Climate Protection*.

Wright, M. M. and R. C. Brown (2007). "Comparative economics of biorefineries based on the biochemical and thermochemical platforms." *Biofuels, Bioproducts and Biorefining* 1: 49-56.

Zhang, Q., J. Chang, T. Wang and Y. XU (2007). "Review of biomass pyrolysis oil properties upgrading and research." *Energy Conversion and Management* 48(1): 87-92.

http://www.abengoabioenergy.es/sites/bioenergy/en/nuevas_tecnologias/proyectos/planta_biomasa/index.html. 20 October 2009.

<http://www.biomatnet.org/secure/Other/S1932.htm>. 20 October 2009.

www.dynamotive.com. 20 October 2009.

3. MODELLING OF BIOLOGICAL FERMENTATION AND PYROLYSIS PROCESSES

SUMMARY

The technical performance of lignocellulosic enzymatic hydrolysis of sugarcane bagasse followed by co-fermentation compared with pyrolysis processes was evaluated, based on currently available technology. Process models were developed for anhydrous bioethanol production from sugarcane bagasse using three different pretreatment methods, i.e. dilute acid, liquid hot water and steam explosion, at various solid concentrations. In addition, two pyrolysis processes were modelled for the production of crude bio-oil from sugarcane bagasse. The processes were designed to achieve energy self-sufficiency, implying that all the process energy needs are supplied internally by utilising the thermal energy available in the solid products, either in the form of lignin residue for bioethanol or char for pyrolysis. For bioethanol production using dilute acid pretreatment, a minimum of 35% solids in the pretreatment reactor was required to render the process energy self-sufficient, while steam explosion is currently energy self-sufficient at 50% pretreatment solid concentrations. Both vacuum pyrolysis and fast pyrolysis could be operated as energy self-sufficient, although some of the char is required to fuel the fast pyrolysis process. The process models indicated that effective process heat integration can result in a 10 to 15% increase in all process energy efficiencies. Process energy efficiencies between 52 and 56% (based on liquid fuel plus thermal energy) were obtained for bioethanol production at pretreatment solids concentrations of 35% and 50%, respectively, while the efficiencies were 70% for both pyrolysis processes. The liquid fuel energy efficiency of the best bioethanol process is 41%, while that of crude bio-oil production before upgrading is 67% and 58% via fast and vacuum pyrolysis, respectively. Efficiencies for pyrolysis processes are expected to decrease by up to 15% should upgrading to a transportation fuel of equivalent quality to bio-ethanol be taken into consideration.

3.1 INTRODUCTION

The use of bioethanol as a substitute for conventional oil-derived transport fuel has grown substantially over the last three decades, due to the expanding sugarcane ethanol and corn ethanol industries in Brazil and the United States, respectively. However, these industries have also been open to criticism since they compete with food markets. Second generation technology has led to the development of lignocellulosic bioethanol that utilise agricultural waste, purpose-grown energy crops or invasive plant species. The method of pretreatment is a key processing step in the production of bioethanol from lignocellulosic biomass such as bagasse, and is important from both a technical and economic point of view. Pretreatment is required to overcome the recalcitrant nature of the lignocellulose and enable enzymatic hydrolysis to proceed at an acceptable rate. Enzymatic hydrolysis is preferred to conventional acid hydrolysis processes for both environmental and economic reasons (Aden et al, 2002, Hamelinck et al, 2005). However, pretreatment is also one of the most energy intensive steps in the process and is therefore a substantial cost factor. Consequently, a wide spectrum of pretreatment methods has been studied intensively over the past decade [Mosier et al, 2005, Wyman et al, 2005]. Hydrothermal pretreatment of sugarcane bagasse has received the most attention, and sufficient data is available for steam explosion, liquid hot water and dilute acid pretreatment to construct process models (Martín et al, 2006, Laser et al, 2002, Aguilar et al, 2002). *Saccharomyces cerevisiae* remains the preferred organism for bagasse hydrolysate fermentation and an adapted strain capable of withstanding high levels of inhibitors has been developed (Martín et al, 2006).

Although transport fuels generally receive the most attention, a substantial portion of the liquid fuel energy market is represented by lower grade fuels. In 2001, residual fuels contributed 17.7% of the world refinery production (International Energy Agency). Pyrolysis is a simple process that is easily applied to biomass for production of bio-oil, which can serve as a replacement for residual or light fuel oil, depending on the quality (Ringer et al, 2006). Experimental data is available for vacuum pyrolysis and fast

pyrolysis of bagasse, where the former produces a nearly equal mixture of char and bio-oil products, while the latter maximises the production of bio-oil.

The technical performances of different process routes can be evaluated by solving the mass and energy balances using process modelling, which also enables process cost estimations. Process models for lignocellulose fermentation have been developed for corn stover, switchgrass and soft woods such as poplar, willow and aspen (Aden et al, 2002, Hamelinck et al, 2005), but the majority of the models used assumptions for nth plant technology. Ringer et al, 2006 developed a process model for a wood chip fast pyrolysis process, based on a pilot facility. Cardona and Sánchez, 2006 developed AspenPlus[®] process models to investigate different process configurations for ethanol production from sugarcane bagasse, although the models were based on technical data obtained for wood chips. In addition, the model did not include boiler and steam turbine sections, which limits the extent to which the effect of steam and heat integration on the overall process efficiency could be considered.

In the following section, different options for biological fermentation and pyrolysis of sugarcane bagasse were compared through process modelling, based on currently available technical data measured for bagasse. The approach to assumptions required for the models was of a conservative nature, in order to reflect the current state of technology as much as possible. The results were used to compare the energy efficiency of biological and pyrolysis processing options, and the effect of heat integration on energy efficiency was assessed using the process models.

3.2 METHODOLOGY

In order to compare different process routes on a consistent basis, process models need to be developed for each process route with the inclusion of heat integration in order to reflect each process realistically. The approach to modelling used throughout this study was to base the models on currently available technology, instead of nth plant technology, which is often assumed in literature.

3.2.1 Biological Processing Process Model

The composition and modelling components that were used to model sugarcane bagasse is given in Appendix A. Three sets of reliable experimental data were used to model dilute acid, liquid hot water and steam explosion pretreatment (Aguilar et al, 2002, Laser et al, 2002, Martín et al, 2002). AspenPlus[®] process modelling software was used, and databanks in AspenPlus[®] were used for process units that could be modelled based on thermodynamics, whereas actual, previously published data was used to calculate stoichiometric yields obtained from units where kinetics played an important role. The process design was loosely based on a process model previously developed by NREL for corn stover (Aden et al, 2002) and to some extent process designs commonly used in the corn bioethanol industry (McAloon et al, 2002). In order to facilitate comparison of the three biological process configurations, the design of all the process steps other than pretreatment was identical. Fermentation data was obtained from a study using the adapted strain of *Saccharomyces cerevisiae* previously developed (Martín et al, 2006).

The process consists of a biological processing section for bioethanol production as well as a thermochemical treatment section where energy is recovered from the lignin residue to supply the energy needs of the process, as depicted in Figure 3.1. The most important design specifications for the bioethanol process are given in Table 3.1. Additional data for the feedstock composition, sources of property data used for biomass components, additional unit design criteria and process flow diagrams are given in Appendix A1, A3 and A6. For the pretreatment and fermentation sections, the ELECNRTL property method was used, since this is the most versatile electrolyte property method

available in AspenPlus® and is suitable for any liquid electrolyte solution. This method makes use of the Redlich-Kwong equation of state to calculate vapour phase properties. The property method used from the distillation section onwards was NRTL, which was also used by Aden et al, 2002, since this method can describe the vapour-liquid and liquid-liquid equilibrium of strongly non-ideal solutions using binary parameters obtained from literature and regression of experimental data, available in the Aspen Physical Property Databanks. The application of the NRTL property method for ethanol distillation is also described in Aden et al, 2002.

3.2.1.1 Pretreatment

Following the process flow in Figure 3.1, the bagasse is received from the sugar mill and the particle size is assumed suitable for pretreatment, except for the dilute acid process, where some milling is required (Hamelinck et al, 2005).

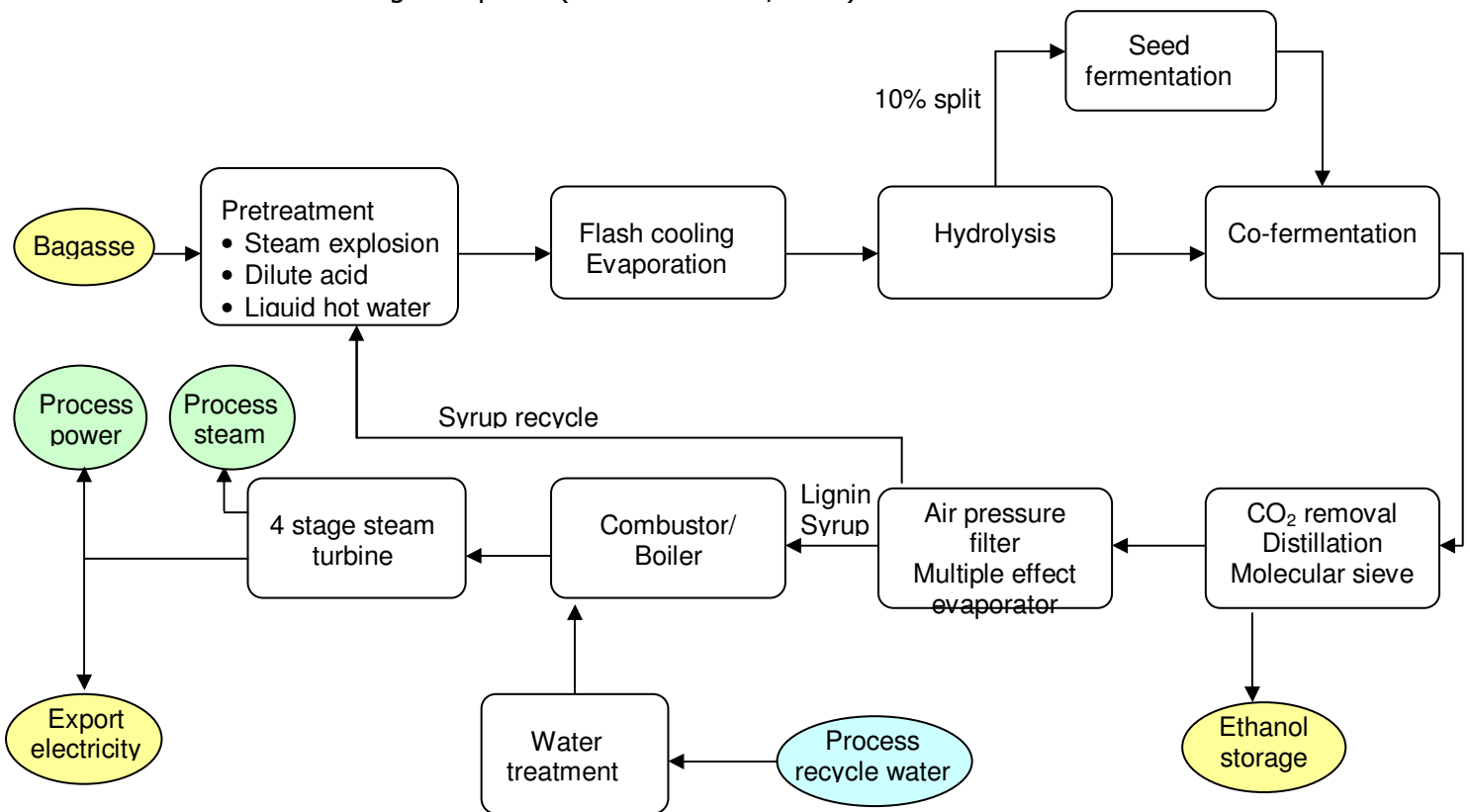


Figure 3.1 Schematic of process flow for bioethanol production.

The bagasse is fed to the pretreatment reactor, which is maintained at the desired temperature using steam generated by the process. Note from Table 3.1 that the pretreatment solids concentrations for liquid hot water, dilute acid and steam explosion were 5, 10 and 50%, respectively. Although the solids content of steam explosion is standard, those of the former two are relatively low compared to some other studies (Hamelinck et al, 2005). However, the most reliable data for sugarcane bagasse used in this study was obtained at these lower solids contents. A list of the pretreatment reactions modelled is given in Appendix A1.

Due to the high solids content required for steam explosion, some of the feed moisture is removed in a pre-heating flash stage. In all cases, approximately 3% excess steam is supplied to account for heat losses and energy loss during decompression. Recycled water is used to adjust the moisture content of the slurry during and after pretreatment, where necessary. In addition, a flash cooling step is required to remove a large fraction of the water present in the pre-hydrolysate. Where the water fraction is below that required for fermentation, as with steam explosion, this is essentially only a cooling step and no heat duty is required, but in the other cases a significant amount of energy is used to evaporate the large quantities of water added during pretreatment. The pH is adjusted to a value of 4.5 and the design specification for solids content at this stage is approximately 20% total solids (Aden et al, 2002).

Table 3.1 Process design specifications for bioethanol production using different pretreatment methods

Design specification	Units	Steam explosion	Liquid hot water	Dilute acid
Pretreatment ^a				
Bagasse moisture content	wt%	46	46	46
Reactor Solids load	wt%	50	5	10 and 35
Reactor temperature	°C	205	210	122
Xylan-xylose conversion	wt%	0.71	0.83	0.90
Cellulose-glucose conversion	wt%	0.07	0.06	0.059
Solids in prehydrolysate	wt%	20	20	20
Hydrolysis and fermentation ^b				
Hydrolysis temperature	°C	65	65	65
Cellulose-glucose conversion	wt%	0.83	0.83	0.83
Hydrolysate split to seed train	%	10	10	10
Fermentation temperature	°C	30	30	30
Glucose-biomass conversion	wt%	0.07	0.07	0.07
Glucose-ethanol conversion	wt%	0.88	0.88	0.88
Xylose-ethanol conversion	wt%	0.44	0.44	0.44
Ethanol recovery ^c				
Beer cleaning: CO ₂ removed	wt%	99.6	99.5	99.6
Overall ethanol recovery	wt%	99.7	99.7	99.7
Evaporation ^d				
Total stillage water evaporated	wt%	66	74	69
Syrup recycled to pretreatment	wt%	25	25	25
Moisture in final residue	wt%	50	50	48
Combustor/Boiler ^e				
Boiler efficiency	%	64	68	68
Steam turbine combined cycle ^f				
Turbine 1 exhaust pressure ^f	kPa	1317	1317	1317
Turbine 2 exhaust pressure	kPa	447	447	447
Turbine 3 exhaust pressure	kPa	172	172	172
Turbine 4 exhaust pressure	kPa	10	10	10

^a Data for pretreatment of sugarcane bagasse obtained from Martín et al, 2002 (steam explosion with 1% H₂SO₄ (dry matter) impregnation of bagasse), Laser et al, 2002 (liquid hot water) and Aguilar et al, 2002 (dilute acid at 2% H₂SO₄). The design specifications and assumptions for the both dilute acid pretreatment models were identical. Detailed reaction data used in the process models is given in Appendix A1.

^b Calculated from data published by Martín et al, 2006 for an adapted co-fermenting yeast strain. Detailed reaction data is given in Appendix A1.

^c Preliminary design based on McAloon et al, 2002. AspenPlus[®] optimisation tools were used for the final design. Design details for the molecular sieve were supplied by UDEC Process, a supplier of separation technology to the local ethanol industry.

^d The pneumatic press described by Aden et al, 2002 was used for the pre-evaporation step, followed by a standard 3-stage multiple effect evaporator.

^e Boiler design was based on that of Aden et al, 2002. The feed water rate was set to match the ratio of the boiler feed lower heating value to boiler feed water rate. Ratio of boiler water to boiler feed was approximately 2.

^f Pressure outlets were taken from Aden et al, 2002. Additional steam requirements were modelled as utilities for liquid hot water (2.5 MPa high pressure steam for pretreatment and 1.3 MPa additional low pressure steam for the rest of the process) and dilute acid pretreatment at 10% (1.3 MPa low pressure steam for the entire process).

Since the fermentation organism used is able to withstand high levels of inhibitors there is no need for detoxification prior to fermentation. The steam explosion hydrolysate used by Martín et al, 2006 to measure the ethanol yields used in this study was obtained under severe conditions forming 4.5g/l and 10g/l furaldehydes and aliphatic acids, respectively. In their previous work, it was shown that the furaldehydes mainly consists of furfural, while acetic acid is the main aliphatic acid (Martín et al, 2002). The furfural concentration in this hydrolysate was substantially higher than the concentrations of 0.13 and 0.5 g/l reported for the liquid hot water and dilute acid hydrolysates, respectively (Laser et al, 2002, Aguilar et al, 2002). The dilute acid hydrolysate contained 3.65 g/l acetic acid while Laser et al, 2002 did not measure significant inhibition from acetic acid formation during liquid hot water pretreatment. Therefore, it is safe to assume that the adapted yeast developed by Martín et al, 2006 would at least be able to achieve the same ethanol yields in these less inhibitory hydrolysates.

3.2.1.2 Hydrolysis and Fermentation

The saccharification and fermentation reaction conditions and conversion data, obtained from Martín et al, 2006 is shown in Table 3.1, and the detailed reactions and design assumptions are given in Appendix A1. Although Martín et al, 2006, did not report any contamination losses, Aden et al, 2002 assumed a loss of 0.3 %, and this value is used as a conservative assumption. To ease comparison between the different pre-treatment

processes, the same design and data was applied to all the three models from this section onwards.

Although it is recognised that simultaneous saccharification and fermentation is often the preferred mode due to cost reductions (Hamelinck et al, 2005), a mode of separate hydrolysis and fermentation was modelled here, since the experimental data used for the modelling was obtained in this manner. This also enables the performance of each step to be studied separately, with each being operated at its optimal temperature. Based on the data of Martín et al, 2006, an enzyme loading of 15 FPU/g cellulose is assumed for enzymatic hydrolysis, and the enzyme is assumed to be purchased. After hydrolysis, a 10% bleed stream is withdrawn from the hydrolysate for seed production in a separate seed reactor train (Aden et al, 2002). The design specifications are set such that sufficient seed biomass is produced to make up 0.2g/l in the hydrolysate. Nutrients, glucose and 35% excess oxygen is supplied in the concentrations given by Martín et al, 2006, which is tabulated in Appendix A3. After fermentation, the product, also referred to as beer, contains between 3.8 and 4% ethanol, and is fed to the recovery section.

3.2.1.3 Ethanol Recovery

The design of this section was loosely based on that of a typical corn-to-ethanol plant (McAloon et al, 2002). At this stage, a small amount of carbon dioxide formed during fermentation is still present in the beer and needs to be removed prior to water-ethanol separation. This is done by using two flash stages, followed by a small water scrubber column, as shown in Figure 3.2.

The beer product is heated using the flash vapour recovered from the conditioning step during pretreatment and then fed to the first flash drum, which effectively removes the majority (95%) of the carbon dioxide, along with 3% of the ethanol. The second flash drum recovers 92% of that ethanol in the liquid phase and 99% of the carbon dioxide in the vapour phase. This vapour is fed to a three-stage water scrubber, along with the

fermentor vent gas and well water at 13°C, which is assumed to be available on site. Any traces of ethanol are captured in the liquid product and returned back to the beer column feed stream. This system achieves a total carbon dioxide removal of 99.6%, with virtually no loss of ethanol. The cleaned beer stream is fed to a beer column where a distillate purity of 55% is achieved with 10 theoretical stages and only 0.3% of the ethanol is lost to the bottoms product, based on the process model. After recovering some of the heat from the stillage stream to heat the feed to the column, the stillage is sent to the following section. The beer column distillate is fed to a rectification column where 18 theoretical stages are required to achieve a distillate purity of 95% ethanol, which is suitable for further purification in a molecular sieve. The optimum column specifications were determined using design tools available in AspenPlus®. More details on the design and performance of this section can be viewed in Appendix A3.

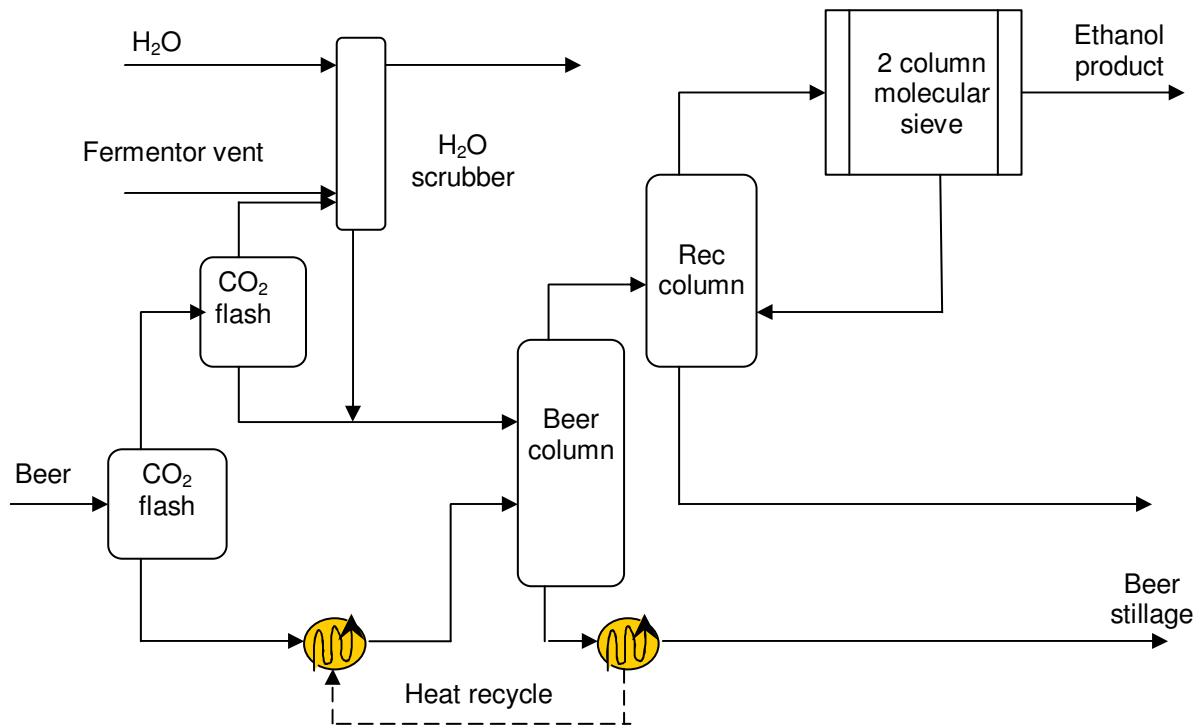


Figure 3.2 Schematic of ethanol recovery process flow in bioethanol process.

The molecular sieve purifies the product stream to 99.5% anhydrous ethanol, while the regenerated stream is recycled back to the rectification column to minimise losses. Performance data for the molecular sieve was obtained from a local supplier (Udecprocess).

3.2.1.4 Residue Separation and Evaporation

The stillage from the beer column contains a significant amount of residual energy and is used to generate superheated steam in a boiler followed by a steam turbine cycle, where the process steam is extracted and electricity generated for use in the process.

Prior to this, the stillage needs to undergo solid-liquid separation and drying to remove excess water while ensuring that the calorific value of the boiler feed is sufficient. A preliminary flash removes 25-30% of the water. High pressure steam and some residual heat from the recovery section are used to supply energy to the flash drum. This is followed by a pneumatic press, which is a pressure belt filter press. Aden et al, 2002 considered several types of solid-liquid separation equipment and found that this press provided the best solids recovery. In the bioethanol models, the pneumatic press effectively separates a solid cake containing between 45 and 50% insoluble solids from the syrup, which is below the specified maximum solids level of 55% (Aden et al, 2002). 25% of this syrup is recycled back to the pretreatment section to improve ethanol conversion. This value should be minimised to limit the effect of accumulation of organic salts in the hydrolysate, and the design value of 25% used by Aden et al, 2002 was based on their experience from a pilot facility. The syrup is further concentrated in a multiple effect evaporator where internal vapour energy is recycled, reducing the net energy input requirement, as outlined in Appendix A3. Of the beer stillage fed to the evaporator section, almost 50% is evaporated as water while 8-10% is recycled to the boiler. This amount of recycled water was limited to minimise the cost of water treatment. The remaining material is sent to the combustor.

3.2.1.5 Combustor and Boiler

The boiler design criteria was based on a circulating fluidised bed combustor described by Aden et al, 2002, which is flexible with respect to varying feed characteristics. After mixing of the syrup and solid cake, the combustor feed calorific value is higher than 10400 kJ/kg (the minimum required value is 5 800 kJ/kg according to Aden et al, 2002) and the moisture contents for all the process models are below the prescribed 52%. Sufficient air is supplied to ensure complete combustion, and a total heat loss from the combustor of 2.6% is assumed (Aden et al, 2002). The ash and gas produced during combustion is sent through a baghouse, the gas is stacked and the ash can be used as an ingredient for the fertiliser already produced at the sugar mill.

The boiler capacity was calculated from the design ratio of the feed material enthalpy to boiler feed water. The amount of high pressure steam from the steam turbine cycle is set to provide enough energy to pre-heat the boiler feed water to approximately 200°C. Energy produced from combustion of the residue material is used to convert the water to superheated steam at 86 bar and approximately 510°C. Although a lower pressure boiler would be cheaper, Aden et al, 2002 was advised that this would lead to a less cost effective turbine system; therefore this design criterion was used. The overall boiler efficiency is between 65 and 69%, compared to 68% reported by Aden et al, 2002.

3.2.1.6 Steam turbine combined cycle

The superheated steam is used to drive a multiple stage steam turbine at four pressure levels (Aden et al, 2002), as shown in Table 3.1. Aden et al, 2002 obtained design and efficiency data from engineering consultants for a turbine system coupled with the boiler described above. An isentropic turbine efficiency of 85% and a 3% loss in electricity at each stage is assumed. Steam is extracted from each stage according to the process requirements, and the final turbine condensate is sent to the water recycle plant where a portion of the water is recycled as boiler feed water. The electricity is used for the process, and any excess is exported to the grid for sale as a by-product.

3.2.2 Pyrolysis Process Model

For pyrolysis, both vacuum pyrolysis and fast pyrolysis processes were modelled. The process designs and heat integration were based on a fast pyrolysis process developed by Ringer et al, 2006, for wood chips. Pyrolysis data used in the models were obtained from our own research group for vacuum pyrolysis of bagasse, and fast pyrolysis data for bagasse was obtained from literature (Piskorz et al, 1998). The process flow diagrams for both options were similar, while the conditions were adjusted for the different data sets.

The same main processing steps consisted of preparation and pretreatment, pyrolysis, condensation and oil recovery, heat recovery and a steam cycle to produce heat and electricity. The pyrolysis process flow diagram is given in Figure 3.3. Additional details of the process and unit design assumptions are given in Appendix A4, and detailed process flow diagrams with stream data are given in Appendix A6. Upgrading of the bio-oil product is not considered here, as sufficient technical information was not available for modelling and application of the oil as residual fuel oil is considered more advantageous (Bridgwater and Peacocke, 2000).

3.2.2.1 Pretreatment and Preparation

The feedstock is received at 46% moisture and dried to 10% moisture using air that is preheated with recycled process heat. Drying is essential as usually all the water present in the feedstock will report to the liquid, reducing the calorific value of the oil product (Bridgwater and Peacocke, 2000). Grinding is required to reduce the average particle size from 4mm to 1mm to match experimental conditions, and based on the performance of KDS Micronex™ technology developed by First American Scientific Corporation, an energy consumption of 75kWh/t for bagasse is assumed (www.fasc.net). The grinding unit is not modelled but the grinding energy is included in the process energy.

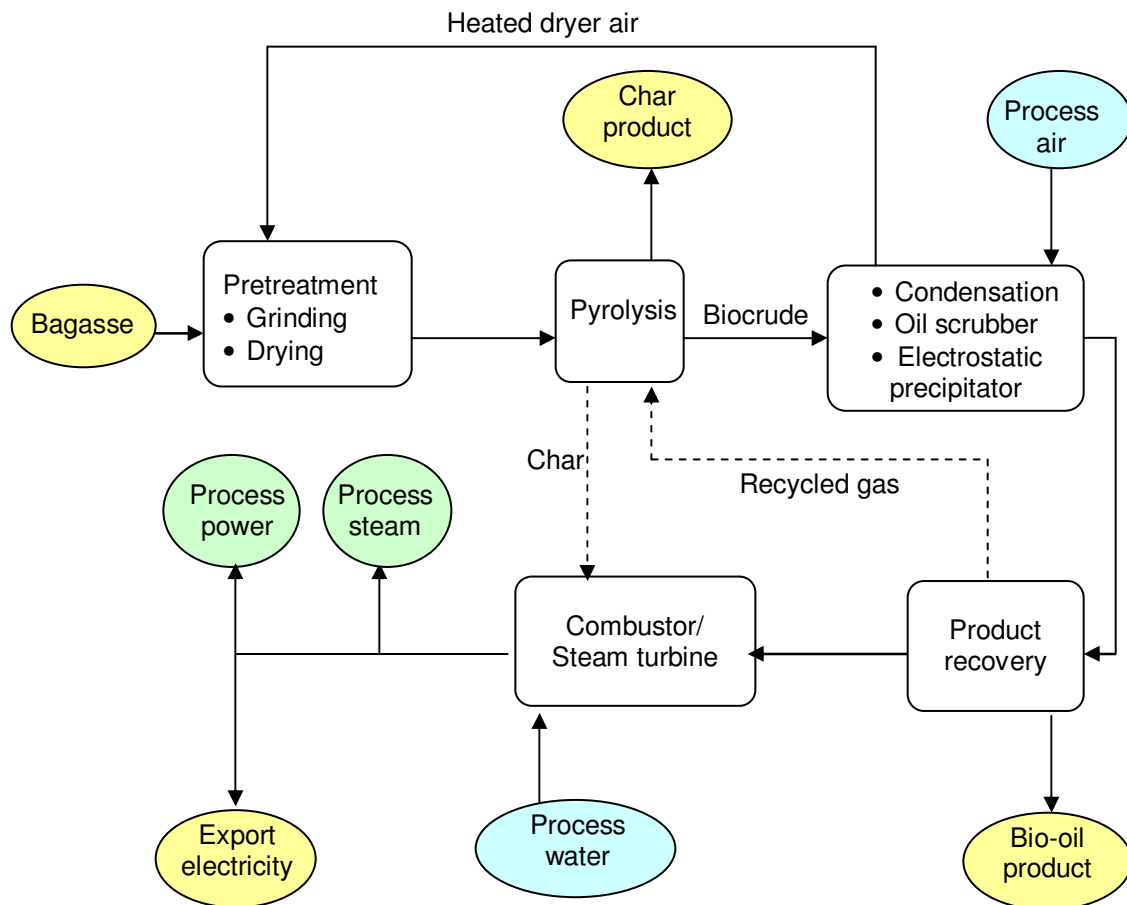


Figure 3.3 Process flow diagram for pyrolysis process. The dashed lines are only applicable to fast pyrolysis.

3.2.2.2 Pyrolysis

The dried material is fed to the following section where pyrolysis takes place. The fast pyrolysis data for bagasse was obtained from a fluidised bed reactor operated at 510°C and ambient pressure (Piskorz et al, 1998). In this model some of the reactor gas is recycled to act as a fluidising gas while also heating the reactor feed. For vacuum pyrolysis, no fluidising gas is required, and the dried bagasse is fed directly to the reactor, which is maintained at 350°C using heat supplied by combustion of the off-gas from the reactor. The pressure is kept at an average of 16 kPa absolute pressure, based on the experimental conditions.

Due to the complexity and non-equilibrium nature of the pyrolysis process, the reactor was modelled as a yield reactor in AspenPlus®; whereby the component yields obtained from the respective pyrolysis processes were derived from the measured experimental

data and set as the output of each pyrolysis reactor. Details of the modelled components for each process and their calculated yields are given in Appendix A2. In both cases the reactor is followed by a cyclone that separates the char from the gas product containing condensable biocrude components and non-condensable gases. For fast pyrolysis, a portion of the char is used to supplement the reactor off-gas fed to the combustor to satisfy the process energy demand, and the rest is stored as a final product. In the case of vacuum pyrolysis, less process energy is required and all the char is recovered as a product.

3.2.2.3 Condensation and Oil Recovery

The gas product from the cyclone is cooled in a series of condensers. Heat recovered from the first condenser is used to generate steam that is sent to the steam turbine cycle, while the second condenser provides energy to pre-heat the air used for drying of the bagasse. This is followed by an oil scrubber, which recovers 80% of the biocrude components to the liquid phase, according to the design of Ringer et al, 2006. The oil recovery is further enhanced by feeding a recycle gas stream from the last oil recovery flash drum to the oil scrubber. An electrostatic precipitator is used to recover 99.9% of the biocrude components lost to the scrubber vapour stream. The brown liquid product consists of an aqueous phase containing water evaporated during pyrolysis as well as reaction water, and an oily phase also referred to as bio-oil. The oil product is sent to the product recovery section where a small portion is recycled to the scrubber and the rest is stored as a product.

3.2.2.4 Combustion and Steam Turbine

At this stage, any non-condensable gas required by the pyrolysis section for use as a fluidising medium in the case of fast pyrolysis is removed, while the remaining off-gas is sent to a combustor where enough air is supplied for complete combustion to be achieved. The combustor is modelled as a stoichiometric reactor similar to the model of Ringer et al, 2006 and AspenPlus[®] calculates the combustion reactions. Since this is a

gas combustor, full combustion may be assumed. Heat generated during combustion is used to supply the energy needs of the pyrolysis reactor, and the product gas is cooled in a series of condensers to recover heat which is used to raise steam for the steam cycle. This steam is mixed with the steam raised during quenching and fed to a steam turbine that generates electricity for use in the process at an isentropic efficiency of 85%. Due to the lower energy demands of vacuum pyrolysis, a small amount of excess electricity is also generated that can be exported to the grid as a by-product.

3.3 RESULTS AND DISCUSSION

Process models were developed to obtain mass and energy balances for an integrated bioethanol plant utilising steam explosion, dilute acid or liquid hot water pretreatment methods at different solid concentrations for sugarcane bagasse. The process and liquid fuel efficiencies obtained from these models were compared to similar process models developed for two modes of pyrolysis, i.e. fast and vacuum pyrolysis. The detailed energy balances obtained from the bioethanol and pyrolysis models are given in Appendix A3.

3.3.1 Bioethanol Process Energy Requirements

The total energy input requirement for all four scenarios studied for bioethanol production are shown in Table 3.2. The 10% dilute acid and 5% liquid hot water processes are clearly not energy self sufficient, and would require an additional energy input, most likely in the form of excess bagasse or coal co-fed to the boiler. The solid concentrations used in these two scenarios were relatively low compared to other studies for other feedstocks. A fourth scenario was thus also modelled to establish the theoretical critical dilute acid pretreatment solids concentration that would result in a breakeven process, i.e. the level where the process is just energy self sufficient, assuming that the same conversions could be obtained at this solids level. It was found that the critical solid load level would be 35%, which compares reasonably well to the model previously developed for dilute acid pretreatment of corn stover at 30% solids (Aden et al, 2002). It is important to stress that this is a theoretical scenario that was included in the study to direct future experimental work and its validity will need to be confirmed with actual measured data for dilute acid pretreatment of bagasse at 35% solids.

Table 3.2 Additional fossil input energy required for bioethanol process using different pretreatment methods.

Pretreatment method		Steam explosion	Dilute acid (theoretical)	Dilute acid	Liquid hot water
<i>Solids in pretreatment</i>		<i>50%</i>	<i>35%</i>	<i>10%</i>	<i>5%</i>
Additional fossil fuel energy	% HHV of biomass input	0%	0%	125%	304%

The increasing energy needs for the lower solids content processes are also reflected in the breakdown of the plant steam requirements, as depicted in Figure 3.4(a). It is clear that the steam required for pretreatment and conditioning (evaporation of the excess water used during pretreatment) is considerably higher for the processes operated at lower pretreatment solid levels. In addition, there is a significant decrease in steam usage from dilute acid pretreatment at 10% to 35%, since lower quantities of water is to be heated, and evaporation of the excess water after pretreatment is not required in the latter case. When the pretreatment solids level is above 35%, the main section requiring significant steam energy is distillation. For example, distillation accounts for 61% of the process steam, compared to 5.5% for pretreatment when steam explosion is used.

A comparison of steam energy requirements from different studies for dilute acid processes is shown in Figure 3.4(b). As mentioned before, Aden et al, 2002 modelled dilute acid pretreatment of corn stover at 30% solids in the pretreatment reactor, while the theoretical scenario developed for bagasse in this study was based on 35% solids and Hamelinck et al, 2005 considered a solids loading in the range of 10 to 30% (w/w). The results in Figure 3.4(b) therefore suggest that 1) steam usage of bioethanol plants utilising lignocellulose is extremely dependent on the solid load of the pretreatment reactor, and 2) the total steam usage is similar for sugarcane bagasse and corn stover.

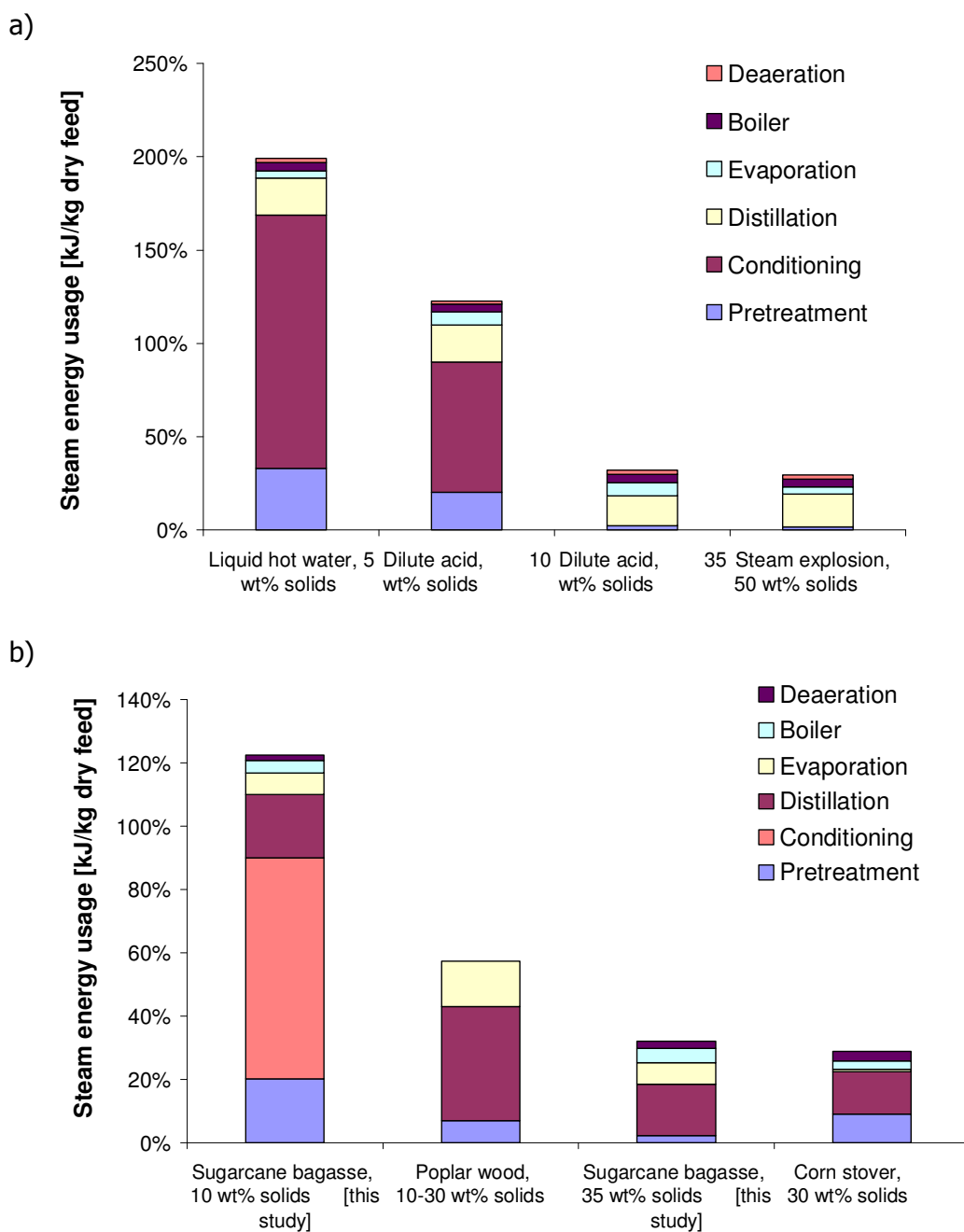


Figure 3.4 Comparison of process steam requirements for bioethanol process: a) Different pretreatment methods for bagasse investigated in this study. b) Dilute acid pretreatment of various feedstocks at different solid levels obtained from this and other studies. Feedstock heating values are: bagasse (19.0 MJ/kg), poplar wood (19.6 MJ/kg, Hamelinck et al, 2005) and corn stover (18.4 MJ/kg, Aden et al, 2002).

As for the process electricity demands, the total electricity for all the bioethanol scenarios are approximately 0.1 kilowatt process electricity required to produce one kilowatt of energy in the form of ethanol. The electricity demands were similar owing to

the identical scale and downstream processing design used for all scenarios. A detailed breakdown of the process energy demands of the bioethanol scenarios can be found in Appendix A3.

3.3.2 Pyrolysis Process Energy Requirements

The process energy requirements for both pyrolysis processes are shown in Table 3.3. The majority of the process energy is consumed during feed drying and in the pyrolysis section. Fast pyrolysis produces more bio-oil and less char than vacuum pyrolysis, as shown in Figure 3.5. The fast pyrolysis mode converts approximately 60% and 10% of the feed energy to bio-oil and saleable char, respectively, compared to roughly 40% for bio-oil and 28% for char during vacuum pyrolysis. However, fast pyrolysis consumes almost twice the amount of energy compared to vacuum pyrolysis, since the process is run at a much higher temperature. The reactor gas and 45% of the char produced was utilised to supply energy for the process. It was also found that for vacuum pyrolysis the process energy losses are higher compared to fast pyrolysis, which is likely caused by the energy consumed to maintain a vacuum. Due to the lower process energy requirements, there is still sufficient energy available in the reactor gas to fuel the process and all the char produced can be sold. Nonetheless, both processes are energy self-sufficient and no additional fossil energy is required to run the plants.

Table 3.3 Process energy requirements for pyrolysis processes as a percentage of total energy input (HHV)

Pyrolysis mode		Fast Pyrolysis	Vacuum Pyrolysis
Feed drying	% HHV input	5.9%	6.0%
Bagasse grinding	% HHV input	2.1%	2.1%
Preheating and reactor energy	% HHV input	19.4%	8.8%
Total process energy	% HHV input	27.4%	16.9%

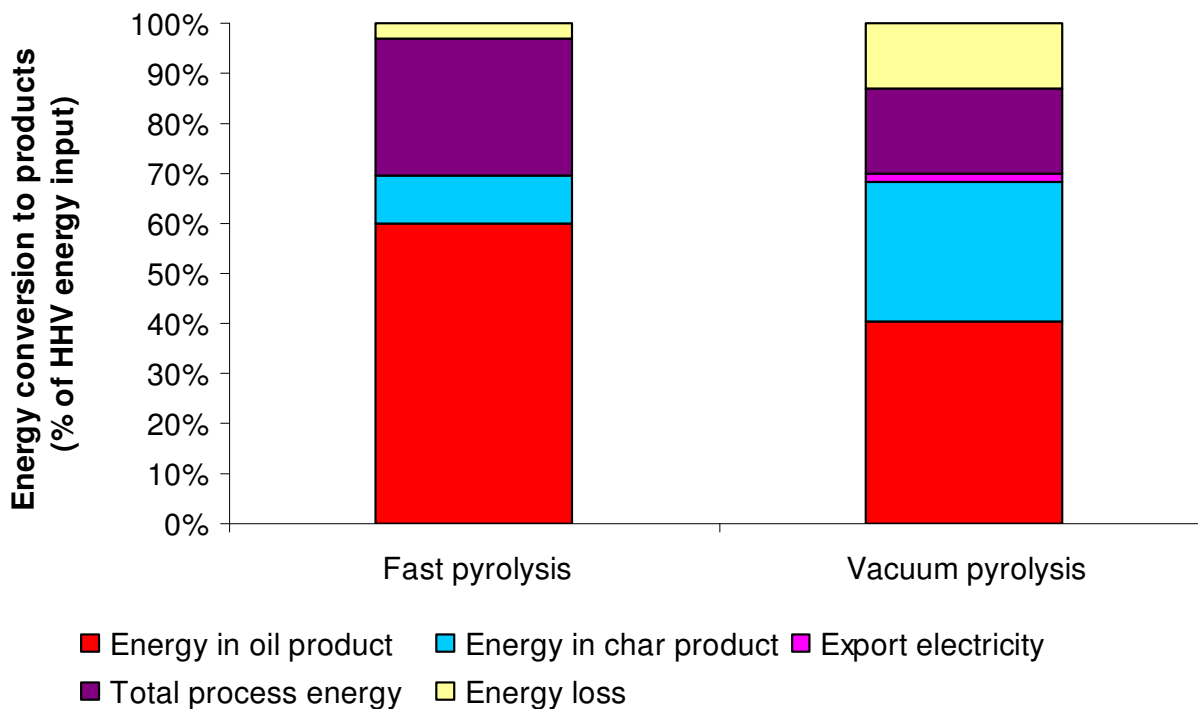


Figure 3.5 Distribution of total process input energy consumed in the process and captured in oil, char and electricity products for pyrolysis processes.

3.3.3 Process energy efficiencies

The distribution of the total input energy for bioethanol production (from biomass and supplementary coal, where applicable) to produce process steam, electricity and final products is given in Figure 3.6 for the four bioethanol scenarios. The steam explosion process is the most efficient at converting the input energy to ethanol, since it also has the lowest energy input requirement. The ethanol energy conversions reflected for liquid hot water and dilute acid pretreatment at 10% solids are much lower compared to the scenarios above 35% pretreatment solids, since these processes require a higher total feed energy owing to co-feeding of fossil energy. Likewise, the energy losses for dilute acid pretreatment at 10% solids and liquid hot water pretreatment seem to be higher compared to the other scenarios, although in reality the designs are similar and the actual energy losses are also similar. However, since the energy loss is calculated by difference from the other yields, which are reduced significantly by the contribution of co-feeding of fossil energy, the graph reflects higher energy losses. In addition, the

need for milling prior to dilute acid pretreatment leads to a slightly higher process electricity requirement compared to steam explosion, as indicated in Figure 3.6.

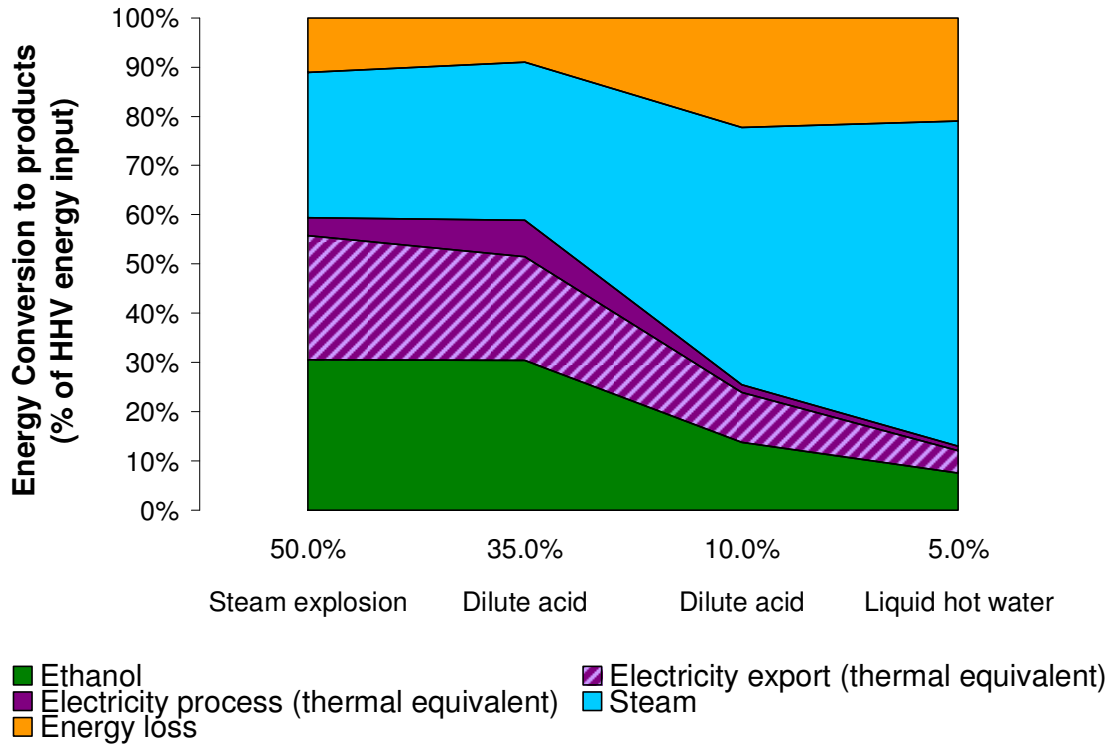


Figure 3.6 Distribution of total process feed energy captured in process steam, electricity and ethanol for bioethanol processes.

Figure 3.7 summarises the energy efficiencies of both the bioethanol and pyrolysis processes. The liquid fuel energy efficiency is expressed on a fuel only basis and is defined as $e_{lf} = (e_{fuel} / (1 - e_{bp}))$, where e_{fuel} is the ethanol or bio-oil energy efficiency and e_{bp} is the by-product energy efficiency, i.e. that of exportable electricity, in thermal units, or char. The energy efficiency of liquid fuels plus thermal products, which will also be referred to as the thermal process energy efficiency, is defined as $e_{lf+th} = (e_{fuel} + e_{lignin} + e_{char} + e_{gas})$, where e_{lignin} , e_{char} and e_{gas} are the energy efficiencies of surplus lignin residue, char and reactor gas prior to electricity generation, in thermal units. A detailed discussion of these definitions can be found in Chapter 2.

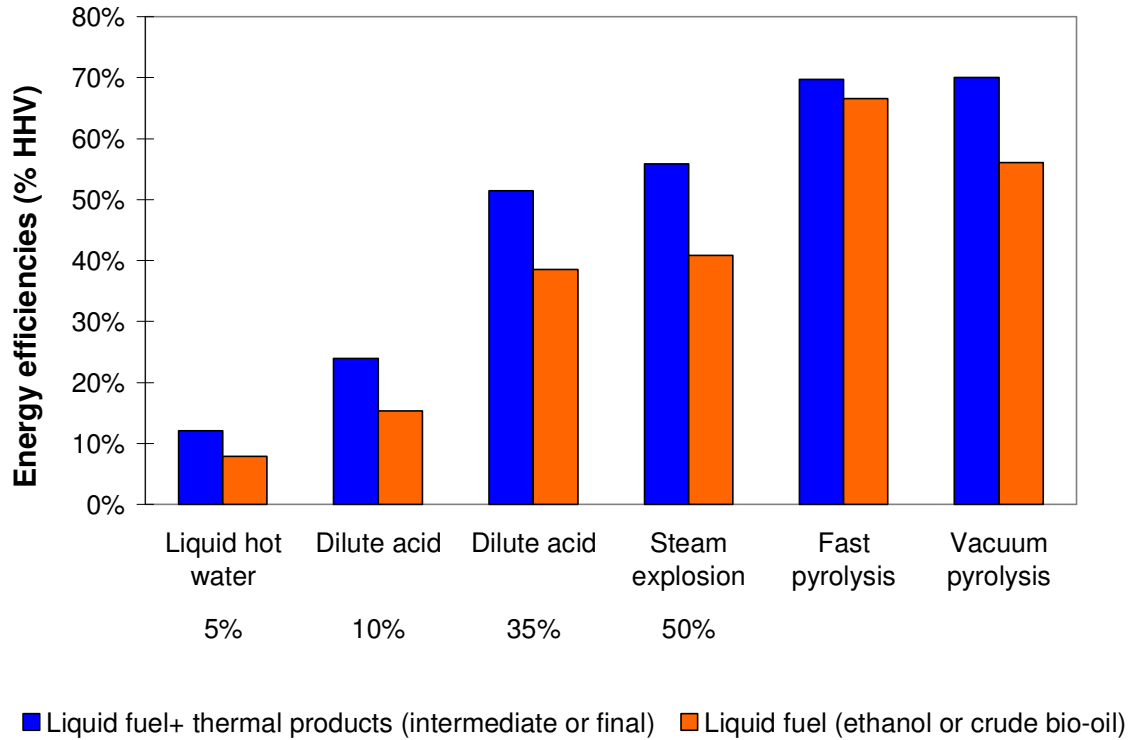


Figure 3.7 Process energy efficiencies and liquid fuel efficiencies for bioethanol and pyrolysis processes.

If one compares the energy efficiencies for **liquid fuels plus thermal products** for the four bioethanol scenarios, the direct correlation between pretreatment solids concentration and energy efficiency is clear once again. Thermal process energy efficiencies of 52 and 56% were achieved at 35% solids dilute acid pretreatment and 50% solids steam explosion, respectively. This is slightly lower than the 56-68% reported by Reith et al, 2002 for lime pretreatment using different feedstocks, while a value of 59% was calculated from the data of Aden et al, 2002. This is probably due to the conservative assumption approach of this study, where the use of experimental data rather than possible or 'ideal' limits resulted in slightly lower efficiencies.

The thermal process energy efficiencies for both vacuum and fast pyrolysis were 70% (Figure 3.7), which is considerably higher than that of lignocellulose fermentation, although this is mostly due to the refinement of bioethanol to a transportation-grade

fuel, which was not performed for pyrolysis bio-oil in the present study. The change in product profiles between fast pyrolysis, producing mostly bio-oil, and vacuum pyrolysis, producing a mixture of bio-oil and char, did not affect the thermal process energy efficiency.

The maximum liquid fuel energy efficiency for the bagasse-to-bioethanol scenarios was 41% using steam explosion pretreatment (Fig. 3.7), compared to 38% reported for poplar wood (Hamelinck et al, 2005), and 54% calculated from the data reported for corn stover (Aden et al, 2002). The liquid fuel efficiencies of 67% and 58% for fast pyrolysis and vacuum pyrolysis, respectively (Fig. 3.7), were higher than for lignocellulose fermentation, although reflecting a crude bio-oil product that is not suitable for use as a transport fuel. Bio-oil upgrading to refined hydrocarbons could reduce the liquid energy efficiency by 9-15%, according to Huber et al, 2006, based on their review of presently available technology for catalytic hydro-treating of bio-oil produced by atmospheric flash pyrolysis followed by refining of the deoxygenated product to gasoline and diesel fuel. It was found that the present and potential process thermal efficiencies of 61 and 68% would be reduced to 52 and 53%, respectively. Assuming the highest range of 15%, the resulting liquid fuel energy efficiency of refined bio-oil from vacuum pyrolysis and bioethanol from steam explosion pretreatment would be in the region of 40-45%, while that of refined bio-oil from fast pyrolysis would be higher, at approximately 52%. According to Wright and Brown, 2007, hydrogen production via thermochemical processing has a liquid fuel efficiency of 50%. Fast pyrolysis therefore has the potential for an excellent transport fuel energy efficiency.

The thermal process energy efficiency was also calculated from the data reported by Cardona and Sánchez, 2006 for dilute acid pretreatment using wood chip experimental data. The resulting efficiency of 42% is significantly lower than the results of this study despite the fact that they assumed higher ethanol yields, which demonstrated the substantial benefits of heat integration to improve process energy efficiencies. The effect of varying levels of heat integration on the liquid fuel efficiency is shown in Figure 3.8 for the bioethanol scenario with steam explosion and fast pyrolysis process. The liquid

fuel efficiency is used for this analysis, since the by-product electricity falls away without a steam cycle. A breakdown of these calculations is also given in Appendix A5. The results show that integration of process heat streams alone led to a 5% and 11% increase in liquid fuel energy efficiency for bioethanol and pyrolysis, respectively, while combining process heat integration with a steam cycle to produce process steam and electricity led to a total increase of 20 and 21% for bioethanol and pyrolysis, respectively. The benefits of process heat integration in the biological process were most evident in the evaporation, recovery and boiler sections, while those of the pyrolysis processes were mostly evident in the pyrolysis and boiler sections. Cardona and Sánchez, 2006, did not model a steam cycle, which explains the lower energy efficiency reported by them.

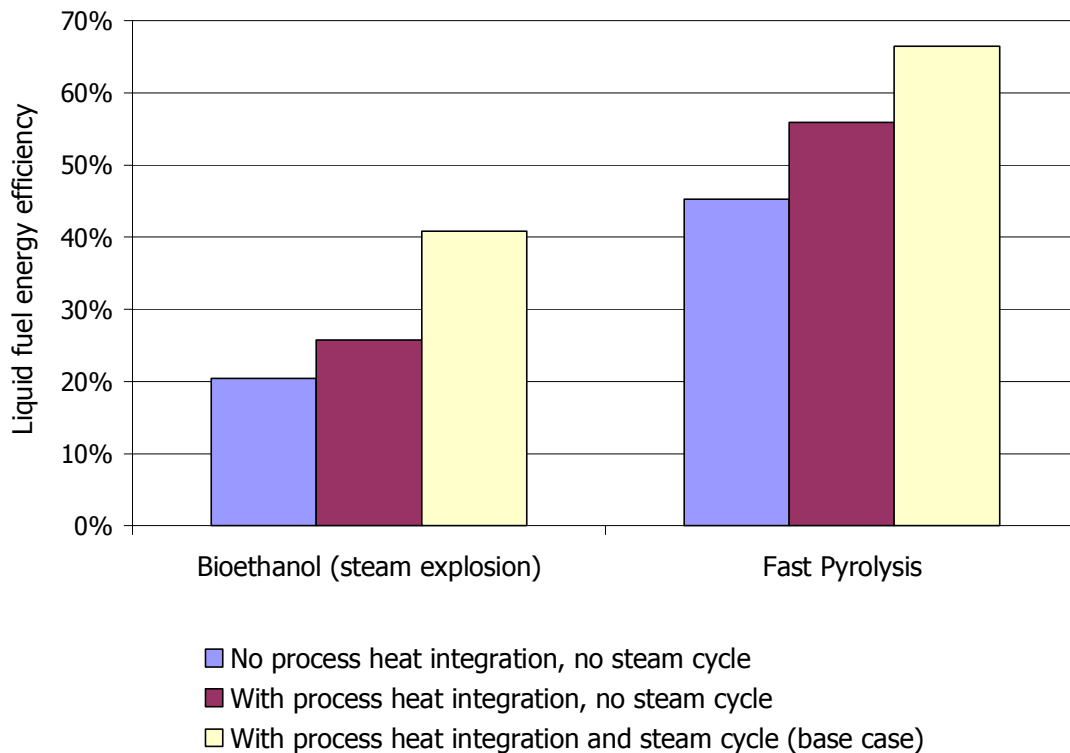


Figure 3.8 Liquid fuel energy efficiencies at different levels of heat integration for bioethanol using steam explosion and fast pyrolysis processes.

The capital and operational cost of the proposed heat integration strategies will dictate their value in commercialisation of these technologies. In addition, in the South African context biofuels processes are not likely to be commercialised as standalone processes,

since integration with existing processes makes a lot more sense. Given the significant effect of heat integration on energy efficiencies for standalone processes shown here, the effect of heat integration between different processes could be very beneficial to the overall efficiency of such biorefineries.

3.4 CONCLUSIONS

- The energy efficiency of processes to produce bioethanol from sugarcane bagasse via enzymatic hydrolysis followed by co-fermentation is highly sensitive to the pretreatment solid concentration. Based on the currently available data, the key to making bioethanol production from bagasse energy self sufficient is to maximise the **solids loading in the pretreatment reactor to at least 35%**, at the highest level of heat integration. Currently, steam explosion is the only pretreatment method that has been successfully tested for bagasse above 35% solids, leading to an energy self-sufficient process, although dilute acid pretreatment has been demonstrated at 30% solids for corn stover, which is a similar feedstock to bagasse based on its composition.
- **Steam explosion** is therefore currently the most energy efficient pretreatment method for bioethanol production from sugarcane bagasse, and the process can produce transport quality bioethanol at a **thermal process energy efficiency of 56% and liquid fuel energy efficiency of 41%**.
- Both **pyrolysis** processes can be operated as **energy self-sufficient** processes, although 45% of the produced char is required to fuel the fast pyrolysis process. The energy in the reactor gas was sufficient to supply the process energy needs of the vacuum pyrolysis process. Both pyrolysis processes exhibited the same **thermal process energy efficiency of 70%**, although the liquid fuel efficiency of fast pyrolysis was superior to vacuum pyrolysis.
- Compared to bioethanol production, fast pyrolysis can achieve a much higher **liquid fuel energy efficiency of 67%**. This stems from the inherent limit in liquid fuel conversion of lignocellulose bioprocessing. However, the produced bio-oil is not a transport quality fuel and it is known that upgrading of bio-oil is currently very expensive. A niche market for crude bio-oil as an industrial heating oil, for example, is considered to be more economical.
- Therefore, pyrolysis is a very efficient process for the production of bio-energy, although not for transport fuels. The production of char as a by-product further

enhances the energy efficiency since energy is converted to electricity, which has a very low energy efficiency.

- Process heat integration increased the liquid fuel energy efficiency of both process routes by between 5% and 11%, while inclusion of a steam cycle led to an increase of 20-21%, and the use of process modelling in this study enabled high levels of integration.

REFERENCES

- Aden, A., M. Ruth, K. Ibsen, J. Jechura, K. Neeves, J. Sheehan and B. Wallace (2002). Lignocellulosic Biomass to Ethanol Process Design and Economics Utilizing Co-Current Dilute Acid Prehydrolysis and Enzymatic Hydrolysis for Corn Stover. Golden, Colorado, US, National Renewable Energy Laboratory.
- Aguilar, R., J. A. Ramírez, G. Garrote and M. Vazquez (2002). "Kinetic study of the acid hydrolysis of sugar cane bagasse." *Journal of Food Engineering* 55: 309-318.
- Botha, T. and H. v. Blottnitz (2006). "A comparison of the environmental benefits of bagasse-derived electricity and fuel ethanol on a life-cycle basis." *Energy Policy* 34: 2654–2661.
- Bridgwater, A. V. and G. V. C. Peacocke (2000). "Fast pyrolysis processes for biomass." *Renewable and Sustainable Energy Reviews* 4: 1-73.
- Cardona, C. A. and O. s. J. Sánchez (2006). "Energy consumption analysis of integrated flowsheets for production of fuel ethanol from lignocellulosic biomass." *Energy* 31: 2447-2459.
- Hamelinck, C. N., G. v. Hooijdonk and A. P. Faaij (2005). "Ethanol from lignocellulosic biomass: techno-economic performance in short-, middle- and long-term." *Biomass and Bioenergy* 28: 384-410.
- Huber, G. W., S. Iborra and A. Corma (2006). "Synthesis of Transportation Fuels from Biomass: Chemistry, Catalysts, and Engineering." *Chemical reviews* 106: 4044-4098.
- Laser, M., D. Schulman, S. G. Allen, J. Lichwa, M. J. A. Jr. and L. Lynd (2002). "A comparison of liquid hot water and steam pretreatments of sugarcane bagasse for bioconversion to ethanol." *Bioresource Technology* 81: 33-44.
- Lavarack, B. P., G. J. Griffin and D. Rodman (2002). "The acid hydrolysis of sugarcane bagasse hemicellulose to produce xylose, arabinose, glucose and other products." *Biomass and Bioenergy* 23: 367-380.
- Martín, C., M. Marcet, O. Almazan and L. J. Jönsson (2006). "Adaptation of a recombinant xylose-utilizing *Saccharomyces cerevisiae* strain to a sugarcane bagasse

hydrolysate with high content of fermentation inhibitors." *Bioresource Technology* 98: 1767-1773.

McAloon, T., F. Taylor, W. Yee, K. Ibsen and R. Wooley (2002). *Determining the Cost of Producing Ethanol from Corn Starch and Lignocellulosic Feedstocks*. Golden, Colorado, US, National Renewable Energy Laboratory.

Piskorz, J. and M. P (1998). "Fast pyrolysis of sweet sorghum and sweet sorghum bagasse." *Journal of Analytical and Applied Pyrolysis* 46: 15-29.

Reith, J., J. Veenkamp, R. Van Ree, W. De Laat, J. Niessen and E. Jong (2002). *Co-production of bio-ethanol, electricity and heat from biomass wastes: Potential and R&D issues*. Petten, The Netherlands, Energy Research Centre of the Netherlands: ECN report CX-01-046.

Ringer, M., V. Putsche and J. Scahill (2006). *Large-Scale Pyrolysis Oil Production: A Technology November 2006 Assessment and Economic Analysis*. Golden, Colorado, US, National Renewable energy Laboratory. NREL/TP-510-37779.

Rocha, J., E. Gómez, J. Pérez, L. Cortez, O. Seye and L. González (2002). *The demonstration fast pyrolysis plant to biomass conversion in Brazil*. World Renewable Energy Congress VII (WREC2002).

Wright, M. M. and R. C. Brown (2007). "Comparative economics of biorefineries based on the biochemical and thermochemical platforms." *Biofuels, Bioproducts and Biorefining* 1: 49-56.

Wyman, C. E., B. E. Dale, R. T. Elander, M. Holtzapple, M. R. Ladisch and Y. Y. Lee (2005). "Coordinated development of leading biomass pretreatment technologies." *Bioresource Technology* 96: 1959–1966.

www.dynamotive.com/en/technology/guelph.html. 28 August 2008.

Energy statistics database, www.data.un.org, 28 August 2008.

<http://www.fasc.net/applications.php>. 26 November 2009.

www.udecprocess.com, personal communication. April 2007.

4. MODELLING OF GASIFICATION AND DOWNSTREAM FISCHER-TROPSCH PROCESSING

SUMMARY

A thermodynamic equilibrium model was used to predict the composition of syngas produced by oxygen-blown biomass gasification at different operating conditions. The effects of temperature, pressure, moisture content, steam to biomass ratio and equivalence ratio (ratio of the amount of oxygen that is fed to the gasifier as a fraction of the oxygen required to achieve full combustion) were studied using sugarcane bagasse and pyrolysis slurry derived from sugarcane bagasse as feed.

Both the equivalence ratio and steam biomass ratio had a negative effect on gasification efficiency and should be minimised within the practical constraints. High moisture in the feedstock had the same effect as steam, but the negative effect on gasification efficiency was even more pronounced. The formation of carbon monoxide and hydrogen was favoured at lower pressures, and due to practical considerations atmospheric gasification was considered in this study.

Taking kinetic limitations into account, the optimum operating conditions to maximise gasification efficiency or to produce the stoichiometric H_2/CO syngas ratio of 2 were determined for each feedstock and integrated with a process model for Fischer-Tropsch liquids production. The maximum overall process efficiency of 51%, of which 40% was in the form of Fischer-Tropsch liquids, corresponded with the maximum gasification efficiency of 75%, based on atmospheric gasification of bagasse with 5% moisture at a temperature of 1100K, equivalence ratio of 0.25 and steam to biomass ratio of 0.75. Operating the gasifier at a steam biomass ratio of 2.25 to yield an equilibrium H_2/CO ratio of 2 increased the Fischer-Tropsch liquid yield to 45%, while inclusion of a shift reactor downstream from the gasifier had the same effect. However, the resulting liquid fuel energy efficiencies were 42% and 49% for the syngas ratio optimised gasifier and shift reactor scenarios, respectively, suggesting that the use of a shift reactor to increase

liquid yields is more energy efficient. Despite this finding, the highest process thermal efficiencies were obtained for the design that did not maximise the Fischer-Tropsch liquid yield, and although process models found in literature make use of a shift reactor, the thermal process energy efficiency can be increased by 10.7% if the shift reactor is excluded. The results obtained for equilibrium gasifier modelling was verified by comparing it with data based on experimental results, and the Fischer-Tropsch process modelling results also compared well with similar designs found in literature.

4.1 INTRODUCTION

Thermochemical processing of biomass to produce second generation biofuels is currently receiving a lot of attention in the biofuels industry. Biomass gasification can be used to produce either electricity and heat, or fuel products that include Fischer-Tropsch fuels, dimethyl-ether, methanol or hydrogen. This study is focused on processes to produce liquid biofuels in a South African context; therefore the application of Fischer-Tropsch (FT) technology for biomass is studied. South Africa has acquired significant experience in Fischer-Tropsch technology due to the presence of Sasol, who have been leaders in commercialisation of this technology, as well as PetroSA.

The synthesis gas used in Fischer-Tropsch production can be obtained from various sources, including coal (CTL), natural gas (GTL) or biomass (BTL). Recently, interest in biomass gasification for Fischer-Tropsch fuels (BTL) has grown substantially. During Fischer-Tropsch synthesis, carbon monoxide and hydrogen (syngas) is converted into straight chain hydrocarbons ranging from CH_4 to waxes (C_{18+}). The range of hydrocarbons in the product can be tailored to optimise for diesel- or naphtha- (petroleum) rich fuel production by adjusting the catalyst, temperature and pressure (Perry and Green, 1997). These synthetic fuels contain no sulphur or other contaminants, making them especially attractive for use in fuel cell vehicles. (Tijmensen et al, 2003).

The main challenge to be overcome for commercialisation of Fischer-Tropsch biofuels is the front end of the process, which includes biomass gasification and syngas cleaning. The aim is to produce a clean, high quality synthesis gas on a constant basis similar to the specifications of coal-derived syngas. In the past, tar formation during biomass gasification was very problematic; however, recent advances in gasification technology has succeeded in producing syngas that is essentially tar free, which is ideal for Fischer-Tropsch synthesis (Wang et al, 2007, Van Paasen et al, 2002). De Filippis et al, 2004, demonstrated that experimental results for bagasse gasification at 800°C and ambient

pressure above equivalence ratios of 0.18 in a two-stage gasifier with nickel catalyst could be successfully predicted using equilibrium modelling.

The latest development in biomass gasifiers is operation at near-equilibrium conditions, and good agreement has been achieved between experimental and equilibrium modelling data (Mahishi and Goswami, 2007, De Filippis et al, 2004, Schuster et al, 2001). Equilibrium modelling is a valuable tool to predict the thermodynamic limits of the gasification system. Several studies have investigated equilibrium modelling of gasification and most of them used the relatively simple Gibbs free energy minimisation method (Altafini et al, 2003, Baratieri et al, 2008, Zainal et al, 2001). Ptasinski et al, 2007 and Prins et al, 2007 studied the effect of varying feedstock compositions on gasification efficiency. Since biomass consists mainly of carbon, hydrogen and oxygen, its composition can be represented on a ternary C-H-O diagram, as shown in Figure 4.1. Gasification occurs when an oxidant is added, moving the product composition in the direction of the carbon boundary line, where all the solid carbon has been converted. In the graph, this line occurs at the 832°C and 600°C isotherms for coal and biomass sludge, respectively. However, if too much oxidant is added, the line from CO₂ to H₂O will be crossed and complete combustion takes place.

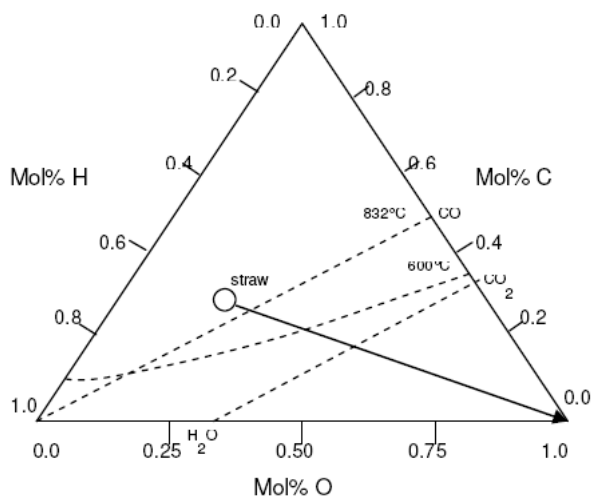


Figure 4.1 Representation of different biomass feedstocks on a ternary C-H-O diagram (redrawn from Ptasinski et al, 2007).

Therefore, the theoretical optimum for gasification corresponds to the carbon-boundary point, where only sufficient oxygen is added to convert all the solid carbon. This theory can also be applied to combined gasification with steam and oxygen, although the authors only considered oxygen as gasifying agent.

Mahishi and Goswami, 2007 used equilibrium modelling to study the effects of operating conditions on hydrogen yields using both steam and oxygen as gasifying media. They found that wood should be gasified at ambient pressure, 1000K, an equivalence ratio of 0.1 and a steam to biomass ratio of 3 to obtain the maximum hydrogen yield, but unfortunately the effect of moisture was not included. A comparison of their equilibrium calculations with experimental data showed that the data correlated best at longer residence times (>1.4s) and temperatures above 800°C.

Process modelling has also been used to evaluate the performance of biomass Fischer-Tropsch processes. Kreutz et al, 2008 compared Fischer-Tropsch synthesis from coal and biomass using experimental data for a fluidised bed gasifier operated at 30 bar and 1000°C. This work was extended to a study comparing the production of Fischer-Tropsch fuels, dimethyl ether and hydrogen using the same modelling basis. Hamelinck et al, 2003 and Tijmensen et al, 2002 also developed Fischer-Tropsch models for willow wood using gasifier data supplied by the Institute of Gas Technology and Batelle Columbus, and different oxidative media and pressures were investigated. Although experimental data is available in literature for bagasse gasification, the gasifiers were not necessarily optimised for the specific downstream application of Fischer-Tropsch synthesis. In addition, none of the previous process modelling studies evaluated the effects of changing operating parameters on gasification efficiency.

In this study, equilibrium modelling of gasification was used to determine two sets of operating parameters for gasification of bagasse or pyrolysis slurry derived from bagasse. Gasification of pyrolysis slurry could offer certain advantages, most notably a

reduction in transport costs due to an increase in volumetric energy density of the feedstock, easier feeding of slurries as opposed to solids and the removal of ash minerals during pyrolysis which can cause slagging during gasification (Van Rossum et al, 2007). The combined effects of temperature, pressure, equivalence ratio, steam to biomass ratio and feedstock moisture content were considered. Although these parameters have been studied before, the combined effects of all five parameters have not been studied in detail. The equilibrium modelling approach was tested by comparing results with experimental data measured for bagasse. The equilibrium gasification results were then applied to a Fischer-Tropsch process model to study the effects of gasification optimisation on downstream processing and the overall process efficiency, and comparisons were made with Fischer-Tropsch models for other feedstocks reported in literature.

4.2 METHODOLOGY

Since biomass gasification and gas cleaning is essentially the only novel part of the Fischer-Tropsch process, the gasification section was studied using equilibrium modelling to study the effects of changing gasification operation on downstream Fischer-Tropsch liquid yields and overall process energy efficiency. For equilibrium modelling of the gasification section, a separate modelling package was used, as is discussed in the following section. Thereafter, the results obtained from the gasification equilibrium modelling work were used as inputs to the Fischer-Tropsch process models, which were developed in AspenPlus®.

4.2.1 Gasification Section Equilibrium Modelling

A five factor central composite design was performed for each feedstock to study the effects of temperature, pressure, moisture content, steam to biomass ratio and equivalence ratio on the predicted equilibrium gas composition and gasification efficiency. A central composite design was used since it allows response surfaces to be studied from a reduced dataset. Instead of a complete three-level factorial dataset, the number of runs is reduced to a two-level factorial dataset with centre and axial points and linear regression is used to obtain the results. All the statistical analyses were performed in STATISTICA, a data analysis software package. An equilibrium model package called Chemical Equilibrium with Applications (CEA), originally developed by the NASA Lewis Research Centre (McBride and Gordon, 1996) was used to perform equilibrium calculations based on the Gibbs energy minimisation method. This package enabled a large number of runs to be performed relatively quickly. The possible product species that were considered included H_2 , H_2O , CO , CO_2 , CH_4 , C_2H_4 , O_2 and solid carbon. The objective is to obtain the mole numbers of the species that will minimise the Gibbs free energy by solving the stoichiometric formulation of the system.

The parameters were varied, based on typical ranges found in literature, as follows: temperature (900-1700 K), pressure (1-40 bar), feed moisture (5-50 wt%), steam to

biomass ratio (0-3, mass basis) and equivalence ratio (0-1). The equivalence ratio is defined as the amount of oxygen that is fed to the gasifier as a fraction of the oxygen required to achieve full combustion. The elemental composition for bagasse ($\text{CH}_{1.49}\text{O}_{0.64}$) was obtained from an assay analysis recently performed on bagasse by a local industry partner. The slurry compositions produced by fast pyrolysis ($\text{CH}_{1.13}\text{O}_{0.32}$) and vacuum pyrolysis ($\text{CH}_{0.85}\text{O}_{0.38}$) were determined from the pyrolysis process models developed in AspenPlus[®], as described in Chapter 3. Due to the presence of high moisture levels and ill-defined structure, the heating value of biomass is often difficult to quantify, especially for bioslurry mixtures (Prins et al, 2007). A statistical correlation was developed by Channiwala and Parikh, 2002 for calculating the higher heating value [MJ/kg] of a wide spectrum of fuels ranging from coal to biomass:

$$HHV = 0.349m_C + 1.1783m_H - 0.1034m_O - 0.0151m_N + 0.1005m_S - 0.0211m_{Ash} \quad [\text{Eq.4.1}]$$

The data generated by the models were used to determine two sets of conditions for gasification of the different feedstocks to 1) maximise the gasification efficiency and 2) obtain a predicted H_2/CO ratio of 2 in the equilibrium gas. The gasification efficiency considered the energy in the biomass, as well as energy required for drying, air separation, steam production and the heat requirements of the gasifier, as shown in Equation 4.2. Depending on the gasifier temperature, pressure and reactant feeds, heat is either required by or emitted from the gasifier. The gasifier duty was calculated from the difference between the product and reactant enthalpy. The product enthalpy was obtained from the equilibrium model, while the reactant enthalpies were calculated from the heat of formation of the feedstock and standard enthalpies of the moisture, steam and oxygen, as described in Appendix B1. The energy consumption of a cryogenic oxygen plant was assumed to be 380kWh/t oxygen (Prins et al, 2007).

$$\text{Gasification efficiency} = \frac{m_{gas} LHV_{gas}}{m_{biomass} LHV_{biomass} + Q_{Drying} + Q_{O_2} + Q_{steam} + Q_{gasifier}} \quad [\text{Eq. 4.2}]$$

where m_i = mass flow rate of component i (kg/h) and Q = duty (W).

$LHV_{\text{bagasse}}=18.31$ MJ/kg, $LHV_{\text{fast pyrolysis slurry}}=25.11$ MJ/kg, $LHV_{\text{vacuum pyrolysis slurry}}=21.99$ MJ/kg.

4.2.2 Fischer-Tropsch Synthesis Process Modelling

The equilibrium gas compositions predicted by the gasification models for different feedstocks at different operating conditions were specified as the feed to the Fischer-Tropsch process models developed in AspenPlus[®]. The process design for Fischer-Tropsch synthesis was based on that of Kreutz et al, 2008, and for easy comparison the process design and specifications were identical. The refinery was not modelled and results from the model of Kreutz et al, 2008 were used to calculate the energy requirements and finished product yields. Detailed refinery models for Fischer-Tropsch processes have been developed in the past, and this portion of the work was not considered to be novel. Once the syngas is produced and conditioned, the source of the syngas has no effect on the downstream process, although the composition does. Therefore, the refinery model of Kreutz et al, 2008 was used, since the synthesis section was also based on their data and therefore the feed to the refinery was similar. The process design used for all the Fischer-Tropsch process models is described below, and detailed design assumptions, performance data and process flow diagrams are given in Appendix B4 and B5. For the purposes of this process description, a simplified process flow diagram is given in Figure 4.2.

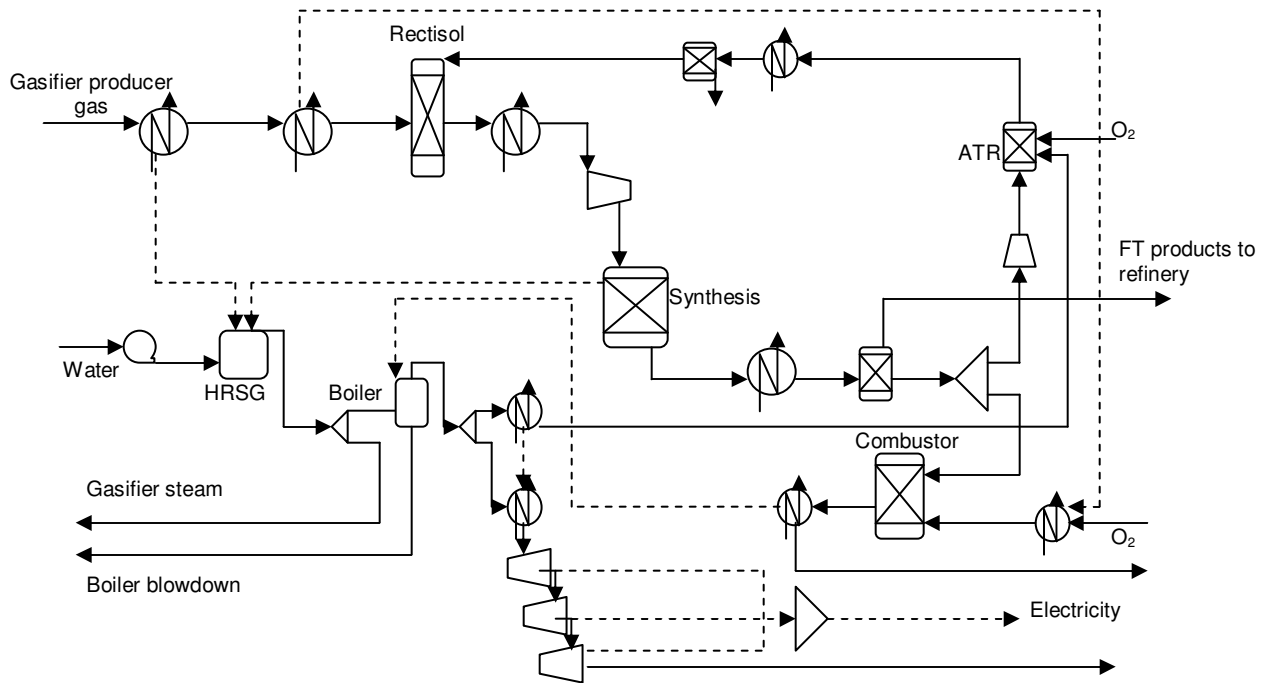


Figure 4.2 Simplified process flow diagram of Fischer-Tropsch downstream processing.

4.2.2.1 Gasification

The equilibrium syngas composition was determined for each scenario. To account for the energy requirements of the gasifier, steam is drawn from the heat recovery section at 500°C and 1 atm, and additional energy requirements of the gasification section, are accounted for, which includes 365kWh per ton 99.5% O₂, 10kJ/kg dry biomass for feedstock handling (Kreutz et al, 2008) and 65kWh/ton water evaporated for bagasse drying (Van Bibber et al, 2007).

4.2.2.2 Gas cleaning and conditioning

After gasification, the ash and particulates are removed from the raw syngas using a cyclone. Since the syngas is assumed to be tar free, no additional tar crackers are required. Based on the work of De Filippis et al, 2004, the presence of a nickel catalyst promotes internal tar cracking sufficiently to achieve equilibrium conditions at 1100K and equivalence ratios above 0.18.

Following the cyclone, the syngas is cooled to 350°C in a heat exchanger using process water and the heat removed from the hot syngas is used to generate steam at 500°C in the steam cycle. Kreutz et al, 2008 assumed a vertical fire-tube syngas cooler for this design, since it minimises deposition fines in the gas and condensed alkali species originating from the ash. A ceramic filter is used to remove any particulates that may have condensed during cooling and the cleaned syngas is further cooled to 40°C. The heat captured from this heat exchanger is partially used to preheat instrument air for the boiler in the heat recovery section, and the balance is available for feedstock drying.

Methane reforming is optional but is not employed here since the gasifier is operated at equilibrium and the contents of methane, ethane and ethene are very low to negligible (below 8% for methane and below 0.1% for ethane and ethene), which does not justify the added cost of reforming. However, a significant amount of carbon dioxide is present in the syngas. In addition, the process design includes recycling of the unconverted syngas exiting the synthesis reactor, which will lead to significant build-up of carbon dioxide in the combined feed to the reactor. CO₂ acts as an inert during synthesis and high levels of CO₂ is therefore undesired as it reduces the conversion efficiency. Although CO₂ removal is expensive, there is a trade-off between the cost of CO₂ removal and the increased Fischer-Tropsch yield associated with the recycle mode of operation (Hamelinck et al, 2003). Considering the aim of this study to compare process routes for production of liquid biofuels, the recycle mode was chosen to maximise the possible yield of Fischer-Tropsch liquids. Based on the recycle design of Kreutz et al, 2008, a Rectisol unit operated at 2 bar and 27°C is used for acid gas removal. Kreutz et al, 2008 discussed different acid gas removal designs for coal and biomass systems. They reported that separate rectisol systems are generally required for coal operations due to the high amount of sulphur species present in the syngas. However, since the sulphur concentrations in biomass-derived syngas are low, co-removal of CO₂ and sulphur is possible in a single absorber column. In this study, the H₂S concentration in the equilibrium syngas was not modelled, and therefore only CO₂ removal is considered, although 100% sulphur removal would be possible according to Kreutz et al, 2008. In addition, a small amount of the H₂, CO and methane in the syngas (less than 4% according to Kreutz et al, 2008) will be removed with the acid gases. Kreutz et al, 2008

built a solvent regeneration cycle into their model, whereby these components are recovered and returned to the syngas. In this study, this feature was not modelled, but the energy and costs required for the regeneration cycle was taken into account based on data given by Kreutz et al, 2008. Additional design parameters for the Rectisol unit are given in Table 4.1. The CO₂ removal is similar to the value assumed by Hamelinck et al, 2003 for a selexol unit.

Table 4.1 Rectisol unit design parameters

Acid gas removal	
CO ₂	97%
Sulphur species	100%
Electricity consumption	1900 kJ/mol(CO ₂ + H ₂ S)
Steam required	6.97 kg/mol(CO ₂ + H ₂ S)

Prior to Fischer-Tropsch synthesis, a water-gas shift reaction may be used to adjust the ratio of hydrogen to carbon monoxide to a value close to 2, which may be required for scenarios that did not optimise the gasifier at a ratio of 2). In the model of Kreutz et al, 2008, the syngas ratio of the synthesis reactor feed was equal to 1.81. Here, the effect of a shift reactor is studied in one of the scenarios. The reactor is modelled as an adiabatic Gibbs free energy minimisation reactor at 330°C and a portion of the stream from the Rectisol unit is split to the shift reactor and recombined with the recycle stream such that the ratio of (H₂-CO₂)/(CO+CO₂) in the combined feed to the synthesis reactor is close to 2. This is simulated with a design specification calculator block in AspenPlus[®]. The design was similar to the single-stage partial water gas shift reactor used by Kreutz et al, 2008, since the use of a two-stage shift reactor was less important due the use of an iron catalyst during Fischer-Tropsch synthesis, and this design also allowed a saving in process steam energy. Additional design details are given in Appendix B4.

4.2.2.3 Fischer-Tropsch synthesis

After adjusting the temperature to 245°C and compressing it to 24.4 bar, the gas is fed to a Fischer-Tropsch synthesis reactor. The model of Kreutz et al, 2008 utilised a slurry-

phased synthesis reactor with an iron catalyst. Due to the enhanced gas-catalyst contact, high once-through conversions of up to 80% can be achieved with these reactors, although their commercial use is more limited than conventional fixed bed reactors. However, one of Sasol's sites is currently using a slurry phased reactor, therefore the technology is currently commercialised. The reactor was modelled as a stoichiometric reactor at 260°C and 23.2 bar, and the key reactions were specified with their fractional conversions, as shown in Table 4.2. Although this modelling approach does not take reaction kinetics into account, the purpose of the model is to simulate an identical reactor to that of the Kreutz model, operated at identical conditions, and this assumption is therefore sufficient for the purposes of this study to solve the mass and energy balances. Since the separation and refining of the Fischer-Tropsch liquid products were not modelled in detail, their fractional conversions were based on their final yields after separation and purification. The molar conversion of carbon monoxide to Fischer-Tropsch products (C₉H₂₀ and C₁₅H₃₂) is 53%. Although higher conversions of up to 80% are possible, this value is more realistic in comparison with the 40% conversion for traditional fixed bed reactors. (Kreutz et al, 2008). In addition, this is only achieved at optimum H₂/CO ratios of around 2, otherwise the conversion will be lower, depending on the degree of limiting reactant.

Table 4.2 Fischer-Tropsch synthesis reactor fractional conversions

Reaction	Fractional conversion	
$\text{CO} + 3\text{H}_2 \rightarrow \text{CH}_4 + \text{H}_2\text{O}$	-0.046 ^a	Eq. 4.3
$4\text{CO} + 8\text{H}_2 \rightarrow \text{C}_4\text{H}_8 + 4\text{H}_2\text{O}$	0.048	Eq. 4.4
$4\text{CO} + 9\text{H}_2 \rightarrow \text{C}_4\text{H}_{10} + 4\text{H}_2\text{O}$	0.533	Eq. 4.5
$9\text{CO} + 19\text{H}_2 \rightarrow \text{C}_9\text{H}_{20} + 9\text{H}_2\text{O}$	0.206	Eq. 4.6
$15\text{CO} + 31\text{H}_2 \rightarrow \text{C}_{15}\text{H}_{32} + 15\text{H}_2\text{O}$	0.324	Eq. 4.6
$\text{CO} + \text{H}_2\text{O} \rightarrow \text{CO}_2 + \text{H}_2$	0.112	Eq. 4.7

^a. The methane synthesis reaction has a negative fractional conversion due to the formation of higher chain length molecules from both the methane present in the feed syngas as well as that formed during synthesis, which leads to a net reduction of methane content in the product stream.

During synthesis, a significant amount of heat is generated (Kreutz et al, 2008), and this heat is captured and combined with the heat from the first syngas cooling step to raise

steam at 510°C using a flash drum. A design specification determines the amount of process water needed in the feed to the drum to achieve the required temperature. After synthesis, the product stream is cooled to 40°C and the recovered waste heat is used to preheat the feed to the synthesis reactor. Any additional heat requirement for preheating of the synthesis reactor feed stream is obtained from the balance of the heat recovered from syngas cooling that is not used for boiler air preheating. In this way, all the heating requirements of the plant are met by using effective heat integration.

Next, the Fischer-Tropsch liquid products are separated from the light gases in the product stream. Since the refinery section is not modelled, the purge gases from the refinery that is normally added to the recycle stream could not be solved directly. In order to overcome this, a mass balance of the light gases (C₁-C₄) was performed over the refinery section of the Kreutz model to determine the average purge gas composition. This is not an unreasonable assumption, considering that the syngas cleaning and Fischer-Tropsch synthesis sections were based on their design, resulting in similar light gases compositions in the crude synthesis products. Based on the mass balance, the light gas stream composition needed to be adjusted to reflect a typical combined light gas stream from Fischer-Tropsch synthesis and refining, being free of water and containing approximately 7.7 wt% CH₄, and this was done using a design specification in AspenPlus[®]. After the light gas stream is adjusted, a 60% split stream is recycled, while the remainder is sent to the boiler and combusted to generate steam for the steam cycle.

4.2.2.4 Recycle

The recycled gas is compressed and an autothermal reformer is used to convert the light hydrocarbon gases to carbon monoxide and hydrogen, using 38 bar steam supplied by the steam cycle and oxygen (185°C, 29 bar) supplied by the air separation unit. The oxygen flow is controlled using a design specification to obtain an outlet temperature equal to 1000°C, while the steam requirement is set equal to 0.63 of the recycle stream mass flow (Kreutz et al, 2008). The reformer is modelled as a Gibbs free energy

minimisation reactor. Hamelinck et al, 2003 also used a reformer but made use of a 2-stage design, which was expected to be more expensive and the single stage reformer described by Kreutz et al, 2008 was found to be sufficient to reform between 89 and 97% of the methane in the recycle stream. The reformed gas is cooled to 40°C and 2 bar and water is knocked out. For the scenario which includes a shift, the product from the shift reactor is combined with the recycle stream before being fed back to the Rectisol unit and combined with the main process stream.

4.2.2.5 Syncrude refining

The detailed process design for the refinery is described by Kreutz et al, 2008, where all the required data was obtained. This section includes a hydrocarbon recovery step, followed by distillation of the syncrude to naphtha, distillate and wax products, which are further refined to produce a mixture of 61% diesel and 39% gasoline blend stocks.

4.2.2.6 Boiler and Steam cycle

The general design used for the boiler and steam turbine cycle was similar to that used for the bioethanol process, the main differences being attributed to the differences in process steam pressures and heat integration requirements. Since the only process steam required for Fischer-Tropsch processing is for the gasifier and reformer, the steam cycle is much less complex. The portion of the flue gas that is not recycled is sent to a boiler, which is modelled as a combustor coupled with a steam generator, although in reality this is a single unit. Air, including an excess of 20%, is preheated to approximately 300°C and fed to the combustor, which is modelled as an adiabatic Gibbs reactor operated at 1.2 bar. In the steam generator, the combustion heat is used to raise superheated steam at 38 bar from a mixture of leftover process steam produced by the recovered process heat and process water. The multistage steam turbine is modelled as a series of three isentropic steam turbines at expanding pressures of 23.6 bar, 2.4 bar and 0.046 bar, and the isentropic and mechanical efficiencies are set at 0.85 and 0.98, respectively (Kreutz et al, 2008). Electricity generated by the three turbines is

combined and the process electricity is subtracted from the generated electricity to obtain the net export electricity.

4.3 RESULTS AND DISCUSSION

4.3.1 Gasification Section Equilibrium Modelling

An example of an output file obtained from the equilibrium model package (Chemical Equilibrium Applications) is shown in Appendix B1. Using all the data generated from these runs, the Pareto charts of standardised effects was obtained from STATISTICA, and these are shown in Appendix B2. The Pareto charts were used to evaluate the most significant standardised effects on the syngas composition and gasification efficiency, in order to aid the identification of trends. For all feedstocks, similar trends were observed, although at different significance levels. For the purposes of this discussion, the analysis of equilibrium gas compositions will focus on bagasse, unless otherwise stated.

First, the prediction capabilities of the equilibrium model was evaluated by comparing the results obtained from the model in this study to the thermodynamic predictions and experimental results for bagasse gasification reported by De Filippis et al, 2004, as depicted in Figure 4.3. The equilibrium gas composition predicted by the equilibrium model agrees very well with the experimental data and is even better than that predicted by De Filippis et al, 2004. The only notable difference in gas compositions was an slight over-prediction in CO₂ accompanied by an equivalent under-prediction in methane. This is due to the fact that a small amount of methane was measured in the experimental data, while all the methane would be reformed by the significant amount of steam at equilibrium conditions. The assumption that equilibrium can be reached in an actual gasifier using bagasse as feedstock is therefore reasonable, although this has only been tested on a bench-scale reactor and for a larger scale apparatus it will be very important to ensure that the operating conditions are sufficient to reach equilibrium.

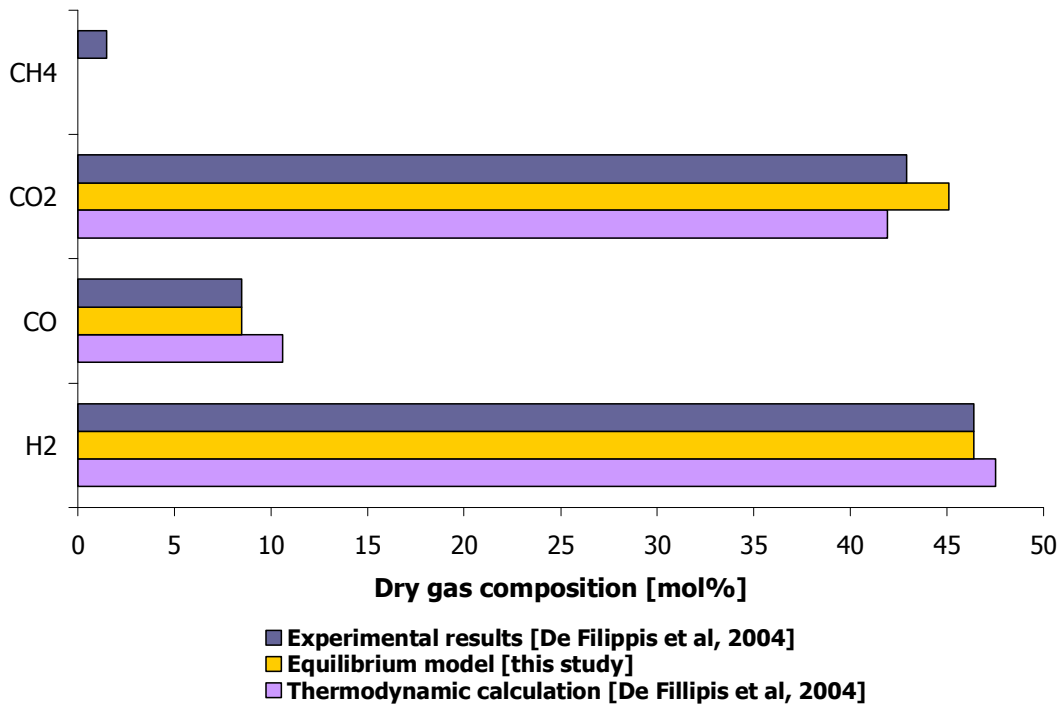


Figure 4.3 Comparison of equilibrium modelling results from this study with prediction modelling and experimental data for bagasse gasification (1 bar, 11% moisture, equivalence ratio=0.18, steam biomass ratio=1.9).

The effect of temperature on the equilibrium gas molar composition is presented in Figure 4.4. Higher **temperatures** favour the formation of CO and H₂ coupled with increased reforming of methane, as depicted in Figure 4.4. The trends observed for the pyrolysis slurries were similar. However, if the temperature is further increased, H₂ is converted to CO and H₂O by the reverse water gas shift reaction, which is favoured at high temperatures. This is also reflected in the quadratic temperature effect observed from the Pareto chart in Appendix B2. In this case, the maximum H₂/CO ratio occurs at between 1200K and 1300K, but this varies according to the other operating variables. The equivalence ratio, pressure and moisture content shown in Figure 4.4 correspond to conditions that were chosen for optimisation, while the steam biomass ratio was chosen as an average value reflecting actual conditions for biomass gasifiers, both of which are discussed later. Also note that the H₂/CO ratio is far below the optimum value of 2 for maximum liquid fuel production, due to the low moisture content and steam to biomass ratio.

According to Ptasinski et al, 2007, the carbon boundary temperature for grass, which has a similar lignocellulosic composition and heating value compared to bagasse, occurs at around 900K, which would correspond to the optimum gasifier temperature. This correlates with the results presented here, as at 900K all the carbon has been converted, and indeed it was found that the highest system efficiency occurred at 900K for all cases due to the increase in external gasifier heat requirements at elevated temperatures. However, this is the theoretical case and is only applicable when the residence time is long enough for equilibrium to be reached. Literature reports that in practice gasifiers need to be operated at elevated temperatures to reduce chemical reaction kinetic and diffusion limitations and ensure complete gasification, ranging from 900K to 1273K (Ptasinski et al, 2001; Mahishi and Goswami, 2007; Prins et al, 2007, Pellegrini et al, 2007). Based on the bagasse gasifier tested by De Filippis et al, 2004, this minimum temperature is assumed to be 1100K for the purposes of this study.

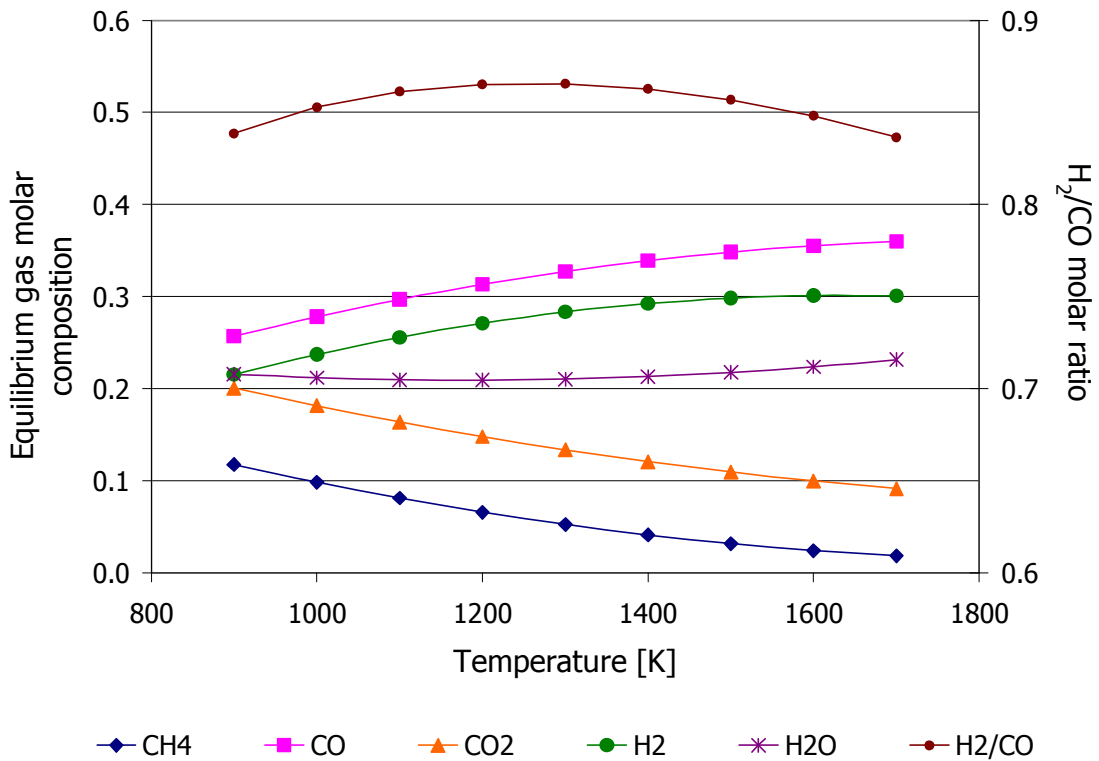


Figure 4.4 Effect of temperature on equilibrium gas compositions for bagasse gasification. (1 bar, 5% moisture, equivalence ratio=0.25, steam biomass ratio=0.5).

The effect of equivalence ratio on the equilibrium gas composition is shown in Figure 4.5. Gasification with oxygen is exothermic; therefore the desired elevation in temperature above the carbon boundary temperature can be achieved by feeding more oxygen to the gasifier. Increasing the **equivalence ratio** leads to over-oxidisation and partial combustion of the syngas to produce H₂O and CO₂ (Prins et al, 2007), as shown in Figure 4.5. As this will decrease the gasification efficiency, the equivalence ratio should be kept to a minimum within the practical constraints. This is also confirmed by the Pareto charts in Appendix B2, which indicate the equivalence ratio to be the most significant factor that negatively affects the gasification efficiency and composition of H₂ and CO in the syngas.

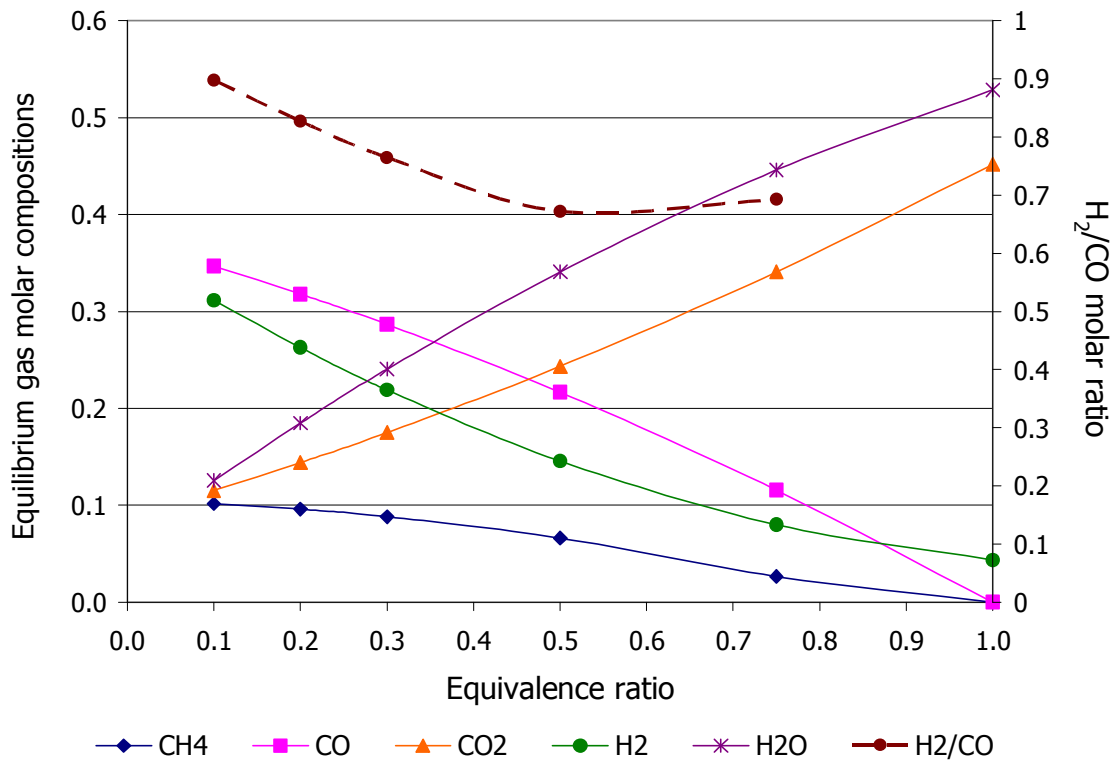


Figure 4.5 Effect of equivalence ratio on equilibrium gas composition for bagasse gasification (1100K, 1 bar, 5% moisture, steam biomass ratio=0.5)

Mahishi and Goswami et al, 2007 found the theoretical optimum conditions for maximum efficiency and hydrogen production from atmospheric gasification of dry biomass to be at 1000K, an equivalence ratio of 0.1 and a steam biomass ratio of 3. However, they did not account for practical considerations such as tar formation. It has been reported in

literature that a 20% secondary air injection above the gasifier freeboard can reduce tar formation by 88.7% (Wang et al, 2008, Kreutz et al, 2007). The results of De Filippis et al, 2004 showed a good correlation between experimental and predicted results for bagasse gasification with no tar formation at equivalence ratios of 0.18 and 0.35. In this study, a minimum equivalence ratio of 0.25 is assumed sufficient to achieve complete gasification.

An increase in gasifier **pressure** leads to reduced partial pressures of CO and H₂ coupled with an increase in CO₂ and H₂O, as reflected in Figure 4.6. This is due to the decrease in the total number of moles at higher pressures (Mahishi and Goswami, 2007), which also leads to a decrease in the H₂/CO ratio. In practice, high pressure gasification may have economic advantages in downstream processing due to smaller equipment sizes, although it has not been commercialised yet (Kreutz et al, 2007, Tijmensen et al, 2002). Higher overall efficiencies could also be achieved if hot gas cleaning is used, but this is still in development, and currently wet gas cleaning is the only available option, in which case the energy losses associated with compression and decompression are high if coupled with a high pressure gasifier. Therefore, the remainder of this work will focus on atmospheric gasification.

It is widely reported that hydrogen-rich syngas can be obtained by **steam** gasification (Mahishi and Goswami, 2007). However, steam gasification is endothermic and decreases the gasification temperature, which necessitates the addition of oxygen to generate heat in the gasifier (Wang et al, 2008, Pellegrini et al, 2007, Mahishi and Goswami, 2007). When oxygen and steam are used as co-gasifying agents, the distribution of H₂ and CO in the product gas can be manipulated by adjusting their relative feeds. Figure 4.7 illustrates the increase in the CO₂ and H₂ yields resulting from the water gas shift reaction as the steam biomass ratio increases. According to the Pareto charts in Appendix B2, the steam biomass ratio has the most significant effect on the equilibrium H₂/CO molar ratio, followed by temperature. This is also clearly shown in Figure 4.7.

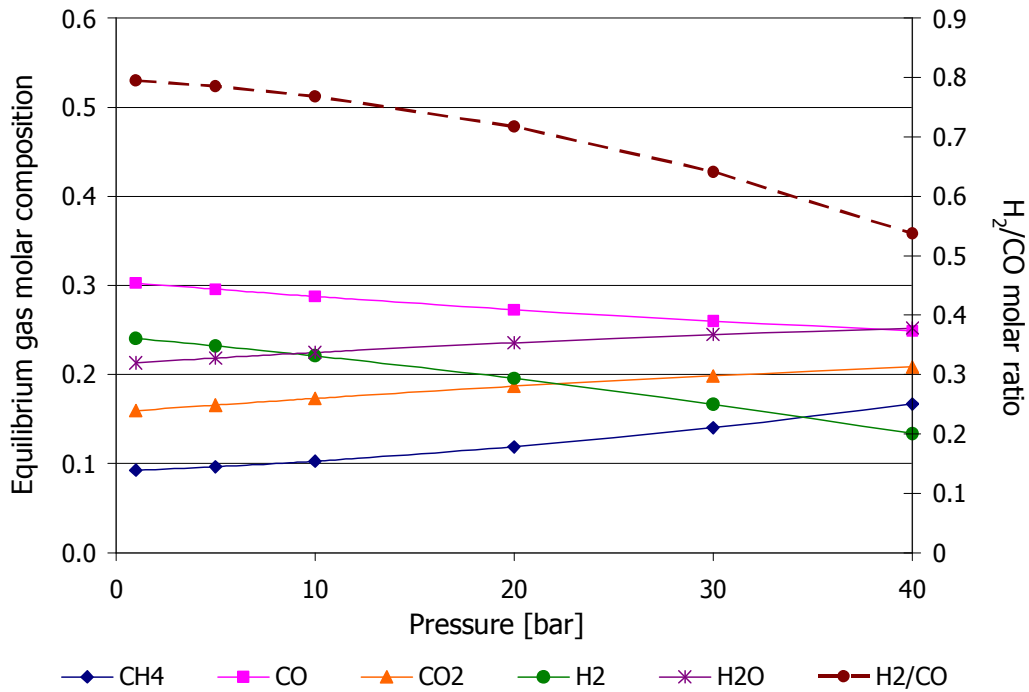


Figure 4.6 Effect of pressure on equilibrium gas composition for bagasse gasification (1100K, 5% moisture, equivalence ratio=0.25, steam biomass ratio=0.5).

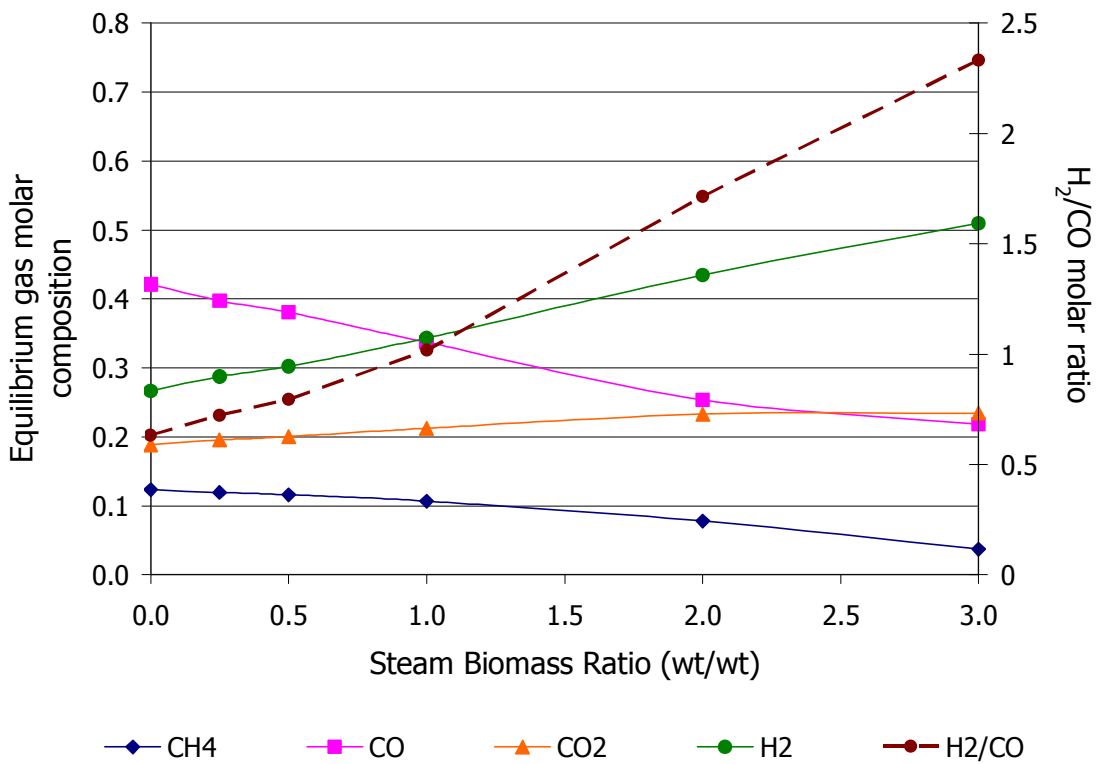


Figure 4.7 Effect of steam biomass ratio on dry equilibrium gas composition for bagasse (1100K, 1bar, 5% moisture, equivalence ratio=0.25).

Similar to steam addition, high **moisture** contents in the biomass also leads to higher hydrogen yields. Figure 4.8(a) shows the combined effect of steam and moisture on the H_2/CO in the equilibrium gas. For example, a H_2/CO ratio of 2 can either be achieved at 5% moisture and a steam biomass ratio of 2.25, or 40% moisture and a steam biomass ratio of 0.5. However, Figure 4.8(b) indicates that the former case results in a gasification efficiency of 60%, while the latter has an efficiency of 55%. This is due to the fact that, at high moisture contents, more energy is consumed for moisture vaporisation, as was also reported by Ptasinski et al, 2007. This leads to a similar, but slightly more pronounced negative effect on gasification efficiency compared to steam addition in the ranges studied. It is therefore more energy intensive to generate electricity for supplying energy to the gasifier externally compared to producing steam and supplying the energy directly with the feed mixture. Normally, the feedstock can be dried using waste heat from the steam turbine cycle (McKendry, 2002, Tijmensen et al, 2002).

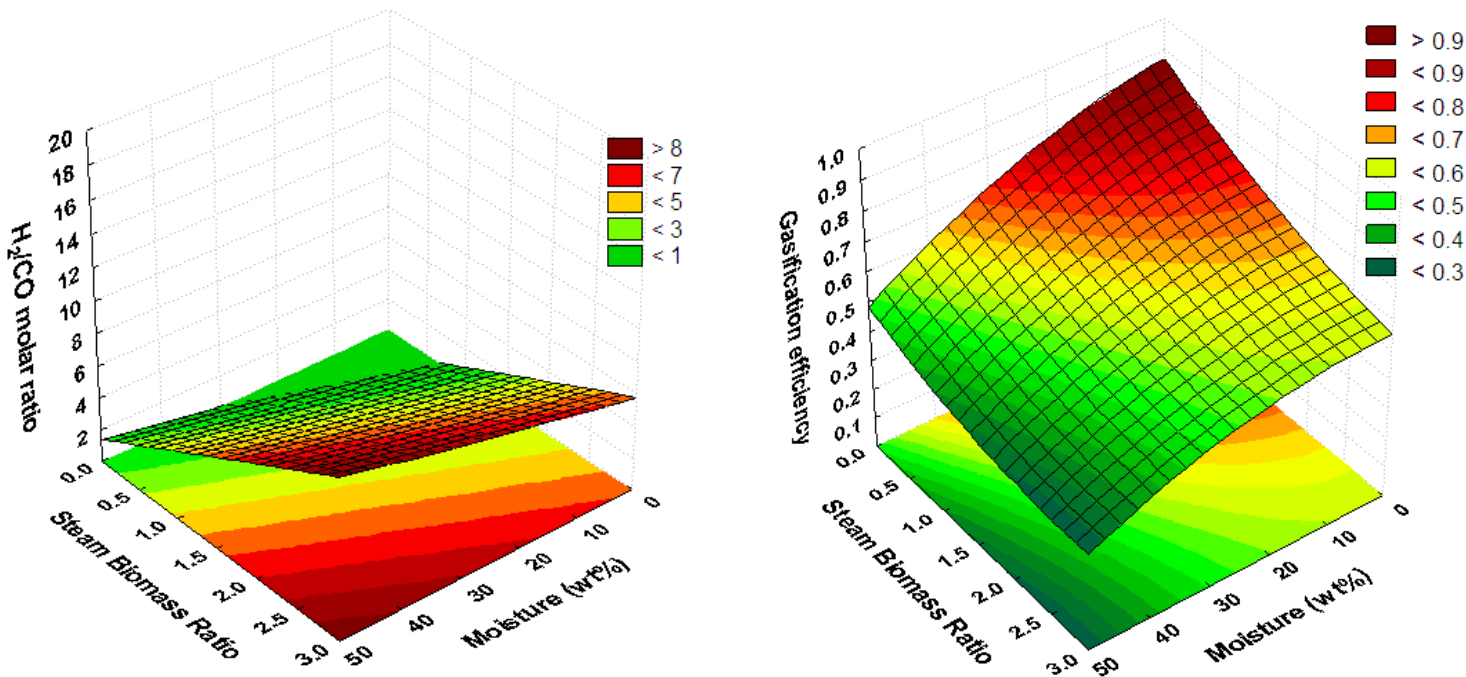


Figure 4.8 Combined effects of steam biomass ratio (wt/wt) and bagasse moisture content (wt%) on predicted (a) equilibrium gas H_2/CO ratio ($R^2=0.98$) and (b) gasification efficiency ($R^2=0.99$). Temperature=1100K, pressure=1bar, equivalence ratio=0.25.

The Pareto chart of standardised effects on the gasifier duty shown in Appendix B2, Figure B2-10 indicates that high equivalence ratios has a very strong negative effect on the gasifier duty. High equivalence ratios lead to higher, more positive gasifier duties, since the gasifier is operated closer to combustion, decreasing the energy in the syngas due to more water and carbon dioxide being formed. This effect is almost three times more significant than that of steam addition. Figure 4.9 shows that, at high equivalence ratios above roughly 0.7, which corresponds to combustion, the gasifier duty becomes positive and energy has to be supplied to maintain the operating temperature. This is due to a decrease in the adiabatic enthalpy resulting from an increasing concentration of oxygen in the feed, which has a zero enthalpy. The effect of steam addition on gasifier duty is interesting. Figure 4.9 indicates that the gasifier duty goes through a minimum at a steam to biomass ratio of about 1.2. This can be explained from the increase in H₂ at increased steam levels, which increase the gas product enthalpy and therefore decrease the gasifier duty, but only up to a point, where steam moderation begins to play a more important role and the decrease in gasifier temperature leads to higher gasifier duties.

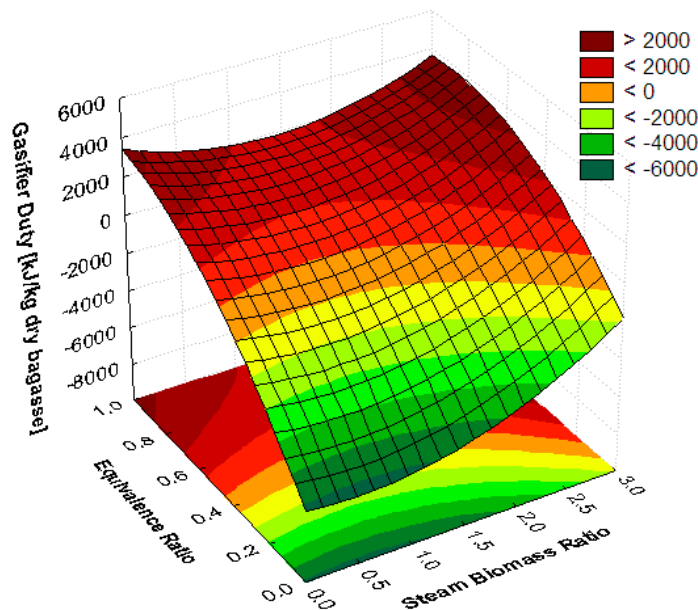


Figure 4.9 Combined effects of steam biomass ratio (wt/wt) and equivalence ratio predicted gasifier duty ($R^2=0.88$). Temperature=1100K, pressure=1bar, moisture=5%. Positive values indicate a net heat input to the gasifier.

As expected, the effect of increased steam and moisture content on the H₂/CO ratio of the equilibrium gas was equivalent for all the feedstocks considered. However, an interesting trend in gasification efficiency was observed for both **pyrolysis slurries**. From Figure 4.10, it is evident that the optimum moisture content for maximum gasification efficiency is not zero as with bagasse, but goes through a maximum. This can be explained by the fact that the slurries have a lower O/C ratio compared to bagasse due to their char content. Prins et al, 2007, determined that fuels with lower O/C ratios exhibit higher carbon boundary temperatures, which is why it is possible in practice to gasify coal below its carbon boundary temperature by moderation with steam. Therefore, for dried pyrolysis slurry, the carbon boundary temperature is slightly higher than the set temperature of 1100K. As the moisture level increases, the composition of the slurry changes up to the point where the operating temperature equals the carbon boundary temperature. The optimum moisture contents to maximise the gasification efficiency for both slurries were determined to be 16.25% using the surface plots. However, the high moisture contents of the slurries also leads to lower gasification efficiencies compared to bagasse.

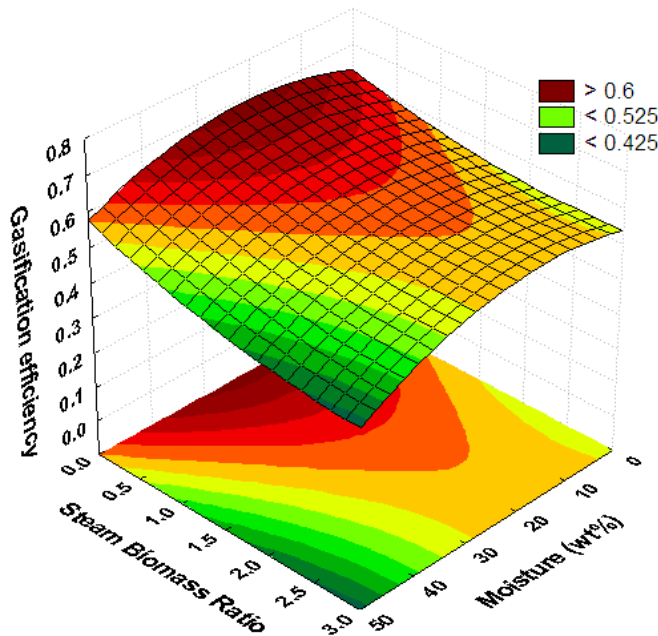


Figure 4.10 Combined effects of steam biomass ratio (wt/wt) and fast pyrolysis slurry moisture content (wt%) on predicted gasification efficiency ($R^2=0.98$).

Using the data generated by the equilibrium modelling, two sets of operating conditions were determined using prediction profiling tools available in STATISTICA®. This method and the intermediate results are described in detail in Appendix B3. Table 4.3 summarises the final **operating conditions** determined for bagasse and pyrolysis slurries using two approaches. In the first case (equilibrium gasifier 1), the gasification efficiency was maximised, while the second approach (equilibrium gasifier 2) was to determine the maximum gasification efficiency that would correspond with a H₂/CO ratio of 2. It was found that gasification of bagasse, having the highest O/C ratio of 0.64, resulted in the highest efficiency in the first case, while fast pyrolysis slurry with the lowest O/C ratio of 0.32 had the lowest efficiency. Setting the H₂/CO ratio equal to 2 lowered the efficiencies of all the feedstocks to more or less 60%.

Table 4.3 Operating conditions for equilibrium gasification of bagasse-derived feedstocks at 1100K, 1 bar and an equivalence ratio of 0.25.

Feedstock	Bagasse		Fast Pyrolysis Slurry		Vacuum Pyrolysis Slurry	
	EG1	EG2	EG1	EG2	EG1	EG2
Optimisation approach*	EG1	EG2	EG1	EG2	EG1	EG2
Moisture [wt%]	5.00	5.00	16.25	16.25	16.25	16.25
Steam Biomass Ratio [wt/wt]	0.75	2.25	0.75	2.00	0.75	2.30
H ₂ /CO molar ratio	0.90	2.00	0.93	2.00	0.75	2.00
Gasification efficiency	74.7	59.6	63.2	57.9	70.4	60.1

*EG1=Equilibrium Gasifier 1, simultaneous optimisation for gasification efficiency and H₂/CO ratio
EG2=Equilibrium Gasifier 2, H₂/CO ratio set equal to 2.

4.3.2 Fischer-Tropsch Process Modelling

The operating parameters and predicted gas compositions of the equilibrium gasifiers used for modelling of the Fischer-Tropsch process scenarios are listed in Table 4.4, along with a comparison with actual gasifier data used for different feedstocks found in literature. The oxygen biomass ratios are given here since the equivalence ratio is dependent on the feedstock and different feedstocks are listed in the table and the gasification efficiencies were calculated from the operational data shown in the table.

First of all, the operating conditions for the equilibrium gasifier 1 mode (EG1) used in this study may be compared with the gasifier data reported by Hamelinck et al, 2003. Although Hamelinck et al, 2003 obtained higher syngas ratios compared to EG1, the fraction of H₂ and CO in the syngas was significantly lower, since they assumed an incomplete carbon conversion (95%) in their model. Small amounts (less than 1%) of tar, ethane and benzene that were also included in their model are not shown here to simplify comparison. Pellegrini et al, 2007 reported that circulating fluidised beds generally operate further away from equilibrium compared to e.g. downdraft gasifiers, and incomplete carbon conversion can therefore be expected.

Table 4.4 Input parameters and gas compositions for equilibrium gasifiers used in Fischer-Tropsch process modelling. FP=fast pyrolysis, VP=vacuum pyrolysis.

Source		FT Bagasse [EG1]	FT Bagasse [EG2]	De Filippis et al, 2004*	Hamelick et al, 2003	Kreutz et al, 2008	Tijmensen et al, 2002	FT FP Slurry [EG1]	FT VP Slurry [EG1]
Feedstock		Bagasse	Bagasse	Bagasse	Willow wood	Switch- and mixed prairie grasses	Poplar wood	Pyrolysis slurry	Pyrolysis slurry
Gasifier type		Equilibrium	Equilibrium	Downdraft with Ni catalyst	Circulating Fluidised bed	GTI Fluidised bed	GTI fluidised bed	Equilibrium	Equilibrium
Temperature	K	1100	1100	1080	1123	1273	1255	1100	1100
Pressure	bar	1	1	1	1.32	29.9	34	1	1
Moisture content	wt%	5	5	11	15	15	15	16.25	16.25
Steam biomass ratio	wt/wt dry biomass	0.75	2.25	1.9	0.49	0.25	0.34	0.75	0.75
Oxygen biomass ratio	wt/wt dry biomass	0.36	0.36	0.26	0.31	0.30	0.30	0.36	0.36
CH ₄	mol%	0.082	0.032 (0.067)	0.003	0.074	0.047	0.082	0.048	0.043
CO	mol%	0.263	0.114 (0.239)	0.182	0.122	0.216	0.150	0.291	0.329
CO ₂	mol%	0.151	0.104 (0.218)	0.298	0.211	0.250	0.239	0.147	0.136
H ₂	mol%	0.236	0.226 (0.475)	0.517	0.201	0.325	0.208	0.270	0.247
H ₂ O	mol%	0.274	0.525 (0)	0.000	0.392	0.158	0.318	0.248	0.248
H₂/CO	mol ratio	0.90	1.98	2.84	1.65	1.50	1.39	0.93	0.75
Gasification efficiency	% LHV	74.7%	59.6%	57.0%	76.0%	77.3%	76.2%	63.0%	70.0%

* De Filippis et al, 2004, gives the dry gas composition, therefore the dry gas composition of EG2 is given in brackets for comparison.

Comparing the equilibrium gasifier gas compositions of EG2 to that measured for bagasse by De Filippis et al, 2004, the operating conditions are found to be similar, except for the significant difference in oxygen biomass ratio. This leads to a lower H₂/CO ratio, as reflected in the table.

Data for the Gas Technology Institute's high pressure fluidised bed gasifier was used by Kreutz et al, 2008 and Tijmensen et al, 2002. The negative effect of increased pressures on syngas compositions is largely outweighed by the positive effect of higher temperatures and lower equivalence ratios, compared to the results for EG1. In the case of Tijmensen et al, 2002, a higher syngas ratio is offset by the lower concentrations of H₂ and CO in the syngas. Kreutz et al, 2008 obtained a better syngas ratio, which could be explained by the secondary air that was injected to the gasifier freeboard. Nevertheless, these fluidised bed gasifiers are known to operate far from equilibrium and many factors will affect the syngas composition that cannot be explained by comparing it with equilibrium modelling. The most important conclusion here is that the syngas produced by the equilibrium gasifiers specifically optimised for bagasse compositions and practical considerations for use in the Fischer-Tropsch models of this study fall within the scope of actual measured data obtained for various biomass feedstocks. Furthermore, the gasification efficiencies are comparable with data from the literature.

In this study, the first equilibrium gasifier mode (EG1) that optimised both the syngas ratio and efficiency was modelled for all feedstocks, while the effect of optimising the gasifier for only the syngas ratio (EG2) was considered for bagasse. In addition, the effect of using EG1 for bagasse gasification in conjunction with a downstream shift reactor was also modelled. The detailed process modelling results for all scenarios are given in Appendix B4, and process flow diagrams are given in Appendix B5.

The gasification section accounts for 44 to 56% of the total **process energy**, when EG1 is used with no shift reactor (see Figure 4.11). This value nearly doubles when the syngas ratio is optimised with EG2. This is attributed to the high steam demand, which also has the effect of lowering the gasifier temperature, increasing the heat requirement of the gasifier. Additional data on the energy requirements for all scenarios are given in Appendix B4. The use of a shift reactor to increase hydrogen yields is clearly more energy efficient. Since the shift reactor product is combined with the recycle stream, the

process energy demand increases by about 8%, due to the higher energy demand of the reformer and recycle compressor. However, this is much lower than the 22% increase in total process energy experienced for the EG2 gasifier mode.

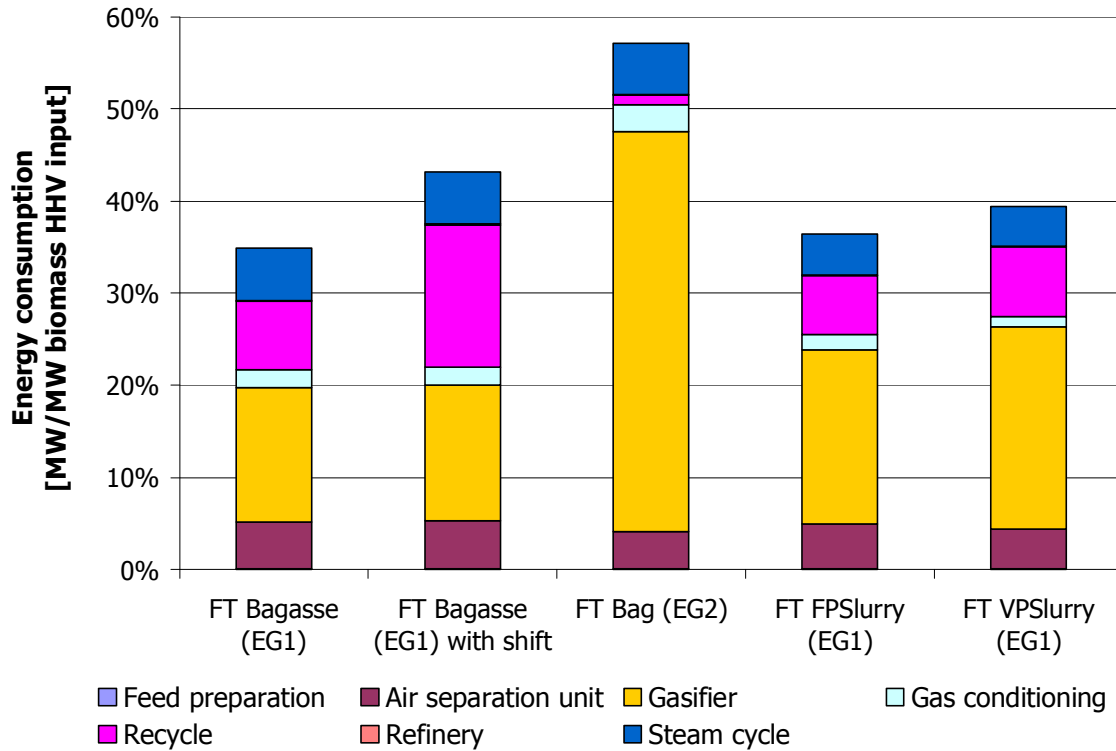


Figure 4.11 Total energy consumption of Fischer-Tropsch processes for different feedstocks and gasifier configurations.

Due to the higher gasification efficiency obtained for bagasse, the total process energy usage is lower compared to the pyrolysis slurry. This is also reflected in the higher thermal process energy efficiency of 59%, at a Fischer-Tropsch liquid energy yield of 40%, as shown in Figure 4.12 for bagasse (EG1). Although the pyrolysis slurry scenarios produced an equivalent amount of surplus electricity, and therefore reasonably high thermal process energy efficiencies, these scenarios were less efficient at producing liquid fuels, resulting in Fischer-Tropsch liquid energy yields between 35 and 36%.

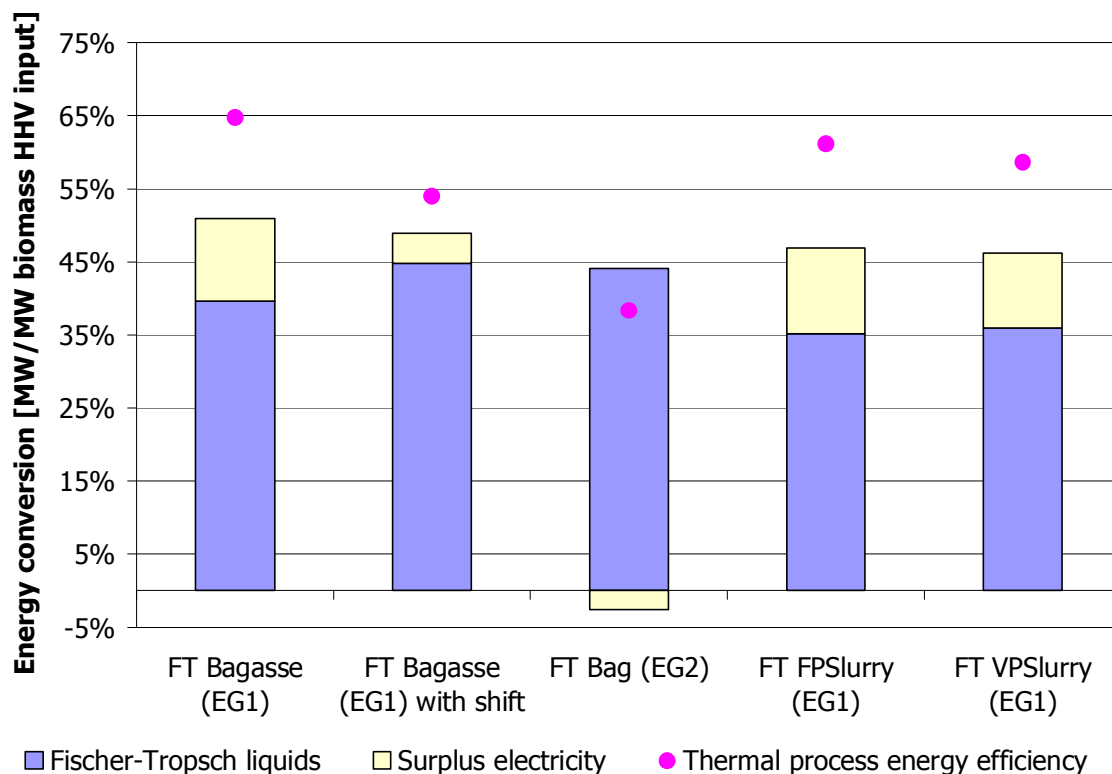


Figure 4.12 Process energy efficiencies for Fischer-Tropsch processing scenarios for different feedstocks. Thermal process energy efficiency = Energy in FT fuel/(1-Electrical energy/0.45).

Adjusting the H₂/CO syngas ratio to 2, either by manipulating the operating conditions of the gasifier (EG2) or by using a shift reactor (EG1 with shift) to maximise liquid fuel production for bagasse result in the same maximum liquid energy yield of 45%. However, the thermal **process energy efficiency** drops from 65% to 54% for a shift reactor, compared to 38% when EG2 is used. This follows from the significant process energy demand of the EG2 scenario, since the gasifier is endothermic in this case, requiring external electricity to supply the energy needs of the gasifier in addition to the increased steam demand. The decrease in energy efficiency using a shift reactor is mainly attributed to the higher energy demands of the recycle stream, as outlined in Appendix B4. If the shift reactor is excluded, the thermal process energy efficiency could therefore be increased by 10.7%.

Kreutz et al, 2008, reported a liquid fuel energy yield of 46%, at a thermal process energy efficiency of 59% using a high pressure gasifier with a shift reactor, which is slightly higher compared to this study. It has to be recognised that neither high pressure nor equilibrium gasifiers have been commercialised yet. However, Hamelinck et al, 2003 obtained a thermal process energy efficiency of 52% using actual data for atmospheric gasification with a shift reactor, which compares well with the result of 54% obtained from this study and confirms the assumption that equilibrium modelling can be successfully applied to study gasifier behaviour and integrated with downstream processing, since it yielded similar results to the experimental gasifier data used in literature.

A breakdown of the **heat integration** effects on the liquid fuel energy efficiency is also shown in Appendix A5 for the scenario using EG1 for bagasse without a shift reactor. It was found that integration of the process heat recovered in the process improved the liquid fuel energy efficiency by 6.7%, while the inclusion of a steam cycle with heat integration led to a total increase of 31%. Due to the significant amount of high quality heat available in the process, the use of a steam cycle to produce process and by-product electricity is therefore very beneficial and this is currently done in coal based Fischer-Tropsch processing.

4.6 CONCLUSIONS

4.6.1 Gasification Equilibrium Modelling

- Both oxygen and steam are required for biomass gasification if the aim is to produce Fischer-Tropsch liquids from the syngas.
- Since gasification with oxygen is exothermic, the gasifier temperature increases with increase in equivalence ratio. However, increasing the equivalence ratio beyond the carbon boundary point leads to over-oxidisation of the syngas and CO and H₂ will convert to CO₂ and H₂O until the syngas is fully combusted. In practice, over-oxidisation of biomass is necessary to obtain sufficiently high temperatures to favour kinetics and ensure complete gasification.
- For bagasse, it is reasonable to assume an equivalence ratio of 0.25 and operating temperature of 1100K to be sufficient. Although increased pressure can also ensure equilibrium conditions and complete gasification at lower equivalence ratios, the energy losses of downstream processing is too high if current state-of the-art wet gas cleaning is used.
- Steam gasification is endothermic and reduces the gasifier temperature, leading to the need for higher equivalence ratios to maintain the gasification temperature required by kinetics, which in turn decreases the useful syngas components due to partial combustion. However, steam gasification produces hydrogen-rich syngas due to the water-gas shift reaction.
- High moisture levels in the feedstock will have the same effect, but leads to lower gasification efficiencies since more energy is consumed to evaporate the moisture. For maximum gasification efficiencies, the moisture content of bagasse should therefore be minimised.
- At a bagasse moisture level of 5%, it was found that a steam biomass ratio of 2.25 would be required to obtain an H₂/CO ratio of 2 for Fischer-Tropsch synthesis at a gasification efficiency of 60% (EG2). This efficiency was lower compared to 75%

obtained for EG1, which produced a syngas ratio of 0.9 at a steam to biomass ratio of 0.75.

- It was found that, due to the higher carbon content of pyrolysis slurries, the carbon boundary temperatures of moisture-free slurries are higher compared to bagasse and the optimum efficiencies for slurry gasification are achieved at 16.25% moisture. The maximum gasification efficiencies for vacuum and fast pyrolysis slurry of about 63% and 70% was achieved using the EG1 mode, which is still lower than that obtained for bagasse. This theoretical limit in gasification efficiency is mainly attributed to the different compositions of these feedstocks. In order to achieve H_2/CO ratios of 2, steam to biomass ratios of 2.0 and 2.3 are required, resulting in gasification efficiencies of 58% and 60% for fast and vacuum pyrolysis slurry, respectively.
- The most important factors that negatively affect the gasifier duty were found to be the equivalence ratio and steam to biomass ratio. At increased equivalence ratios and steam biomass ratios, the gasifier becomes endothermic and heat has to be supplied to maintain the gasifier temperature. A minimum point was also observed for the gasifier duty with varying steam to biomass ratios, which represents the point at which the effect of increasing the syngas ratio (which decreases the gasifier duty) is overshadowed by the moderating effect of steam addition, which lowers the gasifier temperature and increases the gasifier duty.
- Finally, the equilibrium modelling results were compared with experimental data previously reported in literature for bagasse gasification and a good agreement was observed. This justified the use of the equilibrium gasification data for downstream Fischer-Tropsch modelling.

4.6.2 Fischer-Tropsch Process Modelling

- The gasifier data obtained from equilibrium modelling was found to be comparable with gasifier data previously used in literature to model Fischer-Tropsch processing.

- Gasification of bagasse resulted in higher Fischer-Tropsch liquid yields and higher overall process energy efficiencies compared to pyrolysis slurry gasification.
- The highest Fischer-Tropsch thermal process energy efficiency of 59% corresponded with the highest gasification efficiency of 75% for EG1 among the scenarios studied. However, this did not lead to the highest liquid yield, due to the lower syngas ratio produced by the gasifier and the exclusion of a shift reactor, which was used in all of the previous models that were discussed.
- An increase in Fischer-Tropsch liquid energy yield from 40% to 45% can be realised by adjusting the syngas ratio to 2, either by steam addition to the gasifier using EG2 or by the use of a shift reactor coupled with EG1. In both cases, the process energy efficiency will decrease due to higher process energy demand. Using a shift reactor is however far more energy efficient than optimising the gasifier, resulting in thermal process energy efficiencies 54% in the former and 38% in the latter.
- It was concluded that the thermal process energy efficiencies previously reported for Fischer-Tropsch synthesis from atmospheric biomass gasification with a shift reactor could be improved by 10.7% by not using a shift, although 5% less liquid fuel energy would be produced.
- The results obtained from this study compared well with data obtained from previous process models reported in literature, all of which used actual gasifier data as basis for models.
- The applicability of equilibrium modelling to study the effects of gasifier configuration on Fischer-Tropsch processing has been verified, and this approach can be successfully integrated with conventional process modelling for combined gasifier and process optimisation.

REFERENCES

- Altafini, C. R., P. R. Wander and R. M. Barreto (2003). "Prediction of the working parameters of a wood waste gasifier through an equilibrium model." *Energy Conversion and Management* 44: 2763-2777.
- Baratieri, M., P. Baggio, L. Fiori and M. Grigiante (2008). "Biomass as an energy source: Thermodynamic constraints on the performance of the conversion process." *Bioresource Technology* (doi:10.1016/j.biortech.2008.01.006).
- Channiwala, S. and P. Parikh (2002). "A unified correlation for estimating HHV of solid, liquid and gaseous fuels." *Fuel* 81: 1051-1063.
- De Filippis, P., C. Borgianni, M. Paolucci and F. Pochetti (2004). "Gasification process of Cuban bagasse in a two-stage reactor." *Biomass and Bioenergy* 27: 247-252.
- Hamelinck, C. N., A. P. C. Faaij, H. Den Uil and H. Boerrigter (2003). "Production of FT transportation fuels from biomass; technical options, process analysis and optimisation, and development potential." NWS-E-2003-08.
- Kreutz, T. G., E. D. Larson, G. Liu and R. H. Williams (2008). "Fischer-Tropsch Fuels from Coal and Biomass." 25th Annual International Pittsburgh Coal Conference.
- Mahishi, M. H. and D. Y. Goswami (2007). "Thermodynamic optimisation of biomass gasifier for hydrogen production." *International Journal of Hydrogen Energy* 32: 3831-3840.
- McBride, B. J. and S. Gordon (1996). "Computer Program for Calculation of Complex Chemical Equilibrium Compositions and Applications II User manual and Program description."
- McKendry, P. (2002). "Energy production from biomass (part 3): gasification technologies." *Bioresource Technology* 83: 55-63.
- Pellegrini, L. and S. De Oliveira Jr (2007). "Exergy analysis of sugarcane bagasse gasification." *Energy* 32: 314-327.
- Perry, R. H. and D. W. Green (1997). *Perry's Chemical Engineer's Handbook*, McGraw-Hill, Chapter 27.

Prins, M. J., K. J. Ptasinski and Janssen, F.J.J.G. (2003). "Thermodynamics of gas-char reactions: First and second law analysis." *Chemical Engineering Science* 58: 1003-1011.

Ptasinski, K. J., M. J. Prins and Janssen, F.J.J.G. (2007). "Exergetic evaluation of biomass gasification." *Energy* 32: 568-574.

Schuster, G., G. Löffler, K. Weigl and H. Hofbauer (2001). "Biomass steam gasification - an extensive parametric modeling study." *Bioresource Technology* 77: 71-79.

Tijmensen, M. J. A., A. P. C. Faaij, C. N. Hamelinck and M. R. M. v. Hardeveld (2002). "Exploration of the possibilities for production of Fischer-Tropsch liquids and power via biomass gasification." *Biomass and Bioenergy* 23: 129-152.

Van Bibber, L., E. Shuster, J. Haslbeck and M. Rutkowski (2007). *Baseline Technical and Economic Assessment of a Commercial Scale Fischer-Tropsch Liquids Facility*. DOE/NETL-2007/1260, National Energy Technology Laboratory.

Van Paasen, V. B., P. C. A. Bergman and P. A. Neeft (2002). "Primary measures for tar reduction, reduce the problem at the source." *Proceedings of the 12th European Conference and Technology Exhibition on Biomass for Energy, Industry and Climate Protection*.

Van Rossum, G., S. R. A. Kersten and W. P. M. v. Swaaij (2007). "Catalytic and Noncatalytic Gasification of Pyrolysis Oil." *Ind. Eng. Chem. Res.* 46((12)): pp 3959-3967.

Wang, L., C. Weller, D. Jones and M. Hanna (2008). "Contemporary issues in thermal gasification of biomass and its application to electricity and fuel." *Biomass and Bioenergy* doi:10.1016/j.biombioe.2007.12.007.

Zainal, Z. A., R. Ali, Lean, C.H. and Seetharamu, K.N. (2001). "Prediction of performance of a downdraft gasifier using equilibrium modeling for different biomass materials." *Energy Conversion & Management* 42: 1499-1515.

5. BIOLOGICAL AND THERMOCHEMICAL PROCESS ROUTES: COMPARISON OF TECHNICAL PERFORMANCE

SUMMARY

The technical performances of biological fermentation, pyrolysis and Fischer-Tropsch process routes for sugarcane bagasse were compared based on process modelling results previously described. Thermochemical processing of sugarcane bagasse to produce transport biofuels currently produces more liquid fuel energy since it utilises all the available biomass. The process energy efficiencies considering all the end products (liquid fuel and electricity) reported in literature for Fischer-Tropsch processes with the use of a shift reactor were comparable with the results from the shift reactor Fischer-Tropsch scenario in this study. A 2% increase in end product energy efficiency, or 10.7% increase in thermal process energy efficiency, can be obtained by excluding the shift reactor from the design. Compared to Fischer-Tropsch processing, there is significant scope for improvements in the end product energy efficiency of lignocellulosic bioethanol processes by increasing the liquid fuel conversion via enhanced fermentation yields and consolidated bioprocessing. Such improvements will result in end product energy efficiencies comparable to the highest values obtained for Fischer-Tropsch processing of around 50% when pressurised gasifiers are used, or the shift reactor is excluded. At an end product energy efficiency of about 70%, pyrolysis is a very efficient process for the production of crude bio-oil and char, although there are no clear energy benefits from producing transport biofuels via upgrading of pyrolysis oil compared to other processing options for transport fuels.

5.1 INTRODUCTION

Thus far, there has been limited research on the comparison of different biological and thermochemical process routes for the conversion of lignocellulose to liquid fuels. As mentioned before, Laser et al, 2009 compared fourteen mature technologies to identify the most promising scenarios for future development. Their results showed that integration of biological and thermochemical fuel production will ultimately result in the highest efficiency and lowest production costs. The scenario that performed the best applied lignocellulose bioethanol production via consolidated bioprocessing, with methane from the biogas being sold as a co-product, and the lignin-rich residue gasified in a high-pressure, oxygen blown gasifier followed by Fischer-Tropsch synthesis at a 80% single pass CO conversion with syngas recycle. This extensive process integration resulted in a process efficiency of 80%, of which 50% was from bioethanol production and the remaining 30% from Fischer-Tropsch processing.

For current state-of-art technologies, Gnansounou et al, 2005 considered different processing routes for sweet sorghum bagasse to either produce electricity or bioethanol in China. The scarcity value of renewable liquid fuels and the fact that electricity can be produced cheaper from other renewable energy sources, led to the conclusion that it would be more economical to produce bioethanol from the bagasse. Other process routes for renewable liquid fuels were not considered. Wright and Brown, 2007 reviewed a selection of processes to compare the economics of cellulosic ethanol to thermochemical production of methanol, hydrogen or Fischer-Tropsch fuels. Using data from their survey, they adjusted the plant scale, fuel gasoline equivalence, feedstock costs, capital financing and base year. It was found that hydrogen production via gasification currently has the highest fuel conversion efficiency of 50%, followed by Fischer-Tropsch fuels (46%), methanol (45%) and bioethanol (35%). However, pyrolysis was not considered, although this process requires substantially smaller capital investments and offers flexibility with operation. Although bio-oil upgrading to transport quality fuels is currently uneconomical (Bridgwater and Peacocke, 2000, Huber et al,

2006), the process can deliver high yields of a crude liquid biofuels for which a significant market exists.

The definitions used for energy efficiencies of biofuels processes in the literature are not consistent, as described in Chapter 1. This complicates comparison between results obtained from different studies, since the calculated values can vary significantly. Therefore, for the purpose of this study, the technical results were used to calculate three different energy efficiencies, and comparison between these, and data obtained from literature, is discussed.

5.2 COMPARISON OF RESULTS

5.2.1 Comparison of process modelling results from this study for all process routes

The different process efficiencies calculated for the best performing scenarios from this study producing bioethanol, pyrolysis oil or Fischer-Tropsch liquids are summarised in Table 5.1. The highest end product process energy efficiencies (liquid fuel + electricity and/or char) of 70% correspond to the production of crude bio-oil. The liquid fuel energy efficiency reflects the efficiency of a process to produce a liquid fuel, not taking the contribution of by-products into account, and in terms of this definition fast pyrolysis is the most efficient process for producing liquid biofuels at a liquid fuel energy efficiency of 67%.

Table 5.1 Comparison of energy efficiencies for bioethanol, pyrolysis and Fischer-Tropsch processing of sugarcane bagasse. Values in brackets are given for conversion of crude bio-oil to transport fuel (assuming 15% of energy in bio-oil is used for upgrading from Huber et al, 2006) and conversion of char to electricity (45% electrical conversion efficiency).

		ETOH- steam explosion (50% solids)	Fast Pyrolysis	Vacuum Pyrolysis	FT- bagasse (EG1)	FT- bagasse (EG1 with shift)	FT- bagasse (EG2)
Energy conversion to products							
Liquid fuel	$[\text{MW}_{\text{thermal product}} / \text{MW}_{\text{thermal input}}]$	30.5%	60.2% (45.2%)	40.6% (25.6%)	39.5%	44.8%	44.1%
Char/Lignin residue/Gas	$[\text{MW}_{\text{thermal product}} / \text{MW}_{\text{thermal input}}]$	25.3%	9.5% (0%)	27.6% (0%)	25.1%	9.2%	-5.8%
Electricity	$[\text{MW}_{\text{electricity product}} / \text{MW}_{\text{thermal input}}]$	11.4%	0% (4.3%)	1.8% (14.2%)	11.3%	4.1%	-2.6%
Process energy efficiencies							
Liquid fuel	thermal units	40.9%	66.5% (49.9%)	59.4% (37.4%)	52.8%	49.4%	41.5%
Liquid fuel + thermal energy	thermal units	55.9%	69.7% (54.7%)	72.2% (57.2%)	64.7%	54.0%	38.3%
Liquid fuel + electricity and/or char	mixed units	41.9%	69.7%	69.0%	50.9%	49.0%	41.5%

However, since crude bio-oil and char may be considered to be intermediate products compared to transport fuels and electricity, the process and liquid fuel efficiencies were also calculated for bio-oil upgrading to transport fuels and char upgrading to electricity. Huber et al, 2006, reported that bio-oil upgrading will reduce the process energy efficiency by up to 15%, as described in Chapter 3, and the conversion efficiency of char to electricity is assumed to be 45% (Hamelinck et al, 2005). The resulting energy efficiencies for production of transport fuels and electricity from pyrolysis are shown in brackets in Table 5.1.

Therefore, when all three process routes are considered for the production of the same final products, fast pyrolysis of bagasse should be nearly as efficient at producing transport biofuels compared to Fischer-Tropsch synthesis, although the liquid fuel energy efficiency of vacuum pyrolysis would be the lowest of all the other processes. However, if only the bio-oil was upgraded, and the char was sold as a by-product, the resulting energy contained in the upgraded oil and char will be similar to values obtained for bioethanol production and Fischer-Tropsch synthesis including the use of a shift reactor. This implies that, although the efficiency of liquid fuel production is similar to Fischer-Tropsch fuels, this comes at a greater process energy demand in the case of pyrolysis. Huber et al, 2006 stated that, although upgrading of bio-oil from pyrolysis is a promising alternative to other biomass conversion processes from an energy point of view, the costs are still too high and further development is required in this field. Currently, research on pyrolysis is focusing more on reducing the production costs of fast pyrolysis oil and applications of the crude oil product.

In addition, the thermal process energy efficiency of bioethanol production from sugarcane bagasse is currently competitive with Fischer-Tropsch synthesis based on the current process designs found in literature that make use of a shift reactor, although the Fischer-Tropsch thermal process energy efficiency can be increased by 10.7% if a shift reactor is excluded, which will make it more energy efficient than bioethanol production. For both thermochemical and biological processing routes, there is a maximum conversion of biomass energy to liquid fuel. Currently, the maximum obtainable liquid

conversion is 31% for bagasse enzymatic hydrolysis and fermentation, compared to 40-45% for Fischer-Tropsch fuels and 45% for upgraded fast pyrolysis oil, as shown in Table 5.1. The liquid conversion efficiency for the bioethanol process is low due to the high fraction of unfermentable lignin, as well as incomplete fermentation of pentose sugars based on current data.

5.2.2 Comparison of process modelling results for transport fuels production from this study with literature data

Figure 5.1 shows the ranges of end product process energy efficiencies (liquid fuel + electricity) calculated from the results of this study (blue bars) and data from process models found in literature for Fischer-Tropsch and bioethanol processes (orange bars).

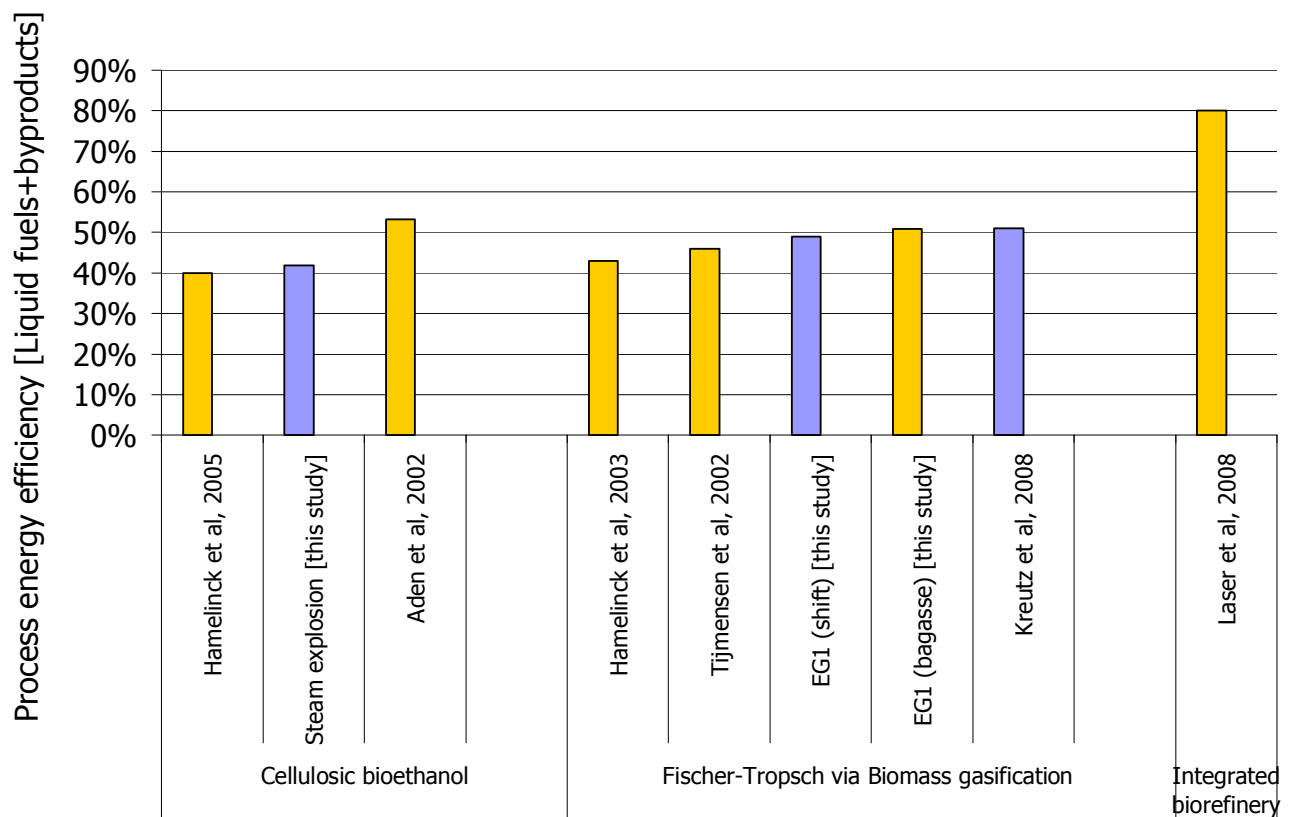


Figure 5.1 Typical ranges of end product process energy efficiencies for bioethanol and Fischer-Tropsch processes calculated from process models in literature and this study. The integrated biorefinery includes both bioethanol and Fischer-Tropsch facilities that operate at efficiencies of 50% and 30%, respectively (based on mature technology).

The data for cellulosic bioethanol obtained from Hamelinck et al, 2005, was based on dilute acid pretreatment of poplar wood, while that of Aden et al, 2002 was based on dilute acid pretreatment of corn stover. The results of this study lie between those of these two studies, and although the design of Aden et al, 2002 was based on pilot plant experience, they assumed a total conversion efficiency for corn stover to ethanol of 48.7%, which is a lot more optimistic than the data currently available for bagasse. However, this provides an indication of the effect that future developments will lead to, and given that the biological conversion yields can be improved to this extent, bioethanol processes will become as efficient as the best Fischer-Tropsch scenarios indicated in Figure 5.1 for pressurised gasifiers or atmospheric designs that exclude a shift reactor.

The range of end product energy efficiencies for Fischer-Tropsch processing shown in Figure 5.1 suggests that the scope for improvement in the energy efficiency of this process route is smaller. Although the exclusion of a shift reactor will lead to a significant increase in thermal process energy efficiency of 10.7%, with regards to the end product energy efficiency the only sensible use of the surplus thermal energy available in the Fischer-Tropsch reactor off-gas is to generate electricity for the process and sell the rest as a by-product. This was made clear from the significant increase of 30% in liquid fuel energy efficiency resulting from the inclusion of a steam cycle in the process design. This will lead to an increase in end product energy efficiency of about 2%, which is smaller than the potential 10% shown for bioethanol production.

Another, more important consideration regarding possible future developments is the option of a biorefinery. The maximum conversion of biomass to liquid fuels can be significantly increased by combining liquid fuels production from biological and thermochemical processing, as opposed to producing electricity from the lignin residue. Consequently, Laser et al, 2008 investigated possible process routes for integrated biorefineries producing both bioethanol and Fischer-Tropsch liquids. Assuming mature technology, they assumed that 50% of the biomass could be converted to bioethanol,

with an additional 10% conversion to Fischer-Tropsch fuels, and an additional 20% from biogas captured during water treatment in a bio-digester. The use of waste heat from the Fischer-Tropsch process for bioethanol production resulted in an overall process energy efficiency of 80%. The main technological advances that would be required to achieve this included more effective pretreatment, the development of consolidated bioprocessing, increased fermentation yields, biomass feeding to a high pressure gasifier with complete tar cracking and advanced process heat integration. This configuration would only be viable if the residues from several bioethanol plants were transported to a central Fischer-Tropsch facility for favourable economies of scale. The question arises whether it would be more economical to rather feed the lignin residue to a fast pyrolysis plant adjacent to the bioethanol plant for the production of crude bio-oil.

It is therefore clear that, when comparing different process routes, the various types of efficiencies need to be considered, since the conclusions could vary depending on the objective of the comparison, namely 1) **which is the most energy efficient process route, or 2) which process route will produce liquid fuels more efficiently, and 3) what is the maturation state of the process?**

The results from this study suggest that thermochemical processes are currently more efficient for producing liquid fuels only, although the thermal process energy efficiencies of bioethanol and Fischer-Tropsch processing are similar. Pyrolysis is very efficient if crude bio-oil is considered, but further upgrading does not offer significant advantages over other process routes for transport fuels.

Fischer-Tropsch processing of syngas from biomass gasification is currently close to commercialisation. Choren has successfully demonstrated wood gasification to produce Fischer-Tropsch diesel at a 45MW input facility, and the full-scale commercial plant producing is set to start operation in 2012 (Van der Drift, 2002). FZK has is also developing a process for the gasification of fast pyrolysis slurry that will be obtained from 100MW pyrolysis plants fed with straw and wood waste to produce Fischer-Tropsch fuels (Van der Drift, 2002). In their case, however, the growth density of the biomass

was found to be important for the feasibility of this process. Although the overall process energy efficiencies will be lower compared to direct biomass gasification, the feeding of slurry to a gasifier is practically less complicated, and this option might prove to have economical advantages since a more energy dense feedstock is transported. As for bioethanol, the first commercial cellulosic bioethanol plant is located in Spain, which operates at an input capacity of 15MW agricultural residues (www.abengoabioenergy.es). Pyrolysis has been commercial for years, and Dynamotive Energy systems Corporation is currently producing biochar and crude pyrolysis oil in Ontario (www.dynamotive.com).

5.3 CONCLUSIONS

- The production of residual fuel oil via pyrolysis is very attractive from a process and liquid energy efficiency point of view, and fast pyrolysis achieved the highest thermal process energy efficiency of 70% and liquid fuel efficiency of 67% for crude bio-oil.
- The upgrading of crude bio-oil to transport fuels will result in a lower thermal process energy efficiency of about 55% compared to 65% that can be obtained for Fischer-Tropsch fuels if no shift reactor is used.
- For the production of transport biofuels, thermochemical processing currently produces more liquid fuel energy than biological fermentation due to the higher conversion of biomass to liquids. Compared to the liquid fuel efficiencies of 50-53% that could be obtained by thermochemical production of transport fuels via pyrolysis or Fischer-Tropsch synthesis, the maximum liquid fuel efficiency of bioethanol from sugarcane bagasse is currently 41%, due to the large portion of unfermentable sugars in the feedstock.
- However, the thermal process energy efficiency of bioethanol production could become comparable with Fischer-Tropsch processing if the fermentation yields for bagasse were increased from 31% to 48%, which could be further increased to 50% with the development of consolidated bioprocessing.
- It is therefore concluded that fast pyrolysis is a promising process for the production of crude bio-oil from sugarcane bagasse to replace residual fuels in the current energy market.
- For the production of transport fuels, there is significant scope for improvement of the liquid fuel energy efficiency of bioethanol processing to become comparable with gasification followed by Fischer-Tropsch synthesis. However, thermochemical processes currently have higher liquid fuel energy efficiencies, since all the lignin is also utilised for conversion to liquid fuels.
- Integrated biorefineries that combine biological fermentation and thermochemical processing could lead to further enhanced process efficiencies, and there is merit in evaluating the integration of bioethanol and pyrolysis processes for future development.

REFERENCES

Bridgwater, A. V. and G. V. C. Peacocke (2000). "Fast pyrolysis processes for biomass." *Renewable and Sustainable Energy Reviews* 4: 1-73.

Gnansounou, E., A. Dauriat and C. E. Wyman (2005). "Refining sweet sorghum to ethanol and sugar: economic trade-offs in the context of North China." *Bioresource Technology* 96: 985–1002.

Hamelinck, C. N., G. v. Hooijdonk and A. P. Faaij (2005). "Ethanol from lignocellulosic biomass: techno-economic performance in short-, middle- and long-term." *Biomass and Bioenergy* 28: 384-410.

Huber, G. W., S. Iborra and A. Corma (2006). "Synthesis of Transportation Fuels from Biomass: Chemistry, Catalysts, and Engineering." *Chemical reviews* 106: 4044-4098.

Laser, M., E. D. Larson, B. E. Dale, M. Wang, N. Greene and L. R. Lynd (2008). "Comparative analysis of efficiency, environmental impact, and process economics for mature biomass refining scenarios." *Biofuels, Bioproducts and Biorefining* 3: 247-270.

Van Der Drift, A. (2002). "An overview of innovative biomass gasification concepts." *Proceedings of the 12th European Conference and Technology Exhibition on Biomass for Energy, Industry and Climate Protection*.

Wright, M. M. and R. C. Brown (2007). "Comparative economics of biorefineries based on the biochemical and thermochemical platforms." *Biofuels, Bioproducts and Biorefining* 1: 49-56.

www.abengoabioenergy.es. 20 November 2009.

www.dynamotive.com. 20 October 2009.

6. ECONOMIC MODELLING FOR BIOETHANOL, PYROLYSIS AND FISCHER-TROPSCH PROCESS ROUTES

SUMMARY

An economic evaluation was performed for various process scenarios previously modelled for bioethanol production, pyrolysis and Fischer-Tropsch synthesis using AspenIcarus[®] software. For bioethanol production from bagasse, steam explosion pretreatment is currently the most economical process and will result in a production cost of \$23.0/GJ at a feedstock price of \$52.2/t for a 600MW plant. For Fischer-Tropsch fuels, the cost of optimising the syngas ratio by steam addition to the gasifier or use of a shift reactor to maximise liquid yields is not economical. Also, gasification of pyrolysis slurries cannot compete on an economic basis with bagasse gasification. The production cost of Fischer-Tropsch fuels is lower than for bioethanol at \$21.6/GJ. Fischer-Tropsch processes require larger capital investments and produce less petrol equivalent products compared to bioethanol, resulting in lower returns. Pyrolysis plants require the lowest capital investment and deliver the highest internal rate of return of 34.2% and 40.5% for fast and vacuum pyrolysis, respectively, which corresponds to return on investments of 29.4% and 37.6%, respectively. Bioethanol with steam explosion leads to an internal rate of return of 14.4%, and this increases to 17.3% at a feedstock price of \$30/t. The return on investment for both bioethanol and Fischer-Tropsch process routes were not found to be attractive based on the current market, although expected increases in product prices could drastically change this outlook. The internal rate of return of Fischer-Tropsch processing is 11 to 16%, depending on the crude oil price.

6.1 INTRODUCTION

The increasing political drive towards promoting biofuels as a replacement for conventional fossil based fuels has led to fast-tracked developments in these technologies to improve the efficiency and economic prospects and attract potential investors. Nevertheless, commercialisation of second generation biofuels is still in its initial stages and with so many technologies available, it is often hard to distinguish the most promising options as so many factors play a role, including the country, target market and future developments.

Economic modelling is a tool often used to perform feasibility studies for new processes that have not been commercialised yet. Several studies have performed detailed economic analyses of either bioethanol, pyrolysis or Fischer-Tropsch processes. For example, Aden et al, 2002, investigated the economics of a corn stover bioethanol process using dilute acid pretreatment. They provided vendor quotes for specialised equipment and process specific units, and they calculated a production cost of \$13.4/GJ. Hamelinck et al, 2005, also compared the economics of bioethanol processes and estimated the production cost of bioethanol via dilute acid pretreatment of wood at \$22/GJ. Ringer et al, 2006, obtained a breakeven bio-oil price of \$7.62/GJ for fast pyrolysis of wood. A number of studies have developed process and economic models for gasification processes, although only some have considered Fischer-Tropsch synthesis applications. Tijmensen et al, 2002, reported Fischer-Tropsch liquid production costs in the range of \$13-\$30/GJ, depending on the process design used and assumed Fischer-Tropsch synthesis yields, and found that pressurised systems resulted in the lowest production costs. Kreutz et al, 2007 also compared coal and biomass gasification for Fischer-Tropsch synthesis and calculated a production cost of \$25.5/GJ for Fischer-Tropsch liquids from biomass.

However, all these previous studies have focused on one specific process route, i.e. either bioethanol production, pyrolysis or gasification. Wright and Brown, 2007 and Huber et al, 2006 published reviews comparing economics of different processes but did

not perform detailed economic modelling. It is difficult to compare economic results from different studies directly due to different biomass sources, cost data applicable to different countries, and process design assumptions, as some studies considered nth plant and others 1st plant technology. In this study, the economic models were based on process models developed for sugarcane bagasse, and cost data was obtained from various sources of literature and selected based on 1st plant technology with a conservative outlook. Although the results from the process models would apply to any location, since it was based on experimental data obtained from various authors and not specific to South African conditions, the results from the economic models are applicable only to South Africa. All the price data for feedstocks and products, biomass availability and transport was applicable to South Africa, and the biomass availability was based on the South African sugar industry. Furthermore, all the settings in AspenIcarus[®] were set to reflect the African context, which adjusts all the location specific data for the project. An extensive knowledge base is available in AspenIcarus[®] that adjusts import freight and taxes, workforce wages and productivity, contingencies, material costs, typical levels of equipment rental and locally versus imported items, etc. In addition, assumptions for investment parameters such as tax and interest rates were also applicable to South Africa.

6.2 METHODOLOGY

The mass and energy balances obtained from the AspenPlus[®] process models described in Chapters 3 and 4 were used to develop an economic model for each scenario using AspenIcarus[®], combined with cost data obtained from literature. Based on their technical performances, the most promising processes were selected for evaluation, as the scenarios that were found to be highly energy inefficient did not warrant further investigation.

The cost data for feedstocks, products and utilities are given in Table 6.1. An exchange rate of 7.5 \$US/ZAR is assumed throughout. The cost of \$62.4/t (\$3.6/GJ) assumed for bagasse is relatively high, compared to that used by previous studies. Aden et al, 2002 and Ringer et al, 2006 both assumed \$30/dry ton for corn stover and wood chips, respectively. However, Kreutz et al, 2008 assumed a cost of \$5/GJ for herbaceous biomass, which included the collection costs for mixed prairie grasses in the United States. Bagasse is an agricultural residue and since the cost of harvesting has already been incurred by the sugar mill, the price should be similar to corn stover. However, the sugar industry considers bagasse as an energy source due to its current application as a boiler fuel, making it more expensive. The detailed general specifications and investment parameters are given in Appendix C1. The investment analysis was based on a 25 year project with 8000 operating hours per year, a tax rate of 30.5% and interest rate of 15.1%. The interest rate was calculated as a weighted average between the prime interest rate of the South African Reserve Bank for July 2009 of 11%, plus 2%, and a desired rate of return to shareholders of 20%, based on a debt/equity ratio of 70:30.

Table 6.1 Cost data for feedstocks, products and utilities (USD₂₀₀₉)

Feedstock			
Coal ¹	3.6	\$/GJ	98.7 \$/t
Bagasse ²	3.6	\$/GJ	62.4 \$/dry t
Cane trash ³	1.8	\$/GJ	31.2 \$/dry t
Products			
Bio-oil ⁴	7.4	\$/GJ	150 \$/kg
Char ⁵	3.6	\$/GJ	98.7 \$/t
Fischer-Tropsch gasoline ⁶	20.9	\$/GJ	705 \$/m ³
Fischer-Tropsch diesel ⁷	19.5	\$/GJ	681 \$/m ³
Ethanol ⁸	20.9	\$/GJ	488 \$/m ³
Electricity ⁹			0.08 \$/kWh
Utilities			
Cooling water ¹⁰			6.96 \$/m ³
Instrument air ¹⁰			0.006 \$/m ³

¹ Provided by local sugar industry.

² Since bagasse is used as a replacement for coal in the sugar mills, the price of bagasse is set equal to that of coal on an energy basis, which equals \$3.6/GJ. Coal HHV=27.5 MJ/kg, Bagasse HHV = 19 MJ/kg.

³ Although cane trash has an energy value similar to bagasse, it is often burned before cane harvesting, which has a negative impact on sucrose yields and the environment. The price of trash is assumed to be half that of bagasse, as it is not currently used for its fuel value.

⁴ As described by Ringer et al, 2006, the selling price of bio-oil varies depending on the quality, and can either be compared to distillate fuel (#2) which sold for \$10.12/GJ in 2000, or residual fuel oil (#6) which sold for \$4.75/GJ. The average crude oil price in 2000 was \$27/barrel, compared to the current level of \$70/barrel. To obtain a likely selling price for bio-oil, a direct linear relationship between the price for fuel oil (#6) and crude oil is assumed, and the bio-oil price is set at 60% of that value, due to uncertainties in the bio-oil market, resulting in a bio-oil price of \$7.40/GJ.

⁵ It is assumed that char could replace coal as an energy source and would achieve the same price.

⁶ The fuel price data for South Africa was obtained from www.dme.gov.za, based on prices in July 2009. On top of the basic petrol price of R3.79/litre, a fuel tax exemption of R1.50/litre applicable for biofuels is added to obtain the Fischer-Tropsch fuel selling price. An exchange rate of \$7.5 US/ ZAR is assumed.

⁷ Same as above. The basic diesel price was R3.76/litre, with a fuel tax exemption of R1.35/litre.

⁸ As a replacement for petrol in the South African transport sector, the price of ethanol can be set equal to the energy equivalent price of petrol, including the tax exemption. 1 kg of ethanol=0.63 kg petrol_{energy basis}.

⁹ Provided by local industry. The electricity rate is equal to R0.60/kWh, 20% higher than the current Eskom rate of R0.504/kWh, which a reasonable rate for green electricity.

In general, the equipment costs for pumps, heat exchangers, flash drums, standard tanks, etc. were estimated using AspenIcarus[®], since costs for these were found to be similar to those reported in literature. A list of these components and their mapping specifications in AspenIcarus[®] for each process route is given in Appendix C2.

The Icarus Evaluation Engine contains a knowledge base of design, cost and scheduling data, methods and models to generate preliminary equipment designs and simulate vendor-costing procedures to develop detailed Engineering-Procurement-Construction (EPC) estimates. Unlike the factored estimation methods normally used in feasibility study level cost estimations, volumetric models are used to produce the quantities of pipe, valves, concrete, steel, and instruments identified by the associated equipment or area. In addition, the required man-hours to produce equipment and install the bulks are produced by craft and engineering discipline. An extensive, proprietary knowledge base also exists that contain site-specific data, such as import freight and taxes, workforce wages and productivity, typical levels of equipment rental and locally versus imported items, etc. For example, the database contains craft workforce wage and productivity rates for each code of account (applicable to each type of craft) and this is used to calculate the total labour costs. Although it is possible that there could be errors in some of these cost items, any possible deviations from reality would be reflected to a similar extent for all the economic models, and it was therefore accepted to be sufficient for the purposes of first level cost estimations.

The base costs for major sections such as air separation units and key equipment units such as boilers and reactors were obtained from a critical review of the literature. A detailed discussion of the considerations for each of these units is also given in Appendix C2, along with a breakdown of their calculated base costs. The CEPCI was used to escalate quoted costs to 2006, since the cost libraries in AspenIcarus[®] was based on 2006, and the total project cost was escalated by AspenIcarus[®] to the specified start date of engineering, 1 January 2010. Scale factors from literature were used to scale quoted equipment to the required size, as shown in Appendix C2. In most cases, built-in installation factors were used to calculate the installed costs, apart from a few

exceptions where there were discrepancies between the AspenIcarus[®] and literature data, in which cases the literature data was used. In some cases, cost data was only available for whole sections, such as feedstock handling, gasifier and gas cleanup sections, refineries, etc, and a custom database with the total installed costs was created in the AspenIcarus[®] equipment model library. More information on all the data used for installation factors and custom database items can be found in Appendix C2.

6.2.1 Feedstock Availability and Delivery Costs

6.2.1.1 Bagasse Supply

The bagasse data was based on a sugar mill located in Mpumalanga that has a cane throughput of 500 tons per hour. The mill produces about 125 tons wet bagasse per hour at 46% moisture. At the moment, the 32 bar low efficiency boiler consumes 87% of this bagasse. However, it has been shown that, with the use of high pressure and high temperature boilers coupled with cogeneration systems, the potential bagasse surplus is 40% (Alonso et al, 2006), while Botha and Von Blottnitz, 2006 assumed a bagasse surplus of 47% in their study using South African data. In addition to this, sugarcane trash and bagasse are produced in roughly equal amounts (Alonso et al, 2006). Therefore, if about half the cane trash were harvested and mixed with bagasse for boiler feed, a surplus of 42% bagasse would be available to feed a 145 MW liquid biofuel plant located next to the sugar mill, at a reduced cost of \$46.5/t feed due to the lower cost of cane trash. These calculations are tabulated in Appendix C1.

6.2.1.2 Plant Scale and Delivery Distance

Economies of scale also play an important role in the economic viability and 145 MW is a relatively small scale. Other studies have used base scales ranging from 367 MW to 660 MW (Tjmensen et al, 2002, Kreutz et al, 2008, Aden et al, 2002 and Hamelinck et al,

2003). Therefore, each scenario was also evaluated at 600 MW, which would require bagasse to be delivered from a number of plants to a central biofuel processing facility.

According to Botha and Von Blottnitz, 2006, the average sugarcane yield in South Africa is 65 tons per hectare. Based on our mill data, each ton of crushed sugarcane produces 0.25 tons of wet bagasse. Assuming 38 crushing weeks in one 12 month cycle and that all the trash is also harvested; one can calculate that a 600 MW plant would require 1.45 million tons of sugarcane residues per year. Our data indicates that one mill can supply 0.77 million tons of surplus bagasse and trash per year, therefore two such mills could supply a 600 MW plant. A map of the northern sugarcane region in South Africa and the locations of the sugarcane mills in that area are given in Figure 6.1. The distance between two of the largest mills that do not have adjacent refineries that consume additional bagasse is 90.6km, which is the average travelling round trip travelling distance assumed for this analysis if the plant is located between the mills.

6.2.1.3 Transport and energy costs of delivery

For scales larger than 145MW, the cost of transport will affect the process economics. The influence of energy and transport costs for feedstock delivery over a range of distances is shown in Figure 6.2. Mauviel et al, 2008, performed a similar assessment for wood chips and assumed that trailers would be used for transport. Based on a trailer volume of 31m³ with a maximum load of 25 tons, and assuming a fuel consumption of 30ℓ per 100 km and bagasse density of 176 kg/m³, one truck can transport 5.46 tons of bagasse per trip. This translates to an energy cost of 0.18 MJ/kg bagasse for a 600 MW plant, which is not significant considering that the higher heating value of bagasse is 19 MJ/kg. The energy cost of pyrolysis slurry delivery to a Fischer-Tropsch facility is even lower. On the other hand, the transport fuel costs are significant. Assuming a fuel price of R8/ℓ (\$1.07/ℓ), the cost of one round trip would be \$5.4/t bagasse. This constitutes 12% of the on-site bagasse cost price and raises the assumed base cost of delivered bagasse for a 600 MW plant to \$52/t. For the pyrolysis slurry, the delivered feedstock cost for a 600MW plant is \$48/t. All data for these calculations are given in Appendix C1.

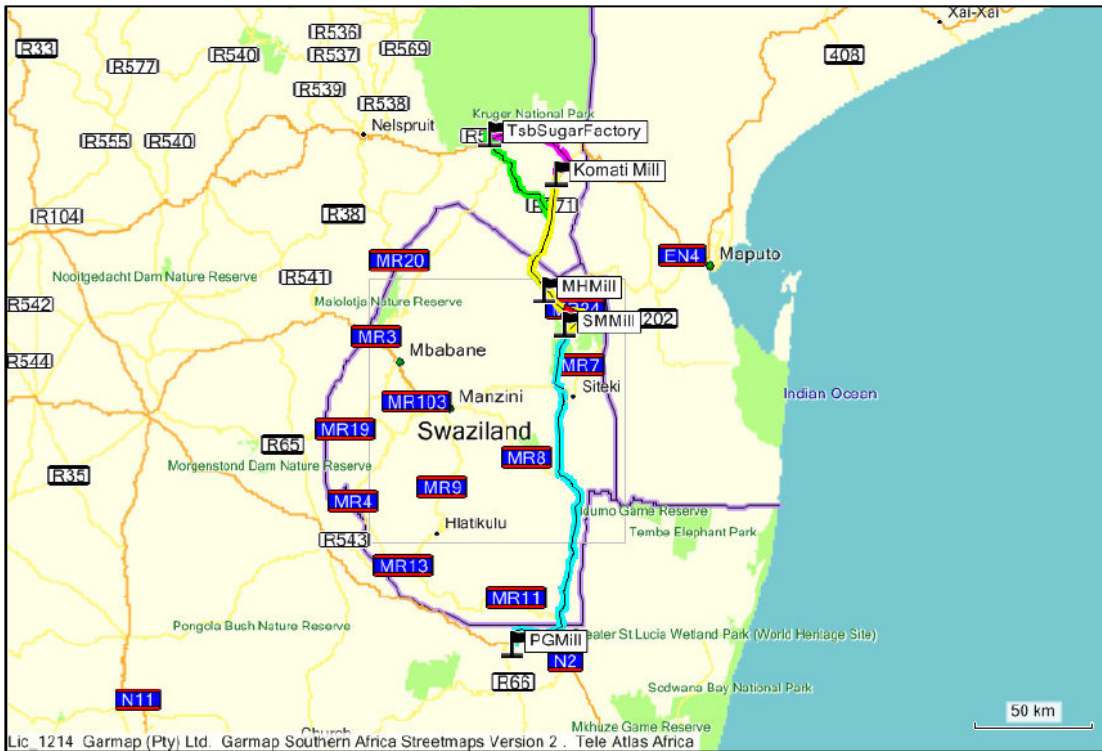


Figure 6.1 Map of sugar mills in northern region of South Africa (Garmap Pty Ltd.).

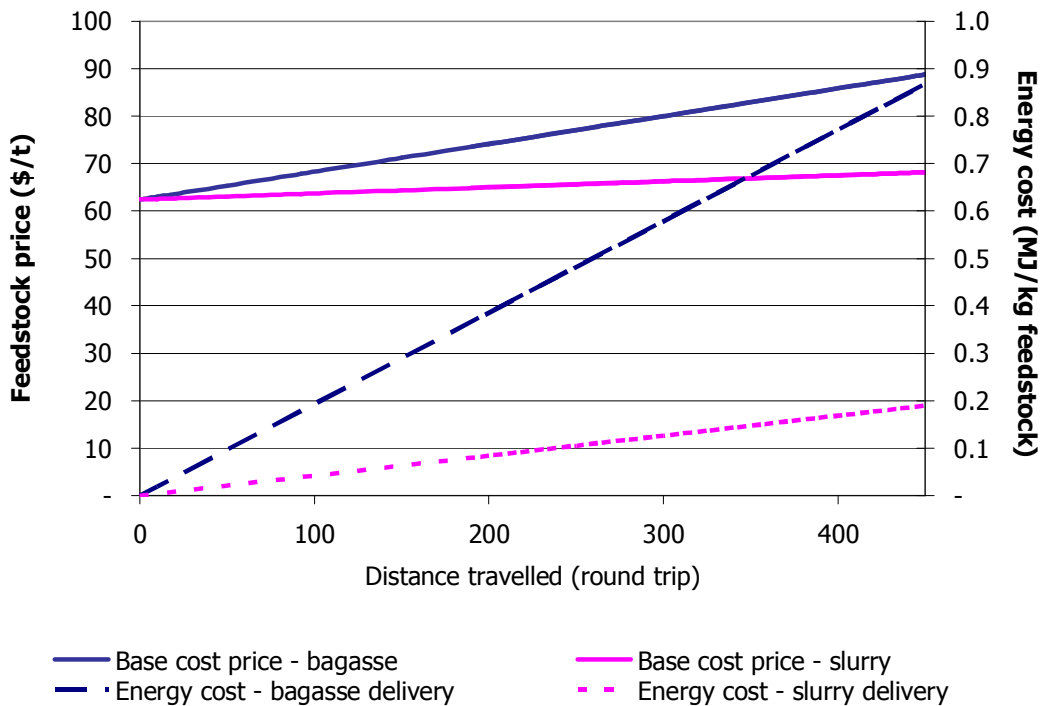


Figure 6.2 Effect of feedstock delivery distance on energy costs and feedstock prices of bagasse and pyrolysis slurry.

6.2.2 Process Equipment and Operating Costs

Based on the process modelling results, the two bioethanol processes that were energy self-sufficient, i.e. those using the steam explosion and dilute acid pretreatment at 35% solids, were investigated. A detailed list of process equipment and the cost data for quoted equipment is given in Appendix C2.

In all cases, the labour costs are calculated by AspenIcarus[®]. For bioethanol, the additional operating costs included the cost of chemicals and disposal fees, as summarised in Table 6.2. According to a market study performed by First Uranium Corporation for a new acid plant, future price projections up to 2014 for sulphuric acid ranged between \$170 and \$265/t (Tait, 2008); therefore a value of \$200/t was assumed for this study. Aden et al, 2002 assumed a purchased cellulase price of \$0.10/gallon ethanol based on negotiations with enzyme suppliers, while Hamelinck et al, 2005 assumed a price of \$0.50/gallon ethanol for the short term, decreasing to \$0.17/gallon ethanol in the medium term. Since then, significant advances have been made in enzyme cost reductions and researchers have made significant progress in developing an enzymatic yeast (personal communication). Given these factors, an enzyme price of \$0.20/gallon ethanol is assumed, which should still be conservative, although a sensitivity analysis was performed at \$0.50/gallon.

Table 6.2 Operating costs for bioethanol scenarios

Sulphuric acid	200	\$/t
Cellulase	0.20	\$/gal EtOH
Corn steep liquor	177	\$/t
Ash disposal	21	\$/t
Lime disposal	21	\$/t

Based on the default value given in AspenIcarus[®], the operating supplies for the pyrolysis processes are assumed to be 25% of the maintenance cost. For the Fischer-Tropsch scenarios, the annual cost of dolomite was based on a consumption of 0.3 kg/kg dry feedstock and a price of \$50/t, while wet gas cleaning costs, including waste

water treatment and sodium hydroxide consumption was assumed to be 0.5% of the total capital investment (Hamelinck et al, 2002).

6.3 ECONOMIC MODELLING RESULTS AND ANALYSIS

A summary of all the economic results is given in Appendix C3. All costs are given in \$US 2009. In order to compare the different fuels on a common basis, the liquid fuel production costs are expressed in \$/GJ fuel. The fuel production costs can also be expressed in relation to the breakeven oil price (BEOP), which represents the price of crude oil at which wholesale prices for petroleum derived fuels would equal the production costs of the equivalent finished biofuel. This method was described by Kreutz et al, 2007, and the wholesale margin of \$0.227 (R0.45, www.dme.gov.za) for the petroleum derived fuel is subtracted from the biofuel production costs to obtain the BEOP. This analysis is not performed for bio-oil, since it is not a transport fuel.

6.3.1 Capital Investment

The contribution of each processing section to the total capital investments for the bioethanol, pyrolysis and Fischer-Tropsch scenarios are given in Figures 6.3, 6.4 and 6.5, respectively. For bioethanol production, it was found that steam explosion pretreatment resulted in the lowest capital investment of \$432.9 million for the 600MW scenario, while that of dilute acid pretreatment was 24% higher. In addition, the benefit of economies of scale is evident from the significant decrease of roughly 35% in specific capital investment (SCI) for a 600MW plant compared to the smaller scale 145MW plants. The boiler steam cycle contributes between 40% and 58% of the total capital investment. For the dilute acid process, the pretreatment section is as expensive as the boiler cycle, due to the higher cost of liquid solids separation associated with the lower solids loading during pretreatment.

The specific capital investment costs for the 600MW dilute acid and steam explosion scenarios, of \$3000/kW and \$2430/kW ethanol, respectively, compare well with those obtained from previous studies. By inflating and scaling the data of Hamelinck et al, 2005 using an overall scaling factor of 0.7 (based on the results of the current study), the SCI values of their dilute acid (short term) and steam explosion (medium term) processes are \$4113/kW and \$2280/kW ethanol, respectively. Likewise, the data of

Aden et al, 2002 reflect an SCI of \$1747/kW ethanol, which is mainly lower due to the higher ethanol conversions assumed in their process model.

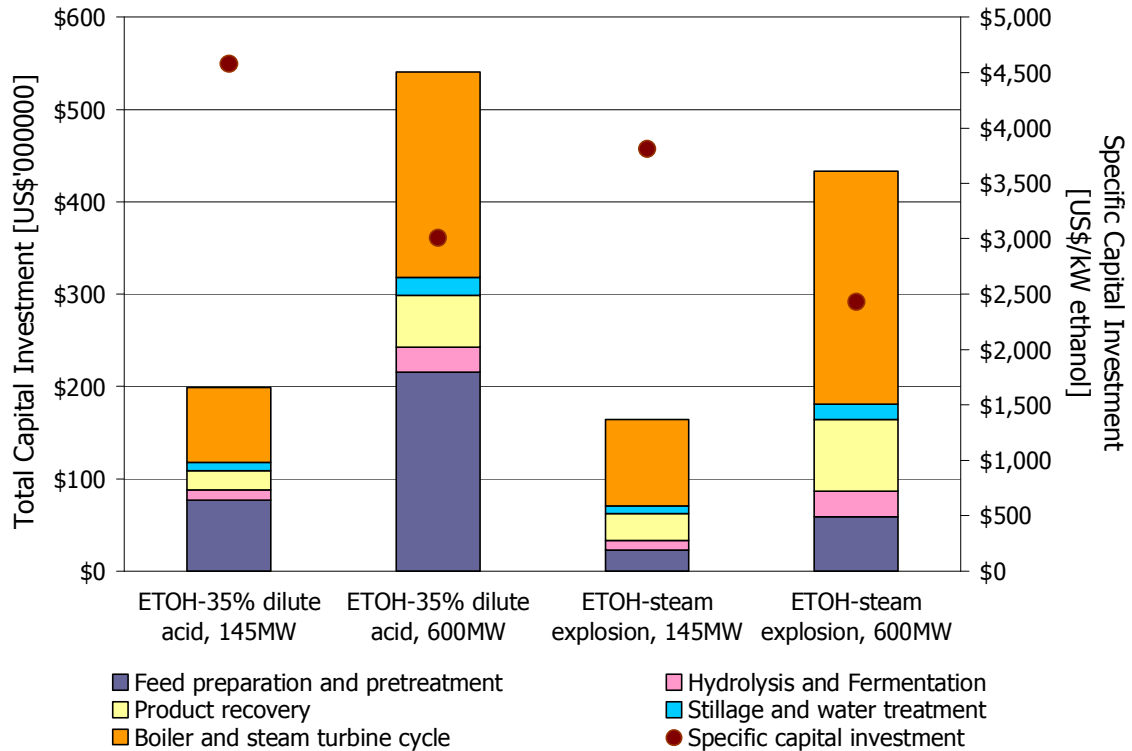


Figure 6.3 Breakdown of capital investment costs for bioethanol scenarios (\$US₂₀₀₉).

The capital investment (TCI) required for a pyrolysis plant is about one third that of a bioethanol plant, since bio-oil is a crude product and there is no included cost of refining. A 600 MW fast pyrolysis plant will cost \$141.7 million, which is 12% higher than the \$126.4 million estimated for vacuum pyrolysis (see Figure 6.4). According to Huber et al, 2006, crude upgrading of atmospheric flash pyrolysis oil followed by product refining would require an additional capital investment of roughly \$300 million, in 2006 terms, although this cost may have been lowered due to recent developments. Nevertheless, it is interesting to note that this value would result in very similar total capital investments for bioethanol and pyrolysis. Fast pyrolysis requires a larger heat recovery and steam turbine cycle due to the higher operating temperature of the pyrolysis reactor.

The effect of economies of scale is even more pronounced for pyrolysis compared to bioethanol processes, and a reduction in SCI of between 44% and 51% was observed when increasing the scale from 145MW to 600MW. Furthermore, the SCI for fast pyrolysis is significantly lower than vacuum pyrolysis, due to the much higher bio-oil yield of fast pyrolysis.

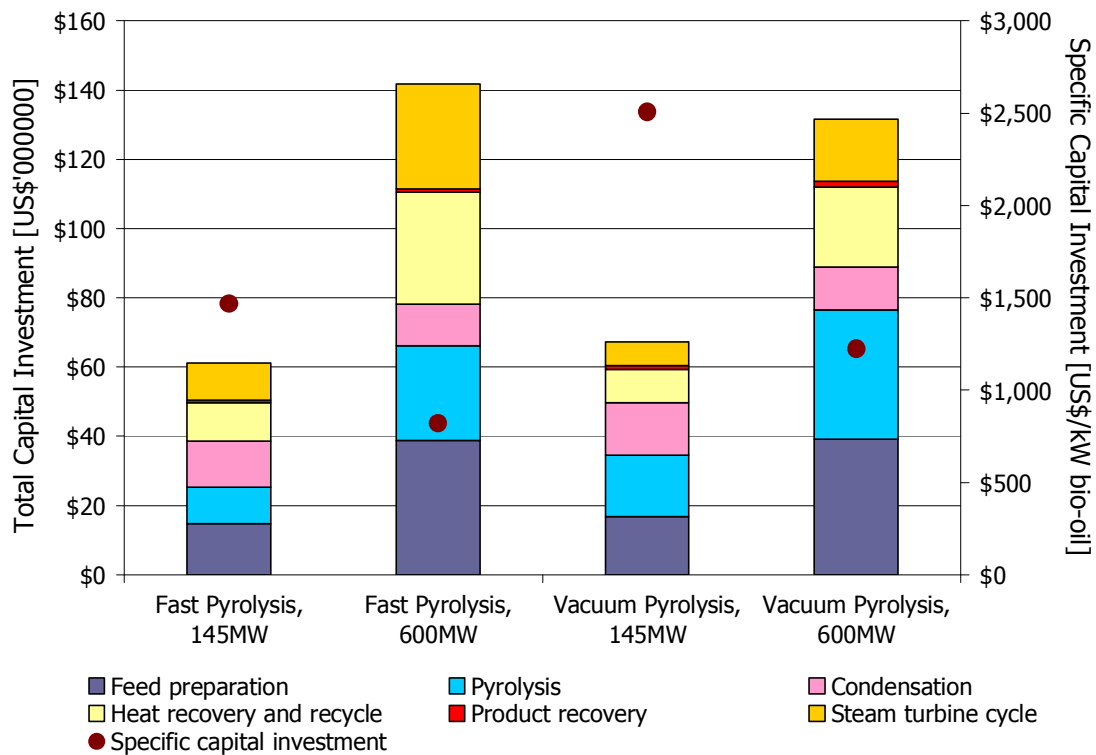


Figure 6.4 Breakdown of capital investments for pyrolysis processes (\$US₂₀₀₉).

From the results published by Ringer and Putsche et al, 2002, the current day specific capital investment would be in the region of \$890/kW bio-oil product for a 127 MW fast pyrolysis plant using wood as feedstock, which is comparable to our 600MW fast pyrolysis scenario at an SCI value of \$821/kW bio-oil.

The total capital investment for a 600 MW Fischer-Tropsch synthesis plant ranged between \$732.9 and \$820.2 million (see Figure 6.5), which is at least 70% more expensive than a cellulosic bioethanol plant, although it yields up to 50% more energy in

liquid fuels. Nevertheless, the specific capital investment is still higher: between \$2640/kW and \$3116/kW Fischer-Tropsch fuel compared to \$2430/kW ethanol for steam explosion pretreatment. The use of a shift reactor to maximise the Fischer-Tropsch liquid yield will double the cost of gas conditioning, while the same increase in liquid yields can be obtained by optimising the gasifier at no additional capital cost. However, operating the gasifier in the G2 mode to produce the optimum syngas ratio of 2 was shown to lead to much lower energy efficiencies in Chapter 4 and 5.

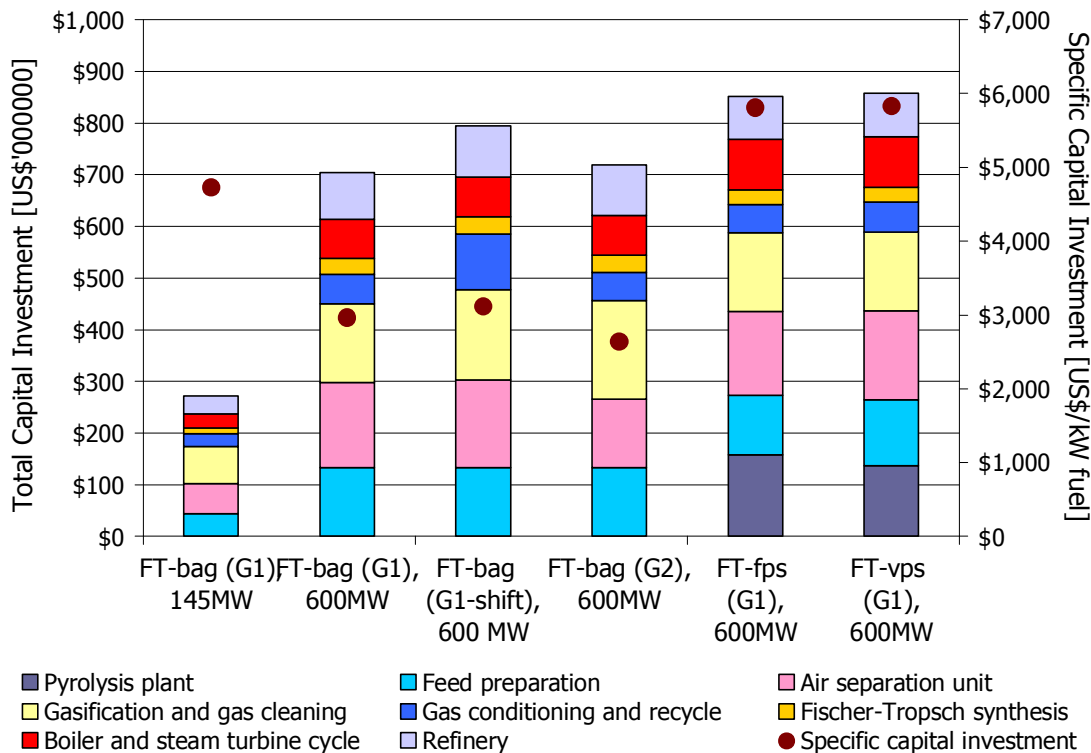


Figure 6.5 Breakdown of capital investments for Fischer-Tropsch scenarios (\$US₂₀₀₉). Gasifier modes: G1= optimised conditions for gasification efficiency and syngas ratio, G2=optimised conditions for syngas H₂/CO ratio equal to 2. Feedstocks: bag=bagasse, fps=fast pyrolysis slurry, vps=vacuum pyrolysis slurry.

The SCI of roughly \$2600-3120/kW for the 600MW Fischer-Tropsch scenarios using bagasse as feed compared to roughly \$2200/kW calculated from the results of Kreutz et al, 2007, which was based on nth plant technology.

Although the delivery cost of pyrolysis slurry to a 600 MW Fischer-Tropsch facility is lower than that of bagasse, the additional capital expenditure is not justified by the lower feedstock costs, based on the assumptions of this study. However, this technology may be feasible under other circumstances. In Europe, FZK is developing a pyrolysis slurry gasification process and found that the process was feasible for a specific area where the grass density was high and the maximum slurry transport distance is about 150 km (Van der Drift, 2002). The major difference between this case and the case for bagasse considered here is the fact that there is no benefit in savings on the collection costs of bagasse. If the bagasse required harvesting prior to processing, slurry gasification might become economically feasible.

6.3.3 Fuel Production Costs

The fuel production cost is made up of the annual capital charges and total operating costs, minus the revenue from any by-products sold, and the results for all the process scenarios studied are shown in Figure 6.6. The production costs of bioethanol and Fischer-Tropsch fuels are also expressed in terms of the breakeven oil price on the right axis. Steam explosion pretreatment at a 600MW scale leads to the lowest ethanol production cost of \$23.0/GJ, with a BEOP of \$81.0/barrel. This is close to the current world price of crude oil, which has fluctuated between \$60 and \$80/barrel over the last 18 months (see Figure 6.7). Moreover, the price of crude oil was well over the \$100/barrel mark a year ago, and is expected to climb again in the next year, which would make bioethanol production with steam explosion pretreatment very competitive with the petroleum industry.

The lowest Fischer-Tropsch fuel production cost was \$21.6/GJ by gasification of bagasse using the G1 gasifier mode and excluding a shift reactor. This corresponded with a breakeven oil price of \$77.3/barrel for a 600MW facility, which is 10% cheaper than bioethanol, and also competitive with recent oil prices. However, 61% of this is Fischer-Tropsch diesel, which has a lower selling price compared to petrol equivalent fuels. At the same time, the fuel production costs for the scenarios aimed at maximising the yield

of Fischer-Tropsch liquids (G1-shift and G2) were 28% and 32% higher, respectively. In other words, the cost of producing the additional 5% of Fischer-Tropsch liquids is very significant and probably not justified.

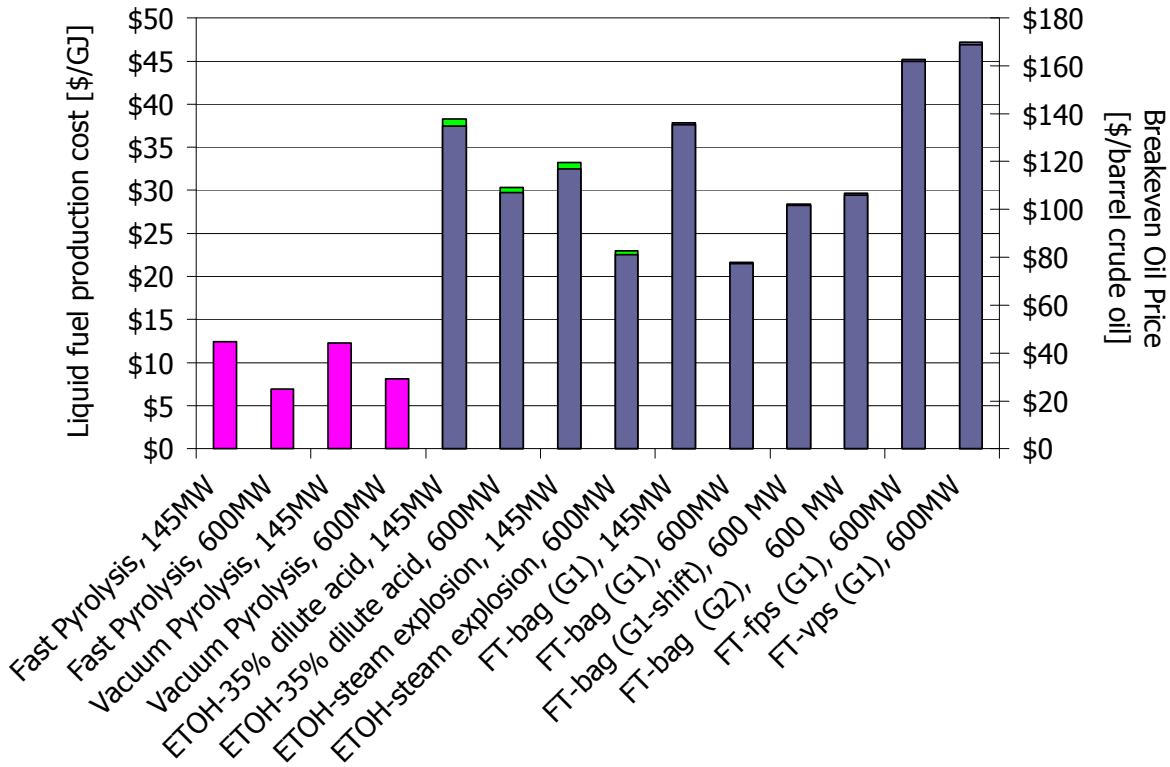


Figure 6.6 Production costs and breakeven oil prices for liquid biofuels from sugarcane bagasse (\$US₂₀₀₉). ETOH=bioethanol production, FT=Fischer-Tropsch synthesis. Breakeven Oil Price is only applicable to bioethanol and Fischer-Tropsch fuels.

Finally, the production costs of bio-oil are less than half that of the refined transport biofuels. Fast pyrolysis oil can be produced at of \$7.0/GJ, while vacuum pyrolysis oil is slightly more costly to produce (\$8.2/GJ), although that is not taking the revenue from char into account. According to Huber et al, 2006, bio-oil upgrading would cost an additional \$6.9/GJ, which would result in a refined fuel production cost of \$13.9/GJ via fast pyrolysis, based on the results for a 600MW plant. Although much research is still needed in the area of bio-oil refining, this is certainly a viable option to further develop.

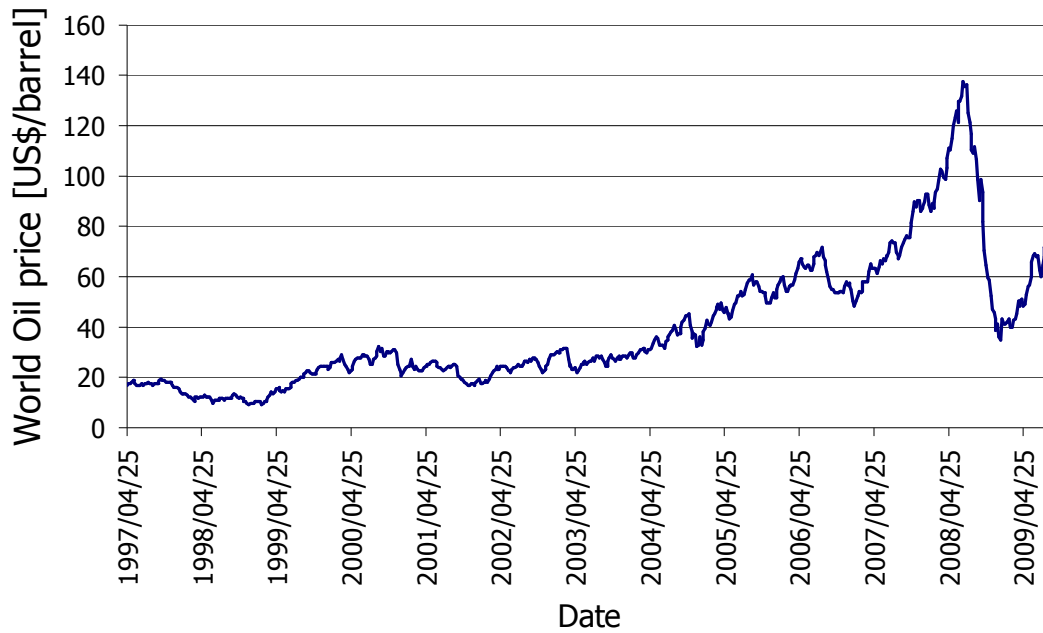


Figure 6.7 World crude oil price statistics for the past 12 years (Energy Information Administration, 2009).

The effect of process energy efficiency on the production costs of liquid fuels was compared using data from this study and the literature discussed before, and the results are shown in Figure 6.8. For bioethanol production, a clear trend was observed between the end product energy efficiency and production costs of bioethanol. This is mainly as a result of a gradual increase in the conversion efficiency of biomass to ethanol, based on the assumptions used in the different studies.

The trend for Fischer-Tropsch synthesis was not as obvious. The results can however be explained if one considers whether a shift reactor was used or not. Neither of the pure EG1 and EG2 scenarios in this study made use of a shift reactor. It has been shown that optimising the gasifier for a syngas ratio of 2 (EG2) was not feasible, since it led to higher capital costs (and therefore production costs) and lower efficiencies. On the other hand, operating the gasifier at the optimum gasification efficiency within practical constraints led to higher end product efficiencies, and lowered the capital and production costs due to the elimination of a shift reactor and a smaller steam cycle compared to the EG2 scenario. Finally, the remaining middle three data points can be

compared, since all make use of a shift reactor. The data suggests that the increase in the Fischer-Tropsch end product energy efficiency caused by an increase in Fischer-Tropsch liquid yields will also increase the production costs of Fischer-Tropsch liquids. This is because increasing the liquid yields generally necessitates more complicated process designs and additional equipment, which was also concluded from the results of this study.

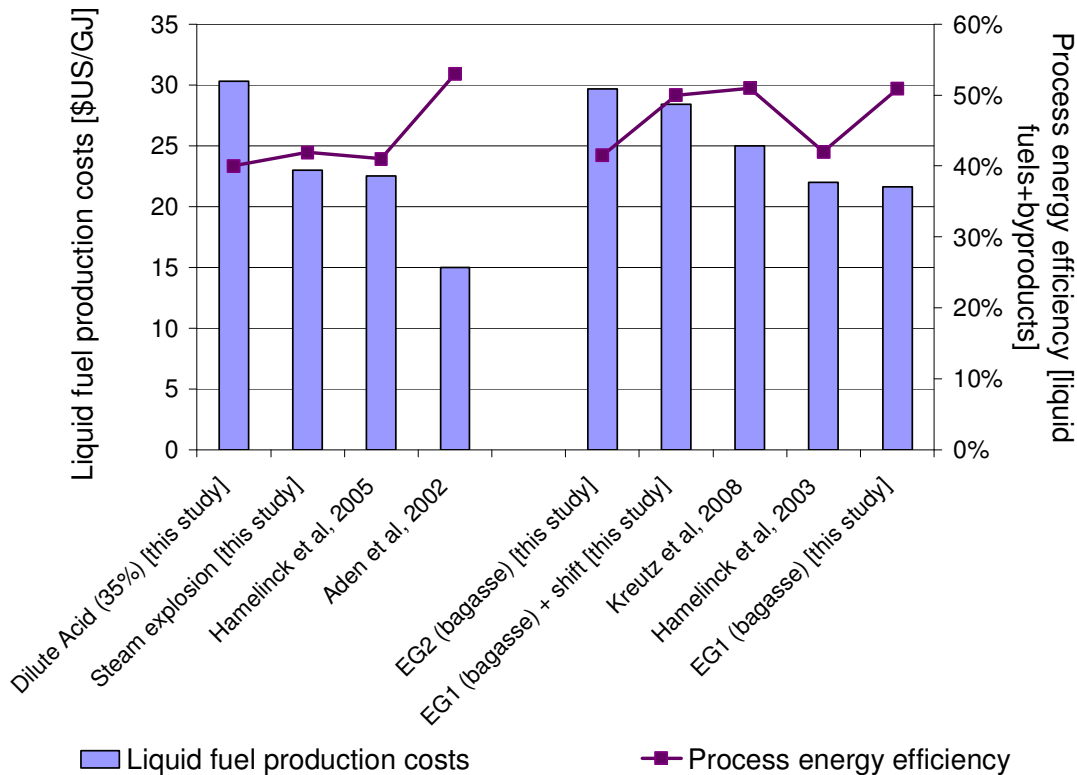


Figure 6.8 Comparison of liquid fuel production costs as a function of end-product process energy efficiencies from this study and literature data.

6.3.4 Investment Analyses and Sensitivity

The fuel production costs are very sensitive to the cost assumptions made. As a general rule of thumb, the uncertainty in capital investments for first level feasibility studies is around 30%. The assumed base price of bagasse is also more than double that assumed for biomass in previous studies, as discussed before. If more of the bagasse could be substituted for sugarcane trash, the cost of the feedstock might be reduced to the same

level of \$30/t. However, if the value of cane trash is assumed to be equal to bagasse, the feedstock would cost \$62/t. The selling price of electricity in South Africa could also change significantly in the near future. In July 2009, Eskom was granted a tariff hike of 31.3%, and it has already requested another 45% per year for the next three years from the national energy regulator. It is therefore likely that the electricity price could double or even triple in the next 2-3 years. The price of char could also rise due to the current construction of new power stations that will increase the demand for coal and therefore the value of char products. The same sensitivity range is therefore considered for char and electricity.

Figure 6.9 shows the sensitivity of the production costs of bioethanol using steam explosion, bio-oil from fast pyrolysis and Fischer-Tropsch liquids via bagasse gasification in the G1 mode to the on-site price of feedstock, total capital investment and by-product selling prices. The by-product for pyrolysis is char, while electricity is the by-product for bioethanol and Fischer-Tropsch synthesis. The sensitivity to variations in interest rate was also considered, but proved to be less important than the other factors.

The production costs of both bioethanol and Fischer-Tropsch fuels could vary by about \$7-9/GJ within the range of total capital investments studied. Therefore, if the total capital investment of a second generation plant is reduced by 30% due to technological learning, the production costs of bioethanol and Fischer-Tropsch fuels could be reduced to about 20.8/GJ and \$16.7/GJ for the 600MW scenarios, respectively. The cost of biomass has a similar effect on transport fuel costs to that of capital investment. Furthermore, considering that bioethanol is a less mature technology compared to Fischer-Tropsch processing and there is more scope for improvement in the liquid yields, it is more likely that future breakthroughs in this technology will decrease the total capital investment, which will lead to similar production costs for both transport fuel processes.

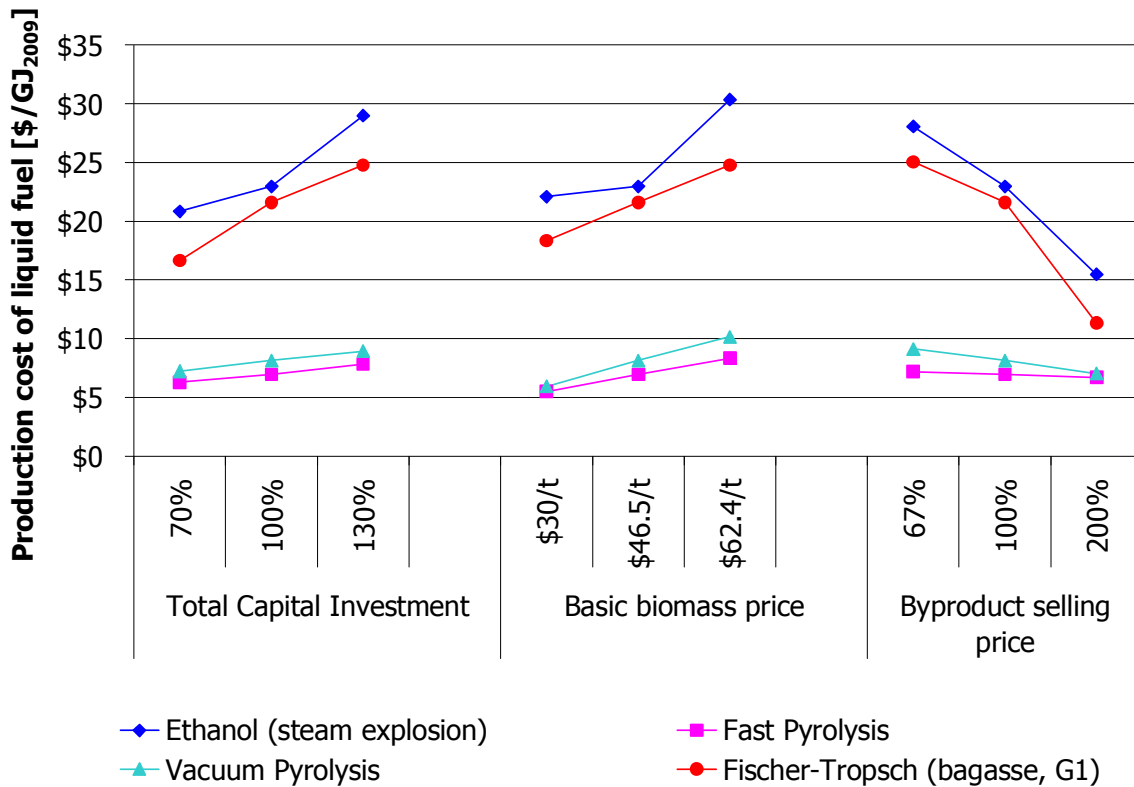


Figure 6.9 Sensitivity of liquid fuel production costs to total capital investment (% variation from base case), on-site price of feedstock (bagasse and trash) and selling prices of by-products (% variation from base case). All the results are applicable to 600MW scenarios.

The sensitivity of bioethanol production costs to the development of consolidated bioprocessing was also evaluated; since an enzyme producing yeast is currently being developed that would reduce the total operating cost by 15%. This would result in an 11% decrease in the bioethanol production cost from about \$23.0/GJ to 20.5/GJ. On the other hand, the effect of higher enzyme costs will have a significant effect on the production cost of bioethanol, and an enzyme cost of \$0.50/gallon ethanol will result in an increase of 15% (from \$23/GJ to \$26/GJ). Reducing the basic bagasse price to \$30/t would decrease the bioethanol production cost to \$22.1/GJ.

The cost of producing bio-oil is less sensitive to variations in capital investment, but more sensitive to the cost of biomass. In fact, the relationship is almost linear, as the production cost can double from an increase in biomass costs of \$30/t to \$62.4/t. The price of char has a more significant effect on vacuum pyrolysis compared to fast pyrolysis, and a 100% increase in the char price will reduce the production costs of vacuum pyrolysis oil by 15%. The sensitivity of bioethanol and Fischer-Tropsch fuels to by-product costs is far more significant than for pyrolysis, even when both char and electricity costs are increased by 100%. This increase in the price of electricity will reduce the production costs of bioethanol and Fischer-Tropsch fuels by 33% (\$15.5/GJ) and 48% (\$11.3/GJ), respectively. This is very important to consider since the price of electricity in South Africa is very likely to double in the short term, while the effect of such an increase on the price of char, coal and biomass, which are inter-related, could be lagged over a longer period. There might be a promising window of opportunity for these technologies to be commercialised in South Africa.

The other side of the argument also holds, in that such high electricity prices would make investment into cogeneration from biomass more attractive, since it also comes at a lower risk. The likely costs of producing electricity in a BIG/GCC plant were estimated from results published by Jin et al, 2006. Using process modelling, they calculated the capital cost of a 983MW plant using an indirectly heated gasifier to be equal to \$1059/kW, that would produce electricity at a LHV efficiency of 48% and a total generating cost of \$0.059/kWh at a biomass cost of \$3.6/GJ (equal to the cost used in this analysis). Converting this value to a 600MW plant using a scaling factor of 0.7, the production cost would be roughly \$0.079/kWh, which is essentially equal to the electricity cost of \$0.08/kWh assumed in this study. However, since electricity is the only product, cogeneration would enjoy the most benefit from an increase in electricity price.

The return on investment, which is defined as the net income before tax, or the difference between the product selling and production price divided by the total fixed capital investment, was calculated for different electricity prices, as shown in Figure

6.10. The results show that a return on investment of 30% (which is desired for investment in new technologies) will be achieved at an electricity price increase of 235%, or an electricity price of \$0.188/kWh. At the current electricity price, the return on investment is not favourable. It should be noted that this is not a detailed analysis and these estimations should be verified with a more detailed approach.

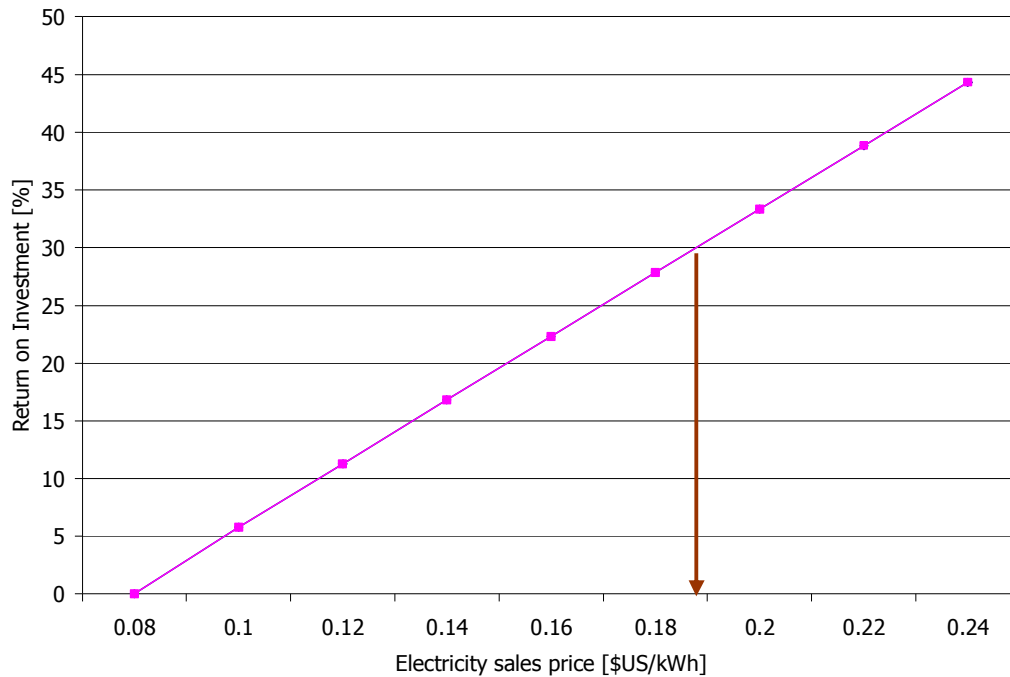


Figure 6.10 Effect of electricity price on the return on investment for a 600MW BIG/GCC cogeneration plant. Cost data was obtained from Jin et al, 006.

The values for the internal rate of return (IRR) and return on investment (ROI) for the best performing scenarios from this study are given in Figure 6.11. The internal rate of return is a discounted interest rate that is comparable to the interest rate given by a bank, while the return on investment provides a measure of the return that an investor can expect each year on a non-discounted basis. It is interesting to note that, although the selling price of pyrolysis oil is the lowest among all the products, these processes deliver the highest returns; the highest being 40.5% and 37.6% for the IRR and ROI, respectively, for vacuum pyrolysis at 600MW. This is due to the significant revenue recovered from the sale of high value char. However, the sale of pyrolysis oil is a relatively high risk and the selling price is also the most uncertain due to the lack of an

established market for bio-oil. The results nevertheless give great merit to the development of such markets.

With regards to transport biofuels, the results suggest that the IRR and ROI for Fischer-Tropsch processes will be lower compared to bioethanol production due to the higher capital investment required, and neither of these is attractive from an investment point of view at the current market prices.

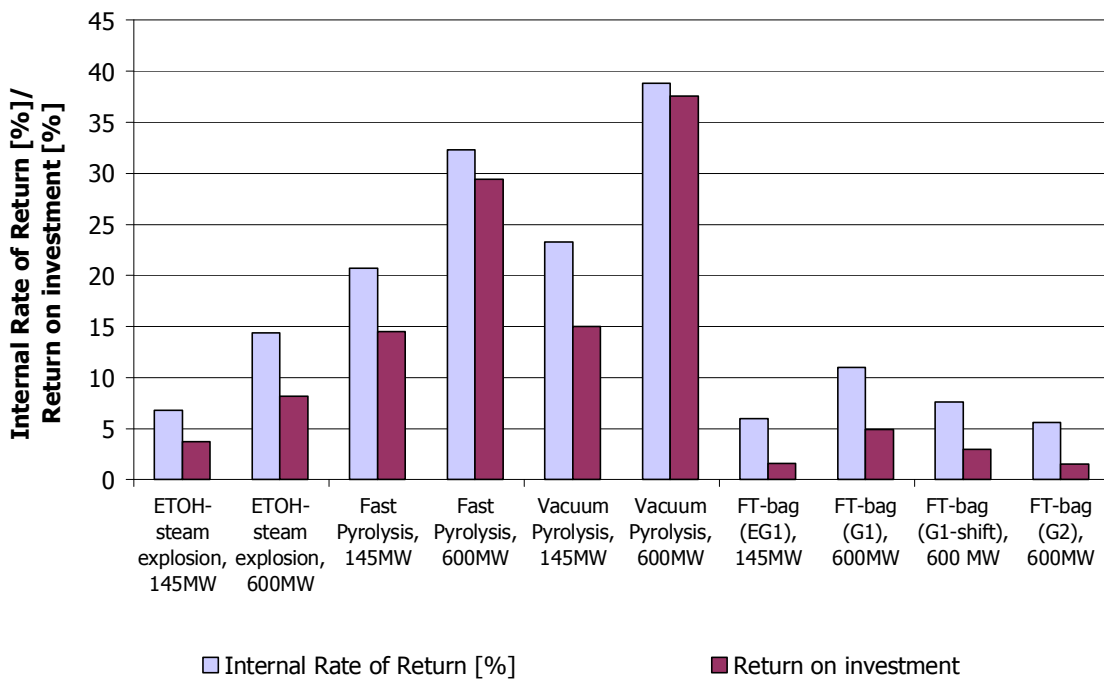


Figure 6.11 Internal rate of return results for best performing process scenarios for production of bioethanol, crude bio-oil and Fischer-Tropsch fuels.

The effect of scale is also evident, and the IRR and ROI for the best 600 MW bioethanol and Fischer-Tropsch scenarios are 14.4% and 11.0%, respectively, and 8.2% and 4.9%, respectively, which is too low considering that banks can currently offer investors a guaranteed return of at least 11%. However, the sensitivity of all the processes to the selling prices for liquid fuels and by-products has been evident. The selling prices for all the liquid fuels are dependent on the crude oil price, while the likely ranges for the cost of char and electricity have been discussed. The effect of product prices on the internal

rate of return is given in Figure 6.12 for the bioethanol, pyrolysis and Fischer-Tropsch scenarios with the lowest respective fuel production costs.

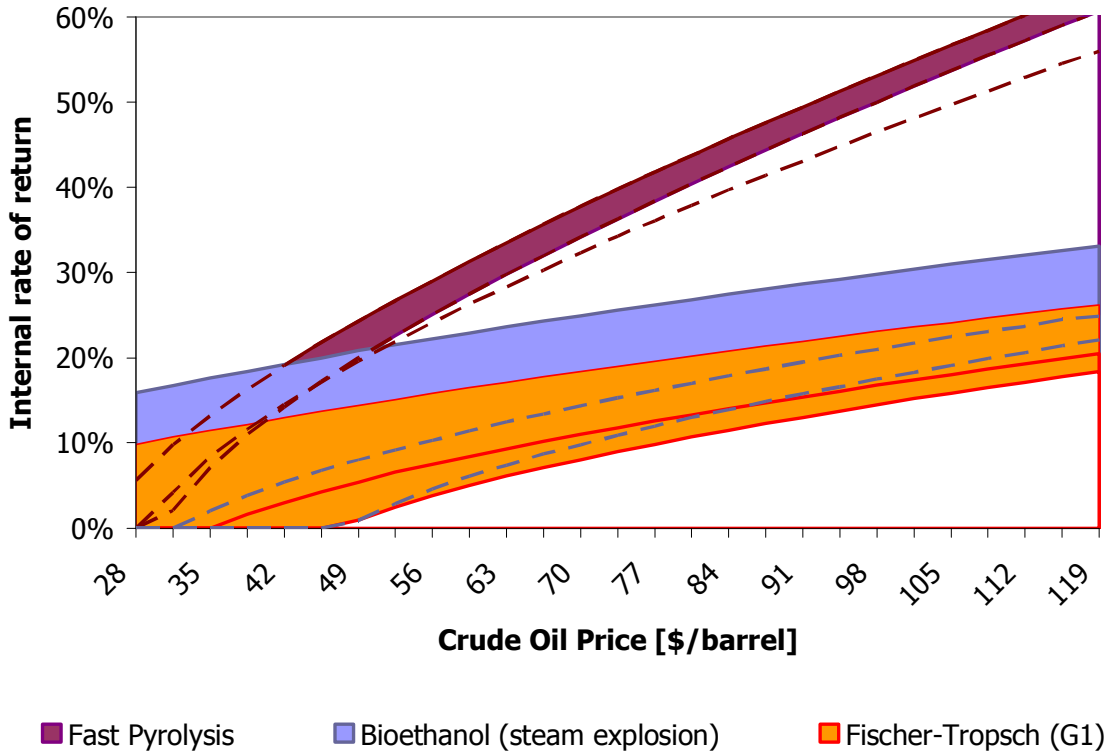


Figure 6.12 Sensitivity of internal rate of return for conversion of bagasse to bioethanol with steam explosion, fast pyrolysis oil and Fischer-Tropsch liquids using G1 gasifier mode. The top band for each process route represents the high by-product price range, the middle band the base case and the lower band the low by-product price range. By-product price ranges: Electricity high=\$0.2/kWh, Electricity low=\$0.04/kWh, Char high=\$197/t, Char low=\$66/t.

The high sensitivity to the electricity price is once again evident. If the crude oil price should rise to \$100/barrel in the next 3 years, and the electricity price should triple, then bioethanol and Fischer-Tropsch liquids can be produced at an internal rate of return of 29% and 21%, respectively, while fast pyrolysis will achieve an internal rate of return of 48%-50%, depending on the char price.

6.4 CONCLUSIONS

- Currently steam explosion pretreatment of bagasse will lead to the lowest production cost for bioethanol of \$23.0/GJ at a breakeven oil price of \$81.0/barrel for a 600MW plant, which is competitive with the current oil price of \$70/barrel.
- Although the yield of Fischer-Tropsch liquids can be increased by using a shift reactor or feeding more steam to the gasifier, these scenarios proved to be less economical. By combined optimisation of the gasification efficiency and syngas ratio, slightly less liquid fuels are produced, but at the lowest production cost of \$21.6/GJ. At a breakeven oil price of \$77.3/barrel, this scenario is also competitive with conventional petroleum derived fuels.
- Gasification of pyrolysis slurry is not currently economical, mainly due to the high base cost of bagasse, and the fact that the bagasse is already collected, negating the cost benefit of transporting pyrolysis slurry versus raw biomass. The small benefit of transporting a more energy dense material does not outweigh the additional cost of a pyrolysis plant.
- Although production of Fischer-Tropsch liquids is slightly cheaper than bioethanol, this difference is insignificant considering the sensitivity of the analysis and future technological advances in bioethanol production are expected to be more significant. In addition, the specific capital investment is higher than for bioethanol (\$2640/kW Fischer-Tropsch fuels versus \$2430/kW ethanol).
- The production of transport fuels from biomass is currently not attractive from an economic point of view, and internal rates of return were below 14.5% while returns on investments were below 9% in all cases. However, the assumptions for cost data was very conservative in this study, and the sensitivity analysis showed that likely increases in product prices will significantly affect the outcome.
- However, from an investment point of view, pyrolysis is currently far more attractive. Vacuum pyrolysis would achieve the maximum internal rate of return of 40.5% compared to 37.6% for fast pyrolysis. The production costs and specific capital

investments are also lower compared to transport fuels: \$6.95/GJ at \$820/kW bio-oil and \$8.16/GJ at \$1200/kW bio-oil for fast and vacuum pyrolysis, respectively.

- In all cases, economies of scale played an important role and, other than crude pyrolysis oil, the production costs for the 145MW scenarios are not currently economical.
- It was shown that the results are most sensitive to the total capital investment, cost of bagasse and product selling prices. For bioethanol or Fischer-Tropsch fuels, likely increases in electricity prices in South Africa will greatly affect the economics, and further market analyses of the cost inputs are required.
- Likewise, the expected increase in the electricity price will make cogeneration from biomass more competitive with biofuels processes. Biomass feedstocks such as bagasse are in high demand and these technologies will have to compete to obtain commercial status. For liquid biofuels, the use as a blending stock could prove to be more desirable. Biorefineries will also be promising from an energy and economic point of view.

REFERENCES

- Aden, A., M. Ruth, K. Ibsen, J. Jechura, K. Neeves, J. Sheehan and B. Wallace (2002). Lignocellulosic Biomass to Ethanol Process Design and Economics Utilizing Co-Current Dilute Acid Prehydrolysis and Enzymatic Hydrolysis for Corn Stover. Golden, Colorado, US, National Renewable Energy Laboratory.
- Alonso, P. W., P. Garzone and G. Cornaccia. (2006). "Agro-industry sugarcane residues disposal: The trends of their conversion into energy carriers in Cuba." *Waste Management*, doi:10.1016/j.wasman.2006.05.001.
- Botha, T. and H. v. Blottnitz (2006). "A comparison of the environmental benefits of bagasse-derived electricity and fuel ethanol on a life-cycle basis." *Energy Policy* 34: 2654–2661.
- Hamelinck, C. N., A. P. C. Faaij, H. Den Uil and H. Boerrigter (2003). "Production of FT transportation fuels from biomass; technical options, process analysis and optimisation, and development potential." NWS-E-2003-08.
- Hamelinck, C. N., G. v. Hooijdonk and A. P. Faaij (2005). "Ethanol from lignocellulosic biomass: techno-economic performance in short-, middle- and long-term." *Biomass and Bioenergy* 28: 384-410.
- Huber, G. W., S. Iborra and A. Corma (2006). "Synthesis of Transportation Fuels from Biomass: Chemistry, Catalysts, and Engineering." *Chemical reviews* 106: 4044-4098.
- Jin, H., E. D. Larson and F. E. Celik (2006, November 20). "Performance and Cost Analysis of Future, Commercially-Mature Gasification-Based Electric Power Generation from Switchgrass." *Biomass and Bioenergy* (article submitted as series to be approved).
- Kreutz, T. G., E. D. Larson, G. Liu and R. H. Williams (2008). "Fischer-Tropsch Fuels from Coal and Biomass." 25th Annual International Pittsburgh Coal Conference.
- Mauviel, G., F. Kies, M. S. Rene and M.Ferrer (2008). "Biomass densification by pyrolysis: An energetic assessment."
- Ringer, M., V. Putsche and J. Scahill (2006). Large-Scale Pyrolysis Oil Production: A Technology November 2006 Assessment and Economic Analysis. Golden, Colorado, US, National Renewable energy Laboratory. NREL/TP-510-37779.

Tait, B. (2008). "First Uranium to build acid plant to secure future supply of sulphuric acid for its uranium plants at reduced costs." News Release, April 21.

Tijmensen, M. J. A., A. P. C. Faaij, C. N. Hamelinck and M. R. M. v. Hardeveld (2002). "Exploration of the possibilities for production of Fischer-Tropsch liquids and power via biomass gasification." Biomass and Bioenergy 23: 129-152.

Wright, M. M. and R. C. Brown (2007). "Comparative economics of biorefineries based on the biochemical and thermochemical platforms." Biofuels, Bioproducts and Biorefining 1: 49-56.

<http://tonto/eia.doe.gov>. 23 November 2009.

www.dme.gov.za. 20 July 2009.

7. CONCLUSIONS

Detailed process models were developed for various process configurations for the production of transport quality bioethanol, crude pyrolysis oil and transport quality Fischer-Tropsch fuels from sugarcane bagasse. This is the first in-depth modelling exercise to consistently compare these process routes using bagasse-specific data that is based on currently available, 1st plant technology. Furthermore, a detailed economic study for liquid biofuels production that is specifically applicable to economic factors in South Africa was presented. Based on results, the following conclusions were made:

7.1 TECHNICAL PERFORMANCE of BIOETHANOL, PYROLYSIS and GASIFICATION FOLLOWED BY FISCHER-TROPSCH PROCESSING

Process models were used to calculate the conversion of energy to products and process energy efficiencies for each scenario. The most important technical results are shown in Table 7.1.

7.1.1 Energy consumption and conversion of feed energy to liquid products

- The bioethanol scenarios utilising liquid hot water pretreatment at 5% solids, and dilute acid pretreatment at 10% solids, are not energy self-sufficient, and it was found that the **solids concentration in the pretreatment reactor** had a strong influence on the overall energy balance. Therefore, the economics for these scenarios were not evaluated. On the other hand, steam explosion pretreatment resulted in a positive energy balance with surplus electricity being available for export to the grid.
- Recognising that the solids load assumed for dilute acid pretreatment was significantly lower compared to previous work conducted with corn stover, the dilute acid process model was used to determine the **critical solids concentration** that would render the process energy self-sufficient. It was

found that, assuming the same pretreatment yields that were experimentally obtained at 10%, there would be enough energy in the residual solids to supply the energy needs for the process at a pretreatment solids load of 35%. This was a theoretical scenario studied and is included since work is currently ongoing to optimise the solids load during dilute acid pretreatment of bagasse.

Table 7.1 Technical and economic performance of the most important process route scenarios for bioethanol, pyrolysis and Fischer-Tropsch processing.

Scenario	Units	ETOH-steam expl	PYR-fast	PYR-vacuum	FT-bag (EG1)	FT-bag (EG1shift)	FT-bag (EG2)
Conversion of feed energy to energy in products							
Liquid fuels	MW/MW HHV input	30.5%	60.2%	40.6%	39.6%	44.8%	44.1%
Electricity	MWe/MW HHV input	11.4%	0.0%	0.8%	11.3%	4.1%	-2.6%
Electricity (thermal equivalent)	MW/MW HHV input	25.3%	0.0%	1.8%	25.1%	9.2%	-5.8%
Char byproduct	MW/MW HHV input	-	9.5%	27.6%	-	-	-
Energy efficiencies							
Liquid fuel		40.9%	66.5%	57.5%	52.9%	49.4%	41.7%
Liquid fuel + thermal energy		55.8%	69.7%	70.0%	64.7%	54.0%	38.3%
Liquid fuel + electricity and/or char		41.9%	69.7%	69.0%	50.9%	49.0%	41.5%
Economic evaluation							
Total project investment cost	M\$	\$432.90	\$141.68	\$126.79	\$705.04	\$794.48	\$719.62
Liquid fuel production costs	\$/GJ HHV	\$22.96	\$6.95	\$8.16	\$21.60	\$28.40	\$29.70
Breakeven oil price	\$/barrel crude oil	\$81.00			\$77.30	\$101.60	\$106.10
Internal rate of return	%	14.40	34.20	40.50	11.00	8.20	6.00
Payback period	years	-	6.29	5.16	-	-	-

Key: ETOH=bioethanol, PYR-fast/vac=fast or vacuum pyrolysis, FT-bag=Fischer-Tropsch processing of bagasse using different equilibrium gasifier modes. Breakeven oil price not calculated for bio-oil, since it is not a transport fuel. Payback periods for Fischer-Tropsch scenarios were longer than the project lifetime.

The process energy efficiencies are defined as follows: 1) Liquid fuel= (energy in liquid fuel)/ (energy in feed-energy in electricity-energy in char) (all in thermal units).

2) Liquid fuel + thermal energy= (thermal energy in liquid fuel + thermal energy in intermediate lignin, char or gas)/energy in feed (all in thermal units).

3) Liquid fuel + electricity and/or char= (energy in liquid fuel + electric energy + energy in char)/energy in feed (mixed units).

- For the energy self-sufficient scenarios, the main process energy consumption was attributed to ethanol distillation, which accounted for more than 60% of the total steam usage. In addition, the maximum conversion of feed energy to **bioethanol** is currently 30.5% for bagasse, as shown in Table 7.1.
- Both the **pyrolysis** scenarios were found to be energy self-sufficient. Fast pyrolysis produced the most liquid fuels at 60.2% conversion of the feed energy to crude bio-oil, in addition to 9.5% saleable char product, as shown in Table 7.1. Since the energy consumption of fast pyrolysis was almost double that of vacuum pyrolysis, the energy in the reactor off-gas had to be supplemented with char to supply the total energy needs of the process.
- Vacuum pyrolysis produced less bio-oil (40.6% conversion of feed energy) but was less energy intensive compared to fast pyrolysis. As a result, all the char produced (27.6% conversion of feed energy) was available for sale as a by-product.
- **Equilibrium modelling of bagasse gasification** compared very well with experimental data, provided that a minimum equivalence ratio of 0.25 and operating temperature of 1100K was used. Although increased pressure can also ensure equilibrium conditions and complete gasification at lower equivalence ratios, the energy losses of downstream processing is too high if current state-of-the-art wet gas cleaning is used.
- Although steam gasification produces hydrogen-rich syngas due to the water-gas shift reaction, the gasifier efficiency decreases with increasing steam to biomass ratios. High moisture levels in the feedstock will have a similar, but more pronounced effect, and the moisture content of bagasse should therefore be minimised for optimum gasification efficiency.
- The **optimum operating conditions** for two equilibrium gasifiers were determined from a statistical analysis of data sets generated by equilibrium modelling of bagasse and bagasse-derived pyrolysis slurry. For bagasse gasification at 1100K, 1 bar and an equivalence ratio of 0.25, the optimum

- gasification efficiency of 74.5% results in a H₂/CO ratio of 0.9 (Equilibrium Gasifier 1). This will produce a Fischer-Tropsch liquid yield of 39.6%, as shown in Table 7.1.
- At a bagasse moisture level of 5%, a steam biomass ratio of 2.25 would be required to obtain the stoichiometric H₂/CO ratio of 2 for **maximum Fischer-Tropsch liquid** yields, resulting in a gasification efficiency of 59.6% (Equilibrium Gasifier 2, Table 7.2), and a final Fischer-Tropsch liquid yield of 44.1% (Table 7.1).
 - However, the it is more energy efficient to use Equilibrium Gasifier 1 coupled with a shift reactor to adjust the H₂/CO ratio to approximately 2 for maximum Fischer-Tropsch liquid yields, since this scenario delivered the highest conversion of biomass energy to liquid transport fuels of 44.8%, and did not decrease the process energy efficiency as much as the scenario using Equilibrium Gasifier 2.
 - Maximising the Fischer-Tropsch liquid conversion by either of the configurations studied will lead to a significant reduction in the thermal process energy efficiency, and the use of a shift reactor with Equilibrium Gasifier 1 reduced the thermal process energy efficiency by 10.7%.
 - Due to their different syngas compositions, gasification of **pyrolysis slurries** followed by Fischer-Tropsch synthesis resulted in 4-5% lower Fischer-Tropsch liquid yields compared to bagasse.

7.1.2 Process and liquid fuel energy efficiencies

- The production of **residual fuel oil** via pyrolysis is very attractive from a process and liquid energy efficiency point of view, and fast pyrolysis achieved the highest thermal process energy efficiency of 70% and liquid fuel efficiency of 67% for crude bio-oil.
- The upgrading of crude bio-oil to transport fuels could result in a lower thermal process energy efficiency of about 55% compared to 65% for Fischer-Tropsch fuels.
- Thermochemical processing of bagasse is currently more energy efficient than biological fermentation for the production of **transport liquid biofuels** due to the higher conversion of biomass to liquids. Compared to the liquid fuel efficiencies of 50-53% obtained by thermochemical production of transport fuels, the maximum liquid fuel efficiency of bioethanol from sugarcane bagasse is currently 41%, due to the large portion of unfermentable sugars in the feedstock. An increase of 18% in ethanol conversion efficiency, which is equivalent to an ethanol conversion efficiency of 49% (close to the theoretical maximum), will result in similar liquid fuel energy efficiencies for thermochemical and biological transport biofuels.
- However, bioethanol production from lignocellulose is further away from mature technology and there is enough scope for **improvements in bioethanol conversion yields** to increase the process energy efficiencies to values similar to Fischer-Tropsch processing using high pressure or equilibrium gasifiers. If one considers only the thermal energy in the liquid fuel and thermal energy in by-products, bioethanol production is currently comparable with Fischer-Tropsch synthesis configurations that make use of a shift reactor.
- The importance of evaluating **different forms of energy efficiency for comparison** between different process routes was evident from the results in this study.

- In all cases, heat integration played an important role and the inclusion of a steam cycle and process heat integration increased liquid fuel energy efficiencies by up to 30%.
- Therefore, the technical results from the process models suggested that fast pyrolysis is a promising process for the production of crude bio-oil from sugarcane bagasse to replace residual fuels in the current energy market, while gasification of bagasse followed by Fischer-Tropsch synthesis to produce transport fuels currently achieves higher liquid fuel conversion efficiencies than bioethanol and for maximum process energy efficiencies, a shift reactor should be excluded. Future developments in bioethanol technology will lead to comparable process energy efficiencies with Fischer-Tropsch synthesis using advanced gasifiers.

7.2 PRODUCTION COSTS AND ECONOMIC PERFORMANCE of BIOETHANOL, PYROLYSIS and GASIFICATION FOLLOWED BY FISCHER-TROPSCH SYNTHESIS

For **bioethanol** production, steam explosion pretreatment of bagasse will currently result in the lowest bioethanol production cost \$23.0/GJ for a 600MW plant.

- It is more economical to produce slightly less **Fischer-Tropsch** liquids and more electricity by optimising the gasification efficiency compared to maximising liquid product yields by using a shift reactor or optimising the gasifier. The lowest Fischer-Tropsch liquid production costs of 21.6/GJ were achieved by combined optimisation of the gasification efficiency and syngas ratio.
- At **breakeven oil prices** of \$81.0 and \$77.3/barrel for the most economical 600MW bioethanol and Fischer-Tropsch scenarios, respectively, both process

- routes are competitive with conventional petroleum derived fuels at recent crude oil prices.
- Gasification of **pyrolysis slurry** is not currently economical, mainly due to the lower conversion yield and high base cost of bagasse, which results in a small proportion of the delivered cost being attributed to transport costs. The small benefit of transporting a more energy dense material does not outweigh the additional cost of a pyrolysis plant.
 - Although production of Fischer-Tropsch liquids is slightly cheaper than bioethanol, the difference is insignificant considering the sensitivity of costs to product selling prices. In addition, the specific capital investment is higher than for bioethanol (\$2640/kW Fischer-Tropsch fuels versus \$2430/kW ethanol). This leads to a higher **return on investment** of 14.4% for bioethanol compared to 11.0% for Fischer-Tropsch fuels.
 - From an investment point of view, production of crude bio-oil via **pyrolysis** proved to be far more attractive than transport fuels production. Vacuum pyrolysis would achieve the maximum return of 40.5% compared to 37.6% for fast pyrolysis. The production costs and specific capital investments are also lower compared to transport fuels: \$6.95/GJ at \$820/kW bio-oil and \$8.16/GJ at \$1200/kW bio-oil for fast and vacuum pyrolysis, respectively.
 - At small scales, only pyrolysis for crude-bio-oil production will currently be economical, and the effect of **economies of scale** was significant for all the process routes.
 - The **sensitivity** of calculated production costs to the total capital investment, cost of bagasse and product selling prices was evident. Due to their higher total capital investment compared to pyrolysis processes, the cost of producing bioethanol and Fischer-Tropsch fuels could be reduced to \$20.8/GJ and \$16.7/GJ, respectively, if the total capital investment is decreased by 30%, which falls within the level of uncertainty of this study. Likewise, a similar increase in production costs can be expected with an increase in capital investment.

- The sensitivity to variations in the **feedstock price** is roughly similar to that of capital investment for production of liquid transport fuels, within the expected ranges that were studied. For crude bio-oil production, variations in the bagasse price would have a significant effect on the production price and internal rate of return, as shown in Figure 7.1.
- For bioethanol or Fischer-Tropsch fuels, likely increases in **electricity prices** in South Africa will greatly affect the economics (Figure 7.1). If the crude oil price should rise to \$100/barrel in the next 3 years and the electricity price should triple, both of which are very possible and even likely, then bioethanol and Fischer-Tropsch liquids could be produced at an internal rate of return of 29% and 21%, respectively, while fast pyrolysis could achieve an internal rate of return of 48%-50%, depending on the char price.
- A detailed market analysis of all the cost inputs is required to shed further light on possible future market trends.

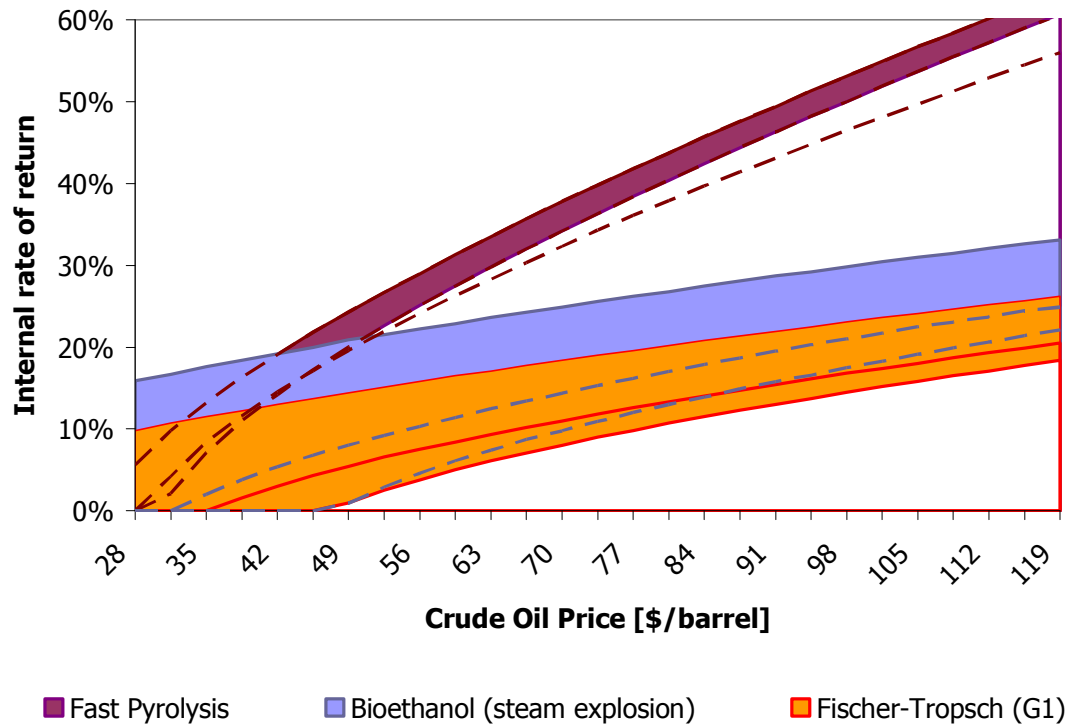


Figure 7.1 Sensitivity of internal rate of return for conversion of bagasse to bioethanol with steam explosion, fast pyrolysis oil and Fischer-Tropsch liquids using G1 gasifier mode. The top band for each process route represents the high by-product price range, the middle band the base case and the lower band the low by-product price range. By-product price ranges: Electricity high=\$0.2/kWh, Electricity low=\$0.04/kWh, Char high=\$197/t, Char low=\$66/t.

7.3 CONTRIBUTIONS

The most important contributions of this work included

- Development of **process models** in AspenPlus® for the biological and thermochemical process routes currently available to produce liquid biofuels from sugarcane bagasse for either the transport or industrial fuel market, **using data either measured or modelled for bagasse** and including heat integration, based on **currently available technology**. Although previous models have

been developed for other lignocellulosic materials, this is the first dedicated to bagasse-specific data and the majority of prior studies considered mature technology, as they were mainly performed to assess future development opportunities for the biofuels industries in developed countries. The selected processes include

- Transport quality *bioethanol* production via biological fermentation coupled with utilisation of the solid residues for cogeneration. The three pretreatment methods considered are dilute acid pretreatment, steam explosion and liquid hot water pretreatment, and the **minimum required solid concentration** during dilute acid pretreatment for a self-sustainable process is determined (**Chapter 3**).
- Pyrolysis to produce crude bio-oil suitable for an industrial fuel and char as a by-product. The two pyrolysis modes considered were fast and vacuum pyrolysis. Data on process modelling of **vacuum pyrolysis** has not been published before in literature (**Chapter 3**).
- Equilibrium modelling to optimise gasification of sugarcane bagasse, as well as **pyrolysis slurries**, followed by Fischer-Tropsch synthesis. This is the first study to **integrate equilibrium modelling** of biomass gasification with process models for Fischer-Tropsch synthesis, and also the first to consider pyrolysis slurries as feedstock. Equilibrium gasification modelling enables a wide range of conditions to be evaluated without the need for extensive experimental runs, and is valid as long as the selected conditions ensure that equilibrium is reached, based on experience in practice (**Chapter 4**).
- Comparison of the technical performance of the three processing routes based on the process modelling results. **Biological and thermochemical process routes** were **compared** on an equivalent basis for processing of sugarcane bagasse to produce liquid biofuels. Previous comparative studies did not consider pyrolysis as an alternative to bioethanol and gasification-based processes such as Fischer-Tropsch synthesis. Furthermore, studies that have compared transport

fuel processes were either conducted in a review form that included different assumptions and feedstocks or assumed mature technology.

- Develop **economic models** of the most promising process scenarios for bioethanol production, pyrolysis and Fischer-Tropsch synthesis and compare the production costs and investment opportunities. The economic models developed in AspenIcarus[®] were specifically relevant to the **South African sugar industry**. Biomass availability was based on data supplied by local producers and the costs of raw materials, liquid fuel and by-products, investment parameters, etc, are applicable to the South Africa context. The fact that sugarcane bagasse is currently used as an energy source, coupled with South Africa's unique energy infrastructure and the significant role of coal energy, both in the synthetic fuels and power supply industries, distinguishes this case study from those of other first world countries.

8. RECOMMENDATIONS FOR FUTURE WORK

The work presented here provides a solid basis for further development of all the concepts developed for the purposes of this study, as well as possible extensions or variations to these concept scenarios. The biofuels industry is a fast developing field and new data is constantly generated with improvements that will undeniably affect the various outcomes described here. It is not only important that new sets of data are incorporated to update the process models on a continuous basis, but also that new experimental data is generated based on the findings of this study and promising technologies that have been identified need to be further developed. Furthermore, many assumptions have been made in all the process models described in this study and need to be verified, either experimentally or by obtaining quoted costs from local industry. Below is a list of suggestions for such future work and possible interesting scenarios that should be investigated.

8.1 BIOETHANOL PROCESSES FOR SUGARCANE BAGASSE

Although reliable data was available in literature for all three pretreatment methods, the hydrolysis and fermentation yields were obtained from only the steam explosion pretreated material. This data was used for consistence and also to reflect the latest technology since it was published in the first year of this study (2006). Although it was ensured that the inhibitor levels of the liquid hot water and dilute acid pretreated materials were lower than that of the steam explosion pretreated material, it has to be verified that the same hydrolysis and fermentation yields can be obtained after all three pretreatment methods, using the same adapted yeast developed by Martín et al, 2006.

In addition, the large-scale production of such a yeast will need to be demonstrated in an industrial environment, and scale-up of especially pretreatment, hydrolysis and fermentation should be done and any adjustments to the yields obtained under these conditions should be made to the models. This is because the highest uncertainty is

linked to the biological treatment of lignocellulose, as the downstream processing is similar to other ethanol distilleries which are currently commercialised.

The theoretical scenario employing dilute acid pretreatment at 35% solids should also be verified experimentally and the possible effects of changes in the reactor solid load should be quantified and applied to the process model, if any changes occur. These levels have been achieved for corn stover in the past (Aden et al, 2002), but nevertheless have to be verified for bagasse.

As the technology progresses towards maturation, the ethanol yields will gradually increase, leading to less residual energy being available for the boiler and steam turbine sections, which could lead to certain processes no longer being energy self-sufficient. Although other authors have investigated several mature technology scenarios (Hamelinck et al, 2005, Laser et al, 2008) by assuming certain n^{th} plant technology developments, a different approach may be followed whereby the required reduction in process energy demand for an energy self-sufficient process is linked to a stepwise increase in ethanol yield. The result would then be similar to the critical pretreatment solids concentration determined in this study, except that it would be applied to the energy demands of the entire process. Furthermore, in this study only combined heat and power systems were considered for residual energy recovery, while other studies have included advanced applications of BIG/GTCC systems (Laser et al, 2008). However, integration of bioethanol processes with pyrolysis of the residual energy has not been investigated, and considering the flexibility of pyrolysis processes and its attractive economics illustrated in this study, this could be an interesting integration opportunity.

8.2 PYROLYSIS PROCESSES FOR SUGARCANE BAGASSE

The most critical factor affecting the viability of pyrolysis processes is the composition and chemical stability of the oil product, which affects its possible applications and therefore its marketability. For example, crude bio-oil has been shown to run well in

pilot-ignition engines, where a small amount of conventional fuel is used to ignite the engine since bio-oil does not ignite easily (Bridgwater et al, 2002). The nature of bio-oil is very dependent on the feedstock composition and reactor configuration and more pilot work needs to be performed, specifically for sugarcane bagasse, to assess the reliability and consistency of the product quality. Also, a detailed analysis on the residual fuel oil market in South Africa will shed more light on the potential local bio-oil market and range of selling prices.

In addition, there was no detailed cost data available for a vacuum pyrolysis reactor, and this had to be estimated using cost ratios of cylindrical tanks at different pressures. Assuming a 30% uncertainty in capital investment costs, this should still fall within the spectrum, but more detailed cost data could reduce the level of uncertainty. The cost implications of building a modular pyrolysis plant have also not been considered in this study, and factors such as the cost of transporting the plant versus transporting the feedstock and the optimum scale for such a plant would provide more insight into the possibilities that this flexible process offers.

In addition, the techno-economics of bio-oil upgrading to transport fuels should be studied in detail based on latest developments, and if applicable, the required developments to make the technology cost effective should be identified.

The concept of a biorefinery is based on the drive to maximise the total process energy efficiency through process integration. In this study, the three different process routes were studied in isolation, although a recent study has evaluated integration of bioethanol and Fischer-Tropsch processing based on mature technology (Laser et al, 2008). Both biological and thermochemical process routes have inherent maximum liquid yields, but process integration enables higher liquid yields by converting the unfermentable portion of the biomass to thermochemical fuels instead of heat and electricity, resulting in higher overall energy efficiencies, since the efficiency of electricity production is low. Therefore, it makes sense to consider the integration of bioethanol production followed by pyrolysis of the residual solids to produce additional bio-oil. So

far work in this area has focused on other thermochemical options, but since pyrolysis requires little capital input and achieves high return rates, it would be an obvious choice.

8.3 GASIFICATION AND FISCHER-TROPSCH PROCESSES FOR SUGARCANE BAGASSE

There is a wide scope of future work still required for gasification process routes of sugarcane bagasse and other lignocellulosic residues. First of all, the validity of equilibrium modelling of sugarcane bagasse gasification has been confirmed by De Filippis et al, 2004. The next step is to scale up this system to verify that equilibrium conditions can still be met at industrial scales.

Furthermore, co-gasification is widely considered in South Africa to be the preferred pre-runner to full-scale biomass gasification, especially at existing facilities that are currently utilising coal. This can be done in separate gasifiers where the produced gas is combined after preliminary cleaning, or simultaneously in the same gasifier. Kreutz et al, 2008 performed process modelling for various co-gasification scenarios using separate experimental gasifier data for mixed grasses and coal. Experimental data for simultaneous co-gasification of sugarcane bagasse in the same gasifier is scarce, and the effect of gasifying a mixture of coal and bagasse on equilibrium gasification should also be addressed in conjunction with process models to assess the effects on process efficiency and economics.

In addition, there are many different downstream process configurations for Fischer-Tropsch synthesis, of which several have been investigated in other studies (Tijmensen et al, 2002, Hamelinck et al, 2003). In this case, the aim was to maximise the Fischer-Tropsch liquid yield, but this does not necessarily lead to the best overall process efficiency or economic performance. The use of a recycle with methane reformer after synthesis does enhance liquid production but also increases costs. There is merit in considering the effect of using a once-through concept with lower liquid yields and

higher electricity production, especially in light of the eminent near-term changes in the South African electricity market. Likewise, if the price of electricity in South Africa is going to triple in the next three years, and the sugar industry is successful in negotiating a favourable rate for green electricity with the national electricity distributor, the economics of producing electricity via cogeneration from sugarcane bagasse is likely to become increasingly attractive, and a detailed study integrating the technological and market effects for the near term should be performed.

The comparison of all the process routes from a life cycle analysis point of view was not addressed in this study. This is obviously a very important aspect and the energy and cost of the supply and final application of the different fuels should be assessed to compare the life cycle efficiencies, emissions and environmental impacts of the process routes studied here.

Finally, there is a serious need to develop an up-to-date, concise local databank for process equipment required for all biomass-related processes in South Africa. This is problematic since 1) there is limited expertise available in South Africa to produce the specialised equipment required for these processes, 2) there is not sufficient funds available to assign contractors to cost these items, and if so, the information is not released to the public since it is treated as intellectual property, and 3) the available data is often between 5 and 10 years old, and given the fast development of this industry, information needs to be updated on a regular basis. The South African government should establish a dedicated task team to collect this data that can be used by academic and research institutions to steer economic evaluations and reduce the level of uncertainty associated with feasibility studies of this nature.

REFERENCES

Aden, A., M. Ruth, K. Ibsen, J. Jechura, K. Neeves, J. Sheehan and B. Wallace (2002). Lignocellulosic Biomass to Ethanol Process Design and Economics Utilizing Co-Current Dilute Acid Prehydrolysis and Enzymatic Hydrolysis for Corn Stover. Golden, Colorado, US, National Renewable Energy Laboratory.

Bridgwater, A. V., A. J. Toft and J. G. Brammer (2002). "A techno-economic comparison of power production by biomass fast pyrolysis with gasification and combustion." *Renewable and Sustainable Energy Reviews* 6: 181-248.

Hamelinck, C. N., A. P. C. Faaij, H. Den Uil and H. Boerrigter (2003). "Production of FT transportation fuels from biomass; technical options, process analysis and optimisation, and development potential." NWS-E-2003-08.

Hamelinck, C. N., G. v. Hooijdonk and A. P. Faaij (2005). "Ethanol from lignocellulosic biomass: techno-economic performance in short-, middle- and long-term." *Biomass and Bioenergy* 28: 384-410.

Laser, M., E. D. Larson, B. E. Dale, M. Wang, N. Greene and L. R. Lynd (2008). "Comparative analysis of efficiency, environmental impact, and process economics for mature biomass refining scenarios." *Biofuels, Bioproducts and Biorefining* 3: 247-270.

Tijmensen, M. J. A., A. P. C. Faaij, C. N. Hamelinck and M. R. M. v. Hardeveld (2002). "Exploration of the possibilities for production of Fischer-Tropsch liquids and power via biomass gasification." *Biomass and Bioenergy* 23: 129-152.

APPENDIX A1 REACTION DATA FOR BIOETHANOL MODELS

Table A1.1 Composition and heating value of sugarcane bagasse supplied by local producer.

Component	Weight fraction	
Glucan	40.6	
Galactan	0.8	
Mannan	0.2	
Xylan	20.0	
Arabinan	1.7	
Lignin	25.5	
Extractives	7.5	
Ash	3.7	
Higher heating value	19.0	MJ/kg

Table A1.2 Chemical formulas and property data sources for biomass components used in AspenPlus® process models. The NREL in-house databank was kindly supplied by Mark Laser, Dartmouth College, NH, USA.

Component name	Chemical Formula	Properties used
Cellulose	$C_5H_{10}O_5$	NREL in-house databank
Galactan	$C_5H_{10}O_5$	Cellulose
Xylan	$C_5H_8O_4$	NREL in-house databank
Arabinan	$C_5H_8O_4$	Xylan
Mannan	$C_5H_8O_4$	Xylan
Glucose	$C_6H_{12}O_6$	NREL in-house databank
Galactose	$C_6H_{12}O_6$	Glucose
Xylose	$C_5H_{10}O_4$	NREL in-house databank
Arabinose	$C_5H_{10}O_4$	Xylose
Mannose	$C_5H_{10}O_4$	Xylose
Cellobiose	$C_{12}H_{22}O_{11}$	Glucose
Microorganism ^a	$CH_{1.8}O_{0.5}N_{0.2}$	NREL in-house databank
Lignin	$C_{10}H_{13.9}O_{1.3}$	NREL in-house databank
Furfural	$C_5H_4O_2$	

^a Since no property data was available for *Saccharomyces cerevisiae spp.* it was assumed that the properties given in the NREL in-house databank for the recombinant *Z. Mobilis* bacterial strain would be similar to that of the recombinant yeast strain used in this study.

Table A1.3 Stoichiometric pretreatment reactions and fractional conversion data used for bioethanol process models. The conversion data was calculated from Laser et al, 2002, Aguilar et al, 2002 and Martín et al, 2002 for liquid hot water, dilute acid and steam explosion pretreatment, respectively.

	Liquid hot water	Dilute Acid	Steam explosion
Pretreatment Reactions	Fractional conversion		
Cellulose (Cisolid) + H ₂ O → Glucose	0.060	0.059	0.070
2Cellulose (Cisolid) + H ₂ O → Cellobiose	^a 0.006	0.006	0.006
Xylan (Cisolid) + H ₂ O → Xylose	0.830	0.900	0.713
Xylan (Cisolid) → Furfural + 2H ₂ O	0.020	0.034	0.180
Galactan (Cisolid) + H ₂ O → Galactose	^b 0.830	0.900	0.713
Arabinan (Cisolid) + H ₂ O → Arabinose	^b 0.830	0.900	0.713
Mannan (Cisolid) + H ₂ O → Mannose	^b 0.830	0.900	0.713

^a Since no data was available for cellobiose conversion, a conversion of 0.6% was assumed, which is slightly lower than the value of 0.7% assumed by Aden et al, 2002.

^b As per the design case of Aden et al, 2002, the conversion of minor hemicellulose carbohydrates (galactan, arabinan and mannan) are assumed to be equal to that of xylan.

Table A1.4 Stoichiometric reactions and conversion data assumed for saccharification and fermentation reactors and conversion data used for bioethanol models. The data reported by Martín et al, 2006 for cellulose hydrolysis and all the fermentation yields were used for all process models.

	Fractional conversion
Saccharification Reactions	
Cellulose(Cisolid) + H ₂ O → Glucose	0.830
Cellobiose + H ₂ O → 2Glucose	^a 1.000
Fermentation reactions	
Glucose → 2 Ethanol + 2CO ₂	0.880
3Xylose → 5 Ethanol + 5CO ₂	0.440
Xylose + H ₂ O → Xylitol + 0.5O ₂	^b 0.010
Glucose + 1.1429 NH ₃ → 5.7143 Microorganism(Cisolid) + 2.5714 H ₂ O + 0.2857 CO ₂	^c 0.085
Xylose + 0.9524 NH ₃ → 4.7619 Microorganism(Cisolid) + 2.1429 H ₂ O + 0.2381 CO ₂	^c 0.043

^a Based on assumption of Aden et al, 2002.

^b Martín et al, 2006 measured xylitol levels below 1g/l in the fermentation broth, which translates to a maximum conversion of 1%.

^c There is no experimental data available on the growth stoichiometry of *Saccharomyces cerevisiae*, since the compositions of various cells in the same culture will not be consistent either (W.van Zyl, personal communication). Therefore, the biomass growth reaction was derived from the assumed elemental composition of the fermenting organism, and ammonia was assumed to be the nutrient source since ammonium phosphate was used in the experimental runs (Martín et al, 2006). The experimental quantities of the nutrients and/or glucose were fed to seed and hydrolysate fermentation reactors as described by Martín et al, 2006, and the unreacted nutrients were purged to reflect actual experimental conditions.

APPENDIX A2 REACTION DATA FOR PYROLYSIS MODELS

Table A2.1 Fast Pyrolysis reactor calculated product yields

Gas product ^a		Mass yield
CO		0.032
CO ₂		0.083
H ₂ O		0.112
CH ₄		0.004
C ₂ H ₂		0.004
		0.235
Liquid + Solid product		
C ₂ H ₄ O ₂	Acetic acid	0.026
C ₃ H ₆ O ₂	Acetol	^b 0.040
C ₇ H ₈ O ₂ -E	Guaicol (pyrolytic lignin)	0.191
C ₈ H ₁₀ O ₃	Modelled as C ₈ H ₁₀ O (3,5 Xylenol)	^b 0.021
CH ₂ O ₂	Formic acid	0.038
C ₁₀ H ₁₂ O ₃	Modelled as C ₁₀ H ₁₂ O ₂ (benzoic acid)	^b 0.090
C ₆ H ₆ O	Phenol	^b 0.003
C ₇ H ₈	Toluene	^b 0.012
C ₅ H ₄ O ₂	Furfural	^b 0.104
C ₆ H ₆	Benzene	^b 0.004
C ₄ H ₈ O ₄	Tetrahydrofuran	0.076
C ₆ H ₁₀ O ₅	Dilactic acid	0.017
CHAR	Solid char	0.142
		0.765
Total		1.000

^a Gas product yields are calculated from the reaction product gas obtained from experimental data (Piskorz et al, 1998) and an additional portion of the product gas that is recycled to the reactor based on the process design (Ringer et al, 2006).

^b It was found that in the liquid product data provided by Piskorz et al, 1998, 44% of the liquid product components were unspecified. The components indicated here were obtained from the complete component list given by Ringer et al, 2006 but not included in the list given by Piskorz et al, 1998. Therefore, the unspecified liquid fraction was modelled as a mixture of these additional or missing components assuming the same distribution from the data of Ringer et al, 2006.

Table A2.2 Vacuum Pyrolysis reactor calculated product yields

Gas product		Mass yield
H2		0.000
CH4		0.002
CO		0.029
CO2		0.080
C2H4		0.000
C2H6		0.000
C3H6		0.000
C3H8		0.001
CH3OH		0.000
C4H10		0.001
C5H12		0.000
		0.114
Liquid and solid product		
H2O		0.395
C2H4O2	Acetic acid	0.199
C3H6O2	Acetol	0.054
C7H8O2-E	Guaicol (pyrolytic lignin)	0.000
C8H10O3	Modelled as C8H10O (3,5 Xylenol)	0.000
CH2O2	Formic acid	0.000
C10H12O3	Modelled as C10H12O2 (benzoic acid)	0.000
C6H6O	Phenol	0.016
C7H8	Toluene	0.000
C5H4O2	Furfural	0.022
C6H6	Benzene	0.000
C4H8O4	Tetrahydrofuran	0.000
C6H10O5	Dilactic acid	0.000
C4H8O2	Butyric acid	0.005
C4H8O-1	Butanone	0.002
C5H8O3		0.005
C5H8O2-D4	Furanone	0.004
C6H6O2	Benzenediol	0.005
C4H8-4	Cyclobutane	0.002
C14H18O3	Modelled as C14H18O4	0.012
C6H6O3	Trihydroxy	0.003
CHAR	Solid char	0.164
		0.886
Total		1.000

APPENDIX A3 ASPENPLUS® RESULTS FOR BIOETHANOL PROCESS MODELS

Table A3.1 Summary of unit design assumptions and performance results for bioethanol process models.

		Steam Explosion	Dilute Acid (35%)	Dilute Acid 10%	Liquid hot water
Pretreatment AREA 100					
Solids concentration		50	35	10	5
Low pressure steam (4.47 bar)	wt% of wet bagasse feed	3.8%	5.0%	33.0%	49.0%
High pressure steam (13.17 bar)	wt% of wet bagasse feed	1.0%	0.8%	36.3%	217.0%
Flash cooling duty	kW/kW bagasse feed HHV	0	0	69.9%	135.8%
Total solids in prehydrolysate	wt% solids	21	21	22	20
pH of prehydrolysate		4.5	4.6	4.6	4.6
Seed fermentation AREA 200					
Prehydrolysate split to seed train	wt% of prehydrolysate	10%	10%	10%	10%
Oxygen feed	wt% of seed stream	7.0%	9.5%	10.1%	6.4%
Glucose feed	wt% of seed stream	0.8%	0.8%	0.8%	0.7%
Nutrient feed	wt% of seed stream	0.5%	0.4%	0.5%	0.4%
Saccharification and Fermentation AREA 300					
Glucose in hydrolysate	wt% of hydrolysate	7.6%	7.2%	7.7%	6.9%
Xylose in hydrolysate	wt% of hydrolysate	3.6%	3.9%	4.1%	3.4%
Unconverted glucose after fermentation ¹	wt% of broth	0.2%	0.2%	0.2%	0.2%
Unconverted xylose after fermentation	wt% of broth	1.9%	2.1%	2.0%	1.8%
Ethanol in fermentation broth	wt% of broth	3.6%	4.0%	3.8%	3.6%
Ethanol lost to reactor vent ²	% of produced ethanol	1.03%	1.17%	1.09%	1.03%
Carbon dioxide lost to reactor vent ²	% of produced CO ₂	96.4%	96.8%	96.6%	96.4%

¹ Accounts for glucose consumption for ethanol production and biomass growth.

² In practice, some ethanol and CO₂ is lost in the reactor vent, therefore this stream is captured and recycled to the ethanol scrubber during product recovery.

Table A3.1 (continued) Detailed unit design assumptions and performance results for bioethanol process models.

		Steam Explosion	Dilute Acid (35%)	Dilute Acid 10%	Liquid hot water
Ethanol recovery AREA 400					
Preheating stage outlet temperature ³	C	46.0	43.0	43.0	46.0
CO2 flash stage 1					
Temperature	C	86	86	86	86
Pressure	bar	0.84	0.84	0.84	0.84
Vapour fraction		0.0039	0.0038	0.0038	0.0036
Ethanol reporting to vapour	% of feed to flash	2.9%	3.0%	3.0%	2.7%
CO2 reporting to vapour	% of feed to flash	95.0%	95.1%	95.1%	94.6%
CO2 flash stage 2					
Temperature	C	38	38	38	38
Pressure	bar	1.11	1.11	1.11	1.11
Vapour fraction		0.18	0.17	0.17	0.19
Ethanol reporting to vapour	% of feed to flash	7.7%	7.4%	7.4%	10.2%
CO2 reporting to vapour	% of feed to flash	99.3%	91.7%	91.7%	98.4%
Ethanol scrubber					
Stages		3	3	3	3
Top stage temperature	C	14.0	14.1	14.1	14.0
Top stage pressure	bar	1.03	1.03	1.03	1.03
Water/feed ratio	wt/wt	1.45	1.45	1.45	1.45
Ethanol recovered to liquid	wt% of feed to scrubber	99.9%	99.9%	99.9%	99.9%
Overall loss of ethanol to scrubber vent	wt% of ethanol feed to recovery	0.0014%	0.0014%	0.0013%	0.0013%
Overall removal of CO ₂	wt% of CO ₂ feed to recovery	99.6%	99.6%	99.6%	99.5%
Beer column					
Stages		10	10	10	10
Feed stage		1	1	1	1
Top stage temperature	C	102.3	102.4	102.4	102.4
Top stage pressure	bar	1.6	1.6	1.6	1.6
Condenser duty	kW/kW bagasse feed HHV	-9.7%	-10.1%	-10.1%	-10.8%
Reboiler duty	kW/kW bagasse feed HHV	13.6%	14.1%	14.1%	14.7%
Ethanol recovery to distillate ⁴	fraction of ethanol in column feed	0.997	0.997	0.997	0.997
Ethanol mass fraction in distillate ⁴		0.55	0.55	0.55	0.55
Rectification column					
Stages		18	18	18	18
Feed stream		8	8	8	8
Recycle stream		12	12	12	12
Top stage temperature	C	86.3	86.4	86.4	86.4
Top stage pressure	bar	1.4	1.4	1.4	1.4
Condenser duty	kW/kW bagasse feed HHV	-2.7%	-2.4%	-2.4%	-2.4%
Reboiler duty	kW/kW bagasse feed HHV	1.4%	1.1%	1.1%	1.1%
Ethanol mass fraction in distillate ⁴		90.85%	90.85%	90.85%	90.85%
Ethanol mass fraction in bottoms ⁴		0.05%	0.05%	0.05%	0.05%
Ethanol lost to bottoms	fraction of total ethanol produced	0.34%	0.34%	0.34%	0.34%
Molecular sieve					
Pre-heating temperature	C	120	120	120	120
Pre-heating pressure	bar	1.38	1.38	1.38	1.38
Molecular sieve temperature	C	115	115	115	115
Regenerate stream outlet pressure	bar	0.3	0.3	0.3	0.3
Product stream outlet pressure	bar	1.29	1.29	1.29	1.29
Ethanol product concentration	wt%	99.5%	99.5%	99.5%	99.5%

³ The fermentation broth is preheated using the hot vapour stream from the pretreatment flash cooling stage.

⁴ Design specifications entered in AspenPlus®.

Table A3.1 (continued) Detailed unit design assumptions and performance results for bioethanol process models.

		Steam Explosion	Dilute Acid (35%)	Dilute Acid 10%)	Liquid hot water
Evaporation AREA500					
Pre-evaporator flash stage					
Temperature	C	75.4	75.4	75.4	75.4
Pressure	bar	0.39	0.39	0.39	0.39
Vapour fraction		0.16	0.19	0.19	0.19
Water evaporated	% of total water evaporated	24%	29%	29%	29%
Pneumatic press					
Temperature	C	70	70	70	70
Pressure	bar	3.2	3.2	3.2	3.2
Solids reporting to cake	% of total solids in feed	98%			
Soluble solids to syrup	% of total soluble solids in feed	90%			
Insoluble solids in solid cake ⁵	wt/wt	40%	46%	44%	44%
Air/feed ratio	wt/wt	0.019	0.020	0.019	0.018
Syrup recycled to pretreatment	wt% of total syrup	25%			
Multiple effect evaporator					
1st stage water evaporated	% of total water evaporated	25%	29%	29%	29%
2nd stage water evaporated	% of total water evaporated	25%	29%	29%	29%
3rd stage water evaporated	% of total water evaporated	25%	13%	13%	13%
Total water evaporated	% of total water in beer stillage	66%	69%	69%	74%
Moisture content of final syrup	wt%	69%	76%	76%	74%

⁵ Maximum solids load is 55% according to Aden et al, 2002.

Table A3.1 (continued) Detailed unit design assumptions and performance results for bioethanol process models.

		Steam Explosion	Dilute Acid (35%)	Dilute Acid 10%)	Liquid hot water
Boiler section AREA600					
Combustor					
Temperature	C	870	870	870	870
Pressure	bar	0.98	0.98	0.98	0.98
Moisture in combined syrup and stillage feed ⁶	wt%	50%	43%	51%	50%
Boiler feed lower heating value ⁷	kcal/kg	2654.73	2403.46	2600.65	2570.37
Boiler feed water/boiler feed energy ⁸	wt/wt	0.076%	0.084%	0.075%	0.078%
Air feed rate/Boiler feed energy ⁹	wt/wt	0.151%	0.180%	0.142%	0.145%
Molar extent of combustion reactions	fractional conversion	0.99	0.99	0.99	0.99
Boiler flash drum					
Temperature	C	572.65	604.85	604.85	680.05
Pressure ¹⁰	bar	87.14	87.14	87.14	87.14
Boiler blowdown		3%	3%	3%	3%
Boiler efficiency ¹¹		64%	63%	68%	68%

⁶ Design value of boiler feed moisture is 50% according to Aden et al, 2002.

⁷ According to the vendor design criteria described by Aden et al, 2002, the minimum lower heating value should be 1111-1389kcal/kg. Their model resulted in a boiler feed lower heating value of 2322 kcal/kg.

⁸ This ratio was used to calculate the required boiler feed water rate, and the criteria was set to be below the value obtained from Aden et al, 2002 of 0.085%.

⁹ In order to supply sufficient air for combustion, this ratio is set to be above the 0.12% obtained from the design of Aden et al, 2002.

¹⁰ The boiler temperature is dependent on the temperature of the boiler feed water and the energy supplied to the flash drum from the combustion reactor.

¹¹ The boiler efficiency is calculated as the energy in the superheated steam divided by the combined energy in the boiler feed water and combustion heat. The data of Aden et al, 2002 resulted in an efficiency of 68%.

Table A3.1 (continued) Detailed unit design assumptions and performance results for bioethanol process models.

		Steam Explosion	Dilute Acid (35%)	Dilute Acid 10%)	Liquid hot water
Water treatment AREA700					
Fresh make up water	% of total boiler feed water	58%	60%	35%	37%
Boiler feed water pump duty	kW/kW bagasse feed HHV	0.87%	0.47%	0.47%	0.44%
Steam turbine cycle AREA800					
Turbine 1					
Pressure	bar	13.17	13.17	13.17	13.17
Steam extracted	wt% of total boiler steam	9.9%	10.9%	28.5%	35.2%
To boiler feed water heating	wt% of total boiler steam	9.1%	10.3%	9.5%	9.3%
To pretreatment reactor	wt% of total boiler steam	0.8%	0.6%	19.0%	25.9%
Turbine 2					
Pressure	bar	4.47	4.47	4.47	4.47
Steam extracted	wt% of total boiler steam	72.8%	73.2%	40.6%	45.6%
To evaporation	wt% of total boiler steam	9.3%	10.3%	15.6%	9.3%
To pretreatment reactor	wt% of total boiler steam	4.0%	4.3%	25.0%	36.3%
To distillation reboilers ¹²	wt% of total boiler steam	59.5%	53.5%	0.0%	0.0%
Turbine 3					
Pressure	bar	1.72	1.72	1.72	1.72
Steam extracted	wt% of total boiler steam	5.2%	5.0%	4.4%	4.3%
To deaerator	wt% of total boiler steam	5.2%	5.0%	4.4%	4.3%
Turbine 4					
Pressure	bar	0.01	0.01	0.01	0.01
Total electricity generated	kWe/kW bagasse feed HHV	13.0%	12.8%	11.4%	9.9%

¹² The liquid hot water and dilute acid pretreatment models did not produce sufficient steam for the distillation reboilers and required additional steam to be bought in.

Table A3.2 Breakdown of process energy demands determined for process models for bioethanol scenarios.

Breakdown of process electricity requirements ($\text{kW}_e/\text{kW}_{\text{HHV}}$ bagasse input)				
Pretreatment method	Steam explosion	Dilute acid	Dilute acid	LHW
<i>Solids in pretreatment reactor</i>	50%	35%	10%	5%
Produced from stillage residue				
Pretreatment ^a	0.21%	2.00%	2.00%	0.16%
Fermentation ^b	0.40%	0.40%	0.40%	0.40%
Distillation ^b	0.40%	0.40%	0.40%	0.40%
Evaporator	0.15%	0.15%	0.15%	0.15%
Water plant	0.45%	0.42%	0.47%	0.49%
Total electricity consumption	1.61%	3.36%	3.42%	1.59%

Breakdown of additional (external) steam requirements ($\text{kW}_{\text{steam}}/\text{kW}_{\text{HHV}}$ bagasse input)				
Pretreatment	0.00%	0.00%	0.00%	56.1%
Conditioning	0.00%	0.00%	69.9%	135.7%
Distillation reboilers	0.00%	0.00%	15.4%	15.8%
Total produced from additional coal or bagasse	0.00%	0.00%	85.4%	207.7%
Boiler efficiency	64.3%	62.9%	62.9%	68.3%
Coal/bagasse energy required for additional steam	0%	0%	135.7%	303.9%

^a Includes the energy requirement for a screw feeder estimated at 0.16% of the biomass energy input (Aden et al, 2002).

^b Data supplied by Aden et al, 2002 to include energy required for agitators during fermentation, reboiler pump around work (since packaged distillation columns were used in this study which does not supply this data).

Table A3.3 Summary of energy balance obtained from process models for bioethanol scenarios.

Pretreatment method		Steam explosion	Dilute acid	Dilute acid	Liquid hot water
<i>Solids in pretreatment reactor</i>	<i>wt %</i>	<i>50.0%</i>	<i>35.0%</i>	<i>10.0%</i>	<i>5.0%</i>
Thermal energy input in feedstock	% HHV	100.0%	100.0%	100.0%	100.0%
Thermal energy in coal	% HHV	0.0%	0.0%	125.0%	303.9%
Total thermal energy input	% HHV	100.0%	100.0%	225.0%	403.9%
Energy in ethanol product	% HHV	30.5%	30.5%	13.8%	7.5%
Residual energy to combustor	% HHV	73.0%	61.4%	77.7%	75.9%
Steam Energy produced for process	% HHV	29.0%	30.0%	52.3%	65.9%
Total Electricity produced	kW _e /kW _{th}	13.0%	12.8%	5.1%	2.4%
Total Electricity produced (thermal equivalent)	% HHV	28.9%	28.5%	11.7%	5.4%
Total energy conversion of biomass	% HHV	88.4%	89.0%	77.7%	78.9%
Process electricity (kWe/kW th)	kW _e /kW _{th}	1.6%	3.4%	0.7%	0.4%
Export electricity (kWe/kWth)	kW _e /kW _{th}	11.4%	9.4%	4.2%	2.1%
Export electricity (thermal equivalent)	% HHV	25.3%	21.0%	10.1%	4.6%
<i>Process thermal energy efficiency^a</i>	<i>% HHV</i>	<i>55.8%</i>	<i>51.5%</i>	<i>23.9%</i>	<i>12.1%</i>
<i>Liquid fuel energy efficiency^a</i>	<i>% HHV</i>	<i>40.9%</i>	<i>38.6%</i>	<i>15.3%</i>	<i>7.9%</i>

^a See description in text.

APPENDIX A4 ASPENPLUS® RESULTS FOR PYROLYSIS PROCESS MODELS

Table A4.1 Detailed unit design assumptions and performance results for pyrolysis process models.

		Fast Pyrolysis	Vacuum Pyrolysis
Pretreatment AREA 100			
Grinder energy consumption	kW/kW bagasse feed HHV	2.1%	2.1%
Dried bagasse moisture content	wt%	3.8%	4.1%
Drier air flow	wt/wt bagasse feed	7.2	7.2
Drier energy consumption	kW/kW bagasse feed HHV	5.9%	6.0%
Pyrolysis AREA 200			
Fluidising gas flow	wt/wt bagasse feed	1.4	0.0
Reactor feed heating energy consumption ¹	kW/kW bagasse HHV	13.6%	0.6%
Reactor energy consumption	kW/kW bagasse HHV	5.8%	8.2%
Reactor product flows			
Biocrude	wt/wt bagasse feed	39.1%	38.1%
Char ²	wt/wt bagasse feed	6.6%	10.5%
Char consumed for process energy	wt/wt bagasse feed	3.0%	0.0%
Reactor gas	wt/wt bagasse feed	6.2%	5.8%
Char product HHV	MJ/kg	25	32
Char product energy yield	kW/kW bagasse feed HHV	9.5%	35.3%

¹ For fast pyrolysis, the majority of the heating energy is ascribed to heating of the fluidising gas.

² More energy is recovered from the vacuum pyrolysis char since more char is produced compared to fast pyrolysis.

Table A4.1 (continued) Detailed unit design assumptions and performance results for pyrolysis process models.

		Fast Pyrolysis	Vacuum Pyrolysis
Quenching AREA 300			
Heat recovery from quenching ³			
For drier air preheating	kW/kW bagasse feed HHV	14.6%	8.4%
For steam generation	kW/kW bagasse feed HHV	0.4%	0.2%
Steam raised from quenching energy		3.5%	3.5%
Steam flow rate	wt/wt bagasse feed		
Steam temperature	C	244	131
Steam pressure	bar	36	36
Oil scrubber			
Scrubber oil-gas recycle stream ⁴	wt/wt quenched feed to scrubber	3.3%	15.3%
Light gas split fraction to gas product	(H ₂ ,CO,CO ₂ ,CH ₄ .C ₂ H ₄ and NH ₃)	100.0%	100.0%
Biocrude split fraction to liquid product		80.0%	80.0%
Electrostatic precipitator			
Light gas split fraction to gas product	(H ₂ ,CO,CO ₂ ,CH ₄ .C ₂ H ₄ and NH ₃)	100.0%	100.0%
Biocrude split fraction to liquid product		99.9%	99.9%
Heat recovery AREA 400			
Air flow to combustor	wt/wt combustible gas feed	20.2	22.9
Energy recovered from combustion gas		28%	26%

³ Fast pyrolysis produces more biocrude compared to vacuum pyrolysis; therefore more energy is recovered during quenching.

⁴ To increase oil product recovery, a portion of the final product is recycled back to the scrubber. The percentage is lower for fast pyrolysis since the fluidising gas is still present in the scrubber feed.

Table A4.2 Summary of energy balance obtained from process models for pyrolysis scenarios.

Pyrolysis mode		Fast pyrolysis	Vacuum pyrolysis
Thermal energy input in feedstock	% HHV	100.0%	100%
Process energy			
Drying	% HHV	5.9%	6.0%
Grinding	% HHV	2.1%	2.1%
Gas heating	% HHV	13.6%	0.6%
Pyrolysis reactor	% HHV	5.8%	8.2%
Total process energy	% HHV	27.4%	16.9%
Energy in oil product	% HHV	60.2%	40.6%
Energy in char product	% HHV	9.5%	27.6%
Energy in export electricity	% HHV	0.0%	1.8%
<i>Process energy efficiency</i>	<i>% HHV</i>	69.7%	70.0%

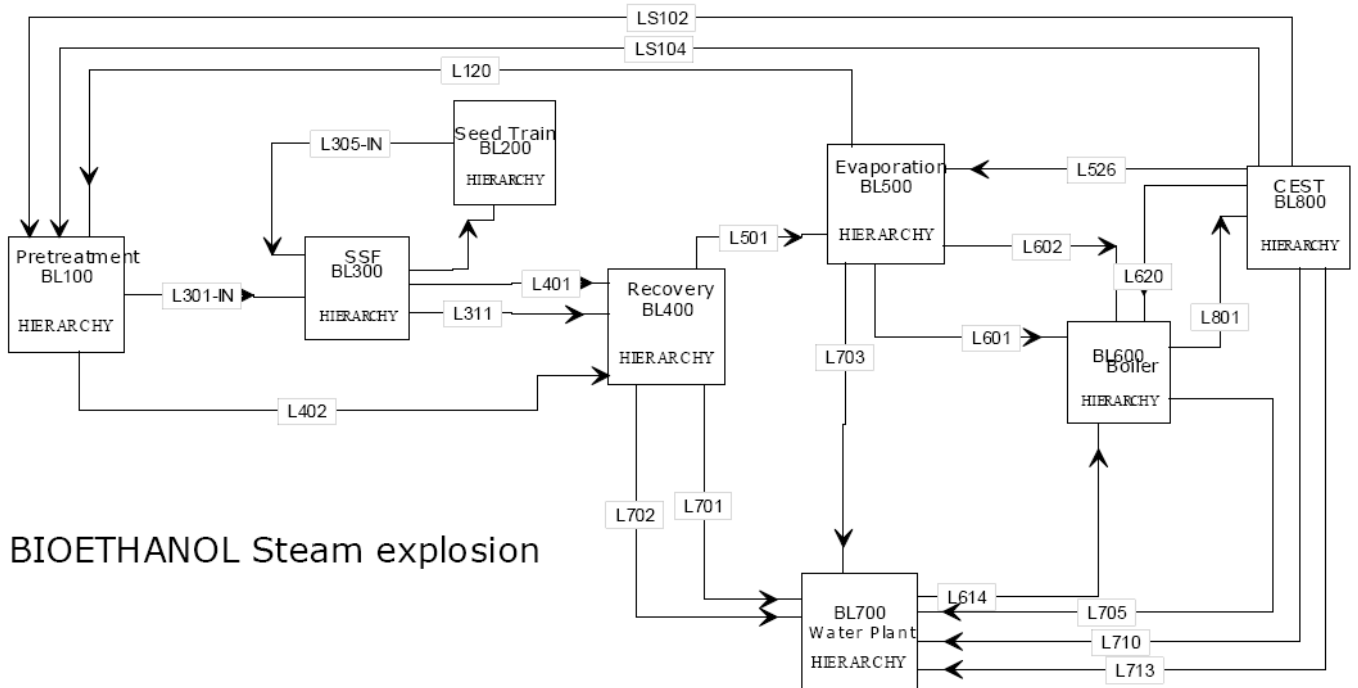
APPENDIX A5 HEAT INTEGRATION CALCULATIONS FOR BIOETHANOL, PYROLYSIS AND FISCHER-TROPSCH PROCESS MODELS

Table A5.1 Calculation of the effect of heat integration on the liquid fuel energy efficiencies of bioethanol production using steam explosion, fast pyrolysis and bagasse gasification using EG1 followed by Fischer-Tropsch synthesis.

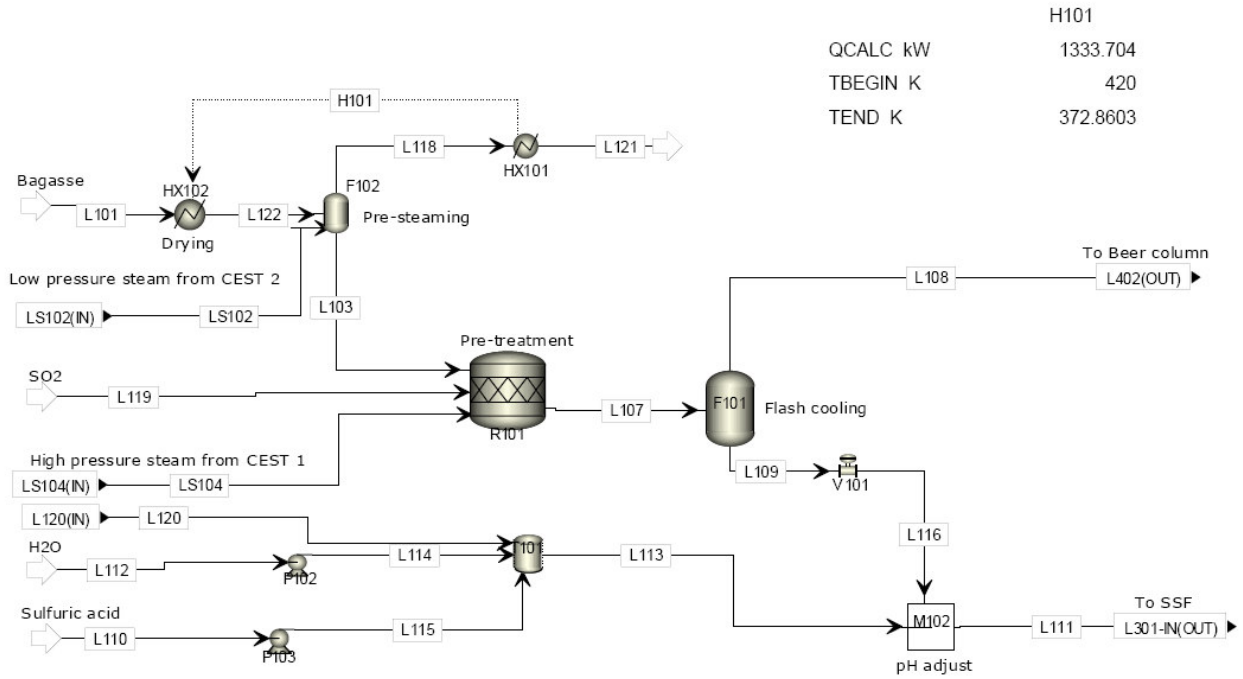
	Bioethanol (steam explosion)	Pyrolysis (fast pyrolysis)	Fischer-Tropsch (EG1-bagasse)
<i>Process heat integration</i>			
Feed drying	0.9%	Grinding	2.1%
Beer column	2.2%	Dryer	5.9%
Molecular sieve	0.1%	Fluidising gas pre-heating	13.6%
Evaporator	22.7%	Pyrolysis reactor	5.8%
Boiler feed energy	4.8%	Boiler feed energy	20.6%
	30.6%	25.3%	42.3%
<i>Process steam produced by steam cycle</i>			
Pretreatment	1.6%		Gasifier
Distillation	7.0%		Autothermal reformer
Evaporation	1.8%		
Boiler feed water heating	1.9%		
Water treatment	0.8%		
	13.0%		21.9%
<i>Process electricity produced by steam cycle</i>			
Electric units [kW_e/kW HHV biomass input]	2.5%		3.4%
Thermal units [kW_{th}/kW HHV biomass input]	5.6%		7.7%
<i>Process energy demands [kW_{th}/kW HHV biomass input]</i>			
No process heat integration, no steam cycle	49.3%		32.9%
With process heat integration, no steam cycle	18.7%		7.7%
Liquid fuel product yield [kW/kW HHV biomass input]	30.5%		60.2%
<i>Liquid fuel energy efficiency</i>			
No process heat integration, no steam cycle	20.4%		45.3%
With process heat integration, no steam cycle	25.7%		55.9%
With process heat integration and steam cycle (base case)	40.9%		66.5%
<i>Improvement in liquid fuel efficiency</i>			
With process heat integration, no steam cycle	5.3%		10.6%
With process heat integration and steam cycle	20.4%		21.2%

APPENDIX A6 PROCESS FLOW DIAGRAMS FOR BIOETHANOL and PYROLYSIS PROCESS MODELS

Appendix A6.1 Process flow diagrams and stream data for bioethanol steam explosion 145 MW scenario. In all the bioethanol models, minor streams and duplicate streams were emitted to reduce the stream tables, but enough stream data is given to solve the complete mass balances.



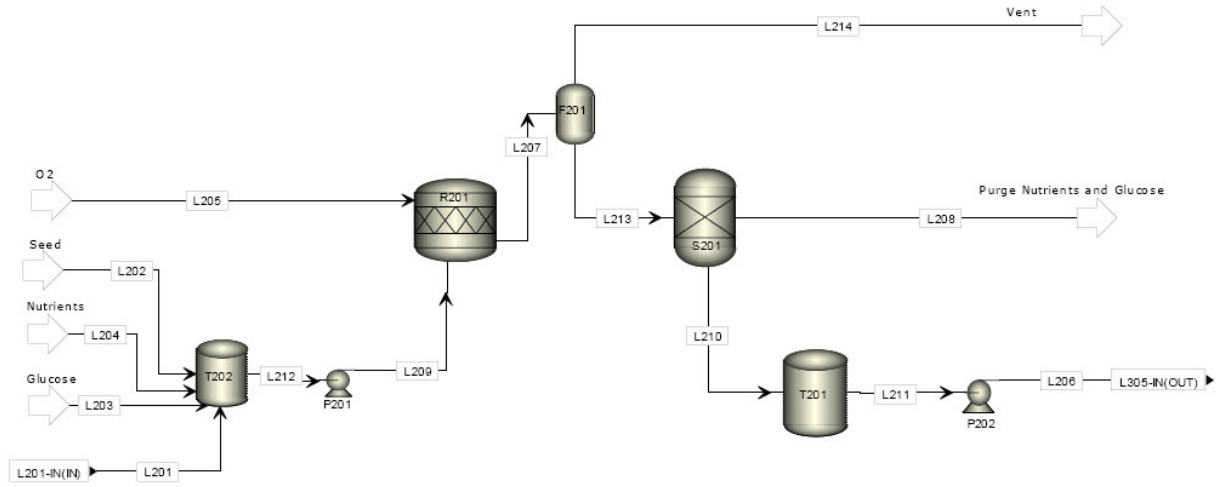
AREA 100



H101
 QCALC KW 1333.704
 TBEGIN K 420
 TEND K 372.8603

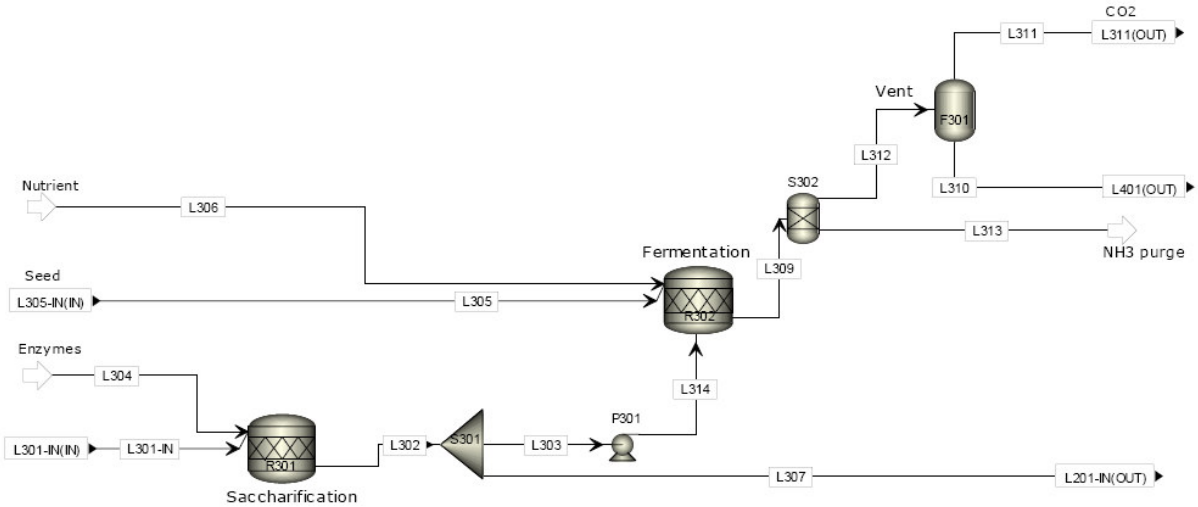
	L101	L103	L107	L108	L109	L110	L111	L113	L119	LS102	LS104
Temperature K	298.1	420	483.1	373.8	373.8	298.1	338.1	298.2	298.1	538	661.4
Pressure bar	1.013	4.337	19.5	1	1	1.013	1.013	1.013	1.013	4.458	13
Vapor Frac	0	0	0	1	0	0	0	0	1	1	1
Mass Flow kg/hr	52800	53392.37	53946.77	6993.487	46953.29	0.127	135477.1	88523.81	290.4	2640	264
Mass Flow TOTAL kg/hr											
GLUCOSE	0	0	833.651	0	833.651	0	905.363	71.712	0	0	0
CELLULOS	10718.4	10718.4	9903.802	0	9903.802	0	9912.227	8.425	0	0	0
XYLOSE	0	0	4277.984	0	4277.984	0	4829.447	551.462	0	0	0
XYLAN	5280	5280	564.96	0	564.96	0	567.799	2.839	0	0	0
LIGNIN	6732	6732	6732	0	6732	0	6765.829	33.829	0	0	0
BIOMASS	0	0	0	0	0	0	11.172	11.172	0	0	0
MICROORG	0	0	0	0	0	0	109.275	109.275	0	0	0
ARABINOS	0	0	395.759	0	395.759	0	510.656	114.898	0	0	0
GALACTOS	0	0	167.317	0	167.317	0	215.893	48.576	0	0	0
MANNOS	0	0	41.829	0	41.829	0	53.973	12.144	0	0	0
ARABINAN	448.8	448.8	100.531	0	100.531	0	101.036	0.505	0	0	0
MANNAN	52.8	52.8	15.154	0	15.154	0	15.23	0.076	0	0	0
GALACTAN	211.2	211.2	60.614	0	60.614	0	60.919	0.305	0	0	0
CELLOB	0	0	67.883	0	67.883	0	67.883	0	0	0	0
XYLITOL	0	0	0	0	0	0	14.209	14.209	0	0	0
EXTRACT	1980	1980	1980	0	1980	0	1989.95	9.95	0	0	0
PROTEIN	0	0	0	0	0	0	0	0	0	0	0
ASH	976.8	976.8	976.8	0	976.8	0	981.709	4.909	0	0	0
ETHANOL	0	0.121	0.14	0.107	0.033	0	1.105	1.072	0	0.195	0.019
H2O	26400	26983.62	26836.89	6702.752	20134.14	0	107475.7	87341.6	0	2627.625	262.762
SO2	0	4.825	296.053	260.269	35.785	0	35.785	0	290.4	8.281	0.828
H3O+	0	0	0.001	0	0	0	0.063	0.063	0	0	0
OH-	0	0	0.001	0	0	0	0	0	0	0	0
FURF	0	2.646	694.122	30.136	663.986	0	850.614	186.628	0	2.679	0.268
HSO4-	0	0	0	0	0	0	0.002	0.001	0	0	0
SO4--	0	0	0	0	0	0	0.158	0.16	0	0	0
SULFU-01	0	0	0	0	0	0.127	0	0	0	0	0
HYDRAZIN	0	1.163	1.285	0.223	1.062	0	1.062	0	0	1.22	0.122

AREA 200



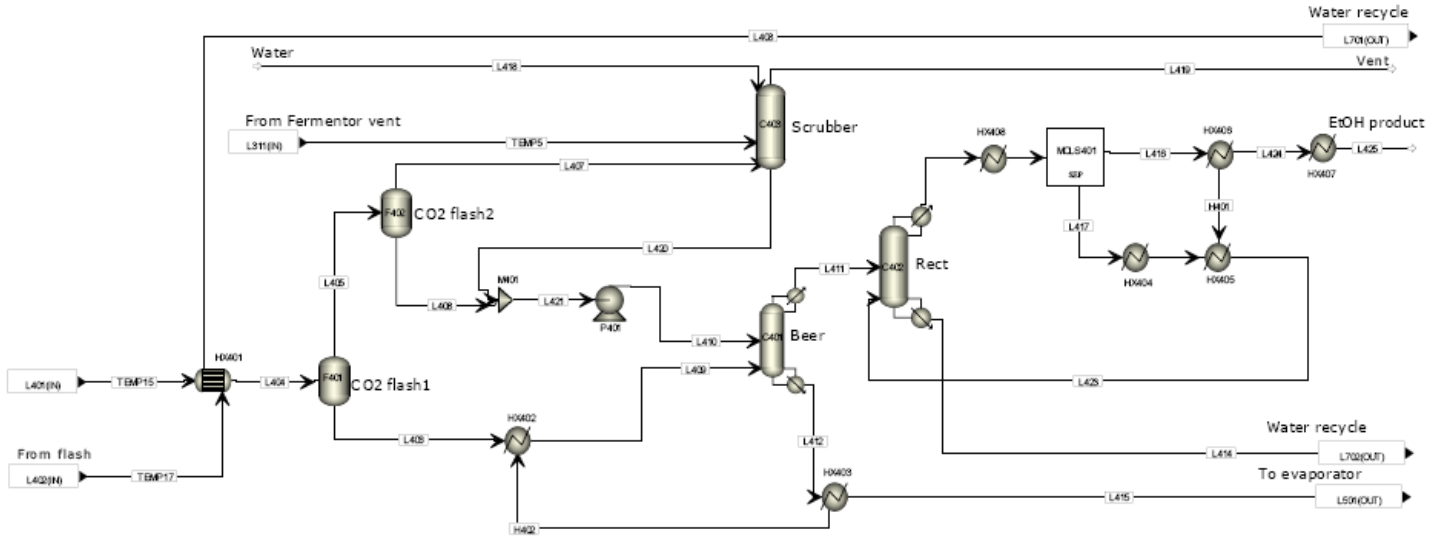
	L201	L202	L203	L204	L205	L206	L207
Temperature K	338.1	303.1	303.1	303.1	303.1	303.2	303.1
Pressure bar	1.013	1.013	1.013	1.013	1.013	1.115	1.013
Vapor Frac	0	0	0	0.88	1	0	0.046
Mass Flow kg/hr	13548.5	0.0	105.6	60.7	924.0	12790.9	14638.8
Mass Flow TOTAL kg/hr							
GLUCOSE	1011.8	0.0	105.6	0.0	0.0	0.0	759.8
CELLULOSE	168.5	0.0	0.0	0.0	0.0	168.5	168.5
XYLOSE	482.9	0.0	0.0	0.0	0.0	482.9	482.9
XYLAN	56.8	0.0	0.0	0.0	0.0	56.8	56.8
LIGNIN	676.6	0.0	0.0	0.0	0.0	676.6	676.6
BIOMASS	1.1	0.0	0.0	0.0	0.0	79.3	79.3
MICROORG	10.9	0.0	0.0	0.0	0.0	10.9	10.9
ARABINOS	51.1	0.0	0.0	0.0	0.0	51.1	51.1
GALACTOS	21.6	0.0	0.0	0.0	0.0	21.6	21.6
MANNOSE	5.4	0.0	0.0	0.0	0.0	5.4	5.4
ARABINAN	10.1	0.0	0.0	0.0	0.0	10.1	10.1
MANNAN	1.5	0.0	0.0	0.0	0.0	1.5	1.5
GALACTAN	6.1	0.0	0.0	0.0	0.0	6.1	6.1
XYLITOL	1.4	0.0	0.0	0.0	0.0	1.4	1.4
EXTRACT	199.0	0.0	0.0	0.0	0.0	199.0	199.0
ASH	98.2	0.0	0.0	0.0	0.0	98.2	98.2
ETHANOL	0.1	0.0	0.0	0.0	0.0	0.1	0.1
H2O	10655.8	0.0	0.0	0.0	0.0	10800.9	10823.4
CO2	0.0	0.0	0.0	0.0	0.0	4.4	409.4
O2	0.0	0.0	0.0	0.0	924.0	0.3	626.3
NH3	0.0	0.0	0.0	27.3	0.0	26.7	27.3
SO2	3.6	0.0	0.0	0.0	0.0	2.9	3.6
H3O+	0.0	0.0	0.0	0.0	0.0	0.0	0.0
FURF	85.1	0.0	0.0	0.0	0.0	85.0	85.1
SO4--	0.0	0.0	0.0	0.0	0.0	0.0	0.0
CELLULAS	0.8	0.0	0.0	0.0	0.0	0.8	0.8
KH2PO4	0.0	0.0	0.0	18.2	0.0	0.2	18.2
MGSO4-01	0.0	0.0	0.0	15.2	0.0	0.2	15.2
HYDRAZIN	0.1	0.0	0.0	0.0	0.0	0.1	0.1

AREA 300



	L301-IN	L302	L303	L304	L305	L306	L307	L309	L310	L311	L312	L313	L314
Temperature K	338.1	338.1	338.1	298.1	303.2	298.1	338.1	303.1	303.2	303.2	303.1	303.1	338.2
Pressure bar	1.013	1.013	1.013	1.013	1.115	1.013	1.013	1.013	1.115	1.115	1.013	1.013	1.165
Vapor Frac	0	0	0	0	0	1	0	0	0	1	0.019	1	0
Mass Flow kg/hr	135477.1	135484.7	121936.2	7.6	12790.9	100.3	13548.5	134827.4	129806.6	4999.6	134806.2	21.2	121936.2
Mass Flow TOTAL kg/hr													
GLUCOSE	905.4	10118.1	9106.3	0.0	0.0	0.0	1011.8	318.7	318.7	0.0	318.7	0.0	9106.3
CELLULOS	9912.2	1685.1	1516.6	0.0	168.5	0.0	168.5	1685.1	1685.1	0.0	1685.1	0.0	1516.6
XYLOSE	4829.4	4829.4	4346.5	0.0	482.9	0.0	482.9	2450.9	2450.9	0.0	2450.9	0.0	4346.5
XYLAN	567.8	567.8	511.0	0.0	56.8	0.0	56.8	567.8	567.8	0.0	567.8	0.0	511.0
LIGNIN	6765.8	6765.8	6089.2	0.0	676.6	0.0	676.6	6765.8	6765.8	0.0	6765.8	0.0	6089.2
BIOMASS	11.2	11.2	10.1	0.0	79.3	0.0	1.1	89.4	89.4	0.0	89.4	0.0	10.1
MICROORG	109.3	109.3	98.3	0.0	10.9	0.0	10.9	874.2	874.2	0.0	874.2	0.0	98.3
ARABINOS	510.7	510.7	459.6	0.0	51.1	0.0	51.1	510.7	510.7	0.0	510.7	0.0	459.6
GALACTOS	215.9	215.9	194.3	0.0	21.6	0.0	21.6	215.9	215.9	0.0	215.9	0.0	194.3
MANNOSE	54.0	54.0	48.6	0.0	5.4	0.0	5.4	54.0	54.0	0.0	54.0	0.0	48.6
ARABINAN	101.0	101.0	90.9	0.0	10.1	0.0	10.1	101.0	101.0	0.0	101.0	0.0	90.9
MANNAN	15.2	15.2	13.7	0.0	1.5	0.0	1.5	15.2	15.2	0.0	15.2	0.0	13.7
GALACTAN	60.9	60.9	54.8	0.0	6.1	0.0	6.1	60.9	60.9	0.0	60.9	0.0	54.8
CELLOB	67.9	0.0	0.0	0.0	0.0	0.0	0.0	0.0	0.0	0.0	0.0	0.0	0.0
XYLITOL	14.2	14.2	12.8	0.0	1.4	0.0	1.4	63.2	63.2	0.0	63.2	0.0	12.8
EXTRACT	1990.0	1990.0	1791.0	0.0	199.0	0.0	199.0	1990.0	1990.0	0.0	1990.0	0.0	1791.0
PROTEIN	0.0	0.0	0.0	0.0	0.0	0.0	0.0	0.0	0.0	0.0	0.0	0.0	0.0
ASH	981.7	981.7	883.5	0.0	98.2	0.0	98.2	981.7	981.7	0.0	981.7	0.0	883.5
ETHANOL	1.1	1.1	1.0	0.0	0.1	0.0	0.1	5186.2	5129.2	57.0	5186.2	0.0	1.0
H2O	107475.7	106558.1	95902.3	0.0	10800.9	0.0	10655.8	106949.1	106869.7	79.4	106949.1	0.0	95902.3
N2	0.0	0.0	0.0	0.0	0.0	0.0	0.0	0.0	0.0	0.0	0.0	0.0	0.0
CO2	0.0	0.0	0.0	0.0	4.4	0.0	0.0	5026.1	170.7	4855.4	5026.1	0.0	0.0
O2	0.0	0.0	0.0	0.0	0.3	0.0	0.0	5.4	0.0	5.4	5.4	0.0	0.0
NH3	0.0	0.0	0.0	0.0	26.7	100.3	0.0	21.2	0.0	0.0	0.0	21.2	0.0
SO2	35.8	35.8	32.2	0.0	2.9	0.0	3.6	35.1	32.8	2.4	35.1	0.0	32.2
FURF	850.6	850.6	765.6	0.0	85.0	0.0	85.1	850.6	850.5	0.1	850.6	0.0	765.6
CELLULAS	0.0	7.6	6.8	7.6	0.8	0.0	0.8	7.6	7.6	0.0	7.6	0.0	6.8

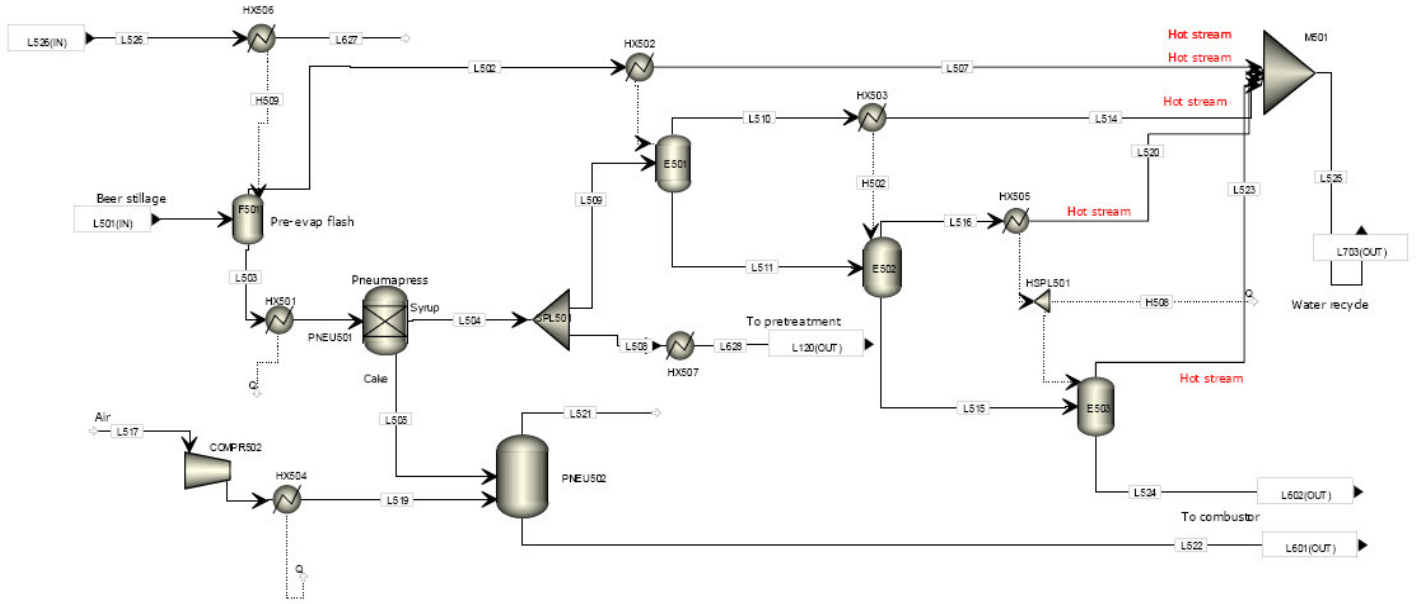
AREA 400



	L403	L404	L405	L406	L407	L408	L409	L410	L411	L412	L413	L414	L416	L417	L418	L419	L420	L423	L425
Temperature K	372.3	319.1	359.1	359.1	311.1	311.1	381.2	295.2	375.4	388.3	359.4	387.5	388.7	388.7	286.1	287.1	294.5	353.1	288.1
Pressure bar	1	2.027	0.841	0.841	1.115	1.115	3.445	1.723	1.551	1.689	1.379	1.655	1.293	0.3	2.07	1.034	1.034	1.52	1.277
Vapor Frac	0.505	0	1	0	1	0	0	0	1	0	1	0	1	1	0	1	0	0	0
Mass Flow kg/hr	6993.5	129806.6	602.5	129204.1	178.0	424.5	129204.1	8050.5	9401.1	127853.5	7111.3	4172.7	5228.4	1882.9	7490.9	5042.5	7626.0	1882.9	5228.4
Mass Flow TOTAL kg/hr																			
GLUCOSE	0.0	318.7	0.0	318.7	0.0	0.0	318.7	0.0	0.0	318.7	0.0	0.0	0.0	0.0	0.0	0.0	0.0	0.0	0.0
CELLULOS	0.0	1685.1	0.0	1685.1	0.0	0.0	1685.1	0.0	0.0	1685.1	0.0	0.0	0.0	0.0	0.0	0.0	0.0	0.0	0.0
XYLOSE	0.0	2450.9	0.0	2450.9	0.0	0.0	2450.9	0.0	0.0	2450.9	0.0	0.0	0.0	0.0	0.0	0.0	0.0	0.0	0.0
XYLAN	0.0	567.8	0.0	567.8	0.0	0.0	567.8	0.0	0.0	567.8	0.0	0.0	0.0	0.0	0.0	0.0	0.0	0.0	0.0
LIGNIN	0.0	6785.8	0.0	6785.8	0.0	0.0	6785.8	0.0	0.0	6785.8	0.0	0.0	0.0	0.0	0.0	0.0	0.0	0.0	0.0
BIOMASS	0.0	89.4	0.0	89.4	0.0	0.0	89.4	0.0	0.0	89.4	0.0	0.0	0.0	0.0	0.0	0.0	0.0	0.0	0.0
MICROORG	0.0	874.2	0.0	874.2	0.0	0.0	874.2	0.0	0.0	874.2	0.0	0.0	0.0	0.0	0.0	0.0	0.0	0.0	0.0
ARABINOS	0.0	510.7	0.0	510.7	0.0	0.0	510.7	0.0	0.0	510.7	0.0	0.0	0.0	0.0	0.0	0.0	0.0	0.0	0.0
GALACTOS	0.0	215.9	0.0	215.9	0.0	0.0	215.9	0.0	0.0	215.9	0.0	0.0	0.0	0.0	0.0	0.0	0.0	0.0	0.0
MANNOS	0.0	54.0	0.0	54.0	0.0	0.0	54.0	0.0	0.0	54.0	0.0	0.0	0.0	0.0	0.0	0.0	0.0	0.0	0.0
ARABINAN	0.0	101.0	0.0	101.0	0.0	0.0	101.0	0.0	0.0	101.0	0.0	0.0	0.0	0.0	0.0	0.0	0.0	0.0	0.0
MANNAN	0.0	15.2	0.0	15.2	0.0	0.0	15.2	0.0	0.0	15.2	0.0	0.0	0.0	0.0	0.0	0.0	0.0	0.0	0.0
GALACTAN	0.0	60.9	0.0	60.9	0.0	0.0	60.9	0.0	0.0	60.9	0.0	0.0	0.0	0.0	0.0	0.0	0.0	0.0	0.0
XYLITOL	0.0	63.2	0.0	63.2	0.0	0.0	63.2	0.0	0.0	63.2	0.0	0.0	0.0	0.0	0.0	0.0	0.0	0.0	0.0
EXTRACT	0.0	1990.0	0.0	1990.0	0.0	0.0	1990.0	0.0	0.0	1990.0	0.0	0.0	0.0	0.0	0.0	0.0	0.0	0.0	0.0
ASH	0.0	981.7	0.0	981.7	0.0	0.0	981.7	0.0	0.0	981.7	0.0	0.0	0.0	0.0	0.0	0.0	0.0	0.0	0.0
ETHANOL	0.1	5129.2	148.0	4981.2	11.8	136.2	4981.2	204.9	5170.6	15.6	6460.6	2.1	5168.5	1292.1	0.0	0.1	68.8	1292.1	5168.5
H2O	6702.8	106869.7	289.6	106580.2	4.1	285.5	106580.2	7827.1	4170.4	110236.8	593.8	4167.4	3.0	590.8	7490.9	32.8	7541.6	590.8	3.0
CO2	0.0	170.7	162.0	8.7	160.9	1.1	8.7	13.7	22.4	0.0	22.4	0.0	22.4	0.0	0.0	5003.7	12.6	0.0	22.4
SO2	260.3	32.8	2.7	30.0	1.2	1.5	30.0	4.5	34.5	0.0	34.5	0.0	34.5	0.0	0.0	0.6	2.9	0.0	34.5
FURF	30.1	850.5	0.3	850.3	0.0	0.3	850.3	0.3	3.2	847.4	0.0	3.2	0.0	0.0	0.0	0.1	0.0	0.0	0.0
CELLULAS	0.0	7.6	0.0	7.6	0.0	0.0	7.6	0.0	0.0	7.6	0.0	0.0	0.0	0.0	0.0	0.0	0.0	0.0	0.0

AREA 500

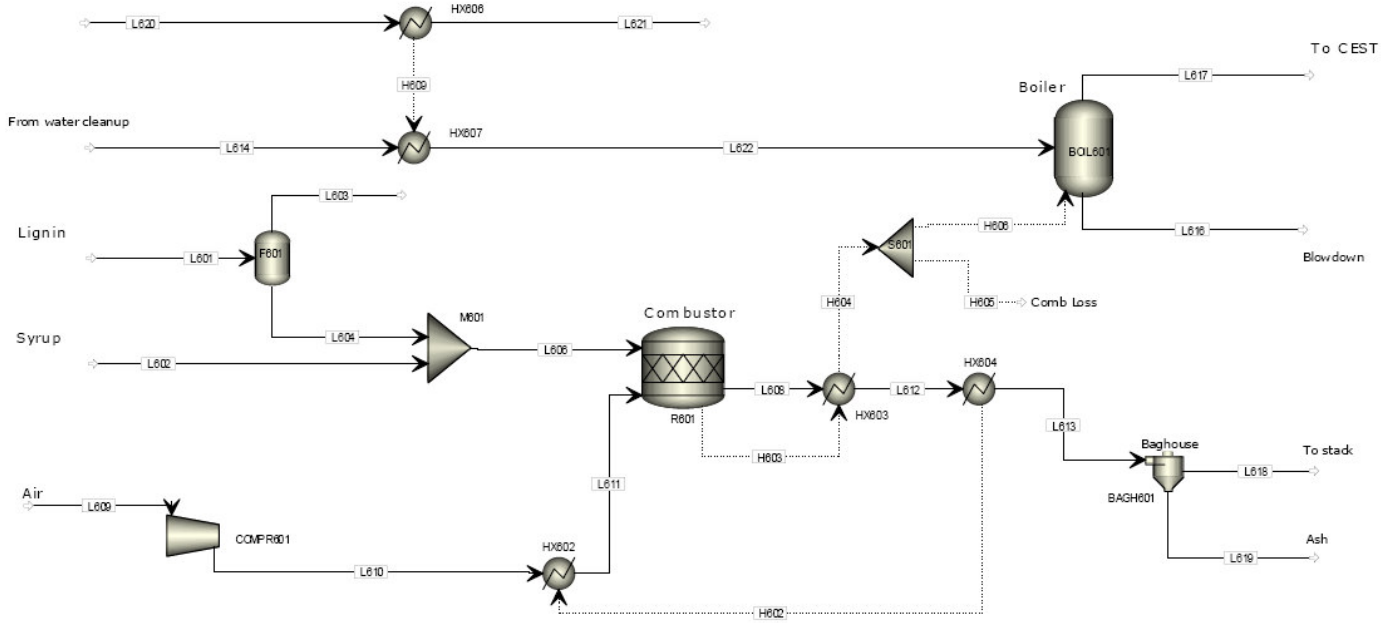
	H502	H504	H505	H506
QCALC kW	10995.9759	616.961312	196.49606	11238.1478
TBEGIN K	339.147143	348.578377	644.629918	334.611975
TEND K	339.147143	343.15	313.15	334.611975



	L502	L503	L504	L505	L509	L510	L511	L515	L516	L519	L522	L524	L525	L628
Temperature K	348.6	348.6	343.1	343.1	343.1	339.1	339.1	334.6	334.6	313.1	337.3	329.3	373.2	298.1
Pressure bar	0.39	0.39	3.242	3.242	3.242	0.26	0.26	0.211	0.211	9.626	3.242	0.162	1.013	1.013
Vapor Frac	1.0	-	-	-	-	1.0	-	-	1.0	1.0	-	-	0.2	-
Mass Flow kg/hr	16,587.4	111,266.1	89,038.7	22,227.5	66,779.0	16,899.1	49,899.9	32,711.7	17,178.2	2,048.8	22,125.7	15,293.3	68,073.0	22,259.7
Mass Flow TOTAL kg/hr														
GLUCOSE	-	318.7	288.8	31.9	215.1	-	215.1	215.1	-	-	31.9	215.1	-	71.7
CELLULOS	-	1,865.1	33.7	1,651.4	25.3	-	25.3	25.3	-	-	1,861.4	25.3	-	8.4
XYLOSE	-	2,450.9	2,205.9	245.1	1,854.4	-	1,854.4	1,854.4	-	-	245.1	1,854.4	-	551.5
XYLAN	-	567.8	11.4	556.4	8.5	-	8.5	8.5	-	-	556.4	8.5	-	2.8
LIGNIN	-	6,765.8	135.3	6,630.5	101.5	-	101.5	101.5	-	-	6,630.5	101.5	-	33.8
BIOMASS	-	89.4	44.7	44.7	33.5	-	33.5	33.5	-	-	44.7	33.5	-	11.2
MICROORG	-	874.2	437.1	437.1	327.8	-	327.8	327.8	-	-	437.1	327.8	-	109.3
ARABINOS	-	510.7	459.6	51.1	344.7	-	344.7	344.7	-	-	51.1	344.7	-	114.9
GALACTOS	-	215.9	194.3	21.6	145.7	-	145.7	145.7	-	-	21.6	145.7	-	48.6
MANNOS	-	54.0	48.6	5.4	36.4	-	36.4	36.4	-	-	5.4	36.4	-	12.1
ARABINAN	-	101.0	2.0	99.0	1.5	-	1.5	1.5	-	-	99.0	1.5	-	0.5
MANNAN	-	15.2	0.3	14.9	0.2	-	0.2	0.2	-	-	14.9	0.2	-	0.1
GALACTAN	-	60.9	1.2	59.7	0.9	-	0.9	0.9	-	-	59.7	0.9	-	0.3
XYLITOL	-	63.2	56.8	6.3	42.6	-	42.6	42.6	-	-	6.3	42.6	-	14.2
EXTRACT	-	1,990.0	39.8	1,950.2	29.8	-	29.8	29.8	-	-	1,950.2	29.8	-	10.0
ASH	-	961.7	16.6	962.1	14.7	-	14.7	14.7	-	-	962.1	14.7	-	4.9
ETHANOL	10.8	4.8	4.3	0.5	3.2	2.7	0.5	0.1	0.5	-	0.4	0.0	14.0	1.1
H2O	16,569.5	93,678.4	84,310.5	9,367.8	63,232.9	16,863.5	46,369.4	29,225.4	17,144.0	-	9,265.8	11,877.9	67,913.5	21,077.6
FURF	18.0	829.5	746.5	82.9	559.9	22.9	636.9	503.2	33.7	-	82.8	432.4	145.4	188.6
CELLULAS	-	7.8	-	7.8	-	-	-	-	-	-	7.8	-	-	-

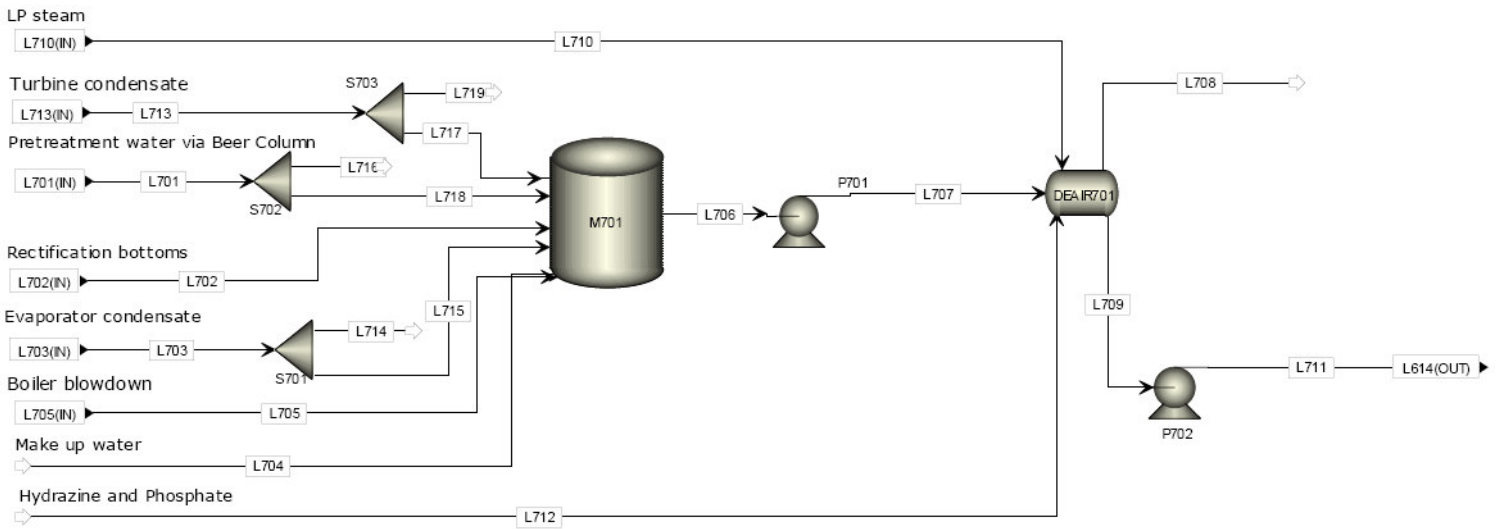
AREA 600

	H604	H605	H609
QCALC KW	56930.1	569.3	4079.1
TBEGIN K	1143.2	1143.2	661.4
TEND K	551.5	551.5	464.7



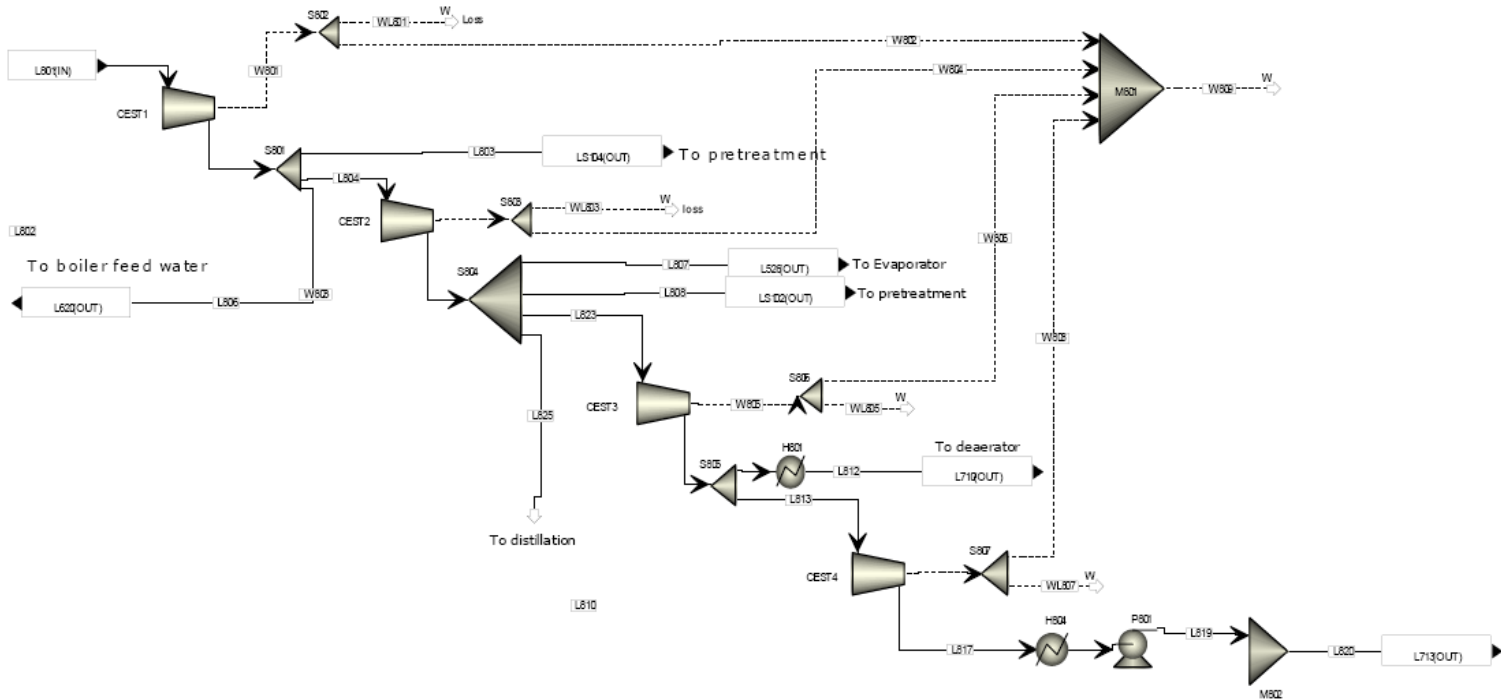
	L603	L604	L606	L608	L611	L612	L613	L614	L616	L617	L622
Temperature K	337.4	337.4	332.3	1143.2	481.8	551.5	430.1	412.2	937.6	937.6	462.1
Pressure bar	1.013	1.013	1.013	0.979	1.027	0.979	0.979	96.26	87.139	87.139	96.26
Vapor Frac	1	0	0	0.992	1	0.99	0.99	0	0	1	0
Mass Flow kg/hr	0.395	22125.325	37418.66	169511.072	132000	169511.072	169511.072	68147.153	0.003	68147.004	68147.097
Mass Flow TOTAL kg/hr											
GLUCOSE	0	31.872	247.007	2.47	0	2.47	2.47	0	0	0	0
CELLULOS	0	1651.377	1676.653	16.767	0	16.767	16.767	0	0	0	0
XYLOSE	0	245.004	1999.482	18.995	0	18.995	18.995	0	0	0	0
XYLAN	0	558.443	564.98	5.65	0	5.65	5.65	0	0	0	0
LIGNIN	0	6630.513	6732	67.32	0	67.32	67.32	0	0	0	0
BIOMASS	0	44.689	78.205	0.782	0	0.782	0.782	0	0	0	0
MICROORG	0	437.1	764.924	764.924	0	764.924	764.924	0	0	0	0
ARABINOS	0	51.066	395.759	3.958	0	3.958	3.958	0	0	0	0
GALACTOS	0	21.589	167.317	1.673	0	1.673	1.673	0	0	0	0
MANNOS	0	5.397	41.829	0.418	0	0.418	0.418	0	0	0	0
ARABINAN	0	99.016	100.531	1.005	0	1.005	1.005	0	0	0	0
MANNAN	0	14.925	15.154	0.152	0	0.152	0.152	0	0	0	0
GALACTAN	0	59.701	60.614	0.606	0	0.606	0.606	0	0	0	0
XYLITOL	0	8.315	48.644	0.489	0	0.489	0.489	0	0	0	0
EXTRACT	0	1950.151	1680	1680	0	1979.997	1979.998	0	0	0	0
ASH	0	962.074	978.8	978.8	0	978.8	978.8	0	0	0	0
ETHANOL	0	0.416	0.419	0.004	0	0.004	0.004	5.028	0	5.028	5.028
H2O	0.063	6265.734	21143.622	31688.994	1716	31688.994	31688.994	67827.701	0	67827.648	67827.848
N2	0.227	0.069	0.069	100147.328	100135.2	100147.329	100147.329	0	0	0	0
CO2	0	0	0	28499.478	0	28499.478	28499.478	0	0	0	0
O2	0.105	0.059	0.059	5324.722	30148.8	5324.722	5324.722	0	0	0	0
CH4	0	0	0	0.924	0	0.924	0.924	0	0	0	0
NO2	0	0	0	0.046	0	0.046	0.046	0	0	0	0
SO2	0	0	0	0.895	0	0.895	0.895	213.761	0	213.761	213.761
CO	0	0	0	0.003	0	0.003	0.003	0	0	0	0
H3O+	0	0.006	0.049	0.049	0	0.049	0.049	0.002	0.002	0	0.002
FURF	0	82.837	515.272	5.153	0	5.153	5.153	69.158	0	69.158	69.158
HSO4-	0	0	0.001	0.001	0	0.001	0.001	0	0	0	0
SO4--	0	0.016	0.123	0.123	0	0.123	0.123	0	0	0	0
CELLULAS	0	7.6	7.6	0.076	0	0.076	0.076	0	0	0	0
KH2PO4	0	0.182	0.182	0.182	0	0.182	0.182	0	0	0	0
MGSO4-01	0	0.152	0.152	0.152	0	0.152	0.152	0	0	0	0
HYDRAZIN	0	0.933	0.933	0.933	0	0.933	0.933	31.501	0	31.501	31.501

AREA 700



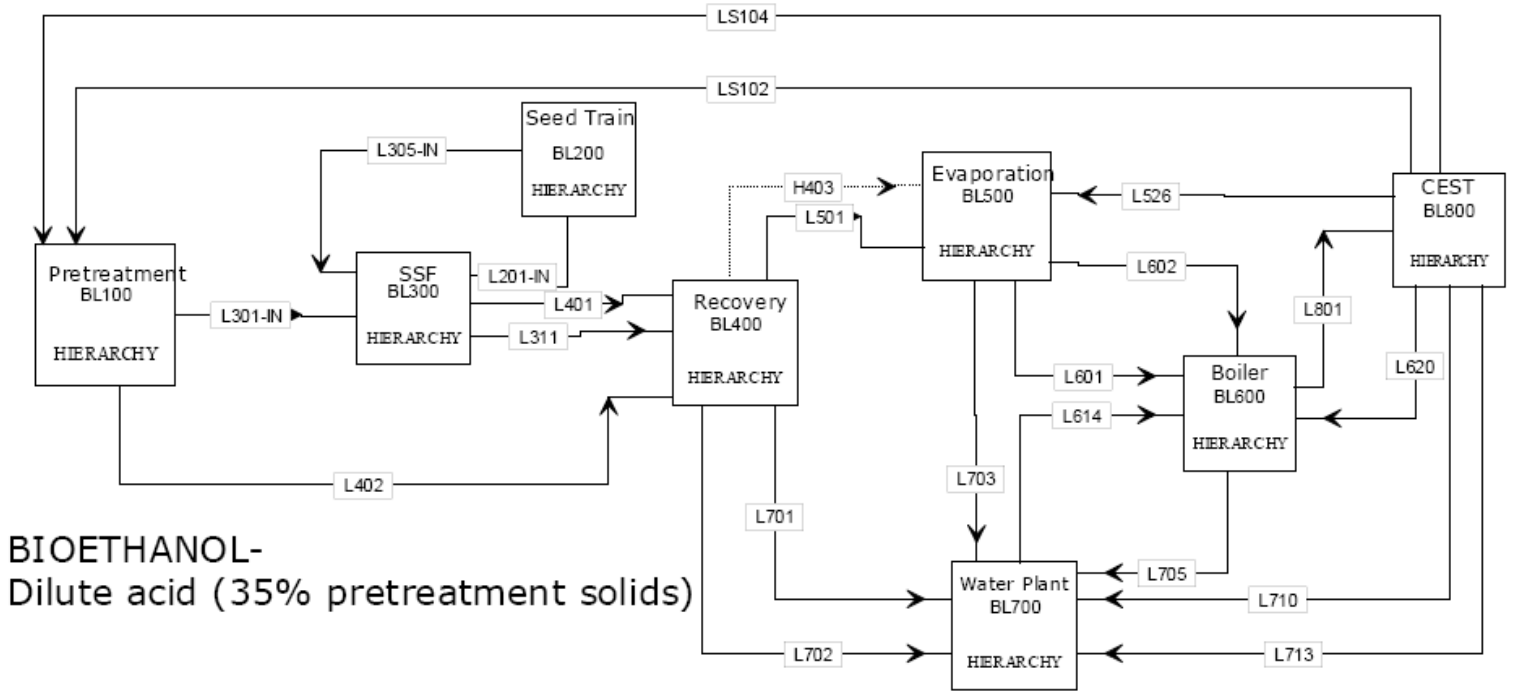
	L704	L706	L707	L708	L709	L711	L712	L715	L717	L718
Temperature K	298.1	374.3	374.4	410.1	410.1	412.2	298.1	373.2	318	372.3
Pressure bar	1.013	1.7	3.445	3.344	3.344	96.26	1.013	1.013	4.2	1
Vapor Frac	0	0	0	1	0	0	0	0.202	0	0.505
Mass Flow kg/hr	34320.0	66285.0	66285.0	1253.1	68147.2	68147.2	26.4	13614.6	8233.3	5944.5
Mass Flow TOTAL kg/hr										
ETHANOL	0.0	5.6	5.6	0.8	5.0	5.0	0.0	2.8	0.6	0.1
H2O	34320.0	65962.1	65962.1	1208.8	67827.7	67827.7	0.0	13582.7	8194.7	5697.3
SO2	0.0	247.1	247.1	43.0	213.8	213.8	0.0	0.0	25.8	221.2
FURF	0.0	66.2	66.2	0.2	69.2	69.2	0.0	29.1	8.4	25.6
HYDRAZIN	0.0	4.0	4.0	0.4	31.5	31.5	26.4	0.0	3.8	0.2

AREA 800

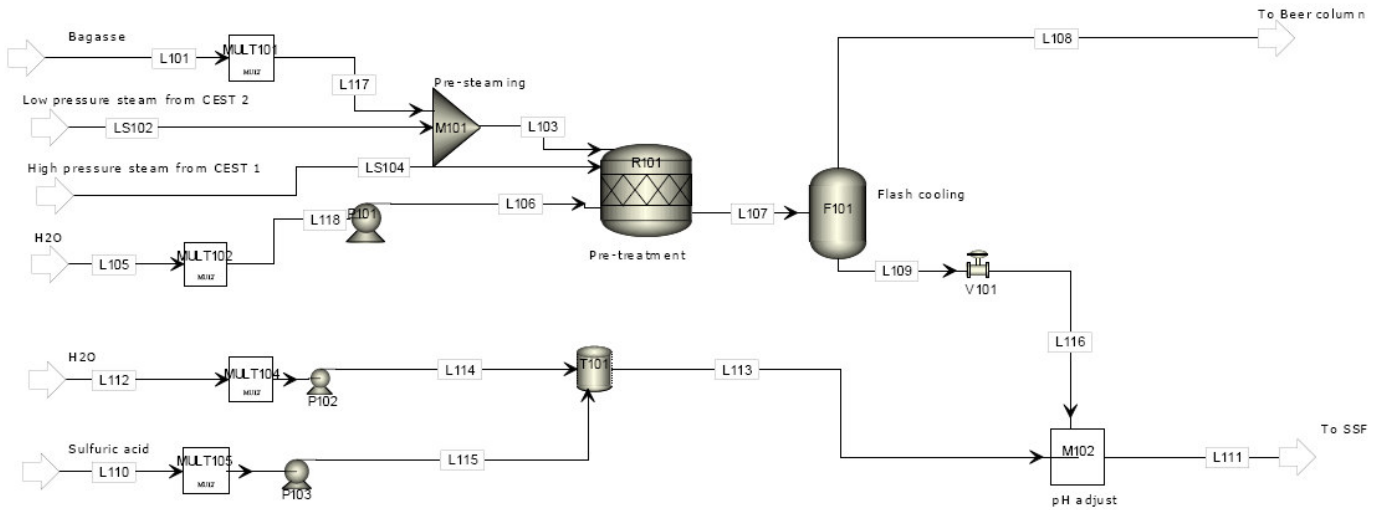


	L801	L802	L803	L804	L805	L806	L807	L808	L810	L812	L813	L820	L823	L825
Temperature K	1080.4	775.7	775.7	775.7	636.2	775.7	636.2	636.2	528.8	387.9	528.8	318.2	636.2	636.2
Pressure bar	87.14	13.00	13.00	13.00	4.46	13.00	4.46	4.46	1.70	1.70	1.70	4.20	4.46	4.46
Vapor Frac	1	1	1	1	1	1	1	1	1	0	1	0	1	1
Mass Flow kg/hr	66541.4	66541.4	528.0	59941.4	59941.4	6072.0	6204.0	2640.0	11497.4	3088.8	8408.6	8408.6	11497.4	39600.0
Mass Flow TOTAL kg/hr														
ETHANOL	0.2	0.2	0.0	0.2	0.2	0.0	0.0	0.0	0.0	0.0	0.0	0.0	0.0	0.1
H2O	2508.6	2508.6	19.9	2259.8	2259.8	228.9	233.9	99.5	433.5	116.4	317.0	317.0	433.5	1492.9
SO2	7.9	7.9	0.1	7.1	7.1	0.7	0.7	0.3	1.4	0.4	1.0	1.0	1.4	4.7
FURF	2.7	2.7	0.0	2.4	2.4	0.2	0.3	0.1	0.5	0.1	0.3	0.3	0.5	1.6
HYDRAZIN	1.1	1.1	0.0	1.0	1.0	0.1	0.1	0.0	0.2	0.1	0.1	0.1	0.2	0.6

Appendix A6.2 Process flow diagrams and stream data for dilute acid pretreatment
(35%) theoretical 145MW scenario

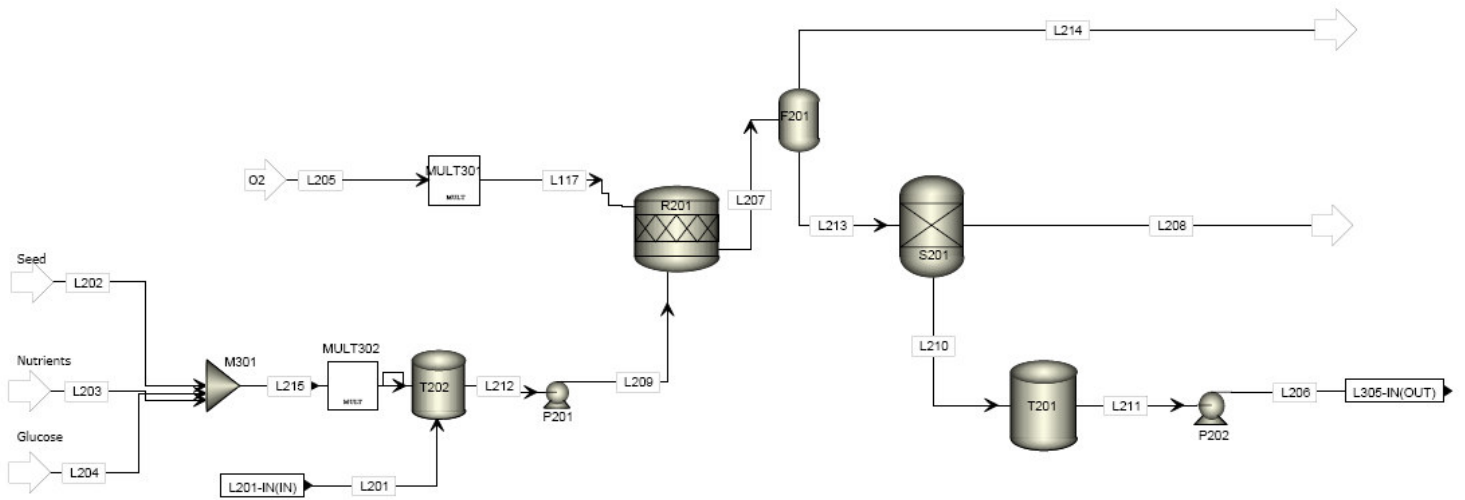


AREA 100



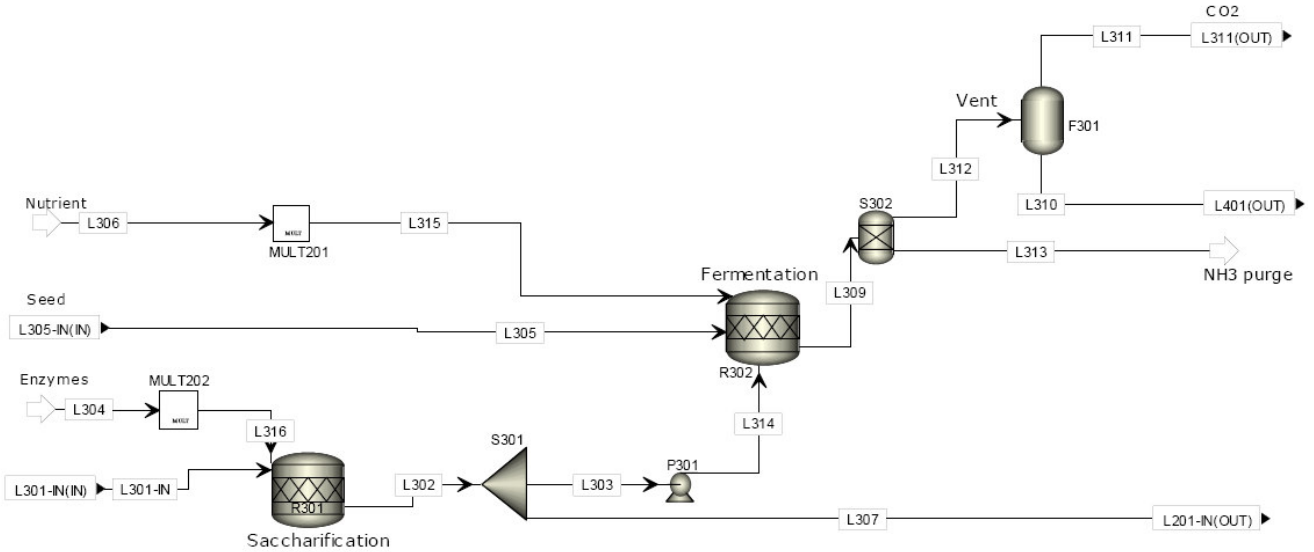
	L106	L107	L108	L109	L111	L113	L117	LS102	LS104
Temperature K	299.2	395	373.4	373.4	338.1	298.2	298.1	683.8	832.5
Pressure bar	19	2.4	1	1	1.013	1.013	1.013	4.479	13.172
Vapor Frac	0	0	1	0	0	0	0	1	1
Mass Flow TOTAL kg/hr	2640.0	82896.0	2381.4	80514.6	130674.8	50160.1	77220.0	2640.0	396.0
Mass Flow TOTAL kg/hr									
GLUCOSE	0.0	702.6	0.0	702.6	702.6	0.0	0.0	0.0	0.0
CELLULOS	0.0	10021.7	0.0	10021.7	10021.7	0.0	10718.4	0.0	0.0
XYLOSE	0.0	5400.0	0.0	5400.0	5400.0	0.0	0.0	0.0	0.0
XYLAN	0.0	348.5	0.0	348.5	348.5	0.0	5280.0	0.0	0.0
LIGNIN	0.0	6732.0	0.0	6732.0	6732.0	0.0	6732.0	0.0	0.0
ARABINOS	0.0	459.0	0.0	459.0	459.0	0.0	0.0	0.0	0.0
GALACTOS	0.0	211.2	0.0	211.2	211.2	0.0	0.0	0.0	0.0
MANNOSE	0.0	52.8	0.0	52.8	52.8	0.0	0.0	0.0	0.0
ARABINAN	0.0	44.9	0.0	44.9	44.9	0.0	448.8	0.0	0.0
MANNAN	0.0	5.3	0.0	5.3	5.3	0.0	52.8	0.0	0.0
GALACTAN	0.0	21.1	0.0	21.1	21.1	0.0	211.2	0.0	0.0
CELLOB	0.0	67.9	0.0	67.9	67.9	0.0	0.0	0.0	0.0
EXTRACT	0.0	3683.7	0.0	3683.7	3683.7	0.0	3683.7	0.0	0.0
ASH	0.0	976.8	0.0	976.8	976.8	0.0	976.8	0.0	0.0
ETHANOL	0.0	0.6	0.2	0.4	0.4	0.0	0.0	0.5	0.1
H2O	2640.0	54035.9	2380.3	51655.6	101815.6	50159.9	49116.3	2638.3	395.7
H3O+	0.0	0.0	0.0	0.0	0.1	0.1	0.0	0.0	0.0
OH-	0.0	0.0	0.0	0.0	0.0	0.0	0.0	0.0	0.0
FURF	0.0	132.0	0.8	131.1	131.1	0.0	0.0	1.2	0.2
HSO4-	0.0	0.0	0.0	0.0	0.0	0.0	0.0	0.0	0.0
SO4--	0.0	0.0	0.0	0.0	0.1	0.1	0.0	0.0	0.0

AREA 200



	L116	L117	L206	L207	L209	L210	L211	L213	L214
Temperature K	308.1	303.1	303.2	303.1	339.5	303.1	303.2	303.1	303.1
Pressure bar	1.013	1.013	1.115	1.013	1.216	1.013	1.013	1.013	1.013
Vapor Frac	0.643	1	0	0.069	0	0	0	0	1
Mass Flow TOTAL kg/hr	166.3	1320.0	12327.129	14573.85	13253.863	12327.129	12327.129	13113.108	1460.742
Mass Flow kg/hr									
GLUCOSE	105.6	0.0	0	752.917	1107.231	0	0	752.917	0
CELLULOS	0.0	0.0	170.369	170.369	170.369	170.369	170.369	170.369	0
XYLOSE	0.0	0.0	539.998	539.998	539.998	539.998	539.998	539.998	0
XYLAN	0.0	0.0	34.848	34.848	34.848	34.848	34.848	34.848	0
LIGNIN	0.0	0.0	673.2	673.2	673.2	673.2	673.2	673.2	0
ARABINOS	0.0	0.0	45.9	45.9	45.9	45.9	45.9	45.9	0
GALACTOS	0.0	0.0	21.12	21.12	21.12	21.12	21.12	21.12	0
MANNOSE	0.0	0.0	5.28	5.28	5.28	5.28	5.28	5.28	0
ARABINAN	0.0	0.0	4.488	4.488	4.488	4.488	4.488	4.488	0
MANNAN	0.0	0.0	0.528	0.528	0.528	0.528	0.528	0.528	0
GALACTAN	0.0	0.0	2.112	2.112	2.112	2.112	2.112	2.112	0
EXTRACT	0.0	0.0	368.372	368.372	368.372	368.372	368.372	368.372	0
ASH	0.0	0.0	97.68	97.68	97.68	97.68	97.68	97.68	0
H2O	0.0	0.0	10222.655	10254.859	10088.778	10222.655	10222.655	10222.655	32.204
O2	0.0	1320.0	0.293	1025.008	0	0.293	0.293	0.293	1024.715
NH3	27.3	0.0	26.351	27.324	27.324	26.351	26.351	26.351	0.973
FURF	0.0	0.0	13.109	13.113	13.113	13.109	13.109	13.109	0.004
CELLULAS	0.0	0.0	20.064	20.064	20.064	20.064	20.064	20.064	0
KH2PO4	18.2	0.0	0.182	18.216	18.216	0.182	0.182	18.216	0
MGSO4-01	15.2	0.0	0.152	15.18	15.18	0.152	0.152	15.18	0

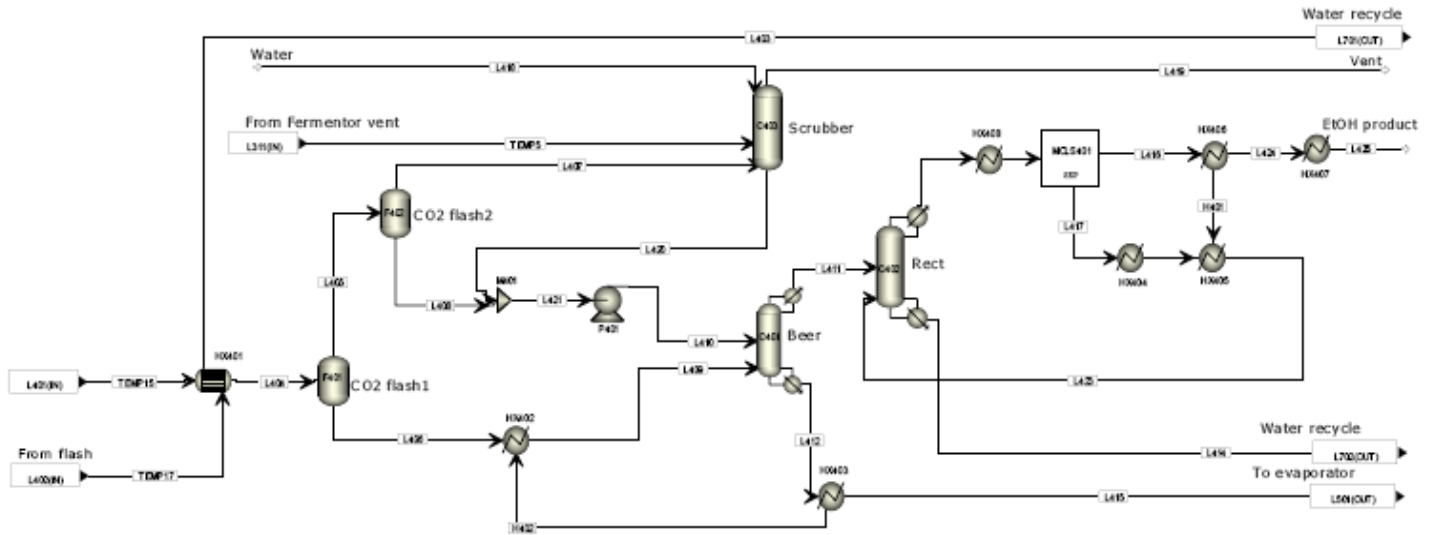
AREA 300



	L302	L303	L307	L309	L310	L311	L312	L313	L315	L316
Temperature K	338.1	338.1	338.1	303.1	303.2	303.2	303.1	303.1	298.1	
Pressure bar	1.013	1.013	1.013	1.013	1.115	1.115	1.013	1.013	1.013	1.013
Vapor Frac	0	0	0	0	0	1	0.02	1	1	
Mass Flow TOTAL kg/hr	130875.4	117787.9	13087.5	130215.3	125102.3	5093.9	130196.2	19.1	100.32	200.64
Mass Flow TOTAL kg/hr										
GLUCOSE	10016.3	9014.7	1001.6	315.5	315.5	0.0	315.5	0.0	0	0
CELLULOS	1703.7	1533.3	170.4	1703.7	1703.7	0.0	1703.7	0.0	0	0
XYLOSE	5400.0	4860.0	540.0	2740.5	2740.5	0.0	2740.5	0.0	0	0
XYLAN	348.5	313.6	34.8	348.5	348.5	0.0	348.5	0.0	0	0
LIGNIN	6732.0	6058.8	673.2	6732.0	6732.0	0.0	6732.0	0.0	0	0
BIOMASS	0.0	0.0	0.0	77.5	77.5	0.0	77.5	0.0	0	0
MICROORG	0.0	0.0	0.0	777.8	777.8	0.0	777.8	0.0	0	0
ARABINOS	459.0	413.1	45.9	459.0	459.0	0.0	459.0	0.0	0	0
GALACTOS	211.2	190.1	21.1	211.2	211.2	0.0	211.2	0.0	0	0
MANNOSE	52.8	47.5	5.3	52.8	52.8	0.0	52.8	0.0	0	0
ARABINAN	44.9	40.4	4.5	44.9	44.9	0.0	44.9	0.0	0	0
MANNAN	5.3	4.8	0.5	5.3	5.3	0.0	5.3	0.0	0	0
GALACTAN	21.1	19.0	2.1	21.1	21.1	0.0	21.1	0.0	0	0
CELLOB	0.0	0.0	0.0	0.0	0.0	0.0	0.0	0.0	0	0
XYLITOL	0.0	0.0	0.0	54.7	54.7	0.0	54.7	0.0	0	0
EXTRACT	3683.7	3315.3	368.4	3683.7	3683.7	0.0	3683.7	0.0	0	0
ASH	976.8	879.1	97.7	976.8	976.8	0.0	976.8	0.0	0	0
ETHANOL	0.4	0.4	0.0	5272.7	5211.3	61.4	5272.7	0.0	0	0
H2O	100887.8	90799.0	10088.8	101271.2	101190.4	80.8	101271.2	0.0	0	0
CO2	0.0	0.0	0.0	5109.0	163.3	4945.7	5109.0	0.0	0	0
O2	0.0	0.0	0.0	6.0	0.0	6.0	6.0	0.0	0	0
NH3	0.0	0.0	0.0	19.1	0.0	0.0	0.0	19.1	100.32	0
FURF	131.1	118.0	13.1	131.1	131.1	0.0	131.1	0.0	0	0
CELLULAS	200.6	180.6	20.1	200.6	200.6	0.0	200.6	0.0	0	200.64
KH2PO4	0.0	0.0	0.0	0.2	0.2	0.0	0.2	0.0	0	0
MGSO4-01	0.0	0.0	0.0	0.2	0.2	0.0	0.2	0.0	0	0

AREA 400

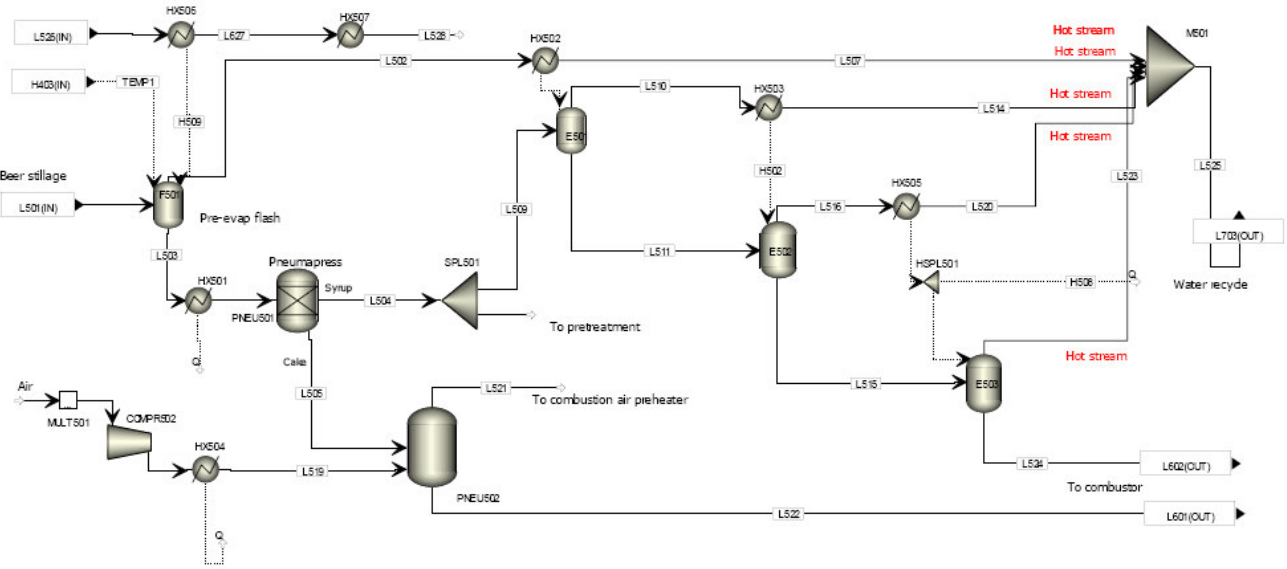
	H401	H402
QCALC KW	74.86909	3125.0119
TBEGIN K	388.7056	388.17302
TEND K	357.65	366.45



	L403	L404	L405	L406	L407	L408	L409	L410	L411	L412	L413	L414	L416	L417	L418	L419	L420	L423	L425
Temperature K	372.3	319.1	359.1	359.1	311.1	311.1	381.2	295.2	375.4	388.3	359.4	387.5	388.7	388.7	286.1	287.1	294.5	353.1	298.1
Pressure bar	1	2.027	0.841	0.841	1.115	1.115	3.445	1.723	1.551	1.689	1.379	1.655	1.293	0.3	2.07	1.034	1.034	1.52	1.277
Vapor Frac	0.505	0	1	0	1	0	0	0	1	0	1	0	1	1	0	1	0	0	0
Mass Flow kg/hr	6993.5	129806.6	602.5	129204.1	178.0	424.5	129204.1	8050.5	9401.1	127853.5	7111.3	4172.7	5228.4	1882.9	7490.9	5042.5	7626.0	1882.9	5228.4
Mass Flow TOTAL kg/hr																			
GLUCOSE	0.0	318.7	0.0	318.7	0.0	0.0	318.7	0.0	0.0	318.7	0.0	0.0	0.0	0.0	0.0	0.0	0.0	0.0	0.0
CELLULOS	0.0	1695.1	0.0	1695.1	0.0	0.0	1695.1	0.0	0.0	1695.1	0.0	0.0	0.0	0.0	0.0	0.0	0.0	0.0	0.0
XYLOSE	0.0	2450.9	0.0	2450.9	0.0	0.0	2450.9	0.0	0.0	2450.9	0.0	0.0	0.0	0.0	0.0	0.0	0.0	0.0	0.0
XYLAN	0.0	567.8	0.0	567.8	0.0	0.0	567.8	0.0	0.0	567.8	0.0	0.0	0.0	0.0	0.0	0.0	0.0	0.0	0.0
LIGNIN	0.0	6765.8	0.0	6765.8	0.0	0.0	6765.8	0.0	0.0	6765.8	0.0	0.0	0.0	0.0	0.0	0.0	0.0	0.0	0.0
BIOMASS	0.0	89.4	0.0	89.4	0.0	0.0	89.4	0.0	0.0	89.4	0.0	0.0	0.0	0.0	0.0	0.0	0.0	0.0	0.0
MICROORG	0.0	874.2	0.0	874.2	0.0	0.0	874.2	0.0	0.0	874.2	0.0	0.0	0.0	0.0	0.0	0.0	0.0	0.0	0.0
ARABINOS	0.0	510.7	0.0	510.7	0.0	0.0	510.7	0.0	0.0	510.7	0.0	0.0	0.0	0.0	0.0	0.0	0.0	0.0	0.0
GALACTOS	0.0	215.9	0.0	215.9	0.0	0.0	215.9	0.0	0.0	215.9	0.0	0.0	0.0	0.0	0.0	0.0	0.0	0.0	0.0
MANNOS	0.0	54.0	0.0	54.0	0.0	0.0	54.0	0.0	0.0	54.0	0.0	0.0	0.0	0.0	0.0	0.0	0.0	0.0	0.0
ARABINAN	0.0	101.0	0.0	101.0	0.0	0.0	101.0	0.0	0.0	101.0	0.0	0.0	0.0	0.0	0.0	0.0	0.0	0.0	0.0
MANNAN	0.0	15.2	0.0	15.2	0.0	0.0	15.2	0.0	0.0	15.2	0.0	0.0	0.0	0.0	0.0	0.0	0.0	0.0	0.0
GALACTAN	0.0	60.9	0.0	60.9	0.0	0.0	60.9	0.0	0.0	60.9	0.0	0.0	0.0	0.0	0.0	0.0	0.0	0.0	0.0
XYLITOL	0.0	63.2	0.0	63.2	0.0	0.0	63.2	0.0	0.0	63.2	0.0	0.0	0.0	0.0	0.0	0.0	0.0	0.0	0.0
EXTRACT	0.0	1990.0	0.0	1990.0	0.0	0.0	1990.0	0.0	0.0	1990.0	0.0	0.0	0.0	0.0	0.0	0.0	0.0	0.0	0.0
ASH	0.0	981.7	0.0	981.7	0.0	0.0	981.7	0.0	0.0	981.7	0.0	0.0	0.0	0.0	0.0	0.0	0.0	0.0	0.0
ETHANOL	0.1	5129.2	148.0	4981.2	11.8	135.2	4981.2	204.9	5170.6	15.6	6460.6	2.1	5168.5	1292.1	0.0	0.1	68.8	1292.1	5168.5
H2O	6702.8	106969.7	289.5	106580.2	4.1	285.5	106580.2	7927.1	4170.4	110236.8	593.8	4167.4	3.0	590.8	7490.9	32.8	7541.6	590.8	3.0
CO2	0.0	170.7	162.0	8.7	160.9	1.1	8.7	13.7	22.4	0.0	22.4	0.0	22.4	0.0	0.0	5003.7	12.6	0.0	22.4
SO2	260.3	32.8	2.7	30.0	1.2	1.5	30.0	4.5	34.5	0.0	34.5	0.0	34.5	0.0	0.0	0.6	2.9	0.0	34.5
FURF	30.1	850.5	0.3	850.3	0.0	0.3	850.3	0.3	3.2	847.4	0.0	3.2	0.0	0.0	0.0	0.0	0.1	0.0	0.0
CELLULAS	0.0	7.6	0.0	7.6	0.0	0.0	7.6	0.0	0.0	7.6	0.0	0.0	0.0	0.0	0.0	0.0	0.0	0.0	0.0

AREA 500

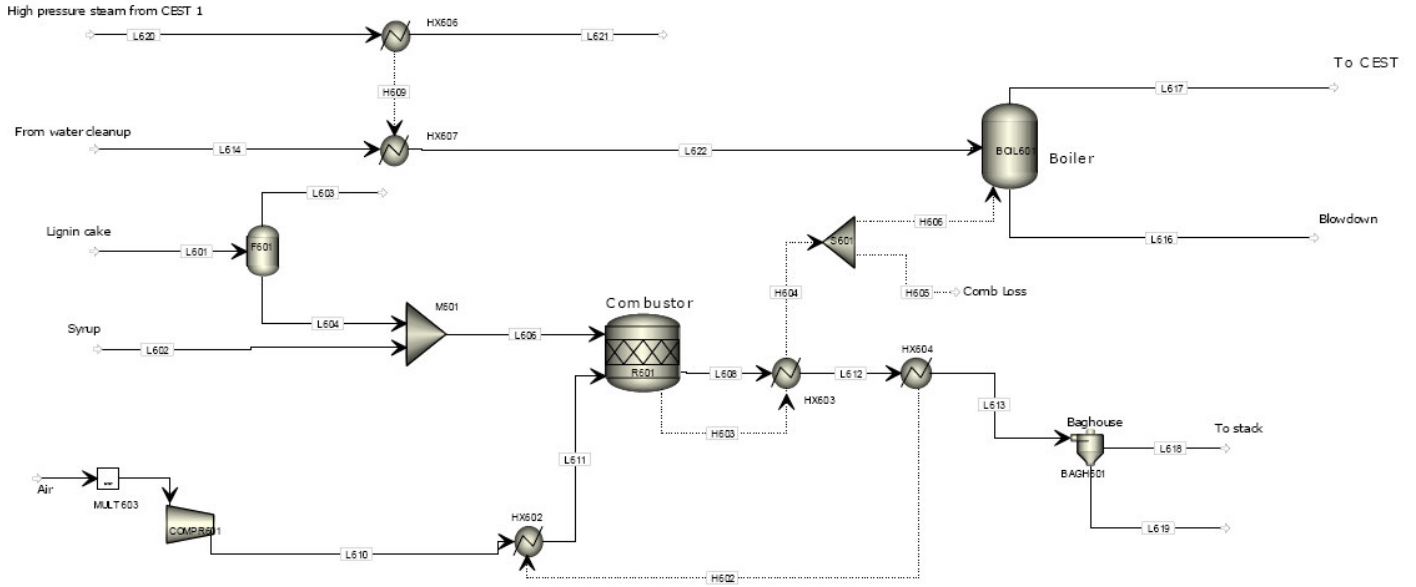
	H502	H504	H505	H506
QCALC kW	10996.0	617.0	196.5	11238.1
TBEGIN K	339.1	348.6	644.6	334.6
TEND K	339.1	343.2	313.2	334.6



	L502	L503	L504	L505	L509	L510	L511	L515	L516	L519	L521	L522	L524	L525	L526
Temperature K	348.6	348.6	343.1	343.1	343.1	339.2	339.2	334.8	334.8	313.1	337	337	330	373.1	663.8
Pressure bar	0.39	0.39	3.242	3.242	3.242	0.26	0.26	0.211	0.211	9.626	3.242	3.242	0.162	1.013	4.479
Vapor Frac	1	0	0	0	0	1	0	0	1	1	1	0	0	0.076	1
Mass Flow TOTAL kg/hr	20,772.8	102,355.4	79,702.8	22,652.6	60,777.1	20,975.3	38,801.8	17,652.2	21,149.7	2,046.6	2,146.6	22,554.6	8,034.9	72,515.0	9,504.0
Mass Flow TOTAL kg/hr															
GLUCOSE	-	315.5	284.0	31.6	213.0	-	213.0	213.0	-	-	-	31.6	213.0	-	-
CELLULOSE	-	1,703.7	34.1	1,669.6	25.6	-	25.6	25.6	-	-	-	1,669.6	25.6	-	-
XYLOSE	-	2,740.5	2,466.4	274.0	1,849.8	-	1,849.8	1,849.8	-	-	-	274.0	1,849.8	-	-
XYLAN	-	348.5	7.0	341.5	5.2	-	5.2	5.2	-	-	-	341.5	5.2	-	-
LIGNIN	-	6,732.0	134.6	6,597.4	101.0	-	101.0	101.0	-	-	-	6,597.4	101.0	-	-
BIOMASS	-	77.5	38.7	38.7	29.1	-	29.1	29.1	-	-	-	38.7	29.1	-	-
MICROORG	-	777.8	388.9	388.9	291.7	-	291.7	291.7	-	-	-	388.9	291.7	-	-
ARABINOS	-	459.0	413.1	45.9	309.8	-	309.8	309.8	-	-	-	45.9	309.8	-	-
GALACTOS	-	211.2	190.1	21.1	142.6	-	142.6	142.6	-	-	-	21.1	142.6	-	-
MANNOS	-	52.8	47.5	5.3	35.6	-	35.6	35.6	-	-	-	5.3	35.6	-	-
ARABINAN	-	44.9	0.9	44.0	0.7	-	0.7	0.7	-	-	-	44.0	0.7	-	-
MANNAN	-	5.3	0.1	5.2	0.1	-	0.1	0.1	-	-	-	5.2	0.1	-	-
GALACTAN	-	21.1	0.4	20.7	0.3	-	0.3	0.3	-	-	-	20.7	0.3	-	-
XYLITOL	-	54.7	49.3	5.5	36.9	-	36.9	36.9	-	-	-	5.5	36.9	-	-
EXTRACT	-	3,683.7	73.7	3,610.0	55.3	-	55.3	55.3	-	-	-	3,610.0	55.3	-	-
ASH	-	976.8	19.5	957.3	14.7	-	14.7	14.7	-	-	-	957.3	14.7	-	-
ETHANOL	12.0	3.8	3.4	0.4	2.6	2.3	0.3	0.0	0.3	-	0.0	0.3	0.0	14.6	1.9
H2O	20,757.0	83,818.6	75,436.8	8,381.9	66,577.6	20,967.4	35,610.2	14,472.2	21,137.9	-	98.3	8,283.6	4,867.4	72,467.1	9,497.7
FURF	3.9	126.8	114.1	12.7	85.6	5.5	80.0	68.6	11.5	-	0.0	12.7	56.1	33.3	4.4
CELLULAS	-	200.6	-	200.6	-	-	-	-	-	-	-	200.6	-	-	-
KH2PO4	-	0.2	-	0.2	-	-	-	-	-	-	-	0.2	-	-	-
MGSO4-01	-	0.2	-	0.2	-	-	-	-	-	-	-	0.2	-	-	-

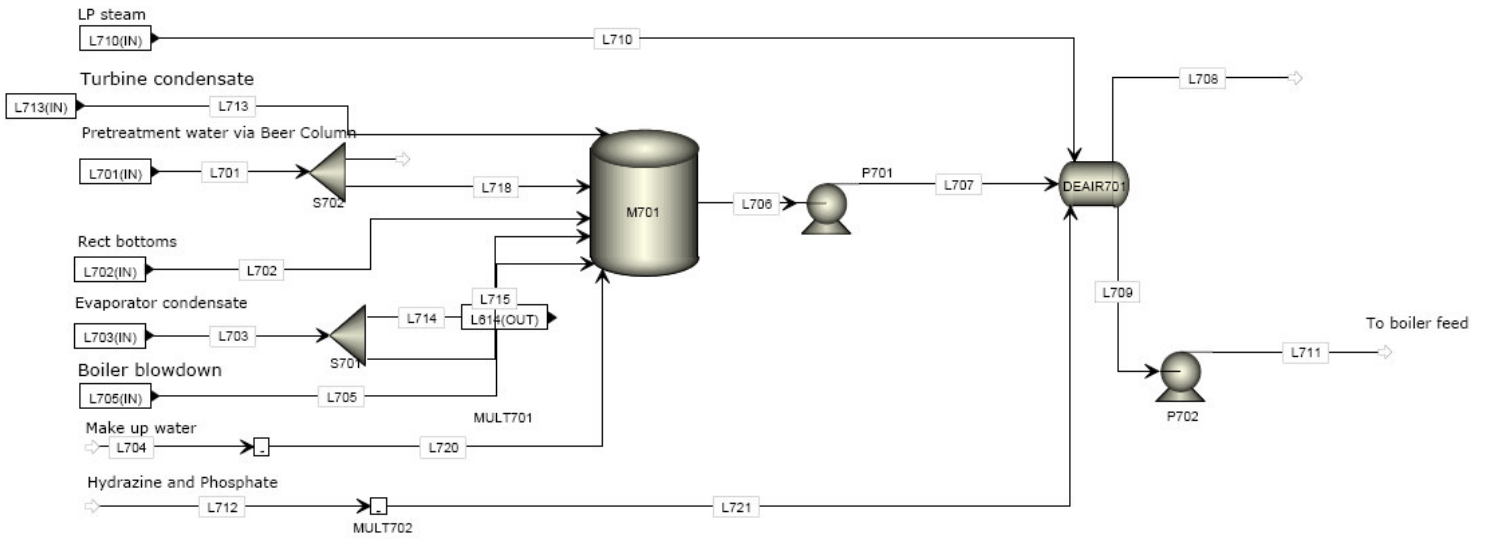
AREA 600

	H604	H606	H609
QCALC kW	60319.8	58751.5	4917.3
TBEGIN K	1143.2	1143.2	832.5
TEND K	551.5	551.5	465.4



	L603	L605	L606	L607	L608	L611	L612	L613
Temperature K	337	298.1	333.3	298.1	1143.2	467.8	551.5	430.1
Pressure bar	1.013	1.013	1.013	1.013	0.979	1.027	0.979	0.979
Vapor Frac	1		0	1	0.997	1	0.997	0.997
Mass Flow TOTAL kg/hr	0.4		30589.2	4.6	162710.7	132000.0	162710.7	162710.7
Mass Flow TOTAL kg/hr								
GLUCOSE	0.0		244.5	0.0	2.4	0.0	2.4	2.4
CELLULOSE	0.0		1695.2	0.0	17.0	0.0	17.0	17.0
XYLOSE	0.0		2123.9	0.0	21.2	0.0	21.2	21.2
XYLAN	0.0		346.7	0.0	3.5	0.0	3.5	3.5
LIGNIN	0.0		6698.3	0.0	67.0	0.0	67.0	67.0
BIOMASS	0.0		67.8	0.0	0.7	0.0	0.7	0.7
MICROORG	0.0		680.6	0.0	680.6	0.0	680.6	680.6
ARABINOS	0.0		355.7	0.0	3.6	0.0	3.6	3.6
GALACTOS	0.0		163.7	0.0	1.6	0.0	1.6	1.6
MANNOSE	0.0		40.9	0.0	0.4	0.0	0.4	0.4
ARABINAN	0.0		44.7	0.0	0.4	0.0	0.4	0.4
MANNAN	0.0		5.3	0.0	0.1	0.0	0.1	0.1
GALACTAN	0.0		21.0	0.0	0.2	0.0	0.2	0.2
XYLITOL	0.0		42.4	0.0	0.4	0.0	0.4	0.4
EXTRACT	0.0		3665.3	0.0	3665.3	0.0	3665.3	3665.3
ASH	0.0		971.9	0.0	971.9	0.0	971.9	971.9
ETHANOL	0.0		0.3	0.0	0.0	0.0	0.0	0.0
H2O	0.1		13151.0	0.0	23615.6	1716.0	23615.6	23615.6
N2	0.2		0.1	0.0	100179.9	100135.2	100179.9	100179.9
O2	0.1		0.1	0.0	5903.9	30148.8	5903.9	5903.9
CH4	0.0		0.0	4.6	1.2	0.0	1.2	1.2
H3O+	0.0		0.0	0.0	0.0	0.0	0.0	0.0
FURF	0.0		68.8	0.0	0.7	0.0	0.7	0.7
CELLULAS	0.0		200.6	0.0	2.0	0.0	2.0	2.0
KH2PO4	0.0		0.2	0.0	0.2	0.0	0.2	0.2
MGSO4-01	0.0		0.2	0.0	0.2	0.0	0.2	0.2

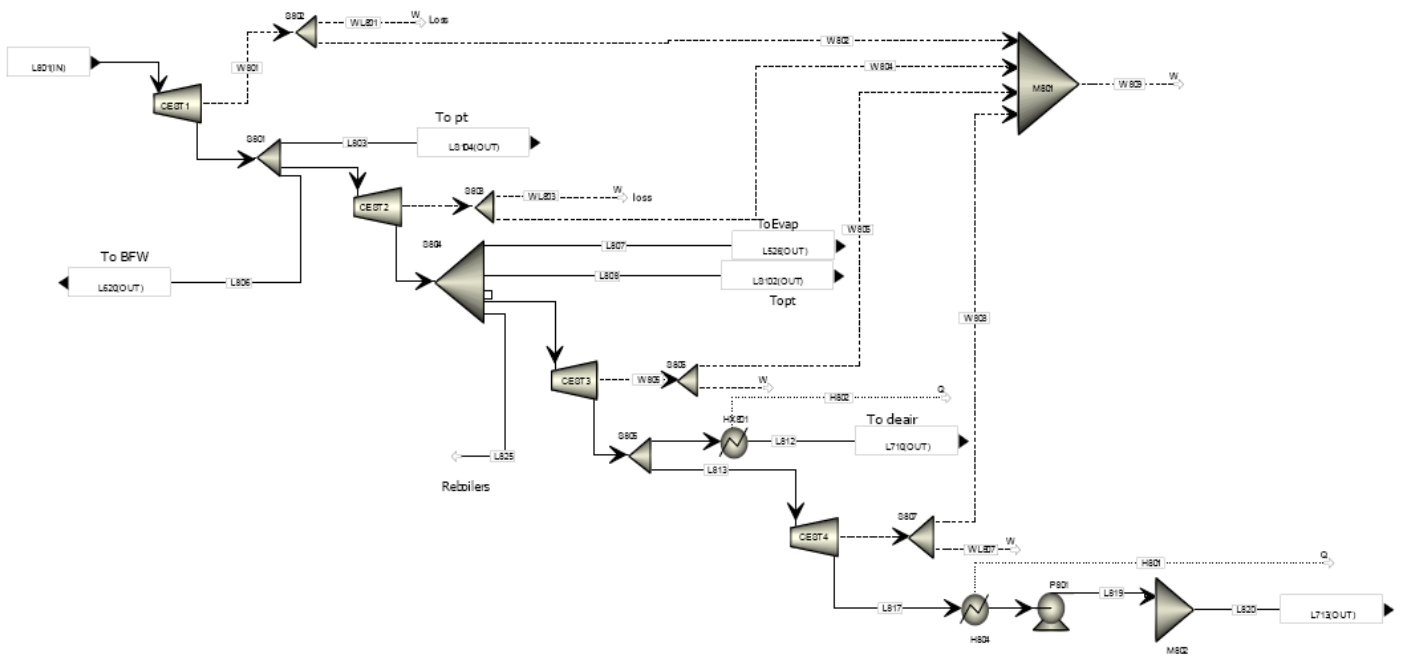
AREA 700



	L706	L707	L708	L709	L711	L712	L715	L718	L720
Temperature K	328.8	328.8		410.1	412.3	298.1	373.1	326.1	298.1
Pressure bar	1.7	3.445	3.344	3.344	96	1.013	1.013	1	1.013
Vapor Frac	0	0		0	0	0	0.076	0	0
Mass Flow TOTAL kg/hr	58906.1	58906.1		62021.5	62021.5	1.0	10877.3	119.1	36960.0
Mass Flow TOTAL kg/hr									
ETHANOL	5.7	5.7		6.3	6.3	0.0	2.2	0.0	0.0
H2O	58891.8	58891.8		61978.8	61978.8	0.0	10870.1	119.0	36960.0
FURF	8.6	8.6		10.0	10.0	0.0	5.0	0.0	0.0
HYDRAZIN	0.0	0.0		26.4	26.4	1.0	0.0	0.0	0.0

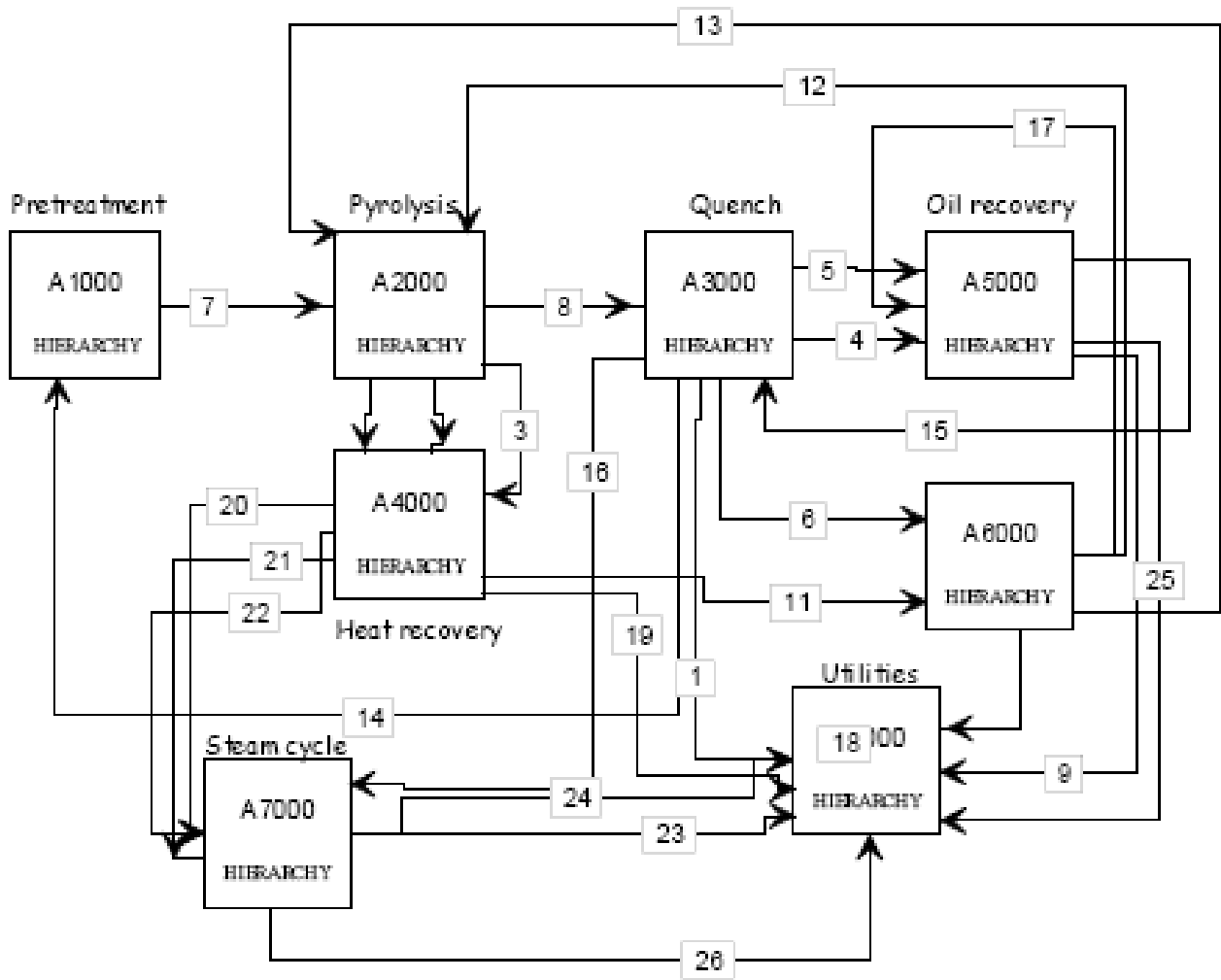
AREA 800

	H801	H802												
QCALC kW	4473.477	2217.543												
TBEGIN K	330.0244	570.5344												
TEND K	319.1379	388.7243												
	W801	W802	W803	W804	W805	W806	W807	W808	W809	WL801	WL803	WL805	WL807	
POWER kW	-11961.95	-11722.71	-4763.558	-4668.287	-622.8499	-610.3929	-858.1134	-840.9511	-17842.34	-239.2389	-95.27116	-12.457	-17.16227	



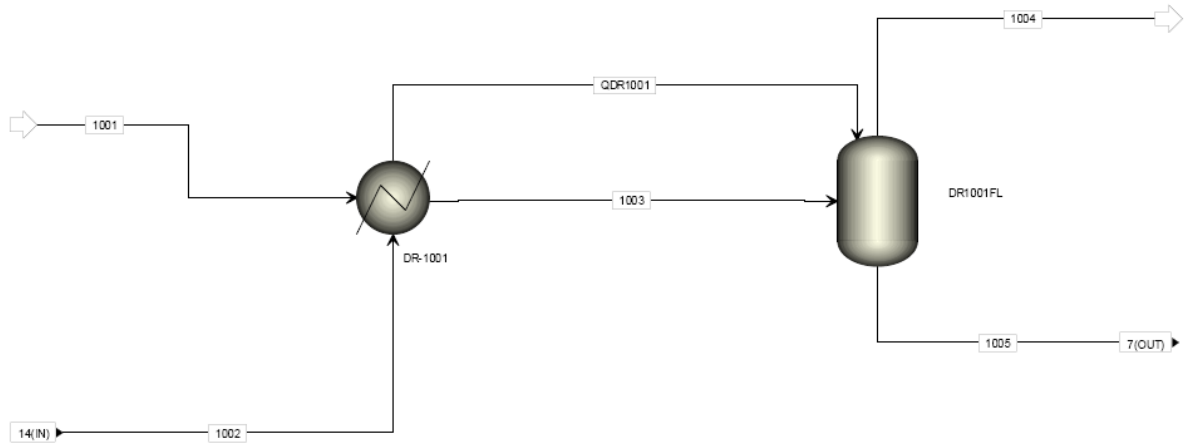
	L802	L803	L804	L805	L806	L807	L808	L810	L812	L813	L817	L820	L825
Temperature K	827.3	832.5	832.5	681.2	832.5	683.8	683.8	569.1	388.7	570.5	330	319.3	683.8
Pressure bar	13.172	13.172	13.172	4.479	13.172	4.479	4.479	1.723	1.723	1.723	0.101	4.2	4.479
Vapor Frac	1	1	1	1	1	1	1	1	0	1	1	0	1
Mass Flow TOTAL kg/hr	61636.9	396.0	54904.9	54904.9	6336.0	9504.0	2640.0	9760.9	3089.0	6671.9	6671.9	6671.9	33000.0
Mass Flow TOTAL kg/hr H2O	61596.2	395.7	54868.6	54868.6	6331.8	9497.7	2638.3	9754.4	3087.0	6667.5	6667.5	6667.5	32978.2

Appendix A6.3 Process flow diagrams and stream data for fast pyrolysis 145MW scenario



AREA 100

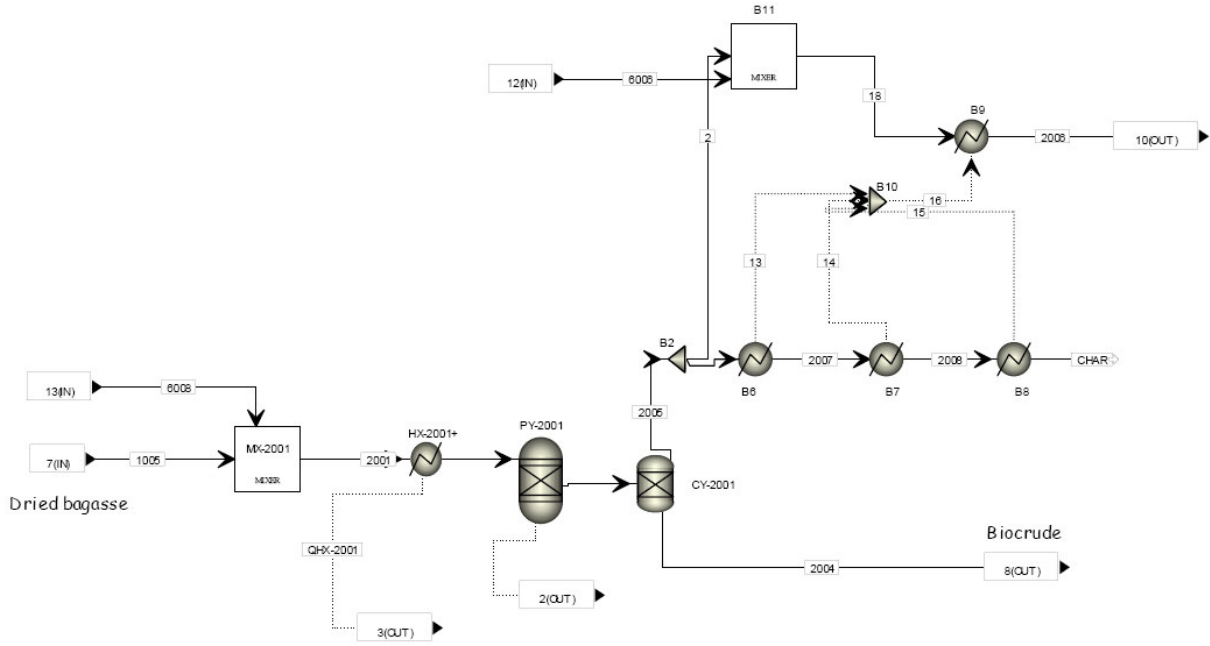
QDR1001
 QCALC Gcal/hr -5.6
 TBEGIN C 52.0
 TEND C 110



	1001	1002	1003	1004	1005
Temperature C	25	214.1	110	56	56
Pressure bar	1.379	1.02	1.379	1.379	1.379
Vapor Frac	0	1	0.998	1	0
Mass Flow kg/hr	41579.1	300000.0	341579.1	319128.6	22450.5
Mass Flow kg/hr					
ASH	769.2	0.0	769.2	0.0	769.2
CELLULOS	8440.6	0.0	8440.6	0.0	8440.6
LIGNIN	5301.3	0.0	5301.3	0.0	5301.3
XYLAN	4157.9	0.0	4157.9	0.0	4157.9
ARABINAN	353.4	0.0	353.4	0.0	353.4
MANNAN	41.6	0.0	41.6	0.0	41.6
GALACTAN	166.3	0.0	166.3	0.0	166.3
N2	0.0	225120.0	225120.0	225117.7	2.3
O2	0.0	68970.0	68970.0	68969.1	0.9
CO2	0.0	120.0	120.0	120.0	0.0
H2O	20789.6	1980.0	22769.6	21111.8	1657.8
AR	0.0	3810.0	3810.0	3810.0	0.0
EXTRACT	1559.2	0.0	1559.2	0.0	1559.2

AREA 200

	13	14	15	16	QHX-2001	QPY-2001
QCALC Gcal/hr	0.0592	0.0515	0.1021	0.2128	-6.1E-15	-5.4356
TBEGIN C	500	400	300		559	559
TEND C	400	300	25		559	500

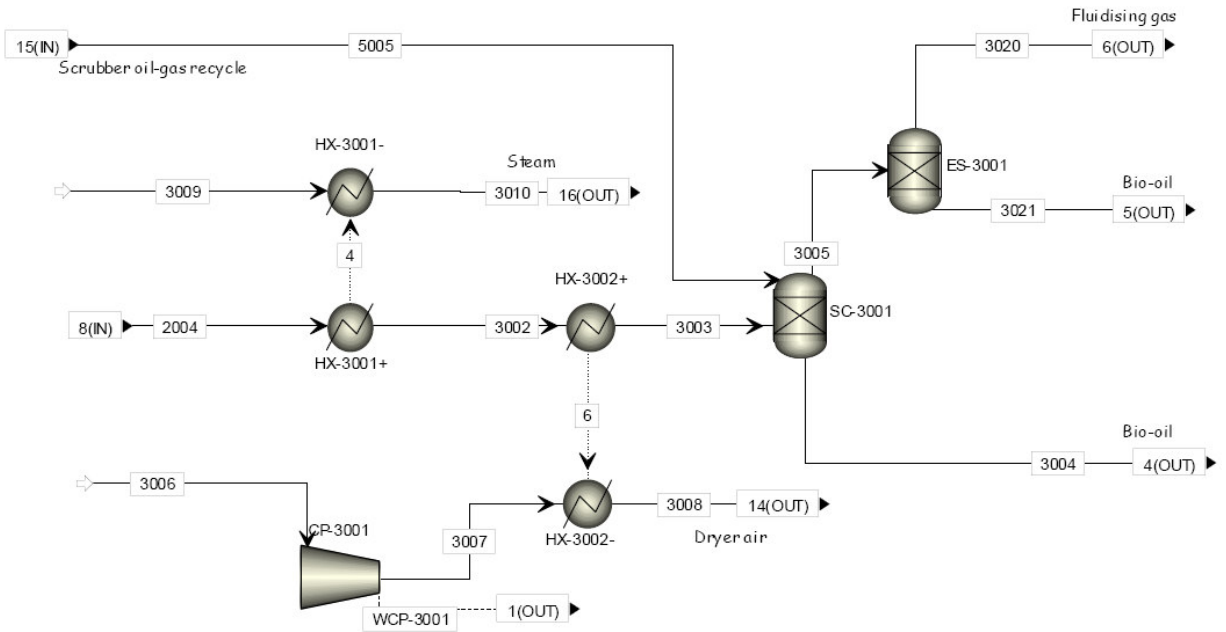


	1	2	18	1005	2001	2002	2003	2005	CHAR
Temperature C			296.9	50	559.5	559.5	500		
Pressure bar	1.379	1.379	1.379	1.379	1.379	1.379	1.379	1.379	1.379
Vapor Frac			1	0	1	1	1		
Mass Flow kg/hr	1493.8	2000.0	4721.2	22450.5	80203.3	80203.3	80203.3	3493.8	1493.8
Mass Flow kg/hr									
CHAR	1164.9	1559.7	1559.7	0.0	0.0	0.0	2724.6	2724.6	1164.9
ASH	328.9	440.3	440.3	769.2	769.2	769.2	769.2	769.2	328.9
CELLULOS	0.0	0.0	0.0	8440.6	8440.6	8440.6	0.0	0.0	0.0
LIGNIN	0.0	0.0	0.0	5301.3	5301.3	5301.3	0.0	0.0	0.0
XYLAN	0.0	0.0	0.0	4157.9	4157.9	4157.9	0.0	0.0	0.0
ARABINAN	0.0	0.0	0.0	353.4	353.4	353.4	0.0	0.0	0.0
MANNAN	0.0	0.0	0.0	41.6	41.6	41.6	0.0	0.0	0.0
GALACTAN	0.0	0.0	0.0	166.3	166.3	166.3	0.0	0.0	0.0
N2	0.0	0.0	0.0	2.3	2.3	2.3	0.0	0.0	0.0
O2	0.0	0.0	0.0	0.9	0.9	0.9	0.0	0.0	0.0
CO	0.0	0.0	703.7	0.0	14934.9	14934.9	15637.4	0.0	0.0
CO2	0.0	0.0	1829.6	0.0	38828.9	38828.9	40667.6	0.0	0.0
H2O	0.0	0.0	0.2	1657.8	1662.6	1662.6	4289.4	0.0	0.0
CH4	0.0	0.0	93.8	0.0	1991.4	1991.4	2085.1	0.0	0.0
C2H4	0.0	0.0	93.8	0.0	1991.4	1991.4	2085.1	0.0	0.0
AR	0.0	0.0	0.0	0.0	0.0	0.0	0.0	0.0	0.0
ACETACID	0.0	0.0	0.0	0.0	0.1	0.1	508.4	0.0	0.0
ACETOL	0.0	0.0	0.0	0.0	0.2	0.2	770.5	0.0	0.0
GUAIACOL	0.0	0.0	0.0	0.0	0.0	0.0	3659.5	0.0	0.0
3-5-X-01	0.0	0.0	0.0	0.0	0.1	0.1	401.1	0.0	0.0
FORMACID	0.0	0.0	0.0	0.0	0.2	0.2	731.6	0.0	0.0
N-PRO-01	0.0	0.0	0.0	0.0	0.4	0.4	1723.7	0.0	0.0
PHENOL	0.0	0.0	0.0	0.0	0.0	0.0	49.2	0.0	0.0
TOLUENE	0.0	0.0	0.0	0.0	0.1	0.1	239.9	0.0	0.0
FURFURAL	0.0	0.0	0.0	0.0	0.4	0.4	2000.1	0.0	0.0
BENZENE	0.0	0.0	0.0	0.0	0.0	0.0	81.0	0.0	0.0
EXTRACT	0.0	0.0	0.0	1559.2	1559.2	1559.2	0.0	0.0	0.0
TETRA-01	0.0	0.0	0.0	0.0	0.0	0.0	1464.0	0.0	0.0
DILACID	0.0	0.0	0.0	0.0	0.0	0.0	325.7	0.0	0.0

AREA 300

	4	6
QCALC Gcal/hr	0.41	13.76
TBEGIN C	500	485
TEND C	485	33

	WCP-3001
POWER KW	67.49

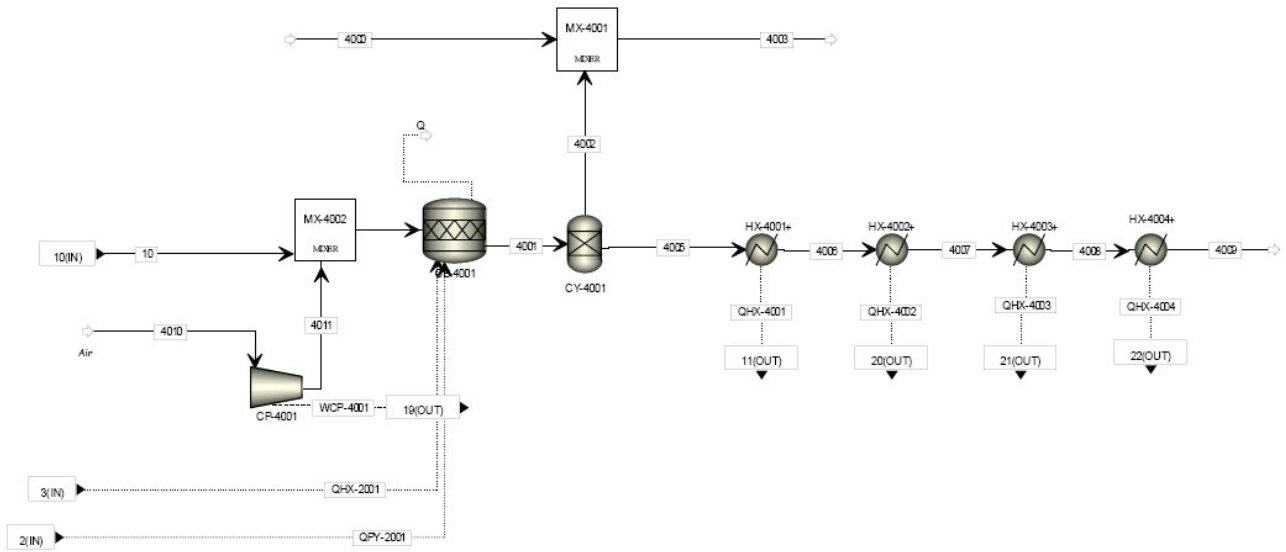


	2004	3002	3003	3004	3005	3006	3007	3008	3009	3010	3020	3021	5005
Temperature C	500	485	33	31.9	31.9	25	25.8	214.1	25	243.5	31.9	31.9	-6.4
Pressure bar	1.379	1.379	1.379	1.379	1.379	1.014	1.02	1.02	1.379	35.508	1.379	1.379	2.758
Vapor Frac	1	1	0.857	0	0.875	1	1	1	0	0.029	1	0	0
Mass Flow kg/hr	76709.5	76709.5	76709.5	11356.8	67902.5	300000.0	300000.0	300000.0	1470.9	1470.9	60471.7	7430.8	2549.8
Mass Flow kg/hr													
N2	0.0	0.0	0.0	0.0	0.0	225120.0	225120.0	225120.0	0.0	0.0	0.0	0.0	0.0
O2	0.0	0.0	0.0	0.0	0.0	68970.0	68970.0	68970.0	0.0	0.0	0.0	0.0	0.0
CO	15637.4	15637.4	15637.4	0.0	15637.4	0.0	0.0	0.0	0.0	0.0	15637.4	0.0	0.0
CO2	40657.5	40657.5	40657.5	0.0	40657.5	120.0	120.0	120.0	0.0	0.0	40657.5	0.0	0.0
H2O	4289.4	4289.4	4289.4	0.0	5045.6	1980.0	1980.0	1980.0	1470.9	1470.9	5.0	5040.5	756.1
CH4	2085.1	2085.1	2085.1	0.0	2085.1	0.0	0.0	0.0	0.0	0.0	2085.1	0.0	0.0
C2H4	2085.1	2085.1	2085.1	0.0	2085.1	0.0	0.0	0.0	0.0	0.0	2085.1	0.0	0.0
AR	0.0	0.0	0.0	0.0	0.0	3810.0	3810.0	3810.0	0.0	0.0	0.0	0.0	0.0
ACETACID	508.4	508.4	508.4	478.5	119.6	0.0	0.0	0.0	0.0	0.0	0.1	119.5	89.7
ACETOL	770.5	770.5	770.5	725.2	181.3	0.0	0.0	0.0	0.0	0.0	0.2	181.1	135.9
GUAICOL	3659.5	3659.5	3659.5	3444.3	861.1	0.0	0.0	0.0	0.0	0.0	0.0	861.1	645.8
3:5-X-01	401.1	401.1	401.1	377.5	94.4	0.0	0.0	0.0	0.0	0.0	0.1	94.3	70.8
FORMACID	731.6	731.6	731.6	688.5	172.1	0.0	0.0	0.0	0.0	0.0	0.2	172.0	129.1
N-PRO-01	1723.7	1723.7	1723.7	1622.3	405.6	0.0	0.0	0.0	0.0	0.0	0.4	405.2	304.1
PHENOL	49.2	49.2	49.2	46.4	11.6	0.0	0.0	0.0	0.0	0.0	0.0	11.6	8.7
TOLUENE	239.9	239.9	239.9	225.8	56.4	0.0	0.0	0.0	0.0	0.0	0.1	56.4	42.3
FURFURAL	2000.1	2000.1	2000.1	1882.4	470.6	0.0	0.0	0.0	0.0	0.0	0.5	470.1	352.9
BENZENE	81.0	81.0	81.0	76.3	19.1	0.0	0.0	0.0	0.0	0.0	0.0	19.1	14.3
TETRA-01	1464.0	1464.0	1464.0	1464.0	0.0	0.0	0.0	0.0	0.0	0.0	0.0	0.0	0.0
DILACID	325.7	325.7	325.7	325.7	0.0	0.0	0.0	0.0	0.0	0.0	0.0	0.0	0.0

AREA 400

	QCB-4001	QHX-2001	QHX-4001	QHX-4002	QHX-4003	QHX-4004	QPY-2001
QCALC Gcal/hr	-16.90	0.00	12.82	3.24	3.12	6.88	-5.44
TBEGIN C	63.42	559.49	1700.00	982.00	792.00	603.00	559.49
TEND C	1700.00	559.49	982.00	792.00	603.00	155.00	500.00

	WCP-4001
POWER kW	12.37

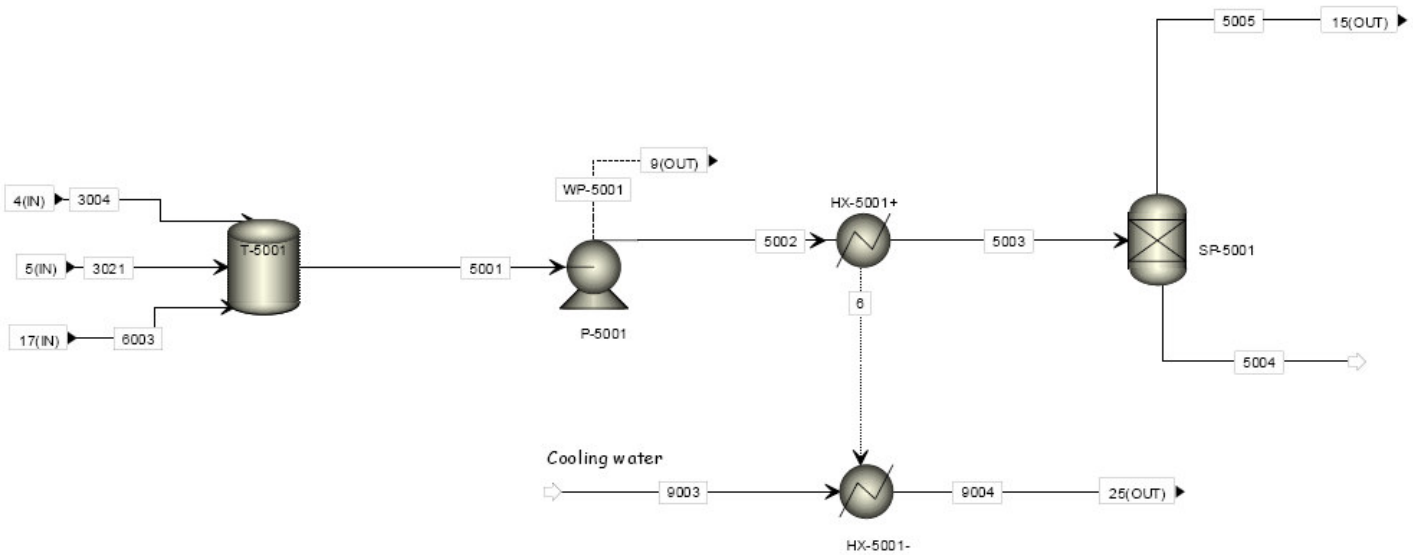


	10	4000	4001	4002	4003	4005	4006	4007	4008	4009	4010	4011
Temperature C	438.3	25	1700		76.5	1700	982	792	603	155	25	25.8
Pressure bar	1.379	1.379	1.02	1.02	1.02	1.02	1.02	1.02	1.02	1.02	1.014	1.02
Vapor Frac	1	0	1		0	1	1	1	1	1	1	1
Mass Flow kg/hr	4721.229	3316.1	59721.229	440.324	3756.424	59280.9	59280.904	59280.9	59280.9	59280.904	55000	55000
Mass Flow kg/hr												
CHAR	1559.676	0	0	0	0	0	0	0	0	0	0	0
ASH	440.324	0	440.324	440.324	440.324	0	0	0	0	0	0	0
N2	0	0	41266.5	0	0	41266.5	41266.5	41266.5	41266.5	41266.5	41266.5	41266.5
O2	0	0	7391.881	0	0	7391.881	7391.881	7391.881	7391.881	7391.881	12644.5	12644.5
CO	703.682	0	0	0	0	0	0	0	0	0	0	0
CO2	1829.589	0	9229.51	0	0	9229.51	9229.51	9229.51	9229.51	9229.51	27.5	27.5
H2O	0.227	3316.1	694.513	0	3316.1	694.513	694.513	694.513	694.513	694.513	363	363
CH4	93.831	0	0	0	0	0	0	0	0	0	0	0
C2H4	93.831	0	0	0	0	0	0	0	0	0	0	0
AR	0	0	698.5	0	0	698.5	698.5	698.5	698.5	698.5	698.5	698.5
ACETACID	0.005	0	0	0	0	0	0	0	0	0	0	0
ACETOL	0.008	0	0	0	0	0	0	0	0	0	0	0
GUAICOL	0	0	0	0	0	0	0	0	0	0	0	0
3:5-X-01	0.004	0	0	0	0	0	0	0	0	0	0	0
FORMACID	0.008	0	0	0	0	0	0	0	0	0	0	0
N-PRO-01	0.018	0	0	0	0	0	0	0	0	0	0	0
PHENOL	0	0	0	0	0	0	0	0	0	0	0	0
TOLUENE	0.003	0	0	0	0	0	0	0	0	0	0	0
FURFURAL	0.021	0	0	0	0	0	0	0	0	0	0	0

AREA 500

6
 QCALC Gcal/hr 0.06304547
 TBEGIN C 3.10E+01
 TEND C 2.50E+01

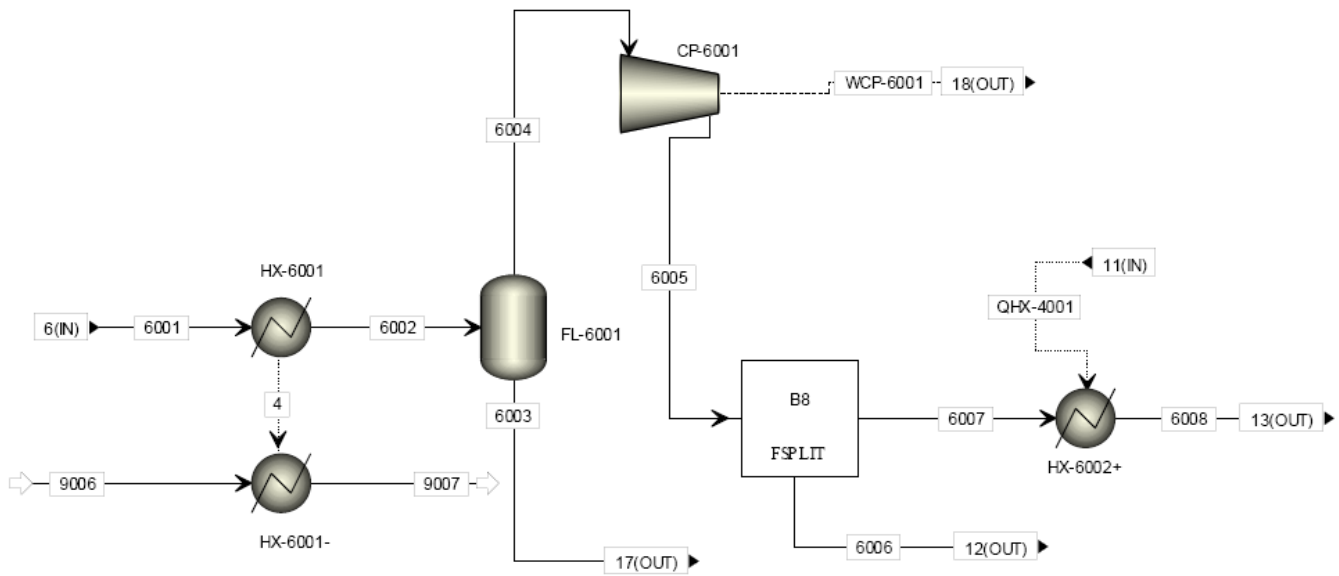
WP-5001
 POWER kW 0.94032435



	3004	3021	5001	5002	5003	5004	5005	9003	9004
Temperature C	31.9	31.9	31	31	25	-6.4	-6.4	21.1	25.7
Pressure bar	1.379	1.379	1.793	2.758	2.758	2.758	2.758	1.034	1.034
Vapor Frac	0	0	0	0	0	0	0	0	0
Mass Flow kg/hr	11,356.8	7,430.8	18,787.5	18,787.5	18,787.5	16,237.9	2,549.7	14,804.8	14,804.8
Mass Flow kg/hr									
H2O	-	5,040.5	5,040.5	5,040.5	5,040.5	4,284.4	756.1	14,804.8	14,804.8
ACETACID	478.5	119.5	598.0	598.0	598.0	508.3	89.7	-	-
ACETOL	725.2	181.1	906.3	906.3	906.3	770.3	135.9	-	-
GUAIACOL	3,444.3	861.1	4,305.4	4,305.4	4,305.4	3,659.6	645.8	-	-
3:5-X-01	377.5	94.3	471.8	471.8	471.8	401.1	70.8	-	-
FORMACID	688.5	172.0	860.5	860.5	860.5	731.4	129.1	-	-
N-PRO-01	1,622.3	405.2	2,027.4	2,027.4	2,027.4	1,723.3	304.1	-	-
PHENOL	46.4	11.6	57.9	57.9	57.9	49.3	8.7	-	-
TOLUENE	225.8	56.4	282.2	282.2	282.2	239.8	42.3	-	-
FURFURAL	1,882.4	470.1	2,352.6	2,352.6	2,352.6	1,999.7	352.9	-	-
BENZENE	76.3	19.1	95.3	95.3	95.3	81.0	14.3	-	-
TETRA-01	1,464.0	-	1,464.0	1,464.0	1,464.0	1,464.0	-	-	-
DILACID	325.7	-	325.7	325.7	325.7	325.7	-	-	-

AREA 600

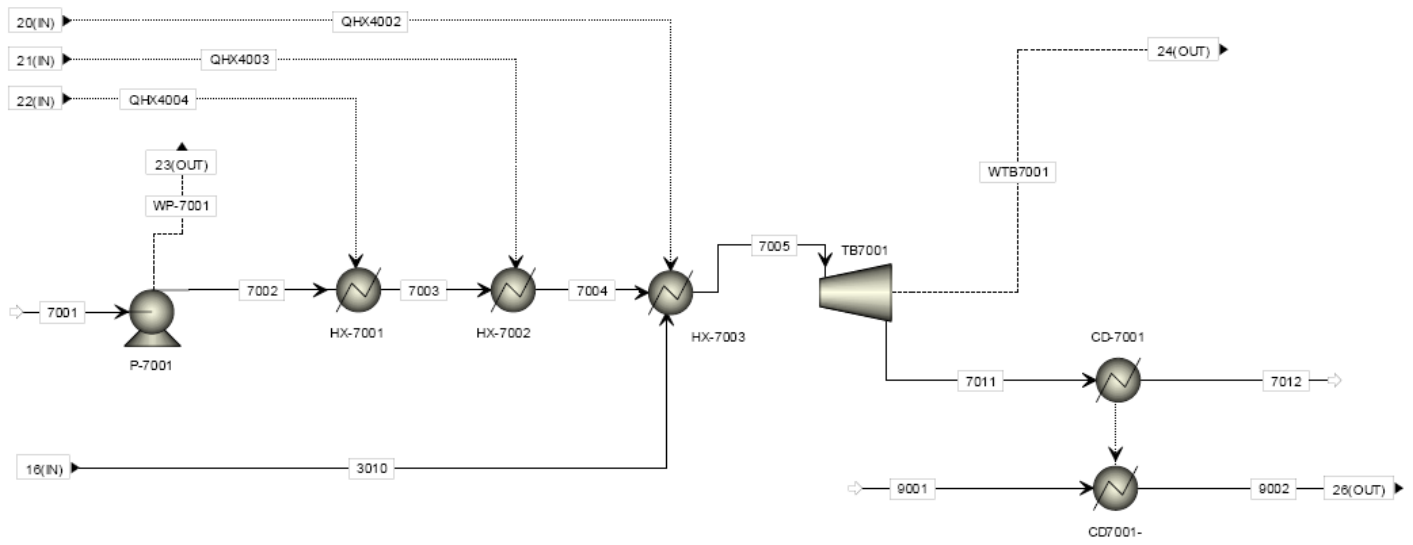
	4	QHX-4001
QCALC Gcal/hr	0.34592103	12.8213654
TBEGIN C	31.8949451	1700
TEND C	7	982
	WCP-6001	
POWER KW	1356.56311	



	6001	6002	6003	6004	6005	6006	6007	6008	9006	9007
Temperature C	31.9	7		7	88.6	88.6	88.6	823.5	4	10
Pressure bar	1.379	1.379	1.379	1.379	3.103	3.103	3.103	3.103	1.034	1.034
Vapor Frac	1	1		1	1	1	1	1	0	0
Mass Flow kg/hr	60471.748	60471.748	0	60471.748	60471.748	2721.229	57750.519	57750.519	64197.7	64197.7
Mass Flow kg/hr										
CO	15637.388	15637.388	0	15637.388	15637.388	703.682	14933.706	14933.706	0	0
CO2	40657.526	40657.526	0	40657.526	40657.526	1829.589	38627.938	38627.938	0	0
H2O	5.046	5.046	0	5.046	5.046	0.227	4.819	4.819	64197.7	64197.7
CH4	2085.144	2085.144	0	2085.144	2085.144	93.831	1991.312	1991.312	0	0
C2H4	2085.144	2085.144	0	2085.144	2085.144	93.831	1991.312	1991.312	0	0
ACETACID	0.12	0.12	0	0.12	0.12	0.005	0.114	0.114	0	0
ACETOL	0.181	0.181	0	0.181	0.181	0.008	0.173	0.173	0	0
3:5-X-01	0.094	0.094	0	0.094	0.094	0.004	0.09	0.09	0	0
FORMACID	0.172	0.172	0	0.172	0.172	0.008	0.164	0.164	0	0
N-PRO-01	0.406	0.406	0	0.406	0.406	0.018	0.387	0.387	0	0
TOLUENE	0.056	0.056	0	0.056	0.056	0.003	0.054	0.054	0	0
FURFURAL	0.471	0.471	0	0.471	0.471	0.021	0.449	0.449	0	0

AREA 700

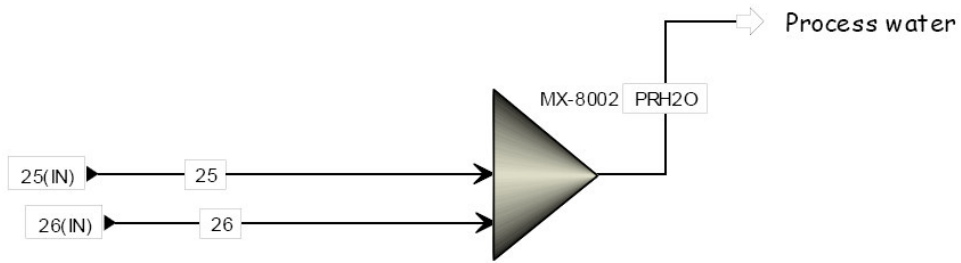
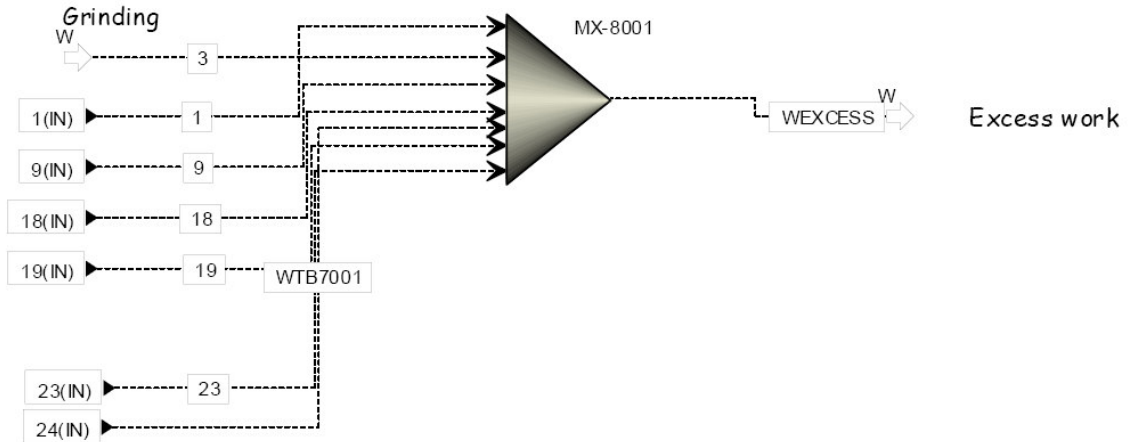
	6	QHX4002	QHX4003	QHX4004
QCALC Gcal/hr	10.1636868	3.23906657	3.12078807	6.87964712
TBEGIN C	225.214039	982	792	603
TEND C	46.4621048	792	603	155
	WP-7001	WTB7001		
POWER KW	7.57248338	-3768.9931		



	3010	7001	7002	7003	7004	7005	7011	7012	9001
Temperature C	243.5	30	30.5	243.5	312.7	642.3	225.2	46.5	21.1
Pressure bar	35.508	1.379	10.411	35.508	35.508	35.508	1.115	0.103	1.103
Vapor Frac	0.029	0	0	0.548	1	1	1	0	0
Mass Flow kg/hr	1470.9	14106	14106	14106	14106	15576.9	15576.9	15576.9	585107
Mass Flow kg/hr H2O	1470.9	14106	14106	14106	14106	15576.9	15576.9	15576.9	585107

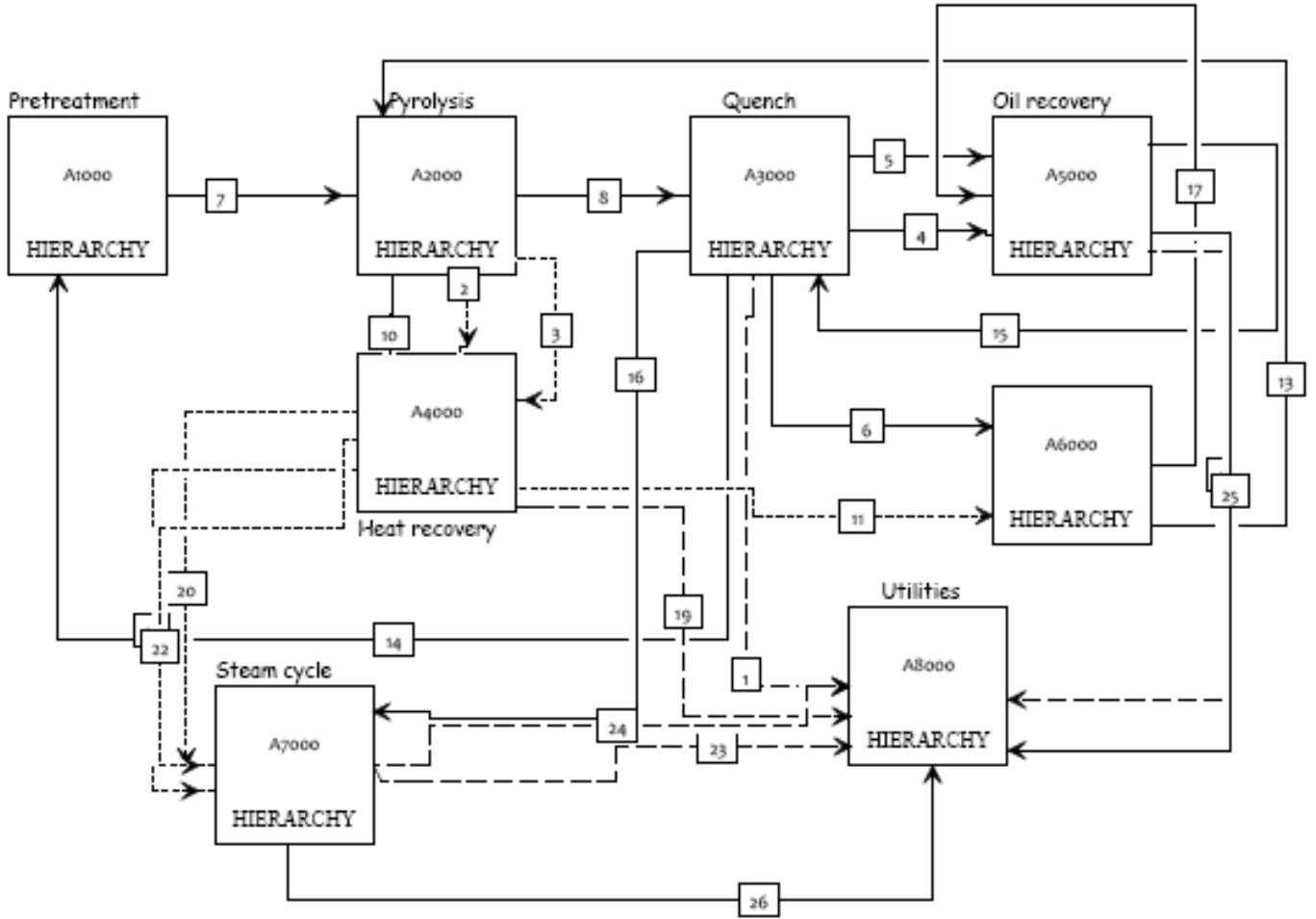
AREA 800

POWER kW	1	3	9	18	19	23	WEXCESS	WTB7001
	67.5	2,338.8	0.9	1,356.6	12.4	7.6	14.8	-3,769.0



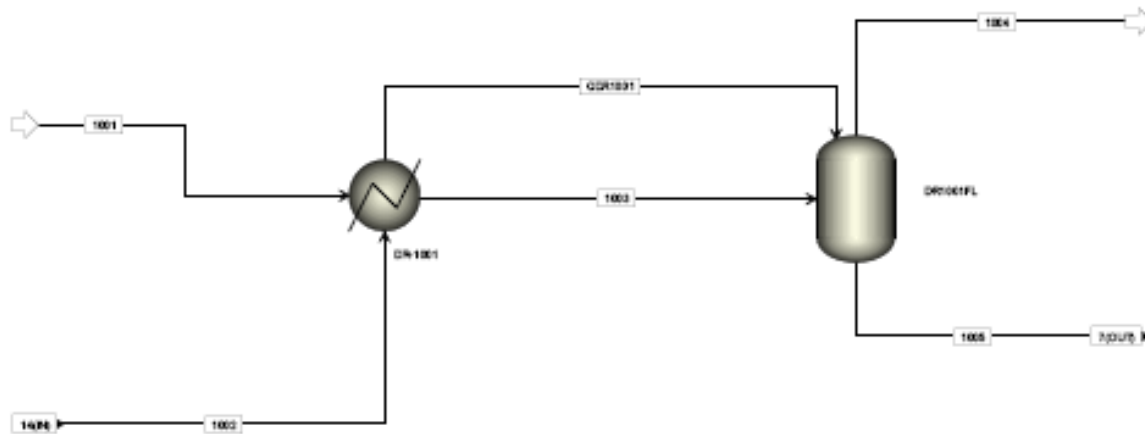
	25	26	PRH2O
Temperature C	25.7	39.8	39.4
Pressure bar	1.034	1.103	1.034
Vapor Frac	0	0	0
Mass Flow kg/hr	14804.8	585107.0	599911.8
Mass Flow kg/hr H2O	14804.8	585107.0	599911.8

Appendix A6.4 Process flow diagrams and stream data for vacuum pyrolysis 145MW scenario



AREA 100

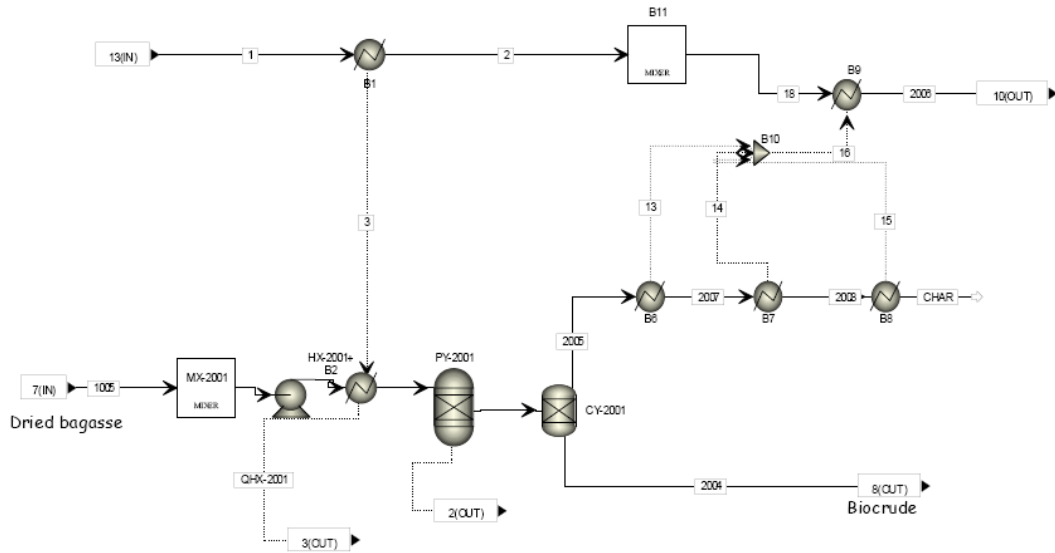
	1	2	QDR1001
QCALC Gcal/hr	5.7	-5.7	-11.5
TBEGIN C	110.0		39.3
TEND C	55.7		110.0



	1001	1002	1003	1004	1005
Temperature C	25	134.4	110	55.7	55.7
Pressure bar	1.379	1.02	1.379	1.379	1.379
Vapor Frac	0	1	0.998	1	0
Mass Flow kg/hr	22348.8	300000	322348.8	318989.8	3359.009
Mass Flow kg/hr					
ASH	789.2	0	789.2	0	789.2
CELLULOS	8440.6	0	8440.6	0	8440.6
LIGNIN	5301.3	0	5301.3	0	5301.3
XYLAN	4157.9	0	4157.9	0	4157.9
ARABINAN	353.4	0	353.4	0	353.4
MANNAN	41.6	0	41.6	0	41.6
GALACTAN	166.3	0	166.3	0	166.3
N2	0.0	225120.0	225120.0	225117.5	2.5
O2	0.0	68970.0	68970.0	68969.1	0.9
AR	0.0	3810.0	3810.0	3810.0	0.0
CO2	0.0	120.0	120.0	120.0	0.0
H2O	20789.6	1980.0	22789.6	20973.3	1796.3
EXTRACT	1559.2	0.0	1559.2	0.0	1559.2

AREA 200

	3	13	14	15	16	QHX-2001	QPY-2001
QCALC Gcal/hr	0.53095578	0.07371668	0.12977594	0.17045692	0.37394954	-2.5166839	7.70794149
TBEGIN C	830	350	300	200		55.6464649	350
TEND C	55	300	200	25		350	350

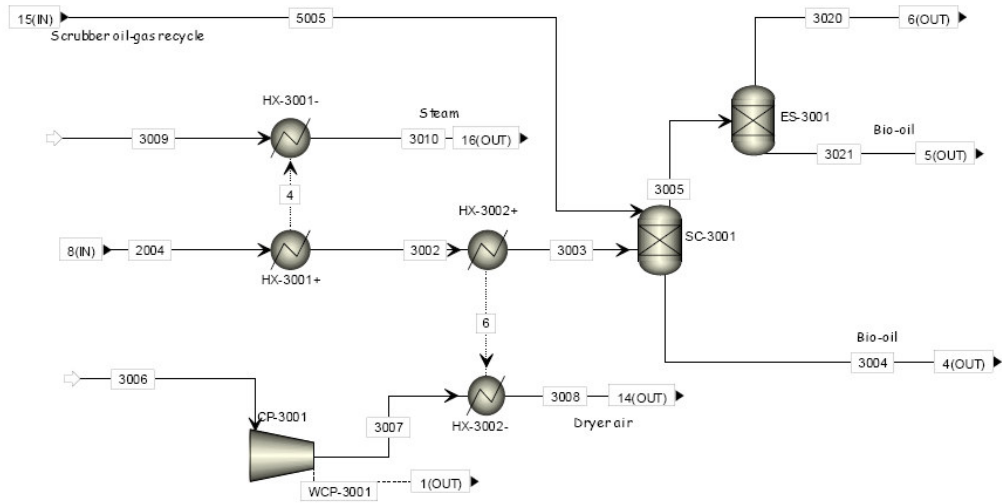


	1	2	4	18	1005	2001	2002	2003	2004	2005	2006	2007	2008	CHAR
Temperature C	830.0	55.0	55.6	55.0	55.7	55.7	350.0	350.0	350.0		622.8			
Pressure bar	1.4	1.4	0.2	1.4	1.4	1.4	0.2	0.2	0.2	0.2	1.4	1.4	1.4	1.4
Vapor Frac	1.0	1.0	0.0	1.0	0.0	0.0	0.9	1.0	1.0		1.0			
Total Flow kg/hr	2401.1	2401.1	22589.3	2401.1	22589.3	22589.3	22589.3	22589.3	18231.9	4357.4	2401.1	4357.4	4357.4	4357.4
Mass Flow kg/hr														
ASH	0	0	769.2	0	769.2	769.2	769.2	769.2	0	769.2	0	769.2	769.2	769.2
CHAR	0	0	0	0	0	0	0	3588.222	0	3588.222	0	3588.222	3588.222	3588.222
CELLULOS	0	0	8440.6	0	8440.6	8440.6	8440.6	0	0	0	0	0	0	0
LIGNIN	0	0	5301.3	0	5301.3	5301.3	5301.3	0	0	0	0	0	0	0
XYLAN	0	0	4157.9	0	4157.9	4157.9	4157.9	0	0	0	0	0	0	0
ARABINAN	0	0	353.4	0	353.4	353.4	353.4	0	0	0	0	0	0	0
MANNAN	0	0	41.6	0	41.6	41.6	41.6	0	0	0	0	0	0	0
GALACTAN	0	0	166.3	0	166.3	166.3	166.3	0	0	0	0	0	0	0
N2	0.0	0.0	2.5	0.0	2.5	2.5	2.5	0.0	0.0	0.0	0.0	0.0	0.0	0.0
O2	0.0	0.0	0.9	0.0	0.9	0.9	0.9	0.0	0.0	0.0	0.0	0.0	0.0	0.0
H2	2.4	2.4	0.0	2.4	0.0	0.0	0.0	2.4	2.4	0.0	2.4	0.0	0.0	0.0
CH4	48.8	48.8	0.0	48.8	0.0	0.0	0.0	48.8	48.8	0.0	48.8	0.0	0.0	0.0
CO	640.2	640.2	0.0	640.2	0.0	0.0	0.0	640.2	640.2	0.0	640.2	0.0	0.0	0.0
CO2	1683.7	1683.7	0.0	1683.7	0.0	0.0	0.0	1683.8	1683.8	0.0	1683.7	0.0	0.0	0.0
C2H4	6.1	6.1	0.0	6.1	0.0	0.0	0.0	6.1	6.1	0.0	6.1	0.0	0.0	0.0
C2H6	10.9	10.9	0.0	10.9	0.0	0.0	0.0	10.9	10.9	0.0	10.9	0.0	0.0	0.0
H2O	8.0	8.0	1796.3	8.0	1796.3	1796.3	1796.3	8642.6	8642.6	0.0	8.0	0.0	0.0	0.0
ACETACID	0.7	0.7	0.0	0.7	0.0	0.0	0.0	4344.4	4344.4	0.0	0.7	0.0	0.0	0.0
ACETOL	0.1	0.1	0.0	0.1	0.0	0.0	0.0	1175.8	1175.8	0.0	0.1	0.0	0.0	0.0
FURFURAL	0.1	0.1	0.0	0.1	0.0	0.0	0.0	473.3	473.3	0.0	0.1	0.0	0.0	0.0
EXTRACT	0.0	0.0	1559.2	0.0	1559.2	1559.2	1559.2	0.0	0.0	0.0	0.0	0.0	0.0	0.0

AREA 300

4 6
 QCALC Gcal/hr 0.160263 7.896515
 TBEGIN C 350 330
 TEND C 330 33

WCP-3001
 POWER kW 67.49482

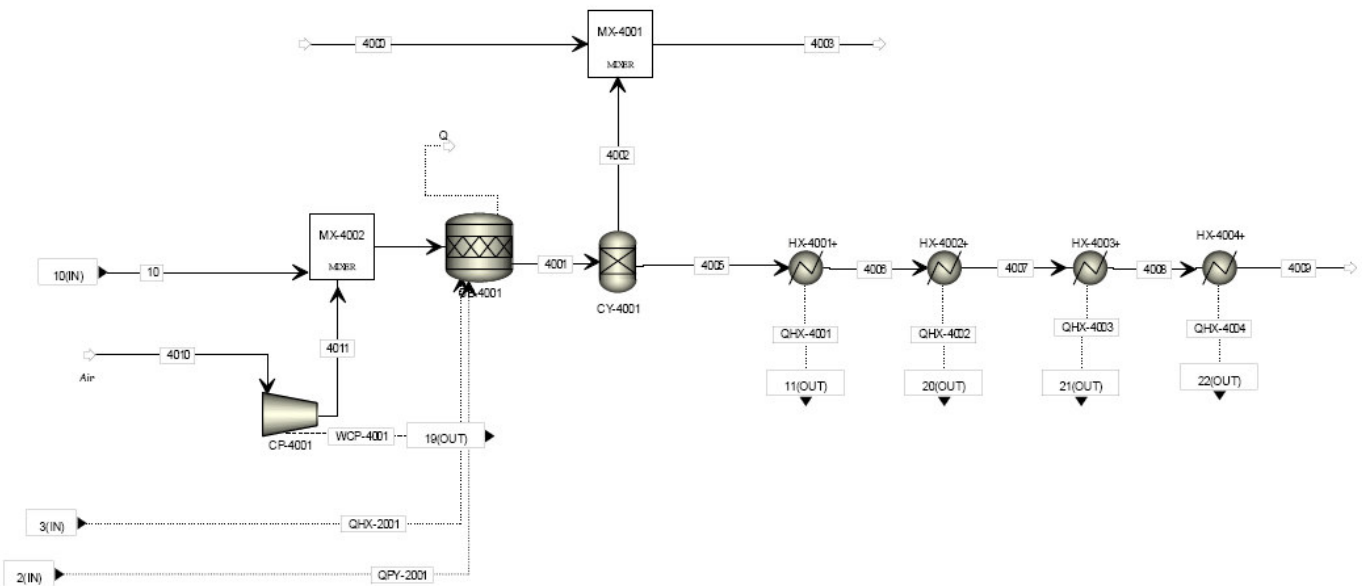


	2004	3002	3003	3004	3005	3006	3007	3008	3009	3010	3020	3021	5005
Temperature C	350.0	330.0	33.0	28.5	28.5	25.0	25.8	134.4	25.0	131.1	28.5	28.5	-6.4
Pressure bar	0.2	1.4	1.4	1.4	1.4	1.0	1.0	1.0	0.0	1.4	35.5	1.4	1.4
Vapor Frac	1.0	1.0	0.1	0.0	0.1	1.0	1.0	1.0	0.0	0.0	1.0	0.0	0.0
Total Flow kg/hr	18231.9	18231.9	18231.9	6773.5	14252.0	300000.0	300000.0	300000.0	1470.9	1470.9	2403.9	11848.1	2793.7
Mass Flow kg/hr													
N2	0.0	0.0	0.0	0.0	0.0	225120.0	225120.0	225120.0	0.0	0.0	0.0	0.0	0.0
O2	0.0	0.0	0.0	0.0	0.0	68970.0	68970.0	68970.0	0.0	0.0	0.0	0.0	0.0
AR	0.0	0.0	0.0	0.0	0.0	3810.0	3810.0	3810.0	0.0	0.0	0.0	0.0	0.0
H2	2.4	2.4	2.4	0.0	2.4	0.0	0.0	0.0	0.0	0.0	2.4	0.0	0.0
CH4	48.8	48.8	48.8	0.0	48.8	0.0	0.0	0.0	0.0	0.0	48.8	0.0	0.0
CO	640.2	640.2	640.2	0.0	640.2	0.0	0.0	0.0	0.0	0.0	640.2	0.0	0.0
CO2	1683.8	1683.8	1683.8	0.0	1683.9	120.0	120.0	120.0	0.0	0.0	1683.9	0.0	0.0
C2H4	6.1	6.1	6.1	0.0	6.1	0.0	0.0	0.0	0.0	0.0	6.1	0.0	0.0
C2H6	10.9	10.9	10.9	0.0	10.9	0.0	0.0	0.0	0.0	0.0	10.9	0.0	0.0
C3H6-2	2.8	2.8	2.8	2.7	0.7	0.0	0.0	0.0	0.0	0.0	0.0	0.7	0.5
C3H8	11.4	11.4	11.4	10.7	2.7	0.0	0.0	0.0	0.0	0.0	0.0	2.7	2.0
CH3OH	3.3	3.3	3.3	3.1	0.8	0.0	0.0	0.0	0.0	0.0	0.0	0.8	0.6
C4H10	15.5	15.5	15.5	14.6	3.7	0.0	0.0	0.0	0.0	0.0	0.0	3.7	2.7
C5H12	9.0	9.0	9.0	8.4	2.1	0.0	0.0	0.0	0.0	0.0	0.0	2.1	1.6
H2O	8642.6	8642.6	8642.6	0.0	10166.3	1980.0	1980.0	1980.0	1470.9	1470.9	10.2	10156.2	1523.7
ACETACID	4344.4	4344.4	4344.4	4088.7	1022.2	0.0	0.0	0.0	0.0	0.0	1.0	1021.2	766.5
ACETOL	1175.8	1175.8	1175.8	1106.6	276.7	0.0	0.0	0.0	0.0	0.0	0.3	276.4	207.5
PHENOL	358.4	358.4	358.4	337.3	84.3	0.0	0.0	0.0	0.0	0.0	0.0	84.3	63.2
FURFURAL	473.3	473.3	473.3	445.4	111.3	0.0	0.0	0.0	0.0	0.0	0.1	111.2	83.5
BUTACID	114.6	114.6	114.6	107.9	27.0	0.0	0.0	0.0	0.0	0.0	0.0	26.9	20.2
2-HYD-01	100.4	100.4	100.4	94.5	23.6	0.0	0.0	0.0	0.0	0.0	0.0	23.6	17.7
FURANONE	86.0	86.0	86.0	80.9	20.2	0.0	0.0	0.0	0.0	0.0	0.0	20.2	15.2
BEZENEDI	100.4	100.4	100.4	94.5	23.6	0.0	0.0	0.0	0.0	0.0	0.0	23.6	17.7
CYCLO-01	43.1	43.1	43.1	40.6	10.1	0.0	0.0	0.0	0.0	0.0	0.0	10.1	7.6
HUMUACID	258.2	258.2	258.2	243.0	60.7	0.0	0.0	0.0	0.0	0.0	0.0	60.7	45.6
TRIHIDRO	57.3	57.3	57.3	54.0	13.5	0.0	0.0	0.0	0.0	0.0	0.0	13.5	10.1
BUTANONE	43.1	43.1	43.1	40.6	10.1	0.0	0.0	0.0	0.0	0.0	0.0	10.1	7.6

AREA 400

	QCB-4001	QHX-2001	QHX-4001	QHX-4002	QHX-4003	QHX-4004	QPY-2001
QCALC Gcal/hr	-18.7	-2.5	12.2	3.1	3.0	6.6	7.7
TBEGIN C	54.4	55.6	1700.0	982.0	792.0	603.0	350.0
TEND C	1700.0	350.0	982.0	792.0	603.0	155.0	350.0

WCP-4001
POWER kW 12.4

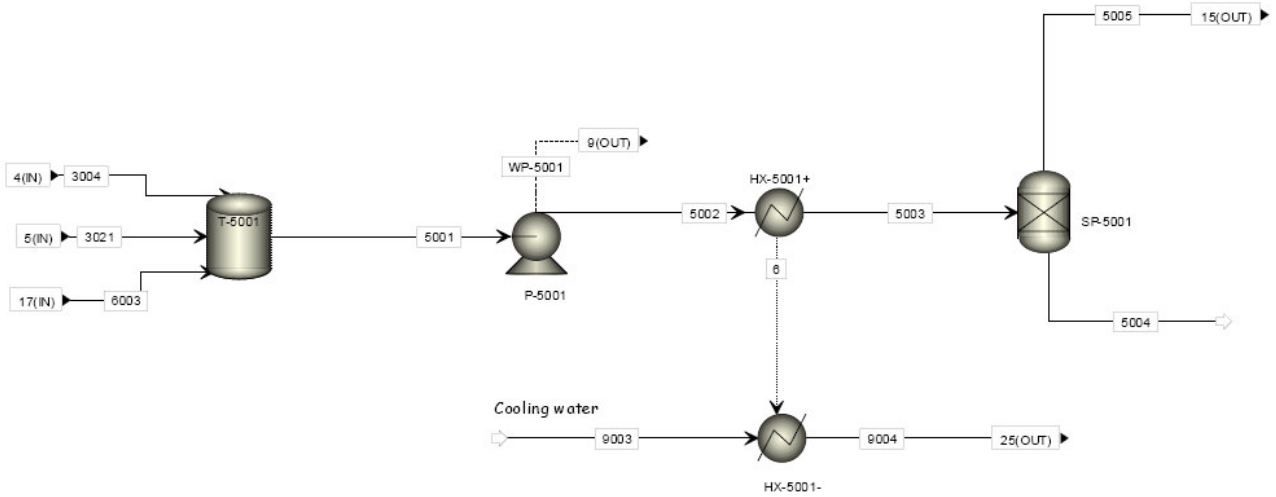


	10	4000	4001	4002	4003	4005	4006	4007	4008	4009	4010	4011	4012
Temperature C	622.8	25.0	1700.0		25.0	1700.0	982.0	792.0	603.0	155.0	25.0	25.8	54.4
Pressure bar	1.4	1.4	1.0		1.0	1.0	1.0	1.0	1.0	1.0	1.0	1.0	14.8
Vapor Frac	1.0	0.0	1.0		0.0	1.0	1.0	1.0	1.0	1.0	1.0	1.0	1.0
Total Flow kg/hr	2401.1	3316.1	57401.2	0.0	3316.1	57401.2	57401.2	57401.2	57401.2	57401.2	55000.0	55000.0	57401.2
Mass Flow kg/hr													
N2	0.0	0.0	41266.5	0.0	0.0	41266.5	41266.5	41266.5	41266.5	41266.5	41266.5	41266.5	41266.5
O2	0.0	0.0	12002.3	0.0	0.0	12002.3	12002.3	12002.3	12002.3	12002.3	12644.5	12644.5	12644.5
AR	0.0	0.0	698.5	0.0	0.0	698.5	698.5	698.5	698.5	698.5	698.5	698.5	698.5
H2	2.4	0.0	0.0	0.0	0.0	0.0	0.0	0.0	0.0	0.0	0.0	0.0	2.4
CH4	48.8	0.0	0.0	0.0	0.0	0.0	0.0	0.0	0.0	0.0	0.0	0.0	48.8
CO	640.2	0.0	0.0	0.0	0.0	0.0	0.0	0.0	0.0	0.0	0.0	0.0	640.2
CO2	1683.7	0.0	2903.7	0.0	0.0	2903.7	2903.7	2903.7	2903.7	2903.7	27.5	27.5	1711.2
C2H4	6.1	0.0	0.0	0.0	0.0	0.0	0.0	0.0	0.0	0.0	0.0	0.0	6.1
C2H6	10.9	0.0	0.0	0.0	0.0	0.0	0.0	0.0	0.0	0.0	0.0	0.0	10.9
H2O	8.0	3316.1	530.2	0.0	3316.1	530.2	530.2	530.2	530.2	530.2	363.0	363.0	371.0
ACETACID	0.7	0.0	0.0	0.0	0.0	0.0	0.0	0.0	0.0	0.0	0.0	0.0	0.7
ACETOL	0.1	0.0	0.0	0.0	0.0	0.0	0.0	0.0	0.0	0.0	0.0	0.0	0.1
FURFURAL	0.1	0.0	0.0	0.0	0.0	0.0	0.0	0.0	0.0	0.0	0.0	0.0	0.1
BUTACID	0.0	0.0	0.0	0.0	0.0	0.0	0.0	0.0	0.0	0.0	0.0	0.0	0.0

AREA 500

6
 QCALC Gcal/hr 0.0
 TBEGIN C 28.9
 TEND C 25.0

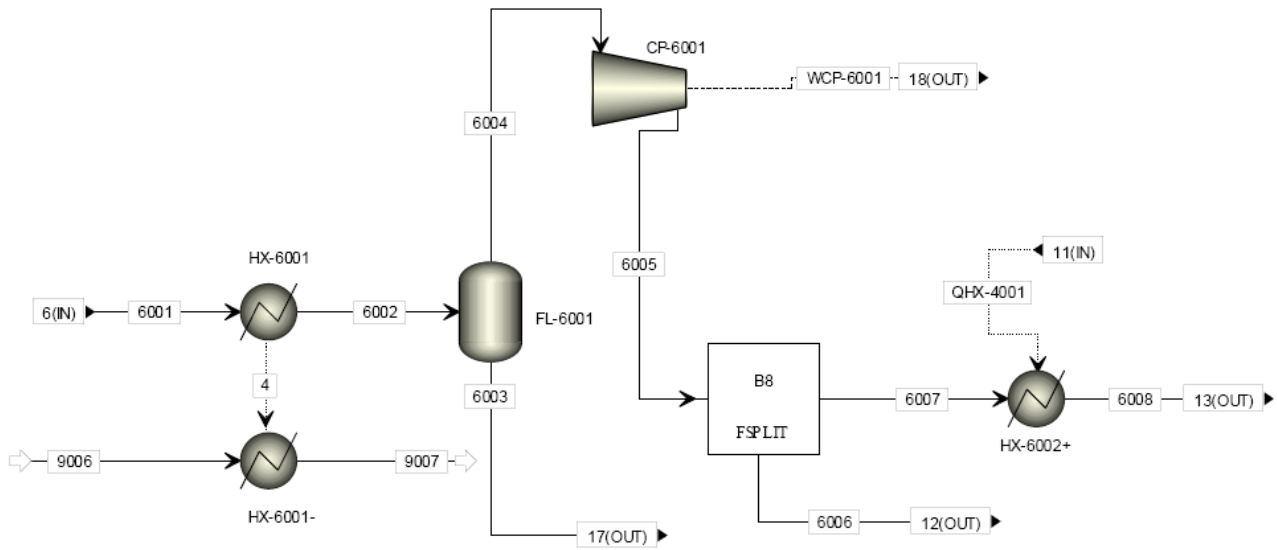
WP-5001
 POWER kW 1.0



	3004	3021	5001	5002	5003	5004	5005	6003	9003	9004
Temperature C	28.5	28.5	28.8	28.9	25.0	-6.4	-6.4	7.0	21.1	24.6
Pressure bar	1.4	1.4	1.8	2.8	2.8	2.8	2.8	1.4	1.0	1.0
Total Flow kg/hr	6773.5	11848.1	18624.4	18624.4	18624.4	15830.7	2793.7	2.8	14804.8	14804.8
Mass Flow kg/hr										
CO2	-	-	0.1	0.1	0.1	0.1	0.0	0.1	-	-
C3H6-2	2.7	0.7	3.3	3.3	3.3	2.8	0.5	-	-	-
C3H8	10.7	2.7	13.4	13.4	13.4	11.4	2.0	-	-	-
CH3OH	3.1	0.8	3.9	3.9	3.9	3.3	0.6	-	-	-
C4H10	14.6	3.7	18.3	18.3	18.3	15.5	2.7	-	-	-
C5H12	8.4	2.1	10.6	10.6	10.6	9.0	1.6	-	-	-
H2O	-	10,156.2	10,158.3	10,158.3	10,158.3	8,634.6	1,523.7	2.2	14,804.8	14,804.8
ACETACID	4,088.7	1,021.2	5,110.2	5,110.2	5,110.2	4,343.6	766.5	0.3	-	-
ACETOL	1,106.6	276.4	1,383.2	1,383.2	1,383.2	1,175.7	207.5	0.2	-	-
PHENOL	337.3	84.3	421.6	421.6	421.6	358.4	63.2	-	-	-
FURFURAL	445.4	111.2	556.6	556.6	556.6	473.2	83.5	0.0	-	-
BUTACID	107.9	26.9	134.9	134.9	134.9	114.6	20.2	0.0	-	-
2-HYD-01	94.5	23.6	118.1	118.1	118.1	100.4	17.7	-	-	-
FURANONE	80.9	20.2	101.2	101.2	101.2	86.0	15.2	-	-	-
BEZENEDI	94.5	23.6	118.1	118.1	118.1	100.4	17.7	-	-	-
CYCLO-01	40.6	10.1	50.7	50.7	50.7	43.1	7.6	-	-	-
HUMUACID	243.0	60.7	303.7	303.7	303.7	258.2	45.6	-	-	-
TRIHYDRO	54.0	13.5	67.4	67.4	67.4	57.3	10.1	-	-	-
BUTANONE	40.6	10.1	50.7	50.7	50.7	43.1	7.6	-	-	-

AREA 600

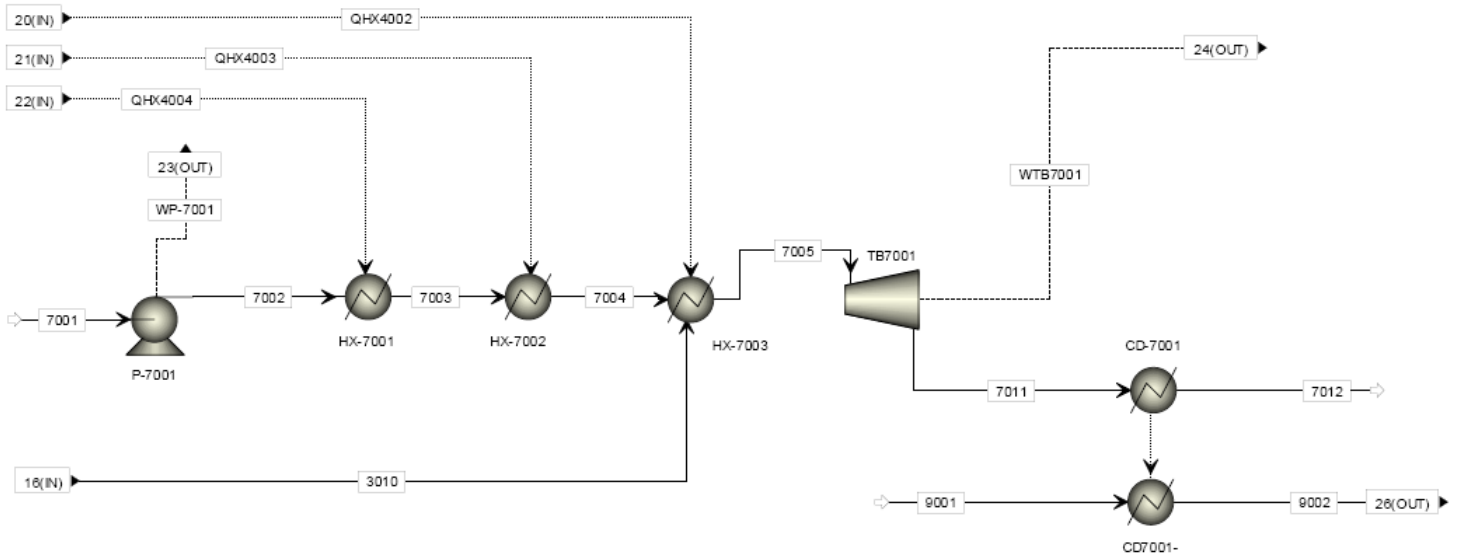
	1	2	4	QHX-4001
QCALC Gcal/hr	-0.6	11.6	0.0	12.2
TBEGIN C	7.0		28.5	1700.0
TEND C	830.0		7.0	982.0



	6001	6002	6003	6007	6008	9006	9007	6008	9006
Temperature C	28.5	7	7	7	830	4	4.2	823.5	4
Pressure bar	1.379	1.379	1.379	1.379	1.379	1.034	1.034	3.103	1.034
Vapor Frac	1	0.998	0	1	1	0	0	1	0
Mass Flow kg/hr	2403.9	2403.9	2.8	2401.1	2401.1	64197.7	64197.7	57750.5	64197.7
Mass Flow kg/hr									
H2	2.407	2.407	0	2.407	2.407	0	0		
CH4	48.791	48.791	0	48.791	48.791	0	0	0	0
CO	640.192	640.192	0.002	640.189	640.189	0	0	0	0
CO2	1683.855	1683.855	0.11	1683.746	1683.746	0	0	0	0
C2H4	6.126	6.126	0	6.126	6.126	0	0		
C2H6	10.94	10.94	0.001	10.939	10.939	0	0		
H2O	10.166	10.166	2.156	8.01	8.01	64197.7	64197.7	0	0
ACETACID	1.022	1.022	0.287	0.735	0.735	0	0	0	0
ACETOL	0.277	0.277	0.186	0.091	0.091	0	0	0	0
FURFURAL	0.111	0.111	0.012	0.099	0.099	0	0	0	0
BUTACID	0.027	0.027	0.011	0.016	0.016	0	0	0	0

AREA 700

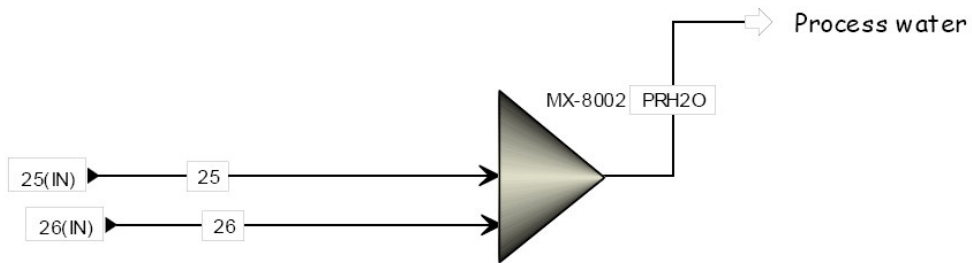
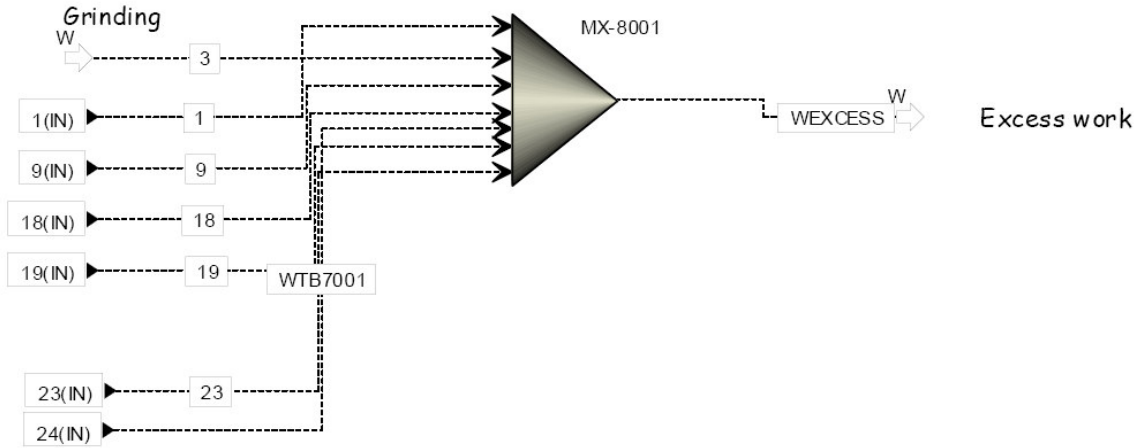
	6	QHX4002	QHX4003	QHX4004
QCALC Gcal/hr	9.7	3.1	3.0	6.6
TBEGIN C	164.7	982.0	792.0	603.0
TEND C	46.5	792.0	603.0	155.0
	WP-7001	WTB7001		
POWER kW	7.6	-3331.6		



	3010	7001	7002	7003	7004	7005	7011	7012	9001
Temperature C	131.1	30	30.5	243.5	250.8	542.9	164.7	46.5	21.1
Pressure bar	35.5	1.4	10.4	35.5	35.5	35.5	1.1	0.1	1.1
Vapor Frac	0.0	0.0	0.0	0.5	1.0	1.0	1.0	0.0	0.0
Mass Flow kg/hr									
H2O	1470.9	14106.0	14106.0	14106.0	14106.0	15576.9	15576.9	15576.9	585107.0

AREA 800

	1	3	9	19	23	WEXCESS	WTB7001
POWER kW	67.5	2338.8	1.0	12.4	7.6	-904.4	-3331.6



	25	26	PRH2O
Temperature C	24.6	39	38.6
Pressure bar	1.034	1.103	1.034
Vapor Frac	0	0	0
Mass Flow kg/hr	14804.8	585107.0	599911.8
Mass Flow kg/hr H2O	14804.8	585107	599911.8

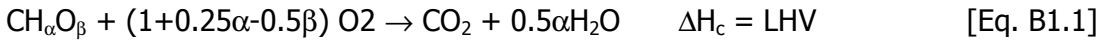
APPENDIX B1 ADDITIONAL DATA FOR EQUILIBRIUM MODELLING OF BAGASSE AND SLURRY GASIFICATION

Table B1.1 Operating conditions for central composite design for gasification runs of each feedstock.

	Temperature	Pressure	Moisture	BSR	ER
1	900	1	5	0	0.1
2	900	1	5	0	1
3	900	0	5	3	0.1
4	900	0	5	3	1
5	900	1	50	0	0.1
6	900	1	50	0	1
7	900	1	50	3	0.1
8	900	1	50	3	1
9	900	40	5	0	0.1
10	900	40	5	0	1
11	900	40	5	3	0.1
12	900	40	5	3	1
13	900	40	50	0	0.1
14	900	40	50	0	1
15	900	40	50	3	0.1
16	900	40	50	3	1
17	1700	1	5	0	0.1
18	1700	1	5	0	1
19	1700	1	5	3	0.1
20	1700	1	5	3	1
21	1700	1	50	0	0.1
22	1700	1	50	0	1
23	1700	1	50	3	0.1
24	1700	1	50	3	1
25	1700	40	5	0	0.1
26	1700	40	5	0	1
27	1700	40	5	3	0.1
28	1700	40	5	3	1
29	1700	40	50	0	0.1
30	1700	40	50	0	1
31	1700	40	50	3	0.1
32	1700	40	50	3	1
33	900	20	25	1.5	0.5
34	1700	20	25	1.5	0.5
35	1300	1	25	1.5	0.5
36	1300	40	25	1.5	0.5
37	1300	20	5	1.5	0.5
38	1300	20	50	1.5	0.5
39	1300	20	25	0	0.5
40	1300	20	25	3	0.5
41	1300	20	25	1.5	0.15
42	1300	20	25	1.5	1
43	1300	20	25	1.5	0.5

B1.1 Calculation of heat of formation for bagasse and bagasse-derived feedstocks

The gasifier duty was calculated as the difference between the product gas enthalpy and that of the feedstock and other reactants. Since the feedstock is fed at standard temperature and pressure, the enthalpy is equal to the **heat of formation** of the feedstock. Since the heat of formation of biomass is not exactly known, it was estimated by using the stoichiometric combustion reaction for dry biomass of composition ($\text{CH}_\alpha\text{O}_\beta$) as follows:



Since the heat of formation for O_2 is zero at the feed conditions of 25°C and 1 atm, the heat of formation of the feedstock was calculated as:

$$\Delta H_f^0(\text{CH}_\alpha\text{O}_\beta) = \Delta H_f^0(\text{CO}_{2(\text{g})}) + 0.5\alpha\Delta H_f^0(\text{H}_2\text{O}_{(\text{g})}) + \text{LHV} \quad [\text{Eq. B1.2}]$$

where $\Delta H_f^0(\text{CO}_{2(\text{g})}) = -393.5$ kJ/mol and $\Delta H_f^0(\text{H}_2\text{O}_{(\text{g})}) = -241.8$ kJ/mol (Perry and Green, 1997). The LHV of the feedstock was determined from the statistical correlation developed by Channiwala and Parikh, 2002 for calculating the HHV of a wide spectrum of fuels from its elemental mass fractions:

$$\text{HHV}_{\text{fuel}}[\text{MJ/kg}] = 0.3491m_C + 1.1783m_H - 0.1034m_O - 0.0151m_N + 0.1005m_S - 0.0211m_{\text{Ash}} \quad [\text{Eq. B1.3}]$$

The LHV was calculated from the HHV by subtracting the heat of evaporation for water (2260 kJ/kg or 40.73 kJ/mol). The results for all feedstocks are given below.

Table B1.2 Feedstock compositions, lower heating values and heats of formation used in equilibrium modelling.

	Bagasse	Fast Pyrolysis slurry	Vacuum Pyrolysis Slurry
Elemental Composition	C H1.49 O0.64	C H1.13 O0.32	C H0.85 O0.38
H/C	1.49	1.13	0.85
O/C	0.64	0.32	0.38
LHV [MJ/kg]	18.31	25.11	21.99
Standard heat of formation [kJ/mol]	-127	-72.77	-81.48

The feedstock mixture enthalpy was calculated by multiplying the mass fraction of each component in the feed mixture with its enthalpy value. The enthalpy of steam at 500K and 1 bar equals -234.9kJ/mol (Perry and Green, 1997).

Table B1.3 Output file from CEA program for equilibrium modelling of bagasse gasification: central composite design run 1

NASA-GLENN CHEMICAL EQUILIBRIUM PROGRAM CEA, AUGUST 30, 1999

BY BONNIE MCBRIDE AND SANFORD GORDON

REFS: NASA RP-1311, PART I, 1994 AND NASA RP-1311, PART II, 1996

! Chemical equilibrium for bagasse gasification - central composite design design 1
problem case=Bagasseccd1 tp t(K)=900 p(bar)=1

o/f=0.14

reac

fuel=bagasse wt%=95 C 0.32 H 0.48 O 0.20 t(k)=298.15 h(kJ/mol)=-127

fuel=H2O wt%=5 t(K)=298

oxid=H2O wt%=0 t(K)=500

oxid=O2 wt%=100 t(K)=298

only H2 CO CH4 CO2 H2O C2H4 O2 C

output siunits

end

OPTIONS: TP=T HP=F SP=F TV=F UV=F SV=F DETN=F SHOCK=F REFL=F
INCD=F

RKT=F FROZ=F EQL=F IONS=F SIUNIT=T DEBUGF=F SHKDBG=F DETDBG=F
TRANSPT=F

T,K = 900.0000

TRACE= 0.00E+00 S/R= 0.000000E+00 H/R= 0.000000E+00 U/R= 0.000000E+00

P,BAR = 1.000000

REACTANT WT.FRAC (ENERGY/R),K TEMP,K DENSITY

EXPLODED FORMULA

F: bagasse .950000 -.152745E+05 298.15 .0000

C .32000 H .48000 O .20000

F: H2O .050000 -.290854E+05 298.00 .0000

H 2.00000 O 1.00000

O: H2O .000000 -.282520E+05 500.00 .0000

H 2.00000 O 1.00000

O: O2 1.000000 -.530002E+00 298.00 .0000

O 2.00000

SPECIES BEING CONSIDERED IN THIS SYSTEM (CONDENSED PHASE MAY HAVE NAME LISTED SEVERAL TIMES) LAST thermo.inp UPDATE: 11/08/99

g 7/97 *C g 8/99 CH4 tpis79 *CO

g 9/99 *CO2 g 1/91 C2H4 tpis78 *H2

g 8/89 H2O tpis89 *O2

O/F = .140000

	EFFECTIVE FUEL	EFFECTIVE OXIDANT	MIXTURE
ENTHALPY	h(2)/R	h(1)/R	h0/R
(KG-MOL)(K)/KG	-.20085249E+04	-.16563198E-01	-.17618660E+04
KG-FORM.WT./KG	bi(2)	bi(1)	b0i
*C	.40387318E-01	.00000000E+00	.35427472E-01
H	.66131821E-01	.00000000E+00	.58010369E-01

O .28017496E-01 .62502344E-01 .32252478E-01
 POINT ITN T C H O
 1 9 900.000 1.124 -9.377 -41.987

THERMODYNAMIC EQUILIBRIUM PROPERTIES AT ASSIGNED
 TEMPERATURE AND PRESSURE

CASE = Bagasseccd1

REACTANT	WT FRACTION (SEE NOTE)	ENERGY KJ/KG-MOL	TEMP K
FUEL bagasse	.9500000	-127000.000	298.150
FUEL H2O	.0500000	-241831.038	298.000
OXIDANT H2O	.0000000	-234901.248	500.000
OXIDANT O2	1.0000000	-4.407	298.000

O/F= .14000 %FUEL= 87.719298 R, EQ. RATIO= 3.096200 PHI, EQ. RATIO= 9.807981

THERMODYNAMIC PROPERTIES

P, BAR 1.0000
 T, K 900.00
 RHO, KG/CU M 2.8570-1
 H, KJ/KG -4141.15
 U, KJ/KG -4491.16
 G, KJ/KG -13906.0
 S, KJ/(KG)(K) 10.8498
 M, (1/n) 21.379

(dLV/dLP)t -1.10690
(dLV/dLT)p 2.8338
Cp, KJ/(KG)(K) 14.2917
GAMMA_s 1.1257
SON VEL,M/SEC 627.7

MOLE FRACTIONS

CH₄ .18875
*CO .46843
*CO₂ .10022
*H₂ .22193
H₂O .02066

* THERMODYNAMIC PROPERTIES FITTED TO 20000.K

PRODUCTS WHICH WERE CONSIDERED BUT WHOSE MOLE FRACTIONS
WERE LESS THAN 5.000000E-06 FOR ALL ASSIGNED CONDITIONS

*C C₂H₄ *O₂

NOTE. WEIGHT FRACTION OF FUEL IN TOTAL FUELS AND OF OXIDANT IN TOTAL
OXIDANTS

APPENDIX B2 STATISTICAL DATA FOR EQUILIBRIUM GASIFIER MODELLING

The model that was used in STATISTICA to fit the equilibrium modelling data included linear and quadratic effects (positive and negative) and the R^2 was evaluated in an ANOVA table. Pareto charts were used to examine the significant effects and generate relevant surface contour plots to analyse the effects of the main factors.

B-2.1 PARETO CHARTS FOR STANDARDIZED FOR SYNGAS RATIO

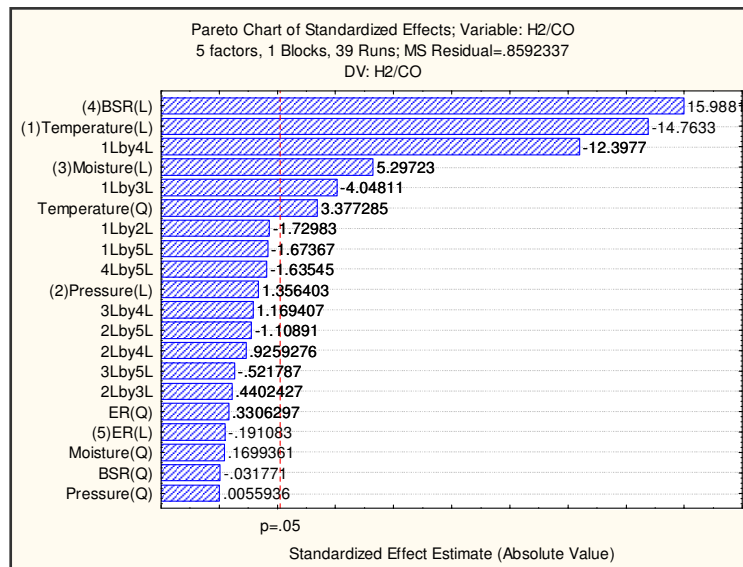


Figure B-2.1 Pareto chart of standardised effects on H_2/CO ratio of equilibrium gas for **bagasse** gasification. ANOVA $R^2=0.98$.

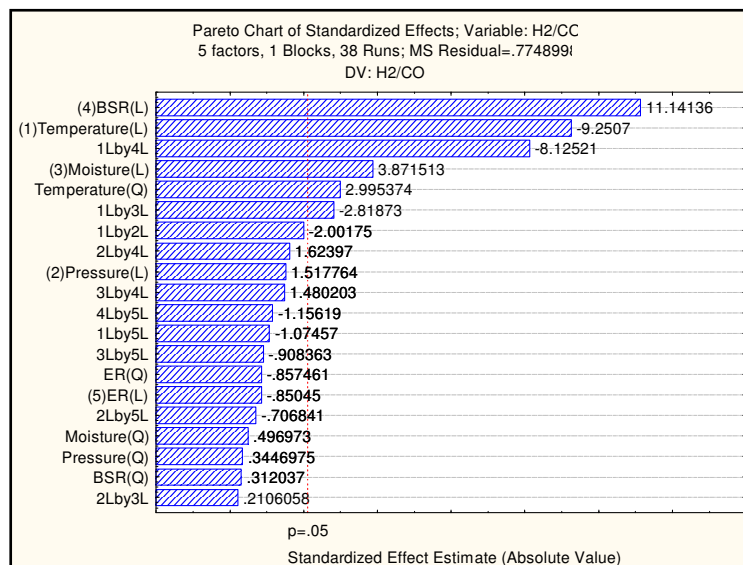


Figure B-2.2 Pareto chart of standardised effects on H_2/CO ratio of equilibrium gas for **fast pyrolysis slurry** gasification. ANOVA $R^2=0.96$.

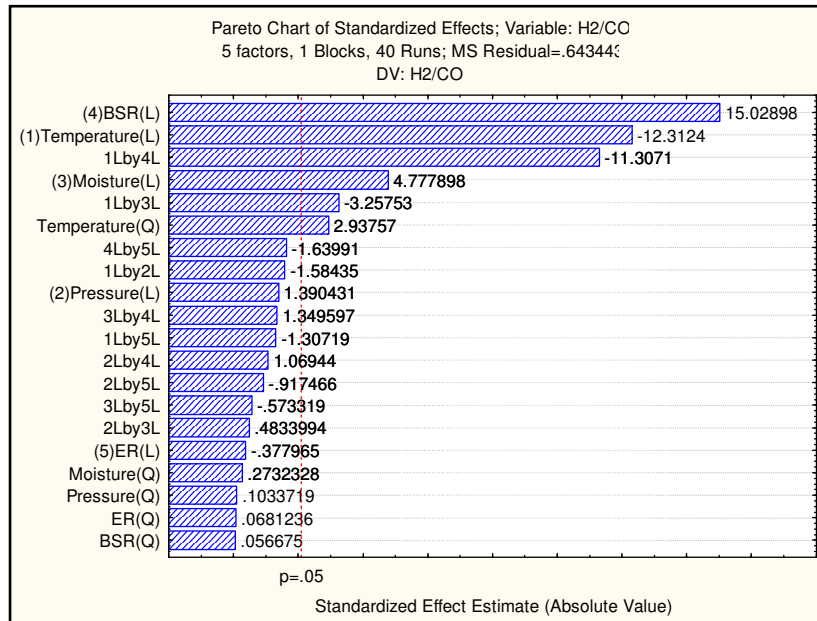


Figure B-2.3 Pareto chart of standardised effects on H₂/CO ratio of equilibrium gas for **vacuum pyrolysis slurry** gasification. ANOVA R²=0.97.

B-2.2 PARETO CHARTS FOR STANDARDIZED FOR SYNGAS COMPOSITION

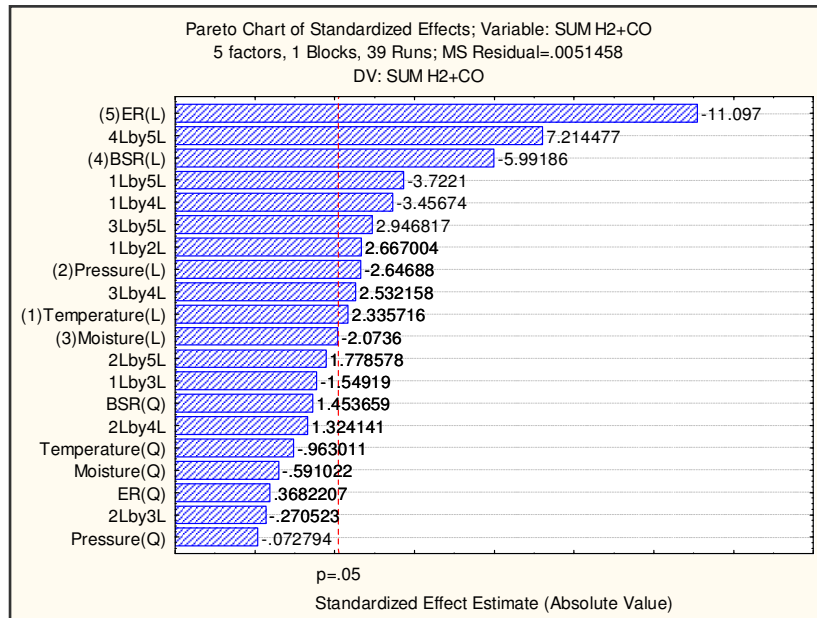


Figure B-2.4 Pareto chart of standardised effects on sum of H₂+CO of equilibrium gas for **bagasse** gasification. ANOVA R²=0.96.

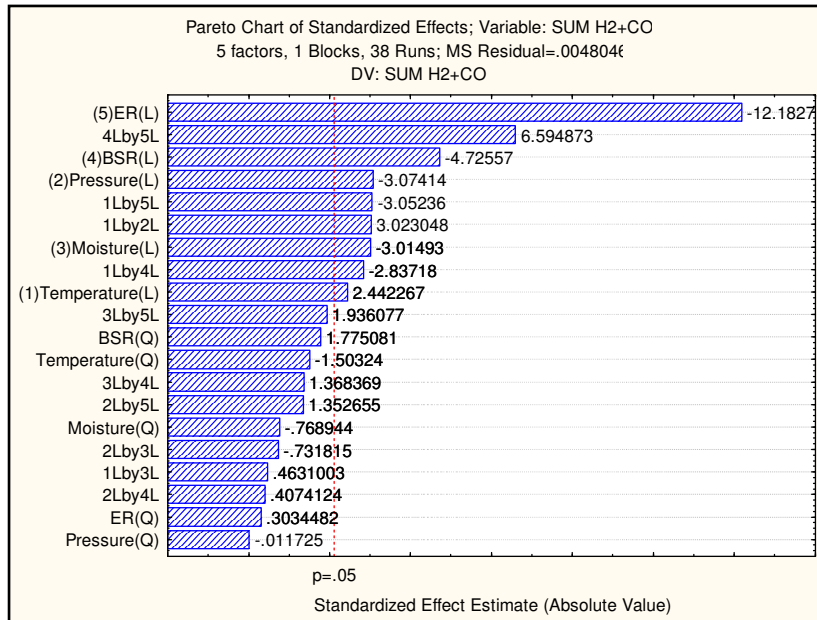


Figure B-2.5 Pareto chart of standardised effects on sum of H₂+CO of equilibrium gas for **fast pyrolysis slurry** gasification. ANOVA R²=0.97.

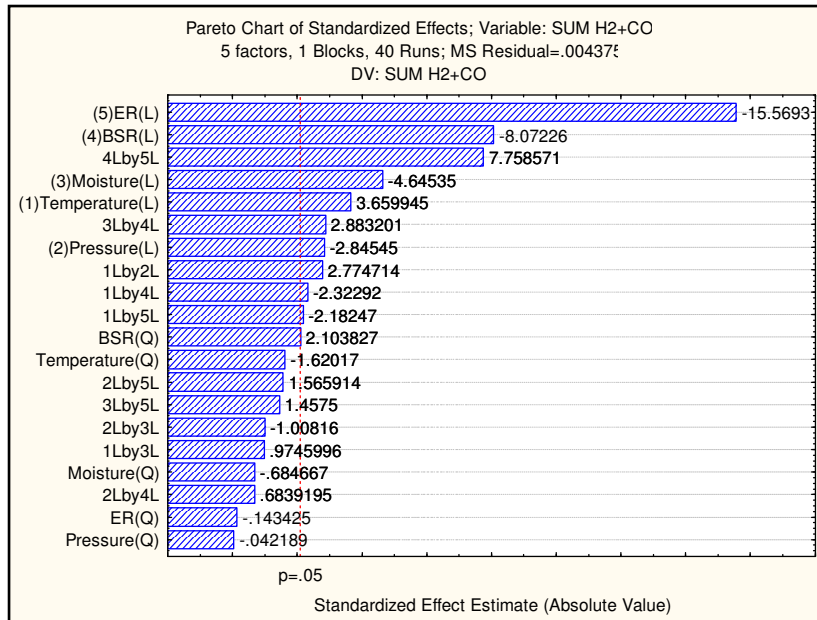


Figure B-2.6 Pareto chart of standardised effects on sum of H₂+CO of equilibrium gas for **vacuum pyrolysis slurry** gasification. ANOVA R²=0.97.

B-2.3 PARETO CHARTS FOR STANDARDIZED FOR GASIFICATION SYSTEM EFFICIENCY

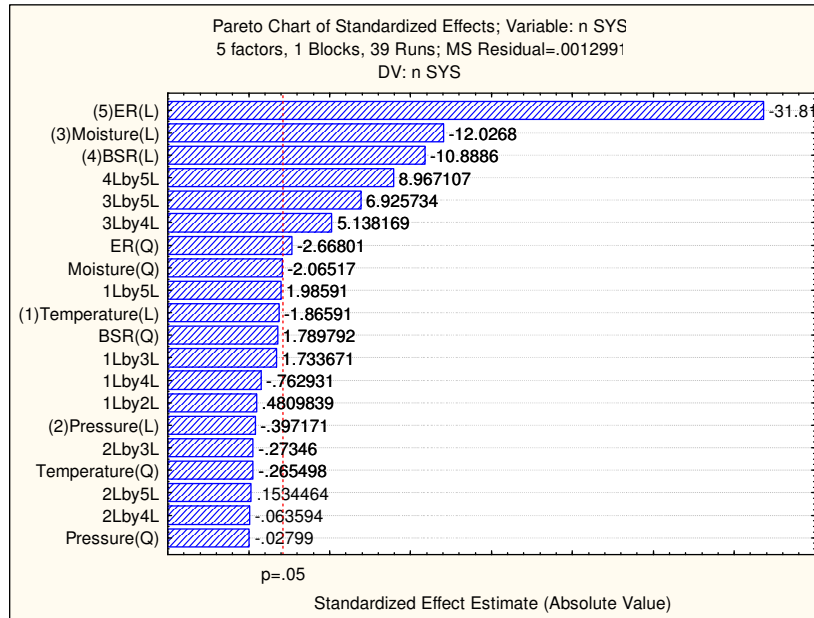


Figure B-2.7 Pareto chart of standardised effects on system efficiency for **bagasse** gasification. ANOVA $R^2=0.99$.

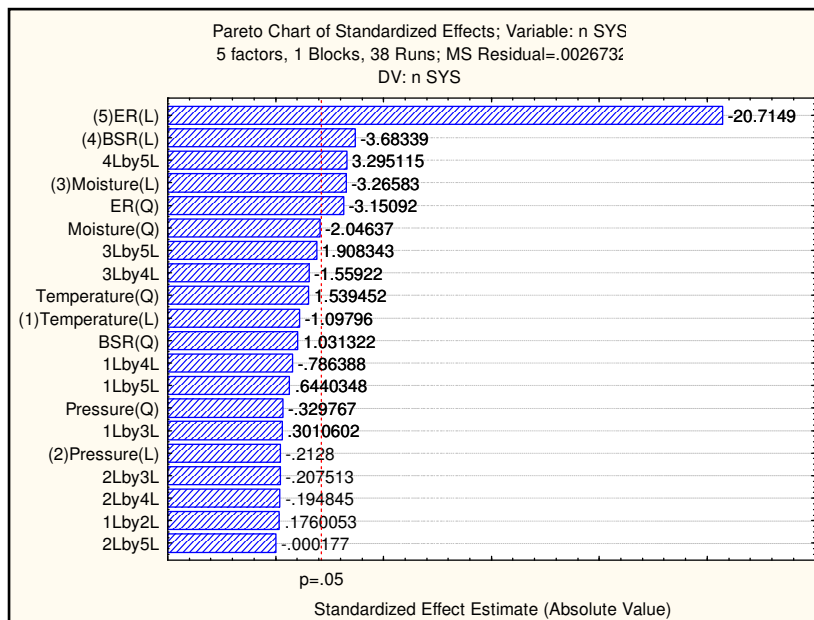


Figure B-2.8 Pareto chart of standardised effects on system efficiency for **fast pyrolysis** slurry gasification. ANOVA $R^2=0.98$.

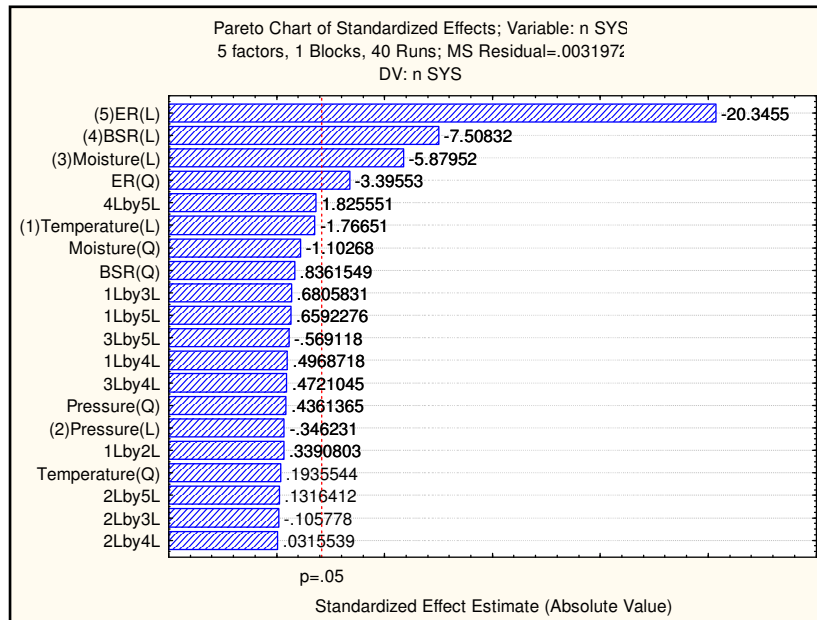


Figure B-2.9 Pareto chart of standardised effects on system efficiency for **vacuum pyrolysis slurry** gasification. ANOVA $R^2=0.98$.

B-2.4 PARETO CHART FOR STANDARDIZED FOR GASIFIER DUTY

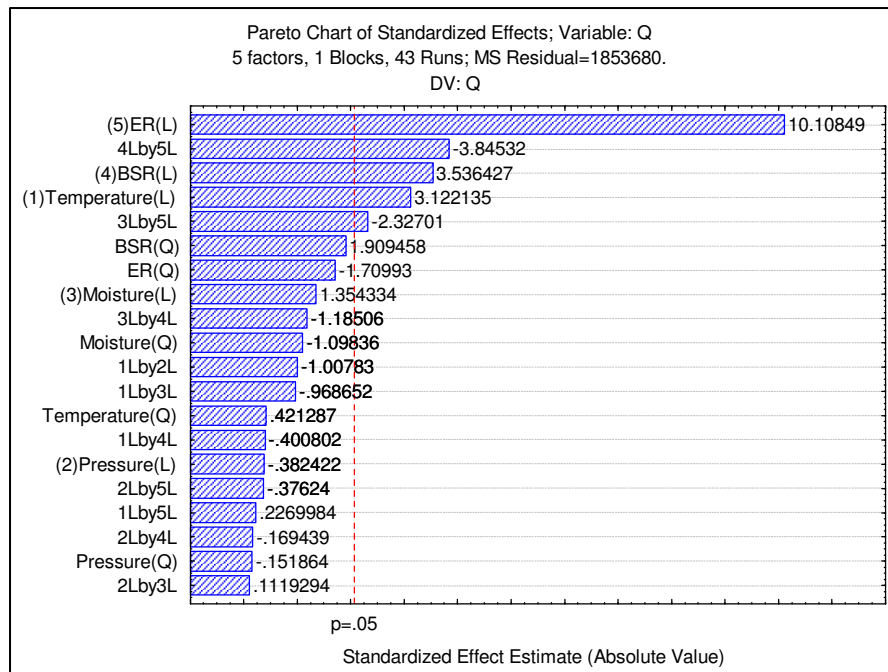


Figure B-2.10 Pareto chart of standardised effects on gasifier duty **bagasse** gasification. ANOVA $R^2=0.88$.

APPENDIX B3 DETERMINATION OF GASIFIER OPERATING CONDITIONS USING EQUILIBRIUM MODELLING

The prediction and profiling tool available in STATISTICA was used to determine operating conditions for two gasifier modes for each feedstock. This was done using the desirability profiler. The relationship between predicted responses on one or more dependent variables and the desirability of responses is called the desirability function. In order to profile the desirability of a response, one needs to specify the desirability function for each chosen dependent variable by assigning a score between 0 (very undesirable) and 1 (very desirable) to the predicted value. The program then calculates the desirability score of each predicted value for each chosen dependent variable by calculating their geometric mean and returns a set of values for the independent variables that would result in the highest possible desirability score for the predicted value of the chosen dependent variable.

The desirability profiler can be used to optimise for one dependent variable at a time, or a set of dependent variables. However, it is important to note that the desirability profiles need to be specified very carefully in order to obtain the best result, and if various dependent variables are optimised at the same time care should be taken to assign the appropriate weight to each desirability profile.

It was therefore decided to determine the desired setting (set value or maximum) for each of the dependent variables listed below individually at first, in order to analyse the effect of assigning a 100% weight on each, followed by a combination of all three dependent variables. This method leads to a better understanding of the impact of each variable on the overall desirability of the system dependent variables as a whole, without creating bias towards one specific variable.

The selected dependent variables were:

- Sum of H₂ and CO (desired components for FT synthesis)
- H₂/CO ratio (target should be close to 2 if a shift reactor is not used)
- Gasification system efficiency (SE)

It is important to note that the reliability of the solver is dependent on the accuracy of the model that was fitted to the data by STATISTICA. This can be measured by evaluating the R² values given in the ANOVA table for each parameter. The R² values for the full data set are given in Table B3.1.

Table B3.1 ANOVA R² values for STATISTICA model

	H ₂ /CO molar ratio	SUM H ₂ +CO	System efficiency
Bagasse	0.98	0.96	0.89
Fast Pyrolysis Slurry	0.96	0.97	0.98
Vacuum Pyrolysis slurry	0.97	0.97	0.98

The model achieved a very good fit for the majority of the parameters, with the exception of the bagasse system efficiency that resulted in a R² value of below 0.9. It was found that for some of the runs, the H₂ and CO concentrations were found to be negligible, resulting in a H₂/CO ratio of infinity. Since STATISTICA ignores any runs with missing parameters in the analysis, the R² value was affected. However, the R² of 0.89 is still good considering the wide spectrum of factors studied.

The prediction profiling and results will now be discussed for each parameter, with a comparison between the various feedstocks.

B3.1 H₂/CO molar ratio

The results for the molar H₂/CO ratio are given in Table B3.2 below. The combined sets of conditions are different for each feedstock. It was found in the analyses of the Pareto charts that the steam to biomass ratio was the most important factor affecting the H₂/CO ratio, while the optimum temperature was found to be 1300K at low steam biomass ratios. However, because the most desirable value for the H₂/CO ratio was set at a value of 2, there would be a number of different solutions for each feedstock that would return this optimum value, as discussed in Chapter 4. It is therefore difficult to optimise for only the H₂/CO ratio in isolation of any other factors, as this would not necessarily result in the best set of conditions for gasification. This can also be seen from the desirability scores obtained for the combined variables in Table B3.2, which are very poor, despite the fact that those for the H₂/CO ratio alone are all equal to 1.

B3.2 Sum of H₂ and CO molar fractions

The set of conditions that maximise the sum of the H₂ and CO molar fractions is shown in Table B3.3. The individual desirability score for each feedstock was close to 1, and in all cases the optimum temperature, steam biomass ratio (SBR) and equivalence ratio (ER) was 1700K, 0 and 0,1, respectively. This is in line with the findings discussed in Chapter 4 that the H₂ and CO concentrations are favoured by higher temperatures, low steam biomass ratios and low equivalence ratios. Some deviations in the optimum values were observed for the pyrolysis slurries in terms of pressure. Although increasing pressure leads to a slightly negative effect on the H₂ and CO fractions, the Pareto charts in Appendix B-2 show that the significance level of this effect is very low. The overall desirability scores obtained for the sum of H₂ and CO fractions range between 0.73 and 0.79, which is the highest so far, but still not close enough to 1.

Table B3.2 Fitted parameters from desirability profiling for H₂/CO molar ratio

	Temperature [K]	Pressure [bar]	Moisture content [w%]	SBR	ER	LHV [kJ/mol]	H ₂ /CO [mol]	SUM H ₂ +CO [mol]	SE	GE	Desirability
Bagasse	1700.00	40.00	5.00	2.25	0.10		2.00				1.00
	1700.00	40.00	5.00	2.25	0.10	116.34	2.00	0.44	0.57	0.40	0.51
Fast Pyrolysis slurry	1500.00	1.00	16.25	3.00	0.55		2.00				1.00
	1500.00	1.00	16.25	3.00	0.55	44.33	2.00	0.26	0.40	0.09	0.30
Vacuum Pyrolysis slurry	1300.00	1.00	50.00	0.75	0.78		2.00				1.00
	1300.00	1.00	50.00	0.75	0.78	7.63	2.00	1.34	0.23	0.04	0.13

Table B3.3 Fitted parameters from desirability profiling for the Sum of H₂ and CO molar fractions

	Temperature [K]	Pressure [bar]	Moisture content [w%]	SBR	ER	LHV [kJ/mol]	H ₂ /CO [mol]	SUM H ₂ +CO [mol]	SE	GE	Desirability
Bagasse	1700.00	1.00	5.00	0.00	0.10			0.95			0.99
	1700.00	1.00	5.00	0.00	0.10	290.43	1.01	0.95	0.87	0.92	0.79
Fast Pyrolysis slurry	1700.00	10.75	5.00	0.00	0.10			0.94			1.00
	1700.00	10.75	5.00	0.00	0.10	314.49	0.73	0.94	0.74	0.65	0.78
Vacuum Pyrolysis slurry	1700.00	20.50	5.00	0.00	0.10			0.93			1.00
	1700.00	20.50	5.00	0.00	0.10	330.25	0.52	0.93	0.73	0.69	0.73

The first desirability score corresponds with the optimised individual variable, while the second for each dataset shows the effect of solving for that individual variable on the overall score for all the dependent variables. SE=gasification system efficiency and GE=gasifier cold gas efficiency.

B3.3 System efficiency

The sets of conditions that lead to the maximum system efficiency are given in Table B3.4 for each feedstock. It is evident that a minimum equivalence ratio and steam biomass ratio will maximise the system efficiency. For both slurries, higher moisture content values are desired. This was ascribed to the fact that the slurries exhibited higher carbon contents and addition of moisture helped to move the composition of the slurry closer to the carbon boundary temperature, as described in Chapter 4.

Furthermore, the overall desirability scores obtained from the sets for maximum system efficiency are very poor, and confirm the previous findings that setting the desired value for an individual parameter will not necessarily optimise the overall process sufficiently.

B3.4 Combined variable

From the individual parameter fittings, it was clear that no single factor could be used effectively to find the desired set of conditions for the overall gasification process. The results obtained from fitting of the all three combined variables are shown in Table B3.5.

First of all, a low equivalence ratio is optimum for all feedstocks and all the target variables. The strong effect of steam addition that was observed for the H_2/CO ratio is featured in the steam biomass ratio setting of 0.75. The combined variable approach resulted in overall desirability scores 0.75 to 0.77, which is an improvement to those obtained for the individual parameters. In all cases, this returned predicted H_2/CO ratios of close to 2.

The desired operating conditions, taking practical considerations into account, are given in Table B3.6. For practical reasons described in Chapter 4, this final optimisation was limited to atmospheric gasifiers, equivalence ratios of 0.25 and a minimum temperature of 1100K. Although these criteria do not lead to the best thermodynamic optimum, the practical optimisation attempted to find the most reasonable operating conditions within

practical constraints that would lead to optimised gasification. As expected, the overall desirability scores are much lower at these conditions, mainly due to the known negative effect of increasing the equivalence ratio, and the scores ranged between 0.48 and 0.57, resulting in gasification system efficiencies of 63-75%. This is mainly due to the known negative effect of increasing the equivalence ratio. In all cases the H_2/CO ratio is far from 2 and a shift reactor will be required for maximum FT synthesis. In the individual optimisation of the H_2/CO ratio, it was found that a steam to biomass ratio of 2.25 would be required to obtain an H_2/CO ratio of 2 for bagasse gasification, given the other practical conditions of 1 bar pressure, 1100K and the optimum of 5% moisture. This was therefore also included as a second equilibrium gasifier option as discussed in Chapter 4.

Table B3.4 Fitted parameters from desirability profiling for system efficiency

	Temperature [K]	Pressure [bar]	Moisture content [w%]	SBR	ER	LHV [kJ/mol]	H ₂ /CO [mol]	SUM H ₂ +CO [mol]	SE	GE	Desirability
Bagasse	900.00	20.50	5.00	0.00	0.10				0.96		1.00
	900.00	20.50	5.00	0.00	0.10	326.38	0.20	0.55	0.96	0.78	0.49
Fast Pyrolysis slurry	900.00	30.25	38.75	0.00	0.10				0.75		1.00
	900.00	30.25	38.75	0.00	0.10	267.20	2.03	0.43	0.75	0.46	0.74
Vacuum Pyrolysis slurry	900.00	1.00	16.25	0.00	0.10				0.83		1.00
	900.00	1.00	16.25	0.00	0.10	308.85	0.02	0.76	0.83	0.62	0.35

Table B3.5 Fitted parameters from desirability profiling for H₂/CO ratio, Sum of H₂ and CO and system efficiency

	Temperature [K]	Pressure [bar]	Moisture content [w%]	SBR	ER	LHV [kJ/mol]	H ₂ /CO [mol]	SUM H ₂ +CO [mol]	SE	GE	Desirability
Bagasse	900.00	1.00	5.00	0.75	0.10		2.22	0.52	0.85		0.78
	900.00	1.00	5.00	0.75	0.10	247.76	2.22	0.52	0.85	0.64	0.72
Fast Pyrolysis slurry	900.00	1.00	16.25	0.75	0.10		1.89	0.57	0.74		0.83
	900.00	1.00	16.25	0.75	0.10	239.41	1.89	0.57	0.74	0.45	0.75
Vacuum Pyrolysis slurry	900.00	1.00	16.25	0.75	0.10		2.04	0.59	0.76		0.85
	900.00	1.00	16.25	0.75	0.10	235.67	2.04	0.59	0.76	0.50	0.77

Table B3.6 Model predictions for adjusted conditions for all feedstocks according to practical considerations

	Temperature [K]	Pressure [bar]	Moisture content [w%]	SBR	ER	LHV [kJ/mol]	H ₂ /CO [mol]	SUM H ₂ +CO [mol]	SE	GE	Desirability
Bagasse	1100.00	1.00	5.00	0.75	0.25	199.96	0.90	0.50	0.75	0.53	0.48
Fast Pyrolysis slurry	1100.00	1.00	16.25	0.75	0.25	188.93	0.93	0.56	0.63	0.36	0.55
Vacuum Pyrolysis slurry	1100.00	1.00	16.25	0.75	0.25	191.37	0.75	0.58	0.70	0.40	0.57

APPENDIX B4 ASPENPLUS® RESULTS FOR FISCHER-TROPSCH PROCESS MODELS

Table B4.1 Detailed unit design assumptions and performance results for Fischer-Tropsch process models.

		FT-bagasse (EG1)	FT-bagasse (EG1shift)	FT-bagasse (EG2)
Gasification				
Feed moisture content	wt%	0.05%	0.05%	0.05%
Steam feed rate	wt/wt dry bagasse feed	75.0%	75.0%	225.0%
Gasifier steam energy consumption	kW/kW bagasse feed HHV	14.6%	14.7%	43.4%
Oxygen feed rate	wt/wt dry bagasse feed	35.5%	35.5%	35.5%
H ₂ /CO molar ratio in syngas		0.90	0.90	1.99
Gas cleaning and conditioning				
Heat recovery from first syngas cooler	kW/kW bagasse feed HHV	10.7%	10.7%	20.3%
Heat recovery from second syngas cooler	kW/kW bagasse feed HHV	12.1%	12.1%	35.8%
Rectisol ¹				
Temperature	C	27.2	27.2	27.2
Pressure	bar	20.0	20.0	20.0
Recycle from autothermal reformer	wt/wt syngas feed to rectisol	36.9%	57.9%	3.4%
Carbon dioxide removed	wt% of total CO ₂ feed to rectisol	0.97	0.97	0.97
Syngas pre-heater				
Temperature	C	245.0	245.0	245.0
Pressure	bar	20.0	20.0	20.0
Shift reactor				
Split to shift reactor	wt/wt of cleaned syngas	-	25.0%	-
Shift reactor pressure	bar	-	2.0	-
H ₂ /CO ratio of inlet stream		-	1.2	-
H ₂ /CO ratio of outlet stream		-	2.6	-
Syngas compressor				
Pressure	bar	24.2	24.2	24.2
Polytropic efficiency		0.8	0.8	0.8
Mechanical efficiency		0.9	0.9	0.9

¹ For simplification, this unit was modelled as a separator block and the fractions reporting to product streams were based on the rectisol mass balance obtained from Kreutz et al, 2009.

Table B4.1 (continued) Detailed unit design assumptions and performance results for Fischer-Tropsch process models.

		FT-bagasse (EG1)	FT-bagasse (EG1shift)	FT-bagasse (EG2)
Fischer-Tropsch synthesis				
H ₂ /CO syngas ratio in reactor feed		0.99	1.98	1.97
Reactor pressure	bar	23.2	23.2	23.2
Reactor temperature	C	260.0	260.0	260.0
Fischer-Tropsch product cooler	C	40.0	40.0	40.0
Methane adjustment for refinery ²	split fraction removed	39.5%	29.2%	60.7%
Fischer-Tropsch liquid yields	wt/wt dry bagasse feed	15.2%	17.2%	17.0%
Fischer-Tropsch diesel	wt/wt dry bagasse feed	9.3%	10.5%	10.4%
Fischer-Tropsch petroleum	wt/wt dry bagasse feed	5.9%	6.7%	6.6%
Fischer-Tropsch liquids HHV	MJ/kg	47.5	47.5	47.5
Fischer-Tropsch liquids energy yield	kW/kW bagasse feed HHV	39.6%	44.8%	44.1%
Split fraction to recycle		60.0%	60.0%	60.0%
Recycle stream				
Autothermal reformer				
Steam feed to reformer	wt/wt recycle stream	0.63	0.63	0.63
Oxygen feed to reformer ³	wt/wt recycle stream	35.7%	17.3%	70.5%
Methane reformed	wt/wt methane in recycle stream	97.3%	92.4%	88.8%
Recycle stream cooler				
Temperature	C	40.0	40.0	40.0
Pressure	bar	2.0	2.0	2.0
Water knocked out	% of total water in recycle	100%	100%	100%

² Since the refinery was not modelled, a mass balance of the light gas components was performed using the data of Kreuz et al, 2008 and it was found that the light gas composition of the recycle stream was similar for all components except methane, which was therefore adjusted using a simulator block to a value of 7.7wt% to reflect a similar composition to that of the Kreuz model.

³ For the EG2 scenario, a significant amount of water in the recycle stream requires more oxygen to achieve the design outlet temperature of 1273K.

Table B4.1 (continued) Detailed unit design assumptions and performance results for Fischer-Tropsch process models.

		FT-bagasse (EG1)	FT-bagasse (EG1shift)	FT-bagasse (EG2)
Combustor				
Air pre-heater temperature	C	325.0	330.2	249.60
Syngas cooling energy split to pre-heater ⁴		45.0%	45.0%	15.0%
Combustor heat	kW/kW bagasse feed HHV	40.1%	38.5%	52.4%
Steam generator feed water ⁵	wt/wt dry bagasse feed	1.62	1.77	2.23
Boiler feed water ⁶	wt/wt dry bagasse feed	2.2	2.1	2.8
Multistage steam turbine				
Isentropic efficiency		0.85	0.85	0.85
Mechanical efficiency		0.98	0.98	0.98
Turbine 1				
Pressure	bar	23.6	23.6	23.6
Electricity generated	kW/kW bagasse feed HHV	6.0%	6.1%	6.3%
Turbine 2				
Pressure	bar	2.38	2.38	2.38
Electricity generated	kW/kW bagasse feed HHV	5.9%	5.9%	6.1%
Turbine 3				
Pressure	bar	0.046	0.046	0.046
Electricity generated	kW/kW bagasse feed HHV	6.9%	7.0%	7.1%
Total process electricity ⁷	kW/kW bagasse feed HHV	7.5%	14.8%	22.1%
Gasifier heating energy required	kW/kW bagasse feed HHV	0.0%	0.0%	14.7%
Total export electricity	kW/kW bagasse feed HHV	11.3%	4.1%	-2.6%

⁴ A portion of the syngas cooling energy is used for pre-heating of the combustion air to approximately 300°C; the remainder is assumed sufficient for drying of the bagasse prior to gasification. For the EG2 scenario, the syngas stream from gasification is much larger, due to the high amount of gasifier steam, therefore a smaller portion of the energy is required for air pre-heating.

⁵ The steam generator feed water flow rate is determined by using a calculator block in AspenPlus based on the design specification ⁶ Similar to the steam generator design specification, a calculator block is used to determine the boiler feed water flow rate that results in a boiler temperature of 800K (527°C) that sets the vapour outlet temperature equal to 500°C.

⁷ For the EG2 scenario, external heat is required to maintain the gasifier temperature due to the high amount of steam being fed to the gasifier. In the other cases, the gasifier is exothermic and heat is released, although the technical feasibility of capturing some of this heat is uncertain and is not considered in this study. For the shift reactor scenario, the larger recycle stream is the main contributor to the increase in process energy. The process energy breakdown is given in Table B4.2.

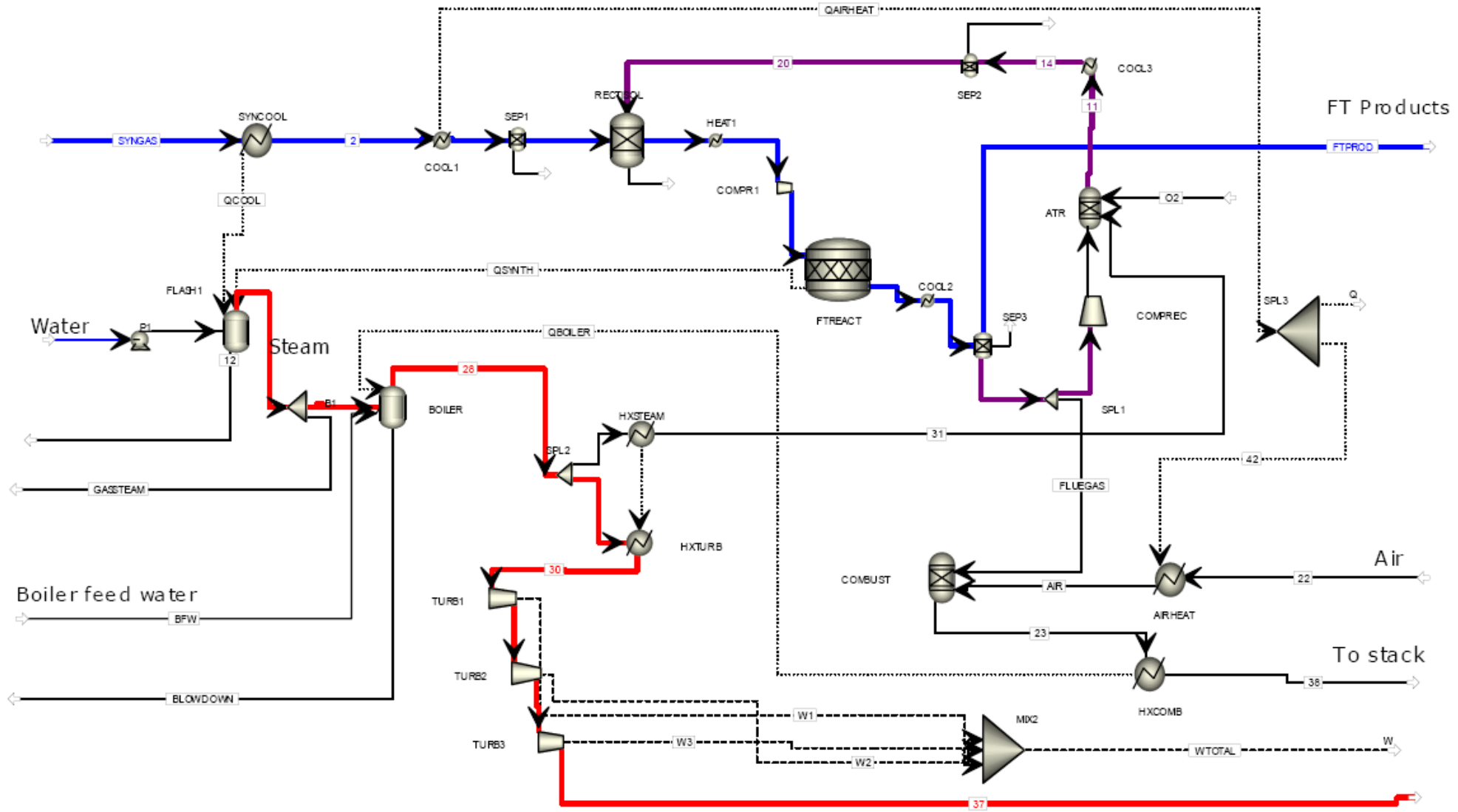
Table B4.2 Breakdown of process energy requirements for Fischer-Tropsch processes

	FT Bagasse (EG1)	FT Bagasse (EG1) with shift	FT Bag (EG2)	FT FPSlurry (EG1)	FT VPSlurry (EG1)
MW/MW bagasse input [HHV]					
Feed preparation	0.13%	0.13%	0.13%	0.12%	0.11%
Air separation unit	5.02%	5.19%	4.01%	4.83%	4.32%
Gasifier	14.59%	14.70%	43.40%	19%	21.95%
Gas conditioning	1.95%	1.99%	2.91%	1.65%	1.05%
Recycle	7.44%	15.44%	1.02%	6.39%	7.58%
Refinery	0.07%	0.07%	0.07%	0.07%	0.06%
Steam cycle	5.68%	5.68%	5.59%	4.43%	4.31%
	34.87%	43.19%	57.13%	36.40%	39.38%

APPENDIX B5 PROCESS FLOW DIAGRAMS FOR FISCHER-TROPSCH PROCESS MODELS

The process flow diagram and stream data for Fischer-Tropsch 145 MW scenario are given here. Only the most promising Fischer-Tropsch process models are given. Minor streams and duplicate streams were omitted to reduce the stream tables, but enough stream data is given to solve the complete mass balances.

Appendix B5.1 Process flow diagram and stream data for Fischer-Tropsch (EG1) bagasse 145 MW scenario.

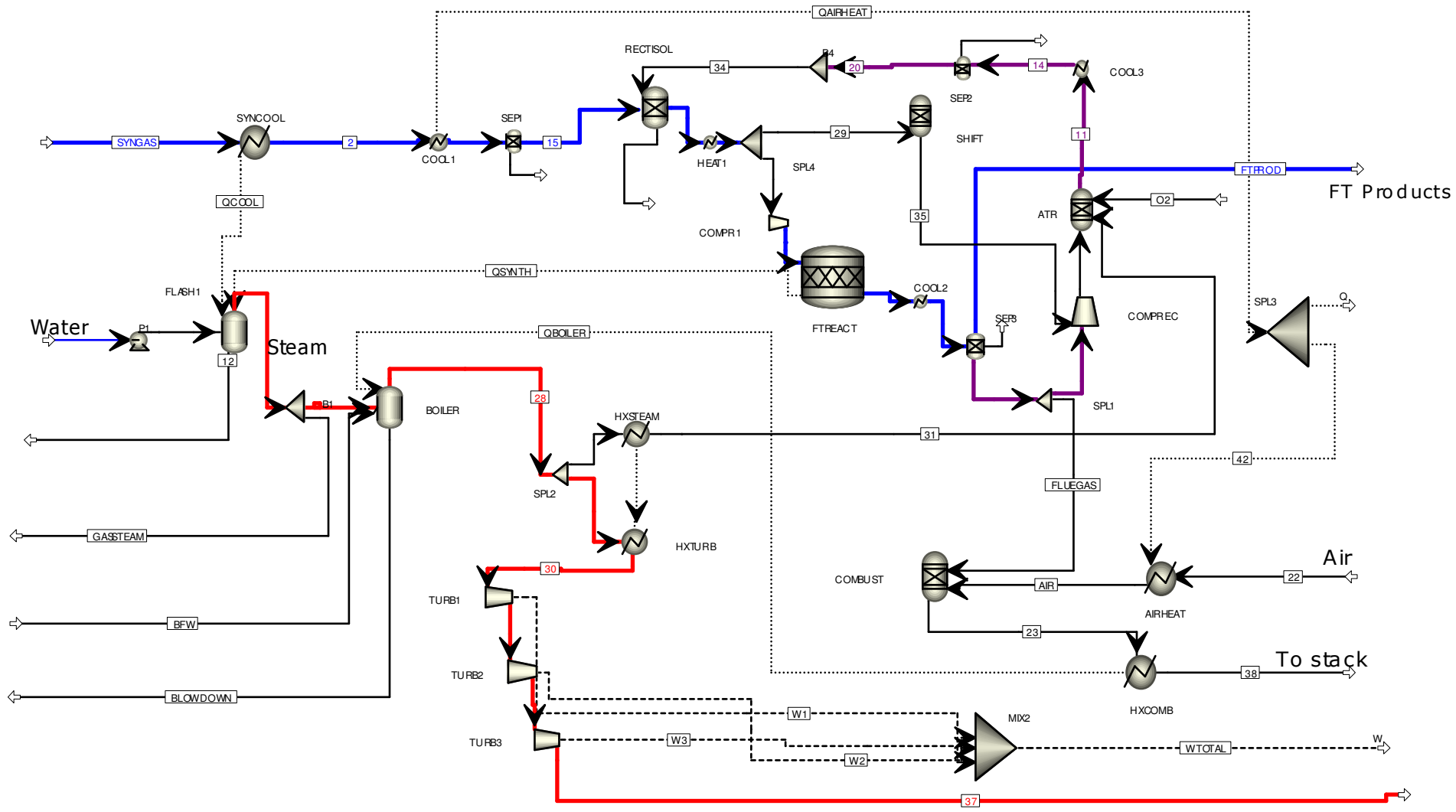


	32	42	43	QAIRHEAT	QBOILER	QCOOL	QSYNTH
QCALC cal/sec	-240002.6	7834015.5	9574907.9	17408923.4	57438528.7	15397400.5	27759717.4
TBEGIN K	781.4	623.2	623.2	623.2	2012.3	1100.0	552.2
TEND K	823.2	313.2	313.2	313.2	373.2	623.2	533.2

	W1	W2	W3	WTOTAL
POWER kW	-36221.8	-35145.4	-41378.3	-112745.5

	2	4	7	10	11	15	17	20	23	28	30	31	37	AIR	BFW	BLOWDOWN	FLUEGAS	FTPROD	GASSTEAM	O2	RAWPROD	RECYCLE	SYNGAS
Feed to block	COOL1	B1	HEAT1	FTREACT	COOL3	RECTISOL	SPL1	RECTISOL	HXCOMB	SPL2	TURB1	ATR		COMBUST	BOILER		COMBUST			ATR	COOL2	COMPREC	SYNCOOL
From block	SYNCOOL	FLASH1	RECTISOL	COMPR1	ATR	SEP1	SEP3	SEP2	COMBUST	BOILER	HXTURB	HXSTEAM	TURB3	AIRHEAT		BOILER	SPL1	SEP3	B1		FTREACT	SPL1	
Temperature K	623.2	783.0	300.4	552.2	1273.1	313.2	313.2	313.2	2012.3	800.0	776.1	823.2	304.6	598.1	298.0		313.2	313.2	783.0	458.2	533.2	313.2	1100.0
Pressure atm	1.0	1.0	19.7	24.1	19.4	2.0	19.7	2.0	1.2	37.5	120.4	37.5	0.0	1.0	1.0	37.5	19.7	19.7	1.0	29.0	22.9	19.7	1.0
Total Flow kg/hr	254800.0	191448.0	229928.0	229928.0	126657.0	254800.0	106068.0	94138.3	424008.0	357850.0	317563.0	40287.0	317563.0	381581.0	255100.0	0.0	42427.2	18014.6	88697.0	22729.8	229928.0	63640.9	254800.0
Mass Flow kg/hr																							
CO	90482.8	0.0	139378.0	139378.0	48895.5	90482.8	62310.7	48895.5	287.7	0.0	0.0	0.0	0.0	0.0	0.0	0.0	24924.3	0.0	0.0	0.0	62310.7	37386.4	90482.8
H2	5844.4	0.0	9977.6	9977.6	4133.2	5844.4	0.0	4133.2	2.8	0.0	0.0	0.0	0.0	0.0	0.0	0.0	0.0	0.0	0.0	0.0	0.0	0.0	5844.4
CO2	81715.9	0.0	3680.7	3680.7	40975.3	81715.9	15444.9	40975.3	78328.0	0.0	0.0	0.0	0.0	0.0	0.0	0.0	6177.9	0.0	0.0	0.0	15444.9	9266.9	81715.9
H2O	60603.5	191448.0	60603.5	60603.5	32518.5	60603.5	0.0	0.0	19621.7	357850.0	317563.0	40287.0	317563.0	0.0	255100.0	0.0	0.0	0.0	88697.0	0.0	100539.0	0.0	60603.5
CH4	16153.0	0.0	16287.3	16287.3	134.3	16153.0	8142.3	134.3	0.0	0.0	0.0	0.0	0.0	0.0	0.0	0.0	3256.9	0.0	0.0	0.0	13447.6	4885.4	16153.0
C4H8	0.0	0.0	0.0	0.0	0.0	0.0	1619.4	0.0	0.0	0.0	0.0	0.0	0.0	0.0	0.0	0.0	647.8	0.0	0.0	0.0	1619.4	971.6	0.0
C4H10	0.0	0.0	0.0	0.0	0.0	0.0	18550.9	0.0	0.0	0.0	0.0	0.0	0.0	0.0	0.0	0.0	7420.3	0.0	0.0	0.0	18550.9	11130.5	0.0
N2	0.0	0.0	0.0	0.0	0.0	0.0	0.0	0.0	301449.0	0.0	0.0	0.0	0.0	301449.0	0.0	0.0	0.0	0.0	0.0	0.0	0.0	0.0	0.0
O2	0.0	0.0	0.0	0.0	0.0	0.0	0.0	0.0	24319.1	0.0	0.0	0.0	0.0	80131.9	0.0	0.0	0.0	0.0	0.0	22729.8	0.0	0.0	0.0

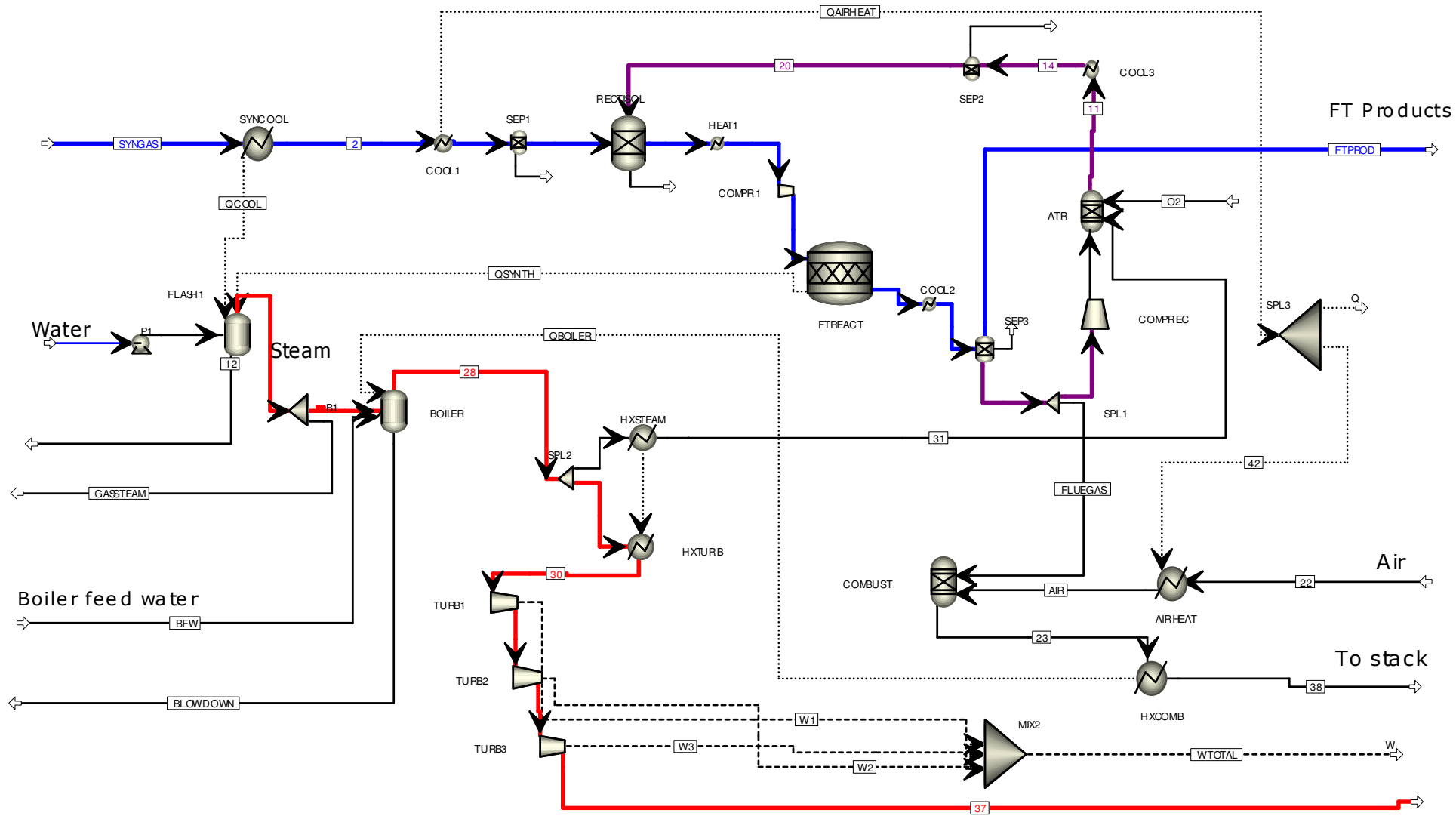
Appendix B5.2 Process flow diagram and stream data for Fischer-Tropsch (EG1) bagasse 145 MW scenario with shift.



	32	42	43	QAIRHEAT	QBOILER	QCOOL	QSYNTH
QCALC cal/sec	-270865.3	7833373.5	9574123.2	17407496.6	55180189.1	15396149.6	31902817.7
TBEGIN K	781.0	623.2	623.2	623.2	1991.9	1100.0	552.9
TEND K	823.2	313.2	313.2	313.2	373.2	623.2	533.2
	W1	W2	W3	WTOTAL			
POWER kW	-36521.1	-35448.9	-41758.0	-113728.0			

	2	4	7	10	11	15	17	20	23	28	30	31	35	37	38	AIR	BFW	FLUEGAS	FTP	GASSTEAM	O2	RAWPROD	RECYCLE	SYNGAS
Feed to block	COOL1	B1	HEAT1	FTREACT	COOL3	RECTISOL	SPL1	RECTISOL	HXCOMB	SPL2	TURB1	ATR	COMP		COMBUST	BOILER	COMBUST				ATR	COOL2	COMP	SYNCOOL
From block	SYNCOOL	FLASH1	RECTISOL	COMPR1	ATR	SEP1	SEP3	SEP2	COMBUST	BOILER	HXTURB	HXSTEAM	SHIFT	TURB3	BOILER	AIRHEAT		SPL1	SEP3	B1		FTREACT	SPL1	
Temperature K	623.1	782.9	300.4	552.9	1273.0	313.1	313.1	313.1	1991.9	799.6	775.0	823.1	759.4	304.6	373.1	603.3	298.0	313.1	313.1	782.9	458.1	533.1	313.1	1100.0
Pressure atm	1.0	1.0	19.7	24.1	19.4	2.0	19.7	2.0	1.2	37.5	120.4	37.5	2.0	0.0	1.0	1.0	1.0	19.7	19.7	1.0	29.0	22.9	19.7	1.0
Vapor Frac	1.0	1.0	0.8	1.0	1.0	0.8	1.0	1.0	1.0	1.0	1.0	1.0	1.0	0.8	1.0	1.0	0.0	1.0	0.0	1.0	1.0	1.0	1.0	1.0
Mass Flow kg/hr	254779.0	209824.9	276656.0	207492.0	195267.2	254779.0	92811.6	147484.9	412028.0	365645.4	320645.4	45000.0	69164.0	320645.4	412028.0	374903.3	245189.5	37124.7	20386.1	89369.0	25416.2	207492.0	55687.0	254779.0
Mass Flow kg/hr																								
CO	90475.5	0.0	179998.3	134998.7	89523.2	90475.5	46654.8	89523.2	217.6	0.0	0.0	0.0	25355.3	0.0	217.6	0.0	0.0	18661.9	0.0	0.0	0.0	46654.8	27992.9	90475.5
H2	5844.0	0.0	15380.4	11535.3	9536.4	5844.0	0.0	9536.4	2.4	0.0	0.0	0.0	4752.4	0.0	2.4	0.0	0.0	0.0	0.0	0.0	0.0	0.0	0.0	5844.0
CO2	81709.2	0.0	3884.8	2913.6	47783.1	81709.2	16226.3	47783.1	70999.1	0.0	0.0	0.0	28429.3	0.0	70999.1	0.0	0.0	6490.5	0.0	0.0	0.0	16226.3	9735.8	81709.2
H2O	60598.6	209824.9	60598.6	45449.0	47782.3	60598.6	0.0	0.0	20316.1	365645.4	320645.4	45000.0	5304.4	320645.4	20316.1	0.0	245189.5	0.0	0.0	89369.0	0.0	91369.5	0.0	60598.6
CH4	16151.7	0.0	16794.0	12595.5	642.3	16151.7	7105.0	642.3	0.0	0.0	0.0	0.0	4198.5	0.0	0.0	0.0	0.0	2842.0	0.0	0.0	0.0	10029.8	4263.0	16151.7
C4H8	0.0	0.0	0.0	0.0	0.0	0.0	1832.6	0.0	0.0	0.0	0.0	0.0	19.5	0.0	0.0	0.0	0.0	733.0	0.0	0.0	0.0	1832.6	1099.5	0.0
C4H10	0.0	0.0	0.0	0.0	0.0	0.0	20992.9	0.0	0.0	0.0	0.0	0.0	1104.6	0.0	0.0	0.0	0.0	8397.2	0.0	0.0	0.0	20992.9	12595.8	0.0
C9H20	0.0	0.0	0.0	0.0	0.0	0.0	0.0	0.0	0.0	0.0	0.0	0.0	0.0	0.0	0.0	0.0	0.0	0.0	7941.8	0.0	0.0	7941.8	0.0	0.0
C15H32	0.0	0.0	0.0	0.0	0.0	0.0	0.0	0.0	0.0	0.0	0.0	0.0	0.0	0.0	0.0	0.0	0.0	0.0	12444.3	0.0	0.0	12444.3	0.0	0.0
N2	0.0	0.0	0.0	0.0	0.0	0.0	0.0	0.0	296173.6	0.0	0.0	0.0	0.0	0.0	296173.6	296173.6	0.0	0.0	0.0	0.0	0.0	0.0	0.0	0.0
O2	0.0	0.0	0.0	0.0	0.0	0.0	0.0	0.0	24319.1	0.0	0.0	0.0	0.0	0.0	24319.1	78729.7	0.0	0.0	0.0	0.0	25416.2	0.0	0.0	0.0

Appendix B5.3 Process flow diagram and stream data for Fischer-Tropsch (EG2) bagasse 145 MW scenario.



	32	42	43	QAIRHEAT	QBOILER	QCOOL	QSYNTH
QCALC cal/sec	-33092.2	7706740.6	43671530.3	51378270.9	75001850.8	29078634.3	30408307.0
TBEGIN K	781.0	623.2	623.2	623.2	2008.7	1100.0	551.0
TEND K	823.2	313.2	313.2	313.2	373.2	623.2	533.2
	W1	W2	W3	WTOTAL			
POWER kW	-37572.1	-36404.6	-42768.9	-116745.6			

	2	4	7	10	11	15	17	20	23	28	30	31	37	AIR	BFW	BLOWDOWN	FLUEGAS	FTPROD	GASSTEAM	O2	RAWPROD	RECYCLE	SYNGAS	
Feed to block	COOL1	B1	HEAT1	FTREACT	COOL3	RECTISOL	SPL1	B4	HXCOMB	SPL2	TURB1	ATR		COMBUST	BOILER					ATR	COOL2	COMPREC	SYNCOOL	
From block	SYNCOOL	FLASH1	RECTISOL	COMPR1	ATR	SEP1	SEP3	SEP2	COMBUST	BOILER	HXTURB	HXSTEAM	TURB3	AIRHEAT		BOILER	SPL1	SEP3	B1		FTREACT	SPL1		
Temperature K	623.2	783.0	300.4	551.0	1273.0	313.2	313.2	313.2	2008.7	799.6	780.3	823.2	304.6	522.7	298.0			313.2	313.2	783.0	458.2	533.2	313.2	1100.0
Pressure atm	1.0	1.0	19.7	24.1	19.4	2.0	19.7	2.0	1.2	37.5	120.4	37.5	0.0	1.0	1.0	37.5	19.7	19.7	1.0	29.0	22.9	19.7	1.0	
Vapor Frac	1.0	1.0	0.4	1.0	1.0	0.5	0.9	1.0	1.0	1.0	1.0	1.0	0.8	1.0	0.0		0.9	0.0	1.0	1.0	1.0	0.9	1.0	
Total Flow kg/hr	432195.0	263885.0	336807.0	336807.0	20299.0	432195.0	43400.0	14701.8	539382.0	333059.0	327559.0	5500.0	327559.0	504662.0	333059.0	0.0	34720.0	20050.7	263885.0	6119.0	336807.0	8680.0	432195.0	
Mass Flow kg/hr																								
CO	75525.9	0.0	84370.8	84370.8	8844.8	75525.9	0.0	8844.8	305.2	0.0	0.0	0.0	0.0	0.0	0.0	0.0	0.0	0.0	0.0	0.0	0.0	0.0	75525.9	
H2	10818.4	0.0	11953.0	11953.0	1134.6	10818.4	1151.5	1134.6	6.5	0.0	0.0	0.0	0.0	0.0	0.0	0.0	921.2	0.0	0.0	0.0	1151.5	230.3	10818.4	
CO2	108847.0	0.0	3404.9	3404.9	4648.3	108847.0	16498.6	4648.3	74513.9	0.0	0.0	0.0	0.0	0.0	0.0	0.0	13198.9	0.0	0.0	0.0	16498.6	3299.7	108847.0	
H2O	224705.0	263885.0	224705.0	224705.0	5597.2	224705.0	0.0	0.0	41554.0	333059.0	327559.0	5500.0	327559.0	0.0	333059.0	0.0	0.0	0.0	263885.0	0.0	268249.0	0.0	224705.0	
CH4	12299.3	0.0	12373.3	12373.3	74.0	12299.3	3299.9	74.0	0.0	0.0	0.0	0.0	0.0	0.0	0.0	0.0	2640.0	0.0	0.0	0.0	8406.8	660.0	12299.3	
C4H8	0.0	0.0	0.0	0.0	0.0	0.0	1802.4	0.0	0.0	0.0	0.0	0.0	0.0	0.0	0.0	0.0	1441.9	0.0	0.0	0.0	1802.4	360.5	0.0	
C4H10	0.0	0.0	0.0	0.0	0.0	0.0	20647.5	0.0	0.0	0.0	0.0	0.0	0.0	0.0	0.0	0.0	16518.0	0.0	0.0	0.0	20647.5	4129.5	0.0	
C9H20	0.0	0.0	0.0	0.0	0.0	0.0	0.0	0.0	0.0	0.0	0.0	0.0	0.0	0.0	0.0	0.0	0.0	7811.1	0.0	0.0	7811.1	0.0	0.0	
C15H32	0.0	0.0	0.0	0.0	0.0	0.0	0.0	0.0	0.0	0.0	0.0	0.0	0.0	0.0	0.0	0.0	0.0	12239.5	0.0	0.0	12239.5	0.0	0.0	
N2	0.0	0.0	0.0	0.0	0.0	0.0	0.0	0.0	398683.0	0.0	0.0	0.0	0.0	398683.0	0.0	0.0	0.0	0.0	0.0	0.0	0.0	0.0	0.0	
O2	0.0	0.0	0.0	0.0	0.0	0.0	0.0	0.0	24319.3	0.0	0.0	0.0	0.0	105979.0	0.0	0.0	0.0	0.0	0.0	6119.0	0.0	0.0	0.0	

APPENDIX C1 GENERAL INPUT DATA FOR ECONOMIC MODELS

Table C1.1 General specifications used for economic models in AspenIcarus®

	Item	Data affected
Process description	Redesigned process	Equipment design allowance: 7%
Process complexity	Typical	
Process control	Digital	
Project Information		
Project location	Africa	Freight (% of material): 4% (domestic) and 8% (ocean) Taxes/Duty (% of material): 4% Equipment rotating spares: 15%
Project type	Grass Roots/Clear field	Power distribution: MAIN substation (Transformers, switchgears) UNIT (MCC, SW Transformer) Operator centre and control centre included
Contingency percent	18	Value provided by local industry
Estimated start date of basic engineering	01-Jan-10	
Soil condition around site	Gravel	Pile type: Steel h-pile - 60-170 tons
Equipment Specification		
Pressure vessel design code	ASME	
Vessel diameter specification	ID	
P and I design level	FULL	

Table C1.2 Main Investment Analysis parameters for economic models

Number of years for analysis	20	
Dividend payout	25	% of net profit
Tax rate	30.5	%/year
Debt/equity ratio	70/30	
Interest rate/desired rate of return	15.1	%/year
Economic life of project	25	
Salvage value	20	% of initial Capital Cost
Depreciation method	Straight line	
Escalation parameters		
Project Capital escalation	8	%/year
Products escalation	8	%/year
Raw materials escalation	8	%/year
Operating and maintenance labour escalation	8	%/year
Utilities escalation	8	%/year
Project Capital parameters		
Working Capital	5	%/year
Operating cost parameters		
Operating supplies	Variable	\$/year
Laboratory charges	70000	\$/year
Operating charges	25	%/year
Plant overhead	50	%/year
G and A expenses	8	%/year
Facility Operation parameters		
Facility type	Petrochemical processing facility	
Operating mode	Continuous processing -24 h	
Length of start-up period	20	weeks
Operating hours per year	8000	H

The tax rate is based on 28% company tax payable on net profit and an additional 10% for dividend payouts. The debt/equity ratio was based on data obtained from the local petrochemical industry. The interest rate/desired rate of return is the weighted average between the assumed interest rate on debt financing (prime+2%) and the desired rate of return for shareholders of 20%, which were also based on parameters used by the petrochemical industry. The escalation factors and laboratory charges are typical values

used by the South African sugar industry. The defaults of AspenIcarus® were used for operating charges, plant overheads and G and A expenses.

Table C1.3 Basis for bagasse availability and delivery cost calculations.

Bagasse supply		
Bagasse surplus	42	%
Trash availability	100	%
Sugarcane yield	65	tons/ha
Wet bagasse and trash yield per tons crushed cane	0.25	
Crushing period per year	38	Weeks
Wet bagasse and trash required for 600 MW plant	1.45	Mt/y
Average distance travelled for 600 MW plant	92.6	km
Energy cost of delivery for 600 MW plant		
Energy consumption per truck	10.5	MJ/km
Bagasse density	176	Kg/m ³
Trailer volume	31	M ³
Limiting weight load of trailer	25	tons
Bagasse load per truck	5.46	T
Bagasse LHV (dry)	18.3	MJ/kg
Energy cost of bagasse delivery	0.18	MJ/kg
Energy cost of slurry delivery	0.04	MJ/kg
Transport cost of delivery for 600 MW plant		
Truck fuel consumption	30	ℓ/100 km
Fuel price	1.07	\$/ℓ
Bagasse base cost price	62.4	\$/t
Trash base cost price	31.2	\$/t
Bagasse and trash on-site base cost price (50% mix)	46.8	\$/t
Transport cost of bagasse delivery	5.40	\$/t
Transport cost of slurry delivery	1.20	\$/t
Delivered base cost price of bagasse for 600 MW plant	52.2	\$/t
Delivered base cost price of slurry for 600 MW plant	48.0	\$/t

APPENDIX C2 PROCESS EQUIPMENT COST DATA

The process equipment that was mapped in AspenIcarus® and the mapping specifications used are given in Table C2.1 and C2.4, along with the base cost data and sources used for quoted equipment. Table C2.2 and C2.5 provides cost data used for process equipment or sections that were specified in the equipment model libraries based on installed costs. Any data of current capacities and installed equipment costs shown apply to the 145 MW scenarios. For the bioethanol process equipment, values are given for the dilute acid pretreatment at 35% scenario, but the same data and factors were applied for the other scenarios. Data for both pyrolysis processes are given in Table C2.3. For the Fischer-Tropsch processes, the installation factors for the autothermal reformer and rectisol unit were taken from literature values, since those assumed by AspenIcarus® were close to 1. The 2006 installed costs are shown for the 145 MW Fischer-Tropsch (G1) scenario for bagasse, and costs for the other scenarios are calculated from the same data.

Table C2.1 Equipment mapping specification and quoted cost data for bioethanol scenarios

	Process model ID	Number of units	Icarus process equipment mapping specification	Material of construction	Base equipment cost source	Base capacity	Capacity unit	Base year	Equipment cost in base year	CEPCI in base year	Scale factor
Pretreatment											
Flash vessel	F101	1	VERTICAL TANK - Flash	SS316	ICARUS						
Prehydrolysate mixing tank	M102	1	AGITATED TANK OPEN TOP	SS304	ICARUS						
Sulfuric acid storage tank	T101	1	PLASTIC STORAGE TANK	Plastic	ICARUS						
Sulfuric acid tank mixer	SULF MIXER	1	STATIC MIXER	304P	ICARUS						
Process pump	P101	1	CENTRIFUGAL PUMP	SS316	ICARUS						
Process pump	P102	1	CENTRIFUGAL PUMP	SS316	ICARUS						
Process pump	P103	1	CENTRIFUGAL PUMP	SS316	ICARUS						
Seed fermentation											
1st Seed fermentor	R201a	2	AGITATED TANK, ENCLOSED, JACKETED	SS304	ICARUS						
Seed feed pump	P202	2	ROTARY LOBE PUMP	SS304	ICARUS						
Seed hold discharge pump	P201	2	ROTARY LOBE PUMP	SS304	ICARUS						
2nd Seed fermentor	R201b	2	AGITATED TANK, ENCLOSED, JACKETED	SS304	ICARUS						
3rd Seed fermentor	R201c	2	AGITATED TANK, ENCLOSED, JACKETED	SS304	ICARUS						
4th Seed fermentor	R201d	2	FLAT BOTTOMED STORAGE TANK	SS304	ICARUS						
4th Seed fermentor cooling coil	R201d-coil	2	BARE PIPE IMMERSION COIL	SS304	ICARUS						
4th Seed fermentor agitator	R201d-agitator	2	SANITARY FIXED PROPELLER	SS	ICARUS						
5th seed fermentor	R201e	2	FLAT BOTTOMED STORAGE TANK	SS304	[1]	727.0	m ³	2000	\$ 148,280	392.0	0.51
5th seed fermentor agitator	R201e-agitator	2	SANITARY FIXED PROPELLER	SS	[1]	727.0	m ³	2000	\$ 10,625	392.0	0.51
5th Seed fermentor cooling coil	R201e-coil	2	BARE PIPE IMMERSION COIL	SS304	ICARUS						
Seed hold tank	T201	1	FLAT BOTTOMED STORAGE TANK	SS304	[1]	872.4	m ³	2000	\$ 162,728	392.0	0.51
Seed hold tank agitator	T201-agitator	1	SANITARY FIXED PROPELLER	SS	[1]	872.4	m ³	2000	\$ 12,898	392.0	0.51
Saccharification and fermentation											
Hydrolysate pump	P301	2	CENTRIFUGAL PUMP	SS304	ICARUS						
Saccharification tank	R301	5	FLAT BOTTOMED STORAGE TANK	SS304	[1]	3596.0	m ³	2000	\$ 499,218	392.0	0.51
Saccharification tank agitator	R301-agitator	5	SANITARY FIXED PROPELLER	SS	[1]	3596.0	m ³	2000	\$ 40,630	392.0	0.51
Saccharification tank cooler	R301-cooler	5	PLATE AND FRAME HEAT EXCHANGER	SS304	ICARUS						
Fermentation tank	R302	5	FLAT BOTTOMED STORAGE TANK	SS304	[1]	3596.0	m ³	2000	\$ 499,218	392.0	0.51
Fermentation tank agitator	R302-agitator	5	SANITARY FIXED PROPELLER	SS	[1]	3596.0	m ³	2000	\$ 40,630	392.0	0.51
Fermentation tank cooler	R302-cooler	5	PLATE AND FRAME HEAT EXCHANGER	SS304	ICARUS						
Beer storage tank	T301	1	FLAT BOTTOMED STORAGE TANK	SS304	ICARUS						
Beer tank agitator	T301-agitator	1	FIXED PROPELLER	SS	ICARUS						

Table C2.1 (continued)

	Process model ID	Number of units	Icarus process equipment mapping specification	Material of construction	Base equipment cost source	Base capacity	Capacity unit	Base year	Equipment cost in base year	CEPCI in base year	Scale factor
Product recovery											
1st CO ₂ Flash vessel	F401	1	FLAT BOTTOMED STORAGE TANK	A515	ICARUS						
2nd CO ₂ Flash vessel	F402	1	FLAT BOTTOMED STORAGE TANK	A515	ICARUS						
Heat exchanger	HX401	1	FIXED TUBE SHEET SHELL AND TUBE EXCHANGER	DEFAULT	ICARUS						
Heat recovery exchanger	HX402	1	FIXED TUBE SHEET SHELL AND TUBE EXCHANGER	DEFAULT	ICARUS						
Heat recovery exchanger	HX403	1	FIXED TUBE SHEET SHELL AND TUBE EXCHANGER	DEFAULT	ICARUS						
Process pump	P401	2	CENTRIFUGAL PUMP	CS	ICARUS						
Water scrubber	Scrubber	1	PACKED TOWER	DEFAULT	[1]	25325.0	kg/h total feed	2000	\$ 127,848	392.0	0.78
Ethanol storage tank	T401	1	FLAT BOTTOMED STORAGE TANK	DEFAULT	ICARUS						
Stillage storage tank	T402	1	FLAT BOTTOMED STORAGE TANK	DEFAULT	ICARUS						
Stillage treatment											
Pre-evaporation flash	F501	1	FLAT BOTTOMED STORAGE TANK	DEFAULT	ICARUS						
1st effect condenser	HX501	1	FIXED TUBE SHEET SHELL AND TUBE EXCHANGER	DEFAULT	ICARUS						
2nd effect condenser	HX504	1	PRE-ENGINEERED U-TUBE EXCHANGER	DEFAULT	ICARUS						
Heat recovery exchanger	HX506	1	FIXED TUBE SHEET SHELL AND TUBE EXCHANGER	DEFAULT	ICARUS						
Heat recovery exchanger	HX507	1	PRE-ENGINEERED U-TUBE EXCHANGER	DEFAULT	ICARUS						
Heat recovery											
Baghouse	BAGH601	1	BAGHOUSE WITH MOTOR SHAKERS	CS	ICARUS						
Heat recovery exchanger	HX602	1	FLOATING HEAD SHELL AND TUBE EXCHANGER	DEFAULT	ICARUS						
Heat recovery exchanger	HX606	1	FLOATING HEAD SHELL AND TUBE EXCHANGER	DEFAULT	ICARUS						
Water plant											
Recycle water pump	P701	2	CENTRIFUGAL PUMP	DEFAULT	ICARUS						
Recycle water hold tank	M701	1	FLAT BOTTOMED STORAGE TANK	DEFAULT	ICARUS						
Steam turbine cycle											
Heat recovery exchanger	BL800.H804	1	FIXED TUBE SHEET SHELL AND TUBE EXCHANGER	DEFAULT	ICARUS						
Heat recovery exchanger	BL800.HX801	1	FIXED TUBE SHEET SHELL AND TUBE EXCHANGER	DEFAULT	ICARUS						
Turbine condensate pump	BL800.P801	2	CENTRIFUGAL PUMP	DEFAULT	ICARUS						
Steam turbine 1	BL800.CEST1	1	ELECTRICITY GENERATOR- STEAM DRIVE	DEFAULT	ICARUS						
Steam turbine 2	BL800.CEST2	1	ELECTRICITY GENERATOR- STEAM DRIVE	DEFAULT	ICARUS						
Steam turbine 3	BL800.CEST3	1	ELECTRICITY GENERATOR- STEAM DRIVE	DEFAULT	ICARUS						
Steam turbine 4	BL800.CEST4	1	ELECTRICITY GENERATOR- STEAM DRIVE	DEFAULT	ICARUS						

^[1] Aden and Ruth et al, 2003.

Table C2.2 Equipment model library cost data for bioethanol scenarios

	Base capacity	Capacity unit	Base year	Equipment cost in base year	CEPCI in base year	Scale factor	Current scale value	Scaled equipment cost in base year	Equipment cost in 2006	Installation factor	Installed cost in 2006	Source ^a
Pretreatment											\$ 10,464,268	
Mill ^b	50.00	ton/h wet biomass	2003	\$ 370,000	402.0	0.70	52.80	\$ 384,385	\$ 477,613	1.00	\$ 477,613	[1]
Mechanical	83.30	ton/h wet biomass	2003	\$ 3,872,000	402.0	0.67	52.80	\$ 2,852,778	\$ 3,544,683	2.00	\$ 7,089,365	[1]
Steam explosion	83.30	ton/h wet biomass	2003	\$ 1,410,000	402.0	0.78	52.80	\$ 988,031	\$ 1,227,665	2.36	\$ 2,897,290	[1]
Dilute acid	83.30	ton/h wet biomass	2003	\$ 14,100,000	402.0	0.78	52.80	\$ 9,880,308	\$ 12,276,651	2.36	\$ 28,972,896	[1]
Product recovery^c												
Beer distillation column	18.47	t/h ethanol	2003	\$ 2,960,000	402.0	0.70	5.28	\$ 1,231,831	\$ 1,530,596	2.75	\$ 4,209,138	[1]
Rectification column	9.23	t/h ethanol	2003	\$ 1,350,000	402.0	0.70	5.28	\$ 913,017	\$ 1,134,457	2.75	\$ 3,119,758	[1]
Molecular sieve	18.47	t/h ethanol	2003	\$ 2,920,000	402.0	0.70	5.28	\$ 1,215,184	\$ 1,509,912	1.00	\$ 1,509,912	[1]
Stillage treatment^c												
Pneumapress	22.47	t/h solids	2000	\$ 1,285,736	392.0	0.60	10.89	\$ 832,456	\$ 1,060,744	1.04	\$ 1,103,174	[2]
First effect evaporator ^d	1217.58	m ² heat exchange area	2000	\$ 537,020	392.0	0.51	326.00	\$ 274,238	\$ 349,444	2.10	\$ 733,832	[2]
Second effect evaporator	1217.47	m ² heat exchange area	2000	\$ 644,386	392.0	0.51	197.00	\$ 254,531	\$ 324,332	2.10	\$ 681,097	[2]
Third effect evaporator	1217.47	m ² heat exchange area	2000	\$ 644,386	392.0	0.51	373.00	\$ 352,480	\$ 449,142	2.10	\$ 943,197	[2]
Heat recovery												
Boiler ^e	235.00	t/h steam	2003	\$ 27,100,000	402.0	0.73	67.24	\$ 10,870,535	\$ 13,507,045	2.20	\$ 29,715,499	[1]

^a Sources: [1] Hamelinck et al, 2003. Euro/US dollar exchange rate (2003) = 1. [2] Aden et al, 2002

^b Milling is only required for dilute acid pretreatment

^c Specific values are given for the dilute acid pretreatment model at 35% solids, the same base cost data are used to calculate the scaled equipment costs for all the other models

^d The heat exchange surface areas for evaporators are obtained from the sizing expert in AspenIcarus®.

^e Boiler costs include combustion chamber, feeders, boiler feed water preheater, steam drums and superheater. The baghouse and steam turbines are costed separately.

Table C.2.3 Process equipment specifications and equipment model library cost data for pyrolysis processes

	Process model ID	Number of units	Icarus process equipment mapping specification	Base equipment cost source	Base/ Current capacity	Base year	Installed equipment cost in base year	CEPCI in base year	Installed equipment cost in 2006
EQUIPMENT MODEL LIBRARY ^a									
Feed preparation				[1]	1	2003	\$ 5,570,000	402	\$ 6,920,933
Pyrolysis				[1]	1	2003	\$ 3,920,000	402	\$ 4,870,746
ICARUS PROCESS EQUIPMENT									
Pyrolysis									
Vacuum pump ^b	P-2001	2	ONE STAGE EJECTOR NON-CONDENSING	ICARUS					
Condensation									
Dryer air compressor	CP-3001	1	CENTRIFUGAL COMPRESSOR	ICARUS					
Wet electrostatic precipitator	ES-3001	1	LOW VOLTAGE ELECTROSTATIC PRECIPITATOR	ICARUS					
1 st biocrude condenser	HX-3001+	1	PRE-ENGINEERED U TUBE EXCHANGER	ICARUS					
2 nd biocrude condenser	HX-3002+	1	PRE-ENGINEERED U TUBE EXCHANGER	ICARUS					
Aerosol scrubber	SC-3001	1	OIL-WATER SEPARATOR	ICARUS					
Heat recovery									
Combustor	CB-4001	1	BOX TYPE PROCESS FURNACE	ICARUS					
Combustor air compressor	CP-4001	1	CENTRIFUGAL COMPRESSOR	ICARUS					
Combustor cyclone	CY-4001	1	CYCLONE DUST COLLECTOR	ICARUS					
Combustion gas cooler	HX-4001+	1	PRE-ENGINEERED U TUBE EXCHANGER	ICARUS					
1 st Heat recovery condenser	HX-4002+	1	PRE-ENGINEERED U TUBE EXCHANGER	ICARUS					
2 nd Heat recovery condenser	HX-4003+	1	PRE-ENGINEERED U TUBE EXCHANGER	ICARUS					
3 rd Heat recovery condenser	HX-4004+	1	PRE-ENGINEERED U TUBE EXCHANGER	ICARUS					
Product recovery									
Product cooler	HX-5001+	1	PRE-ENGINEERED U TUBE EXCHANGER	ICARUS					
Product pump	P-5001	2	CENTRIFUGAL PUMP	ICARUS					
Product mixing tank	T-5001	1	FLAT BOTTOMED STORAGE TANK	ICARUS					
Recycle									
Recycle stream flash	FL-6001-flash vessel	1	VERTICAL TANK - Flash	ICARUS					
Recycle stream condenser	HX-6001	1	PRE-ENGINEERED U TUBE EXCHANGER	ICARUS					
Recycle gas heater	HX-6002+	1	PRE-ENGINEERED U TUBE EXCHANGER	ICARUS					
Steam turbine cycle									
Turbine outlet condenser	CD-7001	1	PRE-ENGINEERED U TUBE EXCHANGER	ICARUS					
Turbine outlet pump	P-7001	2	CENTRIFUGAL PUMP	ICARUS					
Steam turbine	TB7001	1	ELECTRICITY GENERATOR- STEAM DRIVE	ICARUS					
Product storage tank	T7001	1	FLAT BOTTOMED STORAGE TANK	ICARUS					
Product transfer pump	P7001	2	CENTRIFUGAL PUMP	ICARUS					

^a Costs for these non-standard items were available for whole sections only, therefore the total installed costs were specified in the equipment model library.

^b Capital costs for vacuum pyrolysis are assumed to be 17.6% higher than for fast pyrolysis, and will require an additional vacuum pump. The cost ratio was derived from the difference between an atmospheric and vacuum process vessel costed by AspenIcarus[®], since no cost data for vacuum pyrolysis was available.

Table C2.4 Equipment mapping specifications and quoted cost data for Fischer-Tropsch scenarios

	Process model ID	Number of units	Icarus process equipment mapping specification	Base capacity	Capacity unit	Base year	Equipment cost in base year	CEPCI in base year	Scale factor
Gas cleaning and conditioning									
Raw syngas cooling -1 st stage	SYNCOOL	1	PRE-ENGINEERED U TUBE EXCHANGER						
Raw syngas cooling -2 nd stage	COOL1	1	PRE-ENGINEERED U TUBE EXCHANGER						
Rectisol acid gas removal ^a	RECTISOL	1	FLAT BOTTOMED STORAGE TANK	200000	m ³ /h syngas	2007	\$ 28,800,000	525.4	0.63
Fischer-Tropsch feed pre-heater	HEAT1	1	PRE-ENGINEERED U TUBE EXCHANGER						
Fischer-Tropsch feed compressor	COMPR1	1	CENTRIFUGAL COMPRESSOR						
Fischer-Tropsch synthesis									
Fischer-Tropsch reactor ^b	FTREACT	1	AGITATED TANK, ENCLOSED, JACKETED	131	MW _{FT}	2002	\$ 13,376,000	395.6	0.72
Fischer-Tropsch product cooler	COOL2	1	PRE-ENGINEERED U TUBE EXCHANGER						
Recycle									
Recycle compressor	COMPREC	1	CENTRIFUGAL COMPRESSOR						
Autothermal reformer ^c	ATR	1	AGITATED TANK, ENCLOSED, JACKETED	100	m ³ /s feed	2002	\$ 27,368,000	395.6	0.60
Recycle cooler	COOL3	1	PRE-ENGINEERED U TUBE EXCHANGER						
Boiler and steam cycle									
Boiler feed water pump	P1	2	STANDARD ANSI SINGLE STAGE PUMP						
Waste heat flash drum	FLASH1-flash vessel	1	FLAT BOTTOMED STORAGE TANK						
Boiler air preheater	AIRHEAT	1	PRE-ENGINEERED U TUBE EXCHANGER						
Steam boiler unit	BOILER	1	PACKAGED BOILER UNIT						
Reformer steam cooler	HXSTEAM	1	PRE-ENGINEERED U TUBE EXCHANGER						
Turbine feed heater	HXTURB	1	PRE-ENGINEERED U TUBE EXCHANGER						
Steam turbine 1	TURB1	1	ELECTRICITY GENERATOR-STEAM DRIVE						
Steam turbine 2	TURB2	1	ELECTRICITY GENERATOR-STEAM DRIVE						
Steam turbine 3	TURB3	1	ELECTRICITY GENERATOR-STEAM DRIVE						

^a Cost data taken from Kreutz and Larson et al, 2007. The equipment cost is adjusted by 32% to account for the installation costs not taken into account by AspenIcarus[®].

^b Based on the data from Bechtel used by Hamelinck and Faaij et al, 2002, for a 362 m³ reactor operated at 25.2 bar. Installation costs were included in the data.

^c Hamelinck and Faaij et al, 2002, assessed different cost sources and used an average value due to the wide range in literature. Their data is used here and an installation factor of 2.3 is used.

Table C2.5 Equipment model library cost data for Fischer-Tropsch scenarios

	Base capacity	Capacity unit	Base year	Equipment cost in base year	CEPCI in base year	Scale factor	Current scale	Scaled equipment cost in base year	Equipment cost in 2006	Installation factor	Installed cost in 2006
Feed preparation ^a											
Storage	33.5	t/h wet biomass	2002	\$ 1,020,800	395.6	0.65	29.90	\$ 948,086	\$ 1,197,091	2	\$ 2,394,181
Dryer	33.5	t/h wet biomass	2002	\$ 7,480,000	395.6	0.80	29.90	\$ 6,829,717	\$ 8,623,467	2	\$ 17,246,934
Grinding	33.5	t/h wet biomass	2002	\$ 422,400	395.6	0.60	29.90	\$ 394,548	\$ 498,172	2	\$ 996,343
Conveyers	33.5	t/h wet biomass	2002	\$ 360,800	395.6	0.80	29.90	\$ 329,433	\$ 415,955	2	\$ 831,911
Feeding system	33.5	t/h wet biomass	2002	\$ 422,400	395.6	1.00	29.90	\$ 377,008	\$ 476,025	2	\$ 952,049
Air separation unit ^b	576.0	t/day 99.5% oxygen	2002	\$ 24,552,000	395.6	0.75	225.61	\$ 12,155,825	\$ 15,348,419	1.30	\$ 19,952,945
Gasification ^c											
TPS gasifier	69.54	MW HHV input	1999	\$ 3,240,000	390.6	0.70	145.00	\$ 5,419,239	\$ 6,930,133	1.33	\$ 9,217,077
Gas cleaning											
Cyclones	69.54	MW LHV input	1999	\$ 2,570,000	390.6	0.70	145.00	\$ 4,298,594	\$ 5,497,050	1.33	\$ 7,311,077
Baghouse filter	69.54	MW LHV input	1999	\$ 1,620,000	390.6	0.65	145.00	\$ 2,611,871	\$ 3,340,065	1.33	\$ 4,442,287
Gas cooling	69.54	MW LHV input	1999	\$ 2,950,000	390.6	0.70	145.00	\$ 4,934,184	\$ 6,309,844	1.33	\$ 8,392,092
Condensing scrubber	69.54	MW LHV input	1999	\$ 2,570,000	390.6	0.70	145.00	\$ 4,298,594	\$ 5,497,050	1.33	\$ 7,311,077
Water gas shift reactor ^d	8819.00	kmol CO+H ₂ /h	2002	\$ 10,736,000	395.6	0.65	2782.00	\$ 5,071,683	\$ 6,403,704	1.81	\$ 11,590,705
Refinery ^e	286.00	m ³ _{FI} /h	2002	\$ 205,040,000	395.6	0.70	6.28	\$ 14,151,077	\$ 17,867,702	1.00	\$ 17,867,702

^a Costs for feed preparation are taken from Hamelinck and Faaij et al, 2002, which is based on first plant technology (Euro/US dollar exchange rate in 2002 = 0.88). They include costs for iron removal from willow wood, which is not included in this analysis since bagasse is a pre-treated feedstock. The costs assumed by Kreutz and Larson et al, 2007, are much lower but assume nth plant technology, and do not include drying.

^b As stated by Hamelinck and Faaij et al, 2002, costs quoted in literature range significantly. They based theirs on that given by Tijmensen et al, 2002, since it was closely related to the real cost price of oxygen.

^c Since an atmospheric gasifier is used in the simulations, cost data was based on the direct, air-blown, atmospheric TPS gasifier which includes a tar cracker [Tijmensen et al, 2002]. Cost data given by Kreutz and Larson et al, 2007 and Hamelinck and Faaij et al, 2002 was not used since it was based on pressurised gasifier, which are a lot more costly. For consistency, the same source was used to estimate the gas cleaning costs.

^d Large discrepancies between different sources were observed. Scaling and inflating the cost data given in literature, the costs for the current simulation that included a shift ranged from 0.72 MUS [Tijmensen et al, 2002] and 3.99 MUS [Kreutz and Larson et al, 2007] to 11.59 MUS [Hamelinck and Faaij et al, 2002]. Since the data given by Hamelinck and Faaij et al, 2002 was corroborated with two sources and represents the conservative value it is used here.

^e Both Kreutz and Larson et al, 2007 and Hamelinck and Faaij et al, 2002 used data obtained from Bechtel. The cost data was grouped for the entire section by Hamelinck and Faaij et al, 2002 and is used here since the section is not modelled in detail in the simulations.

APPENDIX C3 ECONOMIC RESULTS SUMMARY

Table C3.1 Summary of economic results for selected scenarios of bioethanol, pyrolysis and Fischer-Tropsch process routes.

Scenario	Units	ETOH-dil acid (35)	ETOH-dil acid (35)	ETOH-steam expl	ETOH-steam expl	PYR-fast	PYR-fast	PYR-vacuum	PYR-vacuum	FT-bag (EG1)	FT-bag (EG1shift)	FT-bag (EG2)
Model ID		E1-145	E1-600	E2-145	E2-600	P1-145	P1-600	P2-145	P2-600	F1-600	F1shift-600	F2-600
Energy in biomass feed	MW HHV	145	600	145	600	145	600	145	600	600	600	600
Energy in products												
Liquid fuels	MW HHV	44.2	182.9	44.3	183.1	87.3	361.3	58.8	243.4	237.68	268.98	264.60
Electricity	MWe	13.7	56.6	16.5	68.3	0.0	0.0	1.2	4.9	67.83	24.73	-15.59
Char byproduct	MW HHV					13.7	56.7	40.1	165.8			
Conversion of feed energy to energy in products												
Liquid fuels	MW/MW HHV input	30.5%	30.5%	30.5%	30.5%	60.2%	60.2%	40.6%	40.6%	39.6%	44.8%	44.1%
Electricity	MWe/MW HHV input	9.4%	9.4%	11.4%	11.4%	0.0%	0.0%	0.8%	0.8%	11.3%	4.1%	-2.6%
Electricity (thermal equivalent)	MW/MW HHV input	21.0%	21.0%	25.3%	25.3%	0.0%	0.0%	1.8%	1.8%	25.1%	9.2%	-5.8%
Char byproduct	MW/MW HHV input	-	-	-	-	9.5%	9.5%	27.6%	27.6%	-	-	-
Energy efficiencies												
Liquid fuel		39.9%	39.9%	41.9%	40.9%	69.7%	66.5%	69.0%	57.5%	52.9%	49.4%	41.7%
Liquid fuel + thermal energy		51.5%	51.5%	55.8%	55.8%	69.6%	69.7%	70.0%	70.0%	64.7%	54.0%	38.3%
Liquid fuel + electricity and/or char		38.6%	38.6%	40.9%	41.9%	66.5%	69.7%	57.5%	69.0%	50.9%	49.0%	41.5%
Economic evaluation												
Total project investment cost	M\$	\$198.95	\$540.52	\$163.87	\$432.90	\$61.18	\$141.68	\$62.53	\$126.79	\$705.04	\$794.48	\$719.62
Liquid fuel production costs	\$/GJ HHV	\$38.30	\$30.30	\$33.20	\$22.96	\$12.45	\$6.95	\$12.27	\$8.16	\$21.60	\$28.40	\$29.70
Breakeven oil price	\$/barrel crude oil	\$135.00	\$107.00	\$117.00	\$81.00					\$77.30	\$101.60	\$106.10
Internal rate of return	%	6.40	11.10	6.80	14.40	20.70	34.20	23.30	40.50	11.00	8.20	6.00
Payback period	years	-	19.96	-	-	10.12	6.29	8.68	5.16	-	-	-

Table C3.2 Breakdown of total capital investment for bioethanol process scenarios

	ETOH-dilute acid (35), 145MW	ETOH-dilute acid (35), 600MW	ETOH-steam explosion, 145MW	ETOH-steam explosion, 600MW
Feed preparation and pretreatment	\$ 37,286,100.00	\$ 108,591,700.00	\$ 10,783,300.00	\$ 28,596,600.00
Hydrolysis and Fermentation	\$ 5,586,300.00	\$ 13,592,400.00	\$ 4,976,600.00	\$ 13,455,700.00
Product recovery	\$ 9,999,500.00	\$ 28,180,000.00	\$ 13,379,000.00	\$ 38,009,900.00
Stillage and water treatment	\$ 4,553,400.00	\$ 9,980,800.00	\$ 4,266,700.00	\$ 8,061,000.00
Boiler and steam turbine cycle	\$ 39,525,000.00	\$ 111,974,700.00	\$ 43,722,200.00	\$ 123,041,700.00
	\$ 96,950,300.00	\$ 272,319,600.00	\$ 77,127,800.00	\$ 211,164,900.00
Total capital investment	\$ 198,953,000.00	\$ 540,518,000.00	\$ 163,865,000.00	\$ 432,904,000.00
Specific capital investment	\$ 4,580.54	\$ 3,007	\$ 3,810	\$ 2,432

Table C3.3 Breakdown of total capital investment for pyrolysis process scenarios

	Fast Pyrolysis 145 PYROLYSIS-fast, 145MW	Fast Pyrolysis 600 PYROLYSIS-fast, 600MW	Vacuum Pyrolysis 145 PYROLYSIS- vacuum, 145MW	Vacuum Pyrolysis 600 PYROLYSIS- vacuum, 600MW
Feed preparation	\$ 6,190,000.00	\$ 18,100,000.00	\$ 6,190,000.00	\$ 18,100,000.00
Pyrolysis	\$ 4,360,000.00	\$ 12,800,000.00	\$ 4,806,000.00	\$ 15,053,700.00
Condensation	\$ 5,608,100.00	\$ 5,618,700.00	\$ 5,673,600.00	\$ 5,750,800.00
Heat recovery and recycle	\$ 4,681,200.00	\$ 15,064,100.00	\$ 3,535,700.00	\$ 10,696,300.00
Product recovery	\$ 311,900.00	\$ 436,700.00	\$ 380,000.00	\$ 731,300.00
Steam turbine cycle	\$ 4,484,700.00	\$ 14,104,400.00	\$ 2,558,300.00	\$ 8,366,800.00
	\$ 25,635,900.00	\$ 66,123,900.00	\$ 23,143,600.00	\$ 58,698,900.00
Total capital investment	\$ 61,179,100.00	\$ 141,680,000.00	\$ 62,527,800.00	\$ 126,786,292.80
Specific capital investment [\$/GJ fuel]	\$ 1,468	\$ 821	\$ 2,506	\$ 1,224

Table C3.4 Breakdown of total capital investment for Fischer-Tropsch process scenarios

	FT-Bag (EG), 145MW	FT-Bag (EG1), 600MW	FT-Bag (EG1), 600MW	FT Bag (EG1-shift), 600MW	FT Bag (EG2), 600MW	FT-fps (EG1), 600MW	FT-vps (EG1), 600MW
Pyrolysis plant	\$ -	\$ -	\$ -	\$ -	\$ -	\$ 81,028,000.00	\$ 70,221,000.00
Feed preparation	\$ 22,424,300.00	\$ 22,424,300.00	\$ 68,712,000.00	R 68,712,000.00	\$ 68,712,000.00	\$ 59,224,000.00	\$ 65,687,000.00
Air separation unit	\$ 29,154,300.00	\$ 29,219,700.00	\$ 84,774,000.00	R 87,416,000.00	\$ 67,833,000.00	\$ 83,631,000.00	\$ 88,801,000.00
Gasification and gas cleaning	\$ 36,674,000.00	\$ 36,674,000.00	\$ 78,539,000.00	R 89,857,000.00	\$ 98,822,000.00	\$ 78,539,000.00	\$ 78,539,000.00
Gas conditioning and recycle	\$ 12,471,400.00	\$ 12,490,100.00	\$ 29,345,800.00	R 55,697,900.00	\$ 27,864,700.00	\$ 28,292,700.00	\$ 30,193,200.00
Fischer-Tropsch synthesis	\$ 5,803,300.00	\$ 5,803,300.00	\$ 15,929,400.00	R 17,389,100.00	\$ 17,204,600.00	\$ 14,634,200.00	\$ 14,864,900.00
Boiler and steam turbine cycle	\$ 21,429,000.00	\$ 14,326,200.00	\$ 38,850,600.00	R 39,089,000.00	\$ 39,567,800.00	\$ 50,066,800.00	\$ 49,723,000.00
Refinery	\$ 17,335,800.00	\$ 17,371,500.00	\$ 46,945,000.00	\$ 51,170,000.00	\$ 50,584,000.00	\$ 43,216,000.00	\$ 43,772,000.00
	\$ 145,292,100.00	\$ 138,309,100.00	\$ 363,095,800.00	R 409,331,000.00	\$ 370,588,100.00	\$ 438,631,700.00	\$ 441,801,100.00
Total capital investment	\$ 260,961,000.00	\$ 271,762,000.00	\$ 705,037,000.00	\$ 794,476,000.00	\$ 719,622,000.00	\$ 852,098,000.00	\$ 858,084,000.00
Specific capital investment [\$/GJ fuel]		\$ 4,726	\$ 2,964	\$ 3,116	\$ 2,642	\$ 5,808	\$ 5,830

Table C3.5 Summary of economic indicators for bioethanol steam explosion scenarios

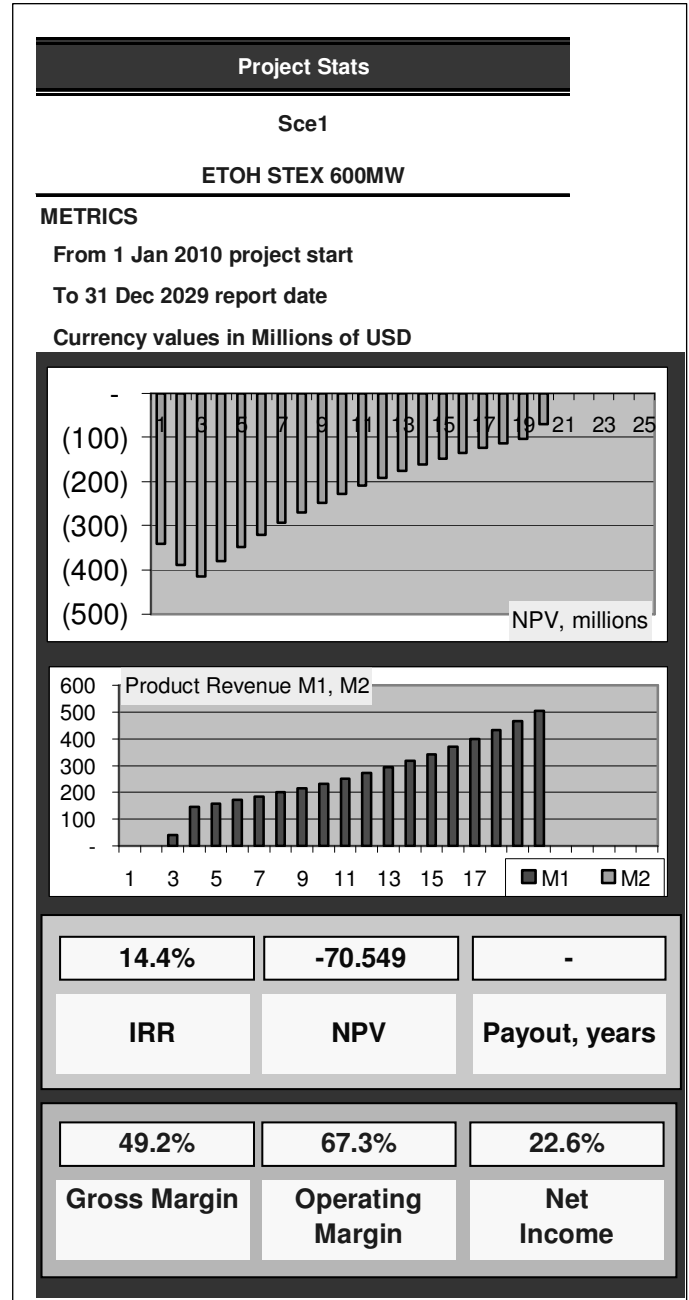
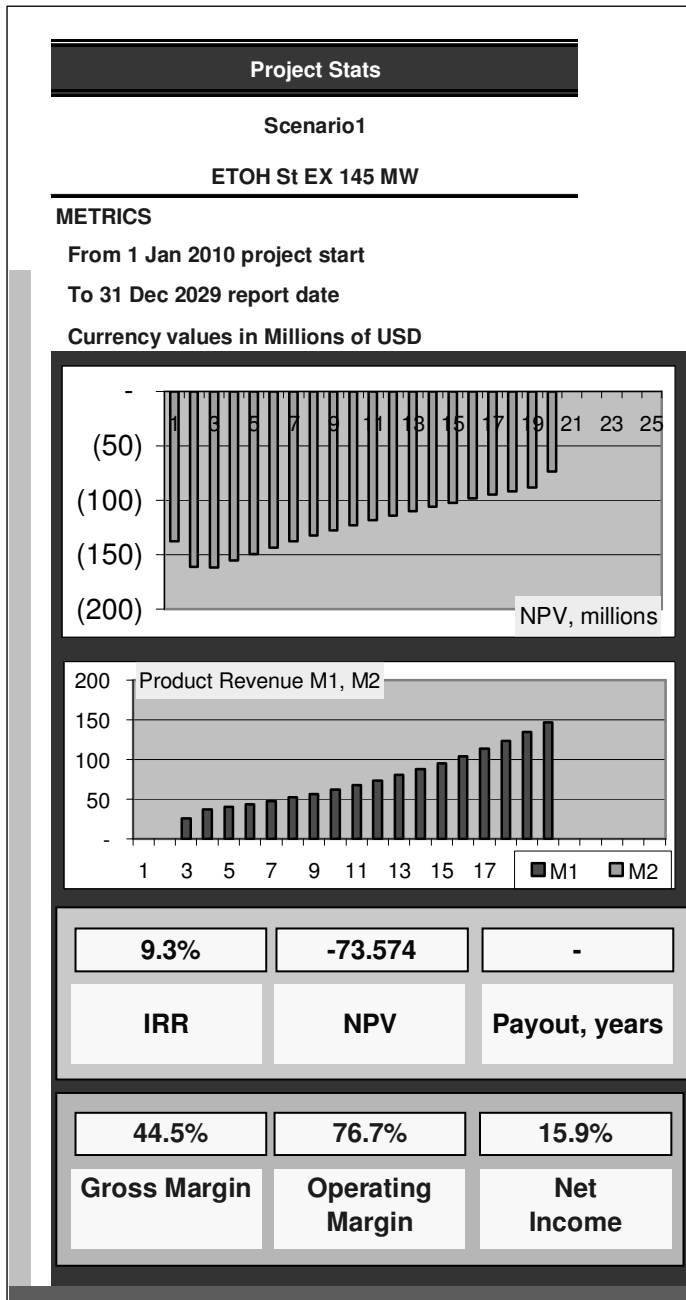


Table C3.6 Summary of economic indicators for vacuum pyrolysis scenarios.

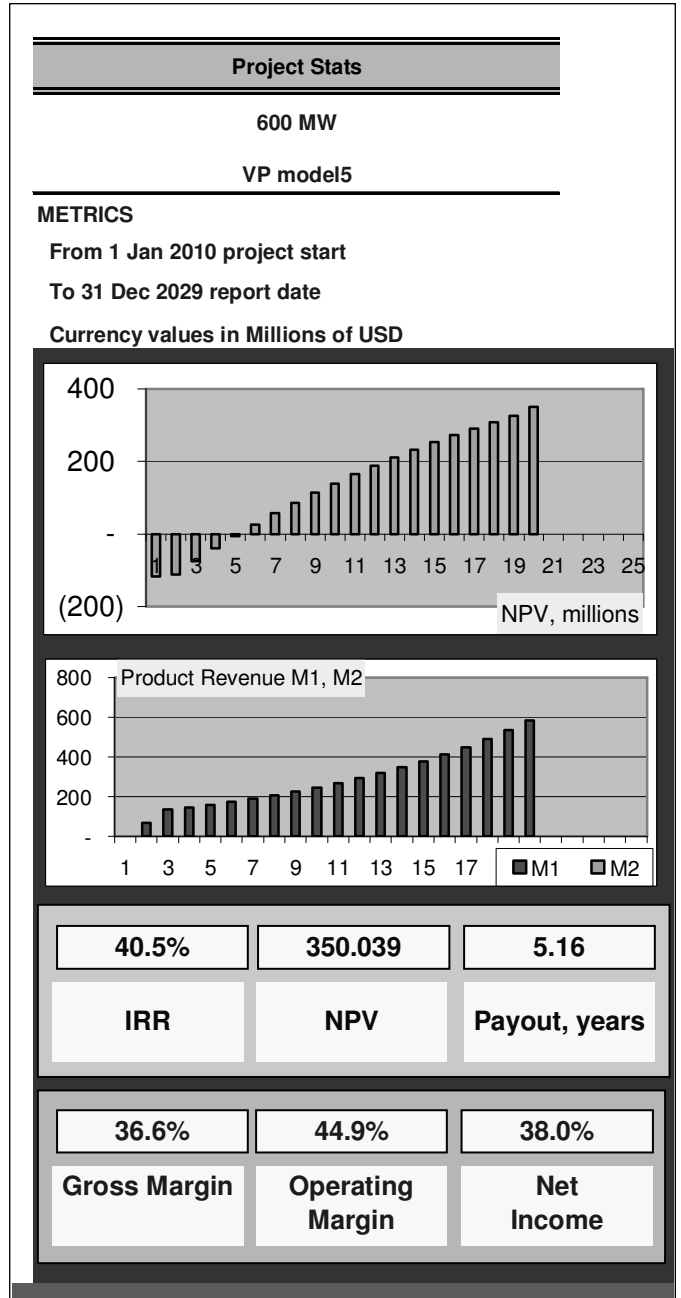
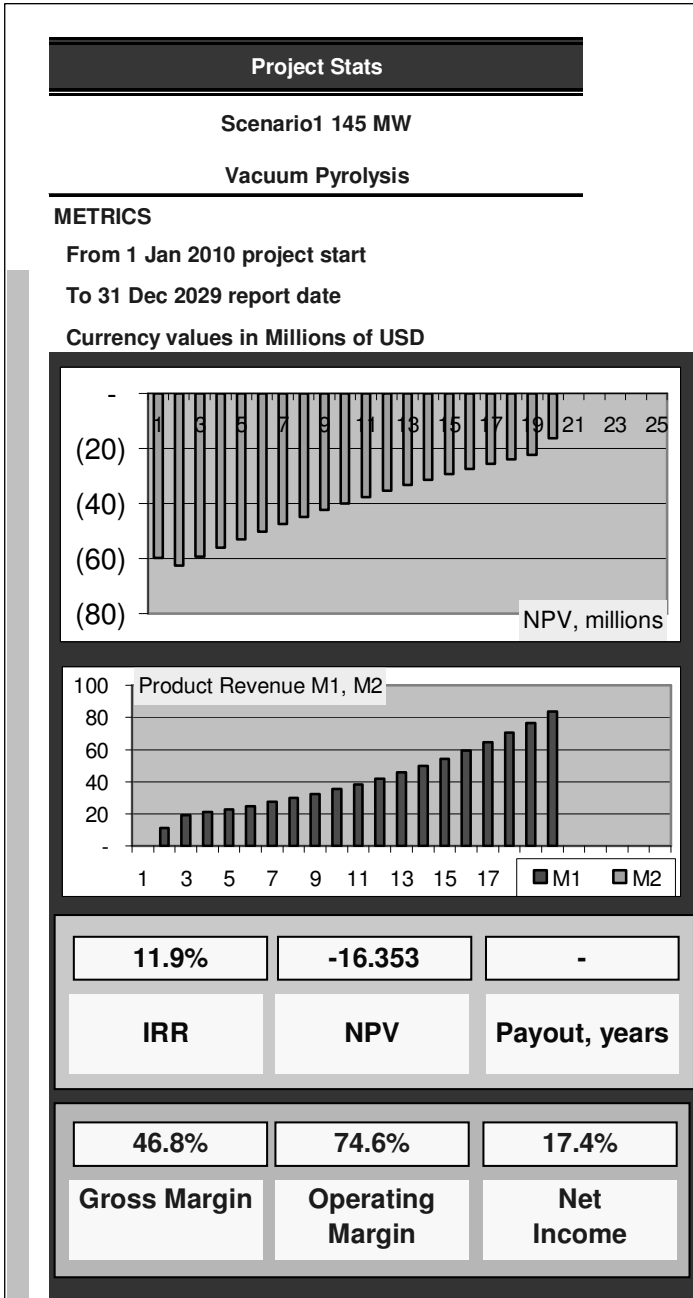


Table C3.7 Summary of economic indicators for fast pyrolysis scenarios

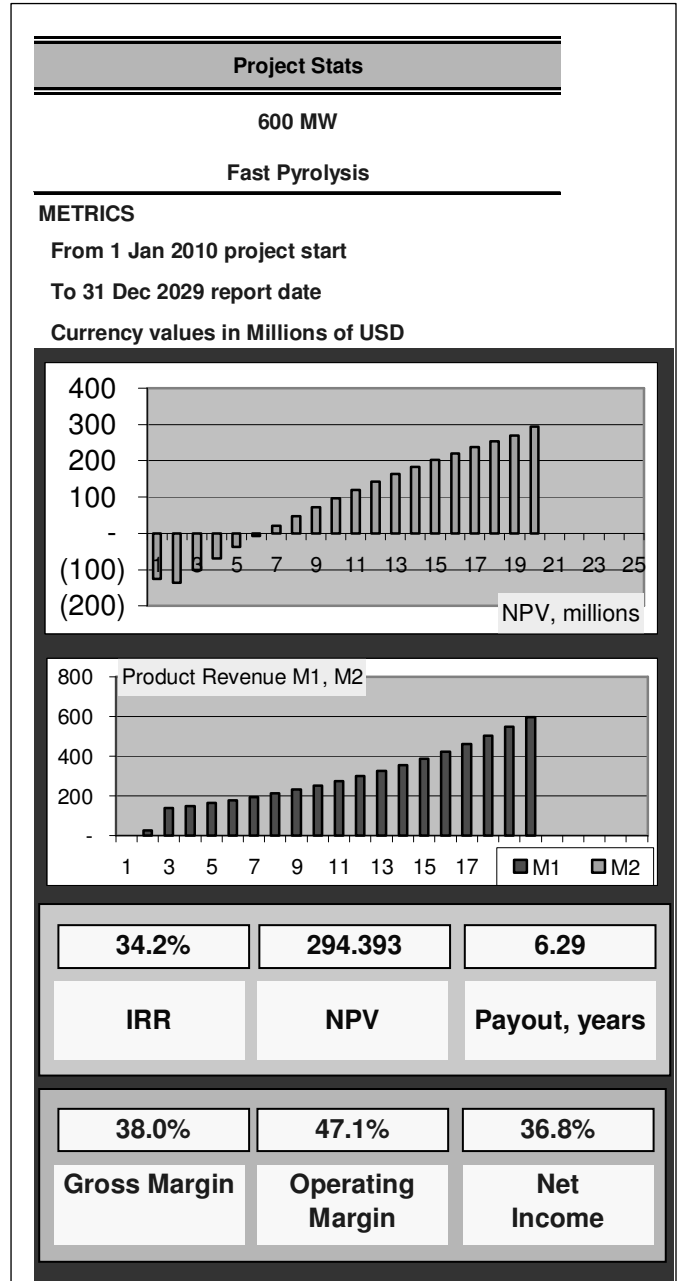
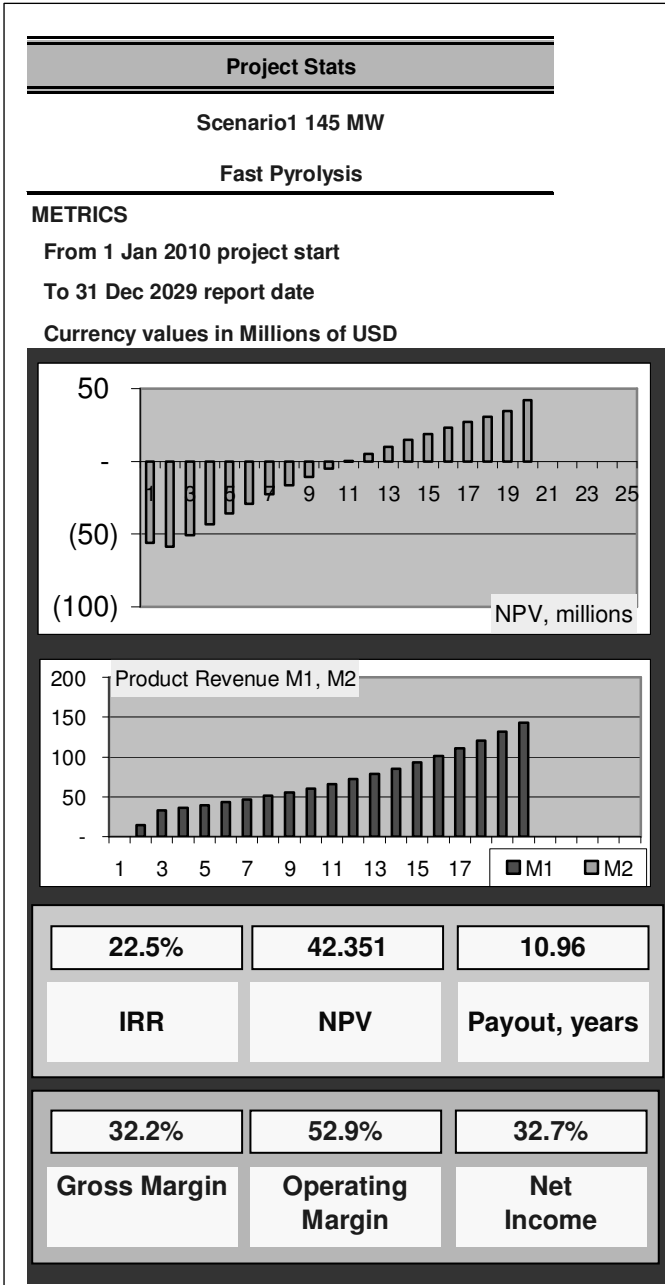


Table C3.8 Summary of economic indicators for Fischer-Tropsch (EG1) bagasse scenarios

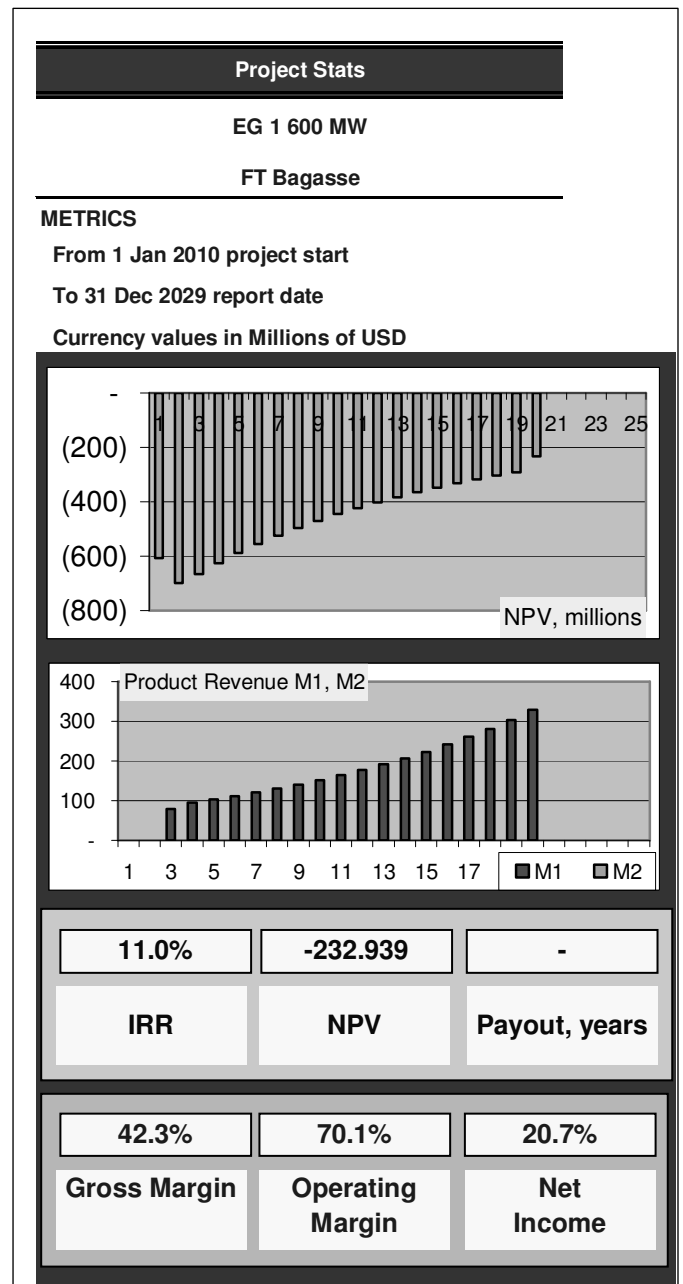
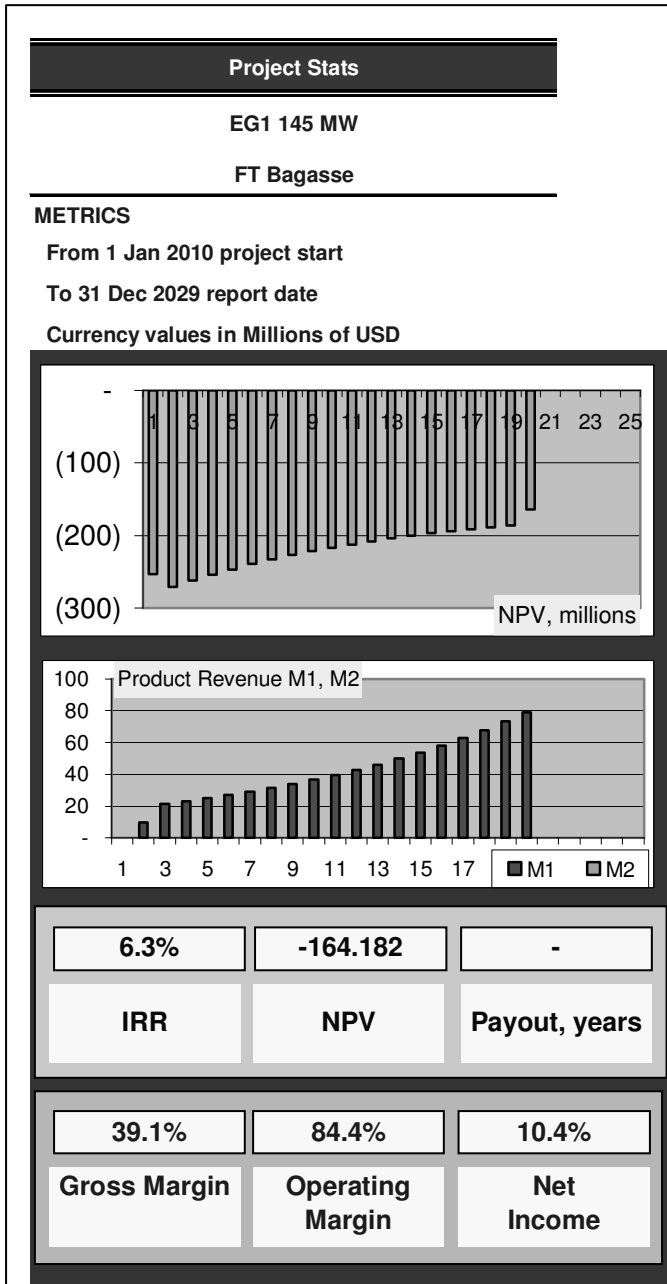


Table C3.9 Summary of economic indicators for Fischer-Tropsch (EG1) with shift and (EG2) bagasse scenarios

